

TEXT and rectangles in blue will NOT show on printed copy

Type final title of thesis or dissertation (M.S. and Ph.D.) below . If your title has changed since your submitted an Application for Graduate Degree, notify Graduate Office.

Tarnishing of a Cu-Al-Zn-Sn Alloy Compared to Commercially Pure Copper: Implications
Toward Antimicrobial Function

A Thesis

Presented to
the faculty of the School of Engineering and Applied Science
University of Virginia

in partial fulfillment
of the requirements for the degree

Master of Science

by

Name

Leanna L. Foster

Month degree is awarded

August

Year

2014

APPROVAL SHEET

The thesis

is submitted in partial fulfillment of the requirements

for the degree of

Master of Science

Leanna L. Foster

AUTHOR *signature*

The thesis has been read and approved by the examining committee:

John R. Scully

Advisor

Robert G. Kelly

Roseanne M. Ford

James A. Smith

Accepted for the School of Engineering and Applied Science:



Dean, School of Engineering and Applied Science

Month degree is awarded

August

Year

2014

Print Form

Abstract

Methicillin-resistant *staphylococcus aureus* (MRSA) is a highly contagious bacterium and is spread mainly by hand-to-surface contact. In 2005, 94,650 patients in the United States contracted MRSA, and 18,650 of these patients died.¹ MRSA is especially prevalent in hospitals, where patients are infected with MRSA by touching surfaces that will, in turn, be touched by other patients whose immune systems may be compromised.

This research is related to the goal of minimizing the spread of antibiotic-resistant diseases in hospitals enabled by corrosive release of Cu^+ and Cu^{2+} from copper alloys in solutions such as human perspiration. At the same time it is desirable to maintain color stability on hospital surfaces by minimizing tarnishing in the form of corrosion product formation. This creates a clearly contradictory situation. Unfortunately, the copper alloys with the best antimicrobial efficacy are often those that tarnish more readily. Conversely, the most corrosion resistant copper alloys in human perspiration often do not exhibit very good antimicrobial efficacy especially after long periods of oxide passivation after abrasion. Nordic Gold (89% Cu, 5% Zn, 5% Al, 1% Sn) was reported to kill MRSA when freshly cleaned. However, Nordic Gold passivated and copper release was limited when exposed to ambient lab conditions for 7 days.² However, kill rate studies have not been conducted in a solution that mimics hospital conditions (i.e. salt transfer from hand perspiration due to frequent skin contact).

The goal of this thesis was to understand tarnishing, copper release and color stability of a 89% Cu- 5% Al-5% Zn-1 % Sn solid solution alloy (Nordic Gold) during corrosion in various “high touch” hospital environments such as full immersion in

synthetic perspiration solution or full immersion in concentrated synthetic perspiration solution simulating the equilibrium conditions at low %RH, as well as during cyclic wetting and drying of synthetic perspiration solution. This alloy was compared to commercially pure Cu, C11000. Additionally, the role of thin oxides such as those formed by prolonged prior air oxidation was examined during subsequent full immersion testing. This was accomplished by tracking the “fate of copper” during oxidation from the elemental state in solid solution through the corrosion process by analysis of the total copper oxidation, the oxide layer formed, as well as solution analysis for dissolved copper. Electrochemical, gravimetric, surface science and solution spectrometry tools were utilized.

In full immersion exposure to synthetic perspiration solution, Nordic Gold exhibited decreased instantaneous corrosion rates, a lesser degree of tarnishing, and a thinner corrosion product layer while maintaining comparable copper ion release rates to C11000. The only corrosion products detected were CuO and Cu₂O on both Nordic Gold and C11000. Additionally, the presence of thin air formed oxides during lab air passivation had minimal effect on subsequent corrosion of C11000, but more noticeable effects on Nordic Gold. Air oxidized Nordic Gold exhibited decreased instantaneous corrosion rates compared to the freshly ground alloy surface, a thinner corrosion layer, but comparable copper release to the freshly ground sample. This behavior is hypothesized to be caused by the complex effect of Nordic Gold’s alloying elements. Sn, Zn, and Al help form a more compact oxide, but still enable the release of similar quantities of Cu cations. This indicates that there is insufficient Zn present to limit Cu

release by suppression of the OCP. The Cu release enhancing effect of Sn seen by Goidanich³ is also operative in Nordic Gold.

Concentrated synthetic perspirations solution was determined to result in a stronger thermodynamic driving force to oxidize copper alloys without direct oxide formation. Following full immersion exposure to concentrated synthetic perspiration, both alloys exhibited increasing instantaneous corrosion rates over time. Nordic Gold was observed to have a thinner compact oxide layer form after exposure to concentrated synthetic perspiration, and released less total metal ions into solution compared to C11000. Prior air oxidation resulted in an increase in Cu release from the alloy. A greater variety of corrosion products, including precipitated $\text{Cu}_2(\text{OH})_3\text{Cl}$, were detected compared to freshly ground alloys where only CuO and Cu_2O were detected.

Corrosion behavior as a result of synthetic perspiration deposition and cyclic wetting and drying was determined to be strongly dependent on the number of cycles samples were exposed to. Nordic Gold and C11000 were observed to have no statistical difference in total oxidation charge determined by mass loss. Evidence of CuO , Cu_2O , $\text{Cu}_2(\text{OH})_3\text{Cl}$ and $\text{Cu}_2(\text{OH})_2\text{CO}_3$ were observed on both alloys. CuO and Cu_2O were theorized to form by direct oxidation while $\text{Cu}_2(\text{OH})_3\text{Cl}$ and $\text{Cu}_2(\text{OH})_2\text{CO}_3$ products were formed by chemical supersaturation of the droplet, resulting in precipitation by homogeneous chemical reaction. Nordic Gold had slightly lower mass gain over 12 dry-wet cycles, suggesting less precipitated corrosion products as governed by these homogeneous chemical reactions. However, Nordic Gold resulted in thinner electrically connected compact oxide layers. These thinner corrosion films enable more copper release from the bulk alloy despite comparable corrosion rate and a lower Cu

composition in the bulk alloy. Moreover, since the overall corrosion rate was similar, ion release was comparable or slightly greater on Nordic Gold. Sn, Al or Zn directly or indirectly enhance Cu release. Based on dissolved Cu concentrations measured, it is suspected that both alloys would provide sufficient Cu^{2+} necessary to kill *E. coli* (HCB1) bacteria in time periods less than 8 hours.

The most significant factor in corrosion behavior was found to be the environmental condition (i.e. full immersion, dry-wet cycles, synthetic perspiration, concentrated synthetic perspiration) given that both alloys possess greater than 89% Cu. While all scenarios facilitate copper ion release at concentrations above those necessary to kill bacteria, concentration build-up in drying-wetting testing with synthetic perspiration solution resulted in the greatest copper ion release rate, followed by full immersion testing with concentrated perspiration solution simulating the concentration just before drying or low %RH. Lastly, full immersion testing with normal concentration synthetic perspiration solution was the least aggressive. Additionally, corrosion layer thickness and Cu ion release varied by solution and alloy. Cyclic wetting and drying in synthetic perspiration yielded Cu based precipitates due to limited droplet volume subject to solubility laws, followed by full immersion with synthetic perspiration solution and lastly full immersion with concentrated perspiration. All solutions generated CuO and Cu_2O corrosion products, with the formation of $\text{Cu}_2(\text{OH})_3\text{Cl}$ especially aided by the high Cl^- content in drying-wetting testing. Additionally, copper carbonate products formed during cyclic drying-wetting in synthetic perspiration, likely due to extended exposure to lab air, thin electrolyte films and the governing solubility laws. It is hypothesized that oxide formation occurs by direct oxidation to form a compact CuO and Cu_2O film, and

by homogeneous chemical precipitation due to supersaturation of the droplet volume with metal cations.

The work in this thesis contributes to the assessment of copper alloys for hospital applications by assessing corrosion behavior as opposed to empirical bacteria kill testing. As such, it evaluates the corrosion process by which a copper alloy is antimicrobial. Results in this thesis indicate that alloy composition and environment are the primary factors controlling corrosion behavior. A complex effect is evident in Nordic Gold alloy with Sn, Zn, and Al. Future work is suggested continue to define the role of corrosion environment on the fate of copper. For instance, antimicrobial efficacy is typically tested in nutrient broths instead of perspiration. Additionally, this work established the methodology and foundation to bridge empirical antimicrobial testing through bacteria kill rates with corrosion studies determining ion release directly from copper alloys.

Acknowledgements

The funding provided by the National Science Foundation under Grant No. DMR-090663, DMR-130999 (Dr. Eric Taleff) and the National Science Foundation Graduate Research Fellowship Grant No. DGE-1315231 has made this project and thesis possible. I would like to specifically thank Dr. John Scully for his guidance, his wealth of knowledge and the opportunity to pursue a line of research that has shaped my future. To all the members of the Center for Electrochemical Science and Engineering – thank you for being a source of encouragement and support when times were rough, and for sharing smiles and laughter when times were good.

Thank you to my parents, who introduced me to science at such a young age, and continued to motivate me every step of the way. You gave me advice, pep talks, and love no matter what time I called, and much needed hugs every time we were together.

Finally, I want to thank my loving husband, Ryan Foster. I appreciate your confidence, patience and love you provided me throughout this project (and our first years of marriage!). You fed me, held me, and challenged me to be the best that I could be. This would not have been possible without you.

Table of Contents

Abstract	1
Acknowledgements	6
List of Figures	11
List of Tables	30
1 Introduction	33
1.1 The Importance of Identifying Color Stable Antimicrobial Alloys	33
1.1.1 Hospital Acquired Infections	33
1.1.2 Mitigating Approaches	33
1.2 A Brief Review of Antimicrobial Copper Alloys	36
1.2.1 EPA-Approved Alloy Systems	36
1.2.2 Antimicrobial Mechanisms	37
1.2.3 Alternative Antimicrobial Metallic Materials	38
1.3 Antimicrobial Efficiency Testing	40
1.3.1 EPA Testing Procedures	40
Label Claims:	43
1.3.2 Copper Development Association Antimicrobial Copper Results	43
1.3.3 In House Disinfection Studies	48
1.4 The Need to Understand the Fate of Oxidized Copper in Copper and Copper Alloys	50
1.4.1 Atmospheric Corrosion and Tarnishing of High Purity Copper	51
1.4.2 Copper Corrosion by Seawater in Full Immersion	61
1.4.3 Copper Corrosion by Human Perspiration in Full Immersion	64
1.5 Effects of Alloying Composition	67
1.5.1 Copper Content	67
1.5.1 Major Alloying Elements	68
1.5.2 Ranking of Alloys	72
1.6 Nordic Gold	77
1.6.1 Color Stability	77
1.6.2 Antimicrobial Activity and Passivation	78
1.7 Critical Unresolved Issues	83
1.8 Thesis Objectives	85
1.8.1 The Fate of Copper	85
1.8.2 Approach	85
1.8.3 Thesis Organization	86

2	The Fate of Copper during Corrosion of Nordic Gold (89% Cu, 5% Zn, 5% Al, 1% Sn) vs. C11000 (>99.9% Cu) in Synthetic Perspiration Solution (0.5% NaCl, 0.1% CH ₄ N ₂ O, 0.1% C ₃ H ₆ O ₃)	89
2.1	Abstract	89
2.2	Introduction	90
2.3	Experimental Procedure	95
2.3.1	Pre-Oxidation Conditions	95
2.3.2	Exposure Experiments	96
2.3.3	E-I Behavior and Open Circuit Potential of C11000 and Nordic Gold	96
2.3.4	Corrosion Rate by OCP-EIS and Mass Loss	97
2.3.5	Corrosion Product Analysis	101
2.3.6	Solution Analysis by ICP-OES	105
2.4	Results	108
2.4.1	E-I Behavior and Open Circuit Potential of C11000 and Nordic Gold	108
2.4.2	Corrosion Rate by OCP-EIS and Mass Loss	112
2.4.3	Surface Analysis of Corrosion Products	122
2.4.4	Copper Ion Release by ICP-OES	144
2.5	Discussion	150
2.5.1	Summary of Results and Findings	150
2.5.2	Effect of Zn, Al, and Sn Alloying Additions and Thin Oxides on Copper Corrosion Electrochemistry in Synthetic Perspiration	155
2.5.3	Effect of Zn, Al, and Sn Alloying Additions and Thin Oxides on Metal Release Rate in Synthetic Perspiration	157
2.6	Conclusions	161
3	The Fate of Copper during Corrosion of Nordic Gold (89% Cu, 5% Zn, 5% Al, 1% Sn) vs. C11000 (>99.9% Cu) in Concentrated Synthetic Perspiration Solution (2 M NaCl, 1 M CH ₄ N ₂ O, 0.11 M C ₃ H ₆ O ₃)	163
3.1	Abstract	163
3.2	Introduction	164
3.3	Experimental Procedure	171
3.3.1	Pre-Oxidation Conditions	172
3.3.2	Exposure Experiments	172
3.3.3	E-I Behavior and Open Circuit Potential of C11000 and Nordic Gold	176
3.3.1	Corrosion Rate by OCP-EIS and Mass Loss	176
3.3.2	Corrosion Product Analysis	180
3.3.3	Solution Analysis by ICP-OES	184

3.3.4	Charge Analysis	187
3.4	Results	189
3.4.1	E-I Behavior and Open Circuit Potential of C11000 and Nordic Gold	189
3.4.2	Corrosion Rate by OCP-EIS and Mass Loss	192
3.4.3	Surface Analysis of Corrosion Products	201
3.4.4	Copper Ion Release by ICP-OES	227
3.5	Discussion	232
3.5.1	Summary of Findings	232
3.5.2	Effect of Concentrated Synthetic Perspiration Solution on Corrosion Behavior compared to Normal Concentration Synthetic Perspiration Solution	235
3.5.3	Effect of Zn, Al, and Sn Alloying Additions and Thin Oxides on Copper Corrosion Electrochemistry in Concentrated Synthetic Perspiration	239
3.5.4	Effect of Zn, Al, and Sn Alloying Additions and Thin Oxides on Metal Release Rate in Concentrated Synthetic Perspiration	241
3.6	Conclusion	244
4	The Fate of Copper during Corrosion of Nordic Gold (89% Cu, 5% Zn, 5% Al, 1% Sn) vs. C11000 (>99.9% Cu) in Synthetic Perspiration Droplets during Wetting and Drying Cycles	246
4.1	Abstract	246
4.2	Introduction	247
4.3	Experimental Procedure	255
4.3.1	Sample Preparations	255
4.3.2	Exposure Solution and Setup	255
4.3.3	Corrosion Rate: Mass Loss by Gravimetric Analysis	257
4.3.4	Corrosion Product Analysis	259
4.3.5	Solution Analysis by ICP-OES	263
4.4	Results	266
4.4.1	Corrosion Rate: Mass Loss by Gravimetric Analysis	266
4.4.1	Surface Analysis of Corrosion Products	267
4.4.2	Tarnishing in Synthetic Perspiration	267
4.4.3	Tarnish Analysis by Optical Spectrophotometry	275
4.4.4	Corrosion Product Analysis by GIXRD	277
4.4.5	Corrosion Product Layer Analysis by Galvanostatic Reduction	281
4.4.6	Copper Ion Release Assessed by ICP-OES	287
4.5	Discussion	289
4.5.1	Summary of Findings	289

4.5.2	Effect of Zn, Al, and Sn Alloying Additions on Copper Corrosion Electrochemistry and Metal Ion Release during Drying and Wetting of Synthetic Perspiration Solution	292
4.5.3	Ability to Achieve Critical Concentration for Antimicrobial Efficacy	294
4.5.4	Effect of Drying and Wetting Synthetic Perspiration Testing on Corrosion Behavior compared to Full Immersion Synthetic Perspiration Solution and Full Immersion Concentrated Synthetic Perspiration Solution	295
4.6	Conclusion	300
5	Future Work	302
	References	304
	Appendix A: Broth Medium Compositions	314

List of Figures

- Figure 1.1. Residual self-sanitizing test protocol schematic.⁵⁴ 42
- Figure 1.2. Viability of methicillin-resistant *staphylococcus aureus* (NTC10442) (MRSA) at 22 °C on copper (C19700, 97.6% Cu), brass (C24000, 81.5% Cu) or stainless steel (S30400) over 360 minutes tested in tryptone soy broth.⁵⁵ 47
- Figure 1.3. Viability of *L. monocytogenes* at 20 °C on various copper alloy surfaces, where antimicrobial efficiency follows copper content in Brain Hearth Infusion Broth.⁵⁷ 47
- Figure 1.4. The effects of tarnishing on *E. coli* 20 °C viability on various copper alloy surfaces in tryptone soy broth.⁵⁷ 48
- Figure 1.5. In house disinfection studies of *E. coli* (HCB1) in solution so synthetic perspiration (0.5% NaCl, 0.1% CH₄N₂O, 0.1% C₃H₆O₃) and Cu²⁺ ions from a CuCl₂ solution at 20 °C, enumerated by most probable number method. 50
- Figure 1.6. Formation sequence for compounds in copper corrosion products formed under sheltered conditions for varying degrees of atmospheric constituents.⁵⁸ 53
- Figure 1.7. Schematic representation of the processes involved in the formation of sulfate components in copper patinas.⁵⁸ 54
- Figure 1.8. Schematic representation of the processes involved in the formation of chloride components of copper patinas.⁵⁸ 54
- Figure 1.9. Schematic representation of the processes involved in the formation of the carboxylic acid components of copper patinas.⁵⁸ 55
- Figure 1.10. Annual release rate of copper and zinc from brass (Cu-Zn), bronze (Cu-Sn), and separate pure metal constituents exposed to identical conditions during 2 years of urban exposure.³ 57
- Figure 1.11. Schematic of copper alloy corrosion in solution droplet akin to atmospheric corrosion at normal relative humidity. 57
- Figure 1.12. E-pH diagram of expected corrosion behavior in chlorinated medium (86 mM Cl⁻, 10 μM Cu⁺ in H₂O at 25 °C) to represent concentrated synthetic perspiration constructed with Medusa software. 61
- Figure 1.13. Evolution of thickness of cuprous oxide (Cu₂O) vs. copper content after hand contact test, corroded by passing between different individuals for various times over a 2 year period.⁷² 66
- Figure 1.14. Binary phase diagram of Cu-Ni.⁹⁶ 69

	12
Figure 1.15. Binary phase diagram of Cu-Sn. ⁹⁶	69
Figure 1.16. Binary phase diagram of Cu-Zn. ⁹⁶	70
Figure 1.17. Binary phase diagram of Cu-Al. ⁹⁶	70
Figure 1.18. Total charge per reduction wave found by galvanostatic reduction analysis of copper alloys exposed to 130 hours of synthetic perspiration. Some alloys had two regions of distinct oxide coloration and were tested separately, labeled oxide 1 and oxide 2. Nordic Gold has the thinnest total oxide layer.	74
Figure 1.19. Grazing incidence x-ray diffraction (GIXRD) of copper alloys freshly ground (a) and after 130 hours of exposure to synthetic perspiration (b).	74
Figure 1.20. Raman spectroscopy of copper alloys freshly ground (a) and after 130 hours of exposure to synthetic perspiration (b).	75
Figure 1.21. Copper ion concentration after copper alloys exposed to 130 hours in synthetic perspiration.	76
Figure 1.22. Viability of methicillin resistant <i>staphylococcus aureus</i> over 6 hours on a freshly cleaned (by alcohol and deionized water) stainless steel, C19700, C24000, and Nordic Gold sample in tryptone soy broth (C19700, C24000, and stainless steel) and unknown broth (Nordic Gold). ²	79
Figure 1.23. Viability of methicillin resistant <i>staphylococcus aureus</i> over 6 hours on freshly cleaned Nordic Gold compared to Nordic Gold samples cleaned (by alcohol and deionized water), then exposed to ambient lab conditions for 7 days in unknown broth. ²	79
Figure 1.24. Viability of <i>C. albicans</i> on dry metallic surfaces at 23 °C. ¹⁰⁷	80
Figure 1.25. Cell viability of <i>Staphylococcus hominis</i> spp. <i>hominis</i> (a), <i>Micrococcus luteus</i> (b), <i>S. aureus</i> (c), and <i>S. epidermidis</i> (d) on unwashed (uw) and washed (w) Euro coins, tested on the center (c) or edge (e) of the coin. ¹⁰⁸ 0.1 € is Nordic Gold.	82
Figure 2.1. Equivalent circuit used to model corrosion behavior of copper alloys.	99
Figure 2.2. Reduction order of copper oxides CuO and Cu ₂ O. ¹²⁵ However, other papers suggest CuO reduces to Cu ₂ O, rather than to CuO to Cu as reported here. ^{126,127}	103
Figure 2.3. Galvanostatic reduction analysis corresponds time to completely reduce a corrosion species (t _i) to inflection points on the galvanostatic reduction spectra, and reduction potential (E _i) to the plateau preceding the inflection point.	105

- Figure 2.4. Comparative calibration curves of Cu in deionized water and synthetic perspiration after 130 hours (no exposure to copper alloys) at 224.7 nm. 107
- Figure 2.5. Procedural flow chart of converting signal obtained by ICP-OES to copper ion release (ions/cm²). 108
- Figure 2.6. Cyclic voltammetry of C11000 and Nordic Gold freshly ground to 1200 grit, exposed to deaerated borate buffer (pH 8.4). 110
- Figure 2.7. Open circuit potential (OCP) of C11000 and Nordic Gold freshly ground to 1200 grit and exposure to synthetic perspiration (23 °C, ambient aeration) for 1 hour. 111
- Figure 2.8. Cyclic polarization (CP) of C11000 and Nordic Gold freshly ground to 1200 grit and exposure to synthetic perspiration (23 °C, ambient aeration) for 1 hour prior to CP. 111
- Figure 2.9. Nyquist plot of C11000 freshly ground to 1200 grit, then exposed to synthetic perspiration solution (23 °C, ambient aeration) for 130 hours, overlaid with model fit by the Simplex method. The exposure area was 0.8 cm². 115
- Figure 2.10. Nyquist plot of Nordic Gold freshly ground to 1200 grit, then exposed to synthetic perspiration solution (23 °C, ambient aeration) for 130 hours, overlaid with model fit by the Simplex method. The exposure area was 0.8 cm². 115
- Figure 2.11. Bode plots of C11000 freshly ground to 1200 grit, then exposed to synthetic perspiration solution (23 °C, ambient aeration) for various times indicated. 116
- Figure 2.12. Bode plots of Nordic Gold freshly ground to 1200 grit, then exposed to synthetic perspiration solution (23° C, ambient aeration) for various times indicated. 116
- Figure 2.13. Bode plots of C11000 and Nordic Gold freshly ground to 1200 grit, then exposed to synthetic perspiration solution (23° C, ambient aeration) for 0 and 130 hours. 117
- Figure 2.14. Bode plots of C11000 and Nordic Gold freshly ground to 1200 grit, furnace oxidized at 170 °C for 60 minutes, then exposed to synthetic perspiration solution (23° C, ambient aeration) for 0 and 130 hours. 118
- Figure 2.15. Bode plots of C11000 and Nordic Gold freshly ground to 1200 grit, air oxidized at ambient lab conditions for 30 days, then exposed to synthetic perspiration solution (23 °C, ambient aeration) for various times. 119
- Figure 2.16. Instantaneous corrosion rate (1/R_p) over time for C11000 freshly ground to 1200 grit, furnace oxidized at 170 °C for 60 minutes, or air oxidized at ambient lab conditions for 30 days, then exposed to synthetic perspiration solution (23 °C, ambient aeration). Data is the average of 3 replicates and error bars are one standard deviation. 120

Figure 2.17. Instantaneous corrosion rate ($1/R_p$) over time for Nordic Gold when freshly ground to 1200 grit, furnace oxidized at 170 °C for 60 minutes, or air oxidized at ambient lab conditions for 30 days, then exposed to synthetic perspiration solution (23 °C, ambient aeration) for various times. Data is the average of 3 replicates and error bars are one standard deviation. 120

Figure 2.18. Instantaneous corrosion rate ($1/R_p$) at 0 hours (left) and 130 hours (right) for C11000 and Nordic Gold when freshly ground to 1200 grit, furnace oxidized at 170 °C for 60 minutes, or air oxidized at ambient lab conditions for 30 days, then exposed to synthetic perspiration solution (23 °C, ambient aeration). Data is the average of a minimum of 3 replicates and error bars reflect one standard deviation. 121

Figure 2.19. Visual analysis of C11000 under freshly ground, furnace oxidized and air oxidized conditions after the indicated time exposure to synthetic perspiration at 23 °C and ambient aeration. 123

Figure 2.20. Visual analysis Nordic Gold under freshly ground, furnace oxidized and air oxidized conditions after the indicated time exposure to synthetic perspiration at 23 °C and ambient aeration. 124

Figure 2.21. Reflectivity of C11000 and Nordic Gold samples when freshly ground to 1200 grit, furnace oxidized at 170 °C for 60 minutes, or air oxidized at ambient lab conditions for 30 days, then exposed to synthetic perspiration solution at 23 °C and ambient aeration for various times. 126

Figure 2.22. Visible light spectrum wavelengths with corresponding observed color¹²⁹. 127

Figure 2.23. Reflectivity of C11000 and Nordic Gold samples when freshly ground to 1200 grit, furnace oxidized at 170 °C for 60 minutes, or air oxidized at ambient lab conditions for 30 days, then exposed to synthetic perspiration solution at 23 °C and ambient aeration for 0 hours (left) and 130 hours (right). 127

Figure 2.24. GIXRD of C11000 and Nordic Gold samples when freshly ground to 1200 grit, furnace oxidized at 170 °C for 60 minutes, or air oxidized at ambient lab conditions for 30 days, prior to exposure to synthetic perspiration solution, where only FCC metallic Cu (PDF Card No. 00-004-0836) peaks are evident. Spectra are shown offset ($y=120$) for ease of comparison. 128

Figure 2.25. GIXRD of C11000 and Nordic Gold samples when freshly ground to 1200 grit, furnace oxidized at 170 °C for 60 minutes, or air oxidized at ambient lab conditions for 30 days, then exposed to synthetic perspiration solution (23 °C, ambient aeration) for various times indicated. The development of Cu_2O is evident in all samples, regardless of composition or pretreatment. Spectra are shown offset ($y=100$) for ease of comparison. 129

Figure 2.26. GIXRD of C11000 and Nordic Gold samples when freshly ground to 1200 grit, furnace oxidized at 170 °C for 60 minutes, or air oxidized at ambient lab conditions for 30 days, after exposure to synthetic perspiration solution (23 °C, ambient aeration) for 130 hours, where only FCC metallic Cu peaks, Cu₂O and CuO peaks are evident. Spectra are shown offset (y=150) for ease of comparison. 130

Figure 2.27. Comparative GIXRD of C11000 and Nordic Gold when freshly ground to 1200 grit followed by exposure to synthetic perspiration solution (23 °C, ambient aeration) for 130 hours. Spectra are shown offset (y=170) for ease of comparison. 131

Figure 2.28. Comparative GIXRD of C11000 and Nordic Gold when freshly ground to 1200 grit, then thermally oxidized at 170 °C for 60 minutes, followed by exposure to synthetic perspiration solution (23 °C, ambient aeration) for 130 hours. Spectra are shown offset (y=170) for ease of comparison. 131

Figure 2.29. Comparative GIXRD of C11000 and Nordic Gold when freshly ground to 1200 grit, then air oxidized at ambient lab conditions, followed by exposure to synthetic perspiration solution (23 °C, ambient aeration) for 130 hours. Spectra are shown offset (y=170) for ease of comparison. 132

Figure 2.30. Galvanostatic reduction of C11000 and Nordic Gold when freshly ground to 1200 grit, thermally oxidized at 170 °C for 60 minutes, or air oxidized at ambient lab conditions for 30 days, followed by exposure to synthetic perspiration solution (23 °C, ambient aeration) for various times indicated. Galvanostatic reductions were conducted at 0.02 mA/cm² on an area of 0.8 cm². 135

Figure 2.31. Galvanostatic reduction of C11000 (left) and Nordic Gold (right) when freshly ground to 1200 grit followed by exposure to synthetic perspiration solution (23 °C, ambient aeration) for 0 and 130 hours. Galvanostatic reductions were conducted at 0.02 mA/cm² on an area of 0.8 cm². 136

Figure 2.32. Galvanostatic reduction of C11000 (left) and Nordic Gold (right) when freshly ground to 1200 grit, thermally oxidized at 170 °C for 60 minutes followed by exposure to synthetic perspiration solution (23 °C, ambient aeration) for 0 and 130 hours. Galvanostatic reductions were conducted at 0.02 mA/cm² on an area of 0.8 cm². 136

Figure 2.33. Galvanostatic reduction of C11000 (left) and Nordic Gold (right) when freshly ground to 1200 grit, air oxidized at ambient lab conditions for 30 days followed by exposure to synthetic perspiration solution (23 °C, ambient aeration) for 0 and 130 hours. Galvanostatic reductions were conducted at 0.02 mA/cm² on an area of 0.8 cm². 137

Figure 2.34. Galvanostatic reduction analysis of inflection points by taking the first derivative of C11000 and Nordic Gold when freshly ground to 1200 grit, thermally oxidized at 170 °C for 60 minutes, or air oxidized at ambient lab conditions for 30 days, followed by exposure to synthetic perspiration solution (23 °C, ambient aeration) for

various times indicated. Galvanostatic reductions were conducted at 0.02 mA/cm^2 on an area of 0.8 cm^2 . 138

Figure 2.35. Galvanostatic reduction over laid with inflection analysis of C11000 and Nordic Gold when freshly ground to 1200 grit, thermally oxidized at $170 \text{ }^\circ\text{C}$ for 60 minutes, or air oxidized at ambient lab conditions for 30 days, followed by exposure to synthetic perspiration solution ($23 \text{ }^\circ\text{C}$, ambient aeration) for 130 hours. Galvanostatic reductions were conducted at 0.02 mA/cm^2 on an area of 0.8 cm^2 . 139

Figure 2.36. Galvanostatic reduction with inflection points (t_i) and associated potentials (E_i) of C11000 (left) and Nordic Gold (right) when freshly ground to 1200 grit then air oxidized at ambient lab conditions for 30 days, followed by exposure to synthetic perspiration solution ($23 \text{ }^\circ\text{C}$, ambient aeration) for 130 hours. Galvanostatic reductions were conducted at 0.02 mA/cm^2 on an area of 0.8 cm^2 . 140

Figure 2.37. Galvanostatic reduction of C11000 and Nordic Gold when freshly ground to 1200 grit, thermally oxidized at $170 \text{ }^\circ\text{C}$ for 60 minutes, or air oxidized at ambient lab conditions for 30 days, followed by exposure to synthetic perspiration solution ($23 \text{ }^\circ\text{C}$, ambient aeration) for various times indicated. Galvanostatic reductions were conducted at 0.02 mA/cm^2 on an area of 0.8 cm^2 . Data is the average of 3 replicates and error bars are one standard deviation. 141

Figure 2.38. Comparative galvanostatic reduction of C11000 and Nordic Gold when freshly ground to 1200 grit followed by exposure to synthetic perspiration solution ($23 \text{ }^\circ\text{C}$, ambient aeration) for 130 hours. Galvanostatic reductions were conducted at 0.02 mA/cm^2 on an area of 0.8 cm^2 . 142

Figure 2.39. Comparative galvanostatic reduction of C11000 and Nordic Gold when freshly ground to 1200 grit then thermally oxidized at $170 \text{ }^\circ\text{C}$ for 60 minutes, followed by exposure to synthetic perspiration solution ($23 \text{ }^\circ\text{C}$, ambient aeration) for 130 hours. Galvanostatic reductions were conducted at 0.02 mA/cm^2 on an area of 0.8 cm^2 . 142

Figure 2.40. Comparative galvanostatic reduction of C11000 and Nordic Gold when freshly ground to 1200 grit then air oxidized at ambient lab conditions for 30 days, followed by exposure to synthetic perspiration solution ($23 \text{ }^\circ\text{C}$, ambient aeration) for 130 hours. Galvanostatic reductions were conducted at 0.02 mA/cm^2 on an area of 0.8 cm^2 . 143

Figure 2.41. Galvanostatic reduction points (t_i, E_i) of C11000 (left) and Nordic Gold (right) when freshly ground to 1200 grit, thermally oxidized at $170 \text{ }^\circ\text{C}$ for 60 minutes, or air oxidized at ambient lab conditions for 30 days, followed by exposure to synthetic perspiration solution ($23 \text{ }^\circ\text{C}$, ambient aeration) for 130 hours. Galvanostatic reductions were conducted at 0.02 mA/cm^2 on an area of 0.8 cm^2 . Data is the average of 3 replicates and error bars are one standard deviation. 143

Figure 2.42. Galvanostatic reduction points (t_i, E_i) of C11000 and Nordic Gold when freshly ground to 1200 grit, thermally oxidized at 170 °C for 60 minutes, or air oxidized at ambient lab conditions for 30 days, followed by exposure to synthetic perspiration solution (23 °C, ambient aeration) for 130 hours. Galvanostatic reductions were conducted at 0.02 mA/cm² on an area of 0.8 cm². Data is the average of 3 replicates and error bars are one standard deviation. 144

Figure 2.43. Copper release of C11000 and Nordic Gold when freshly ground to 1200 grit, thermally oxidized at 170 °C for 60 minutes, or air oxidized at ambient lab conditions for 30 days, followed by exposure to synthetic perspiration solution (23 °C, ambient aeration) over time. Synthetic perspiration solution was exposed to 0.8 cm² of copper of the copper alloy coupon, with a surface to volume ratio of 2.67 cm²/L. Data is the average of 3 replicates and error bars are one standard deviation. 146

Figure 2.44. Copper release from C11000 when freshly ground to 1200 grit, thermally oxidized at 170 °C for 60 minutes, or air oxidized at ambient lab conditions for 30 days, followed by exposure to synthetic perspiration solution (23 °C, ambient aeration) over time, expressed as ppm in solution (left) and amount Cu²⁺ in 300 mL divided by electrode area (0.8 cm²) (right) over time. Synthetic perspiration solution was exposed to 0.8 cm² of copper of the copper alloy coupon, with a surface to volume ratio of 2.67 cm²/L. Data is the average of 3 replicates and error bars are one standard deviation. 147

Figure 2.45. Copper ion release from Nordic Gold when freshly ground to 1200 grit, thermally oxidized at 170 °C for 60 minutes, or air oxidized at ambient lab conditions for 30 days, followed by exposure to synthetic perspiration solution (23 °C, ambient aeration) over time, expressed as ppm in solution (left) and amount Cu²⁺ in 300 mL divided by electrode area (0.8 cm²) (right) over time. Synthetic perspiration solution was exposed to 0.8 cm² of copper of the copper alloy coupon, with a surface to volume ratio of 2.67 cm²/L. Data is the average of 3 replicates and error bars are one standard deviation. 147

Figure 2.46. Copper release from C11000 and Nordic Gold when freshly ground to 1200 grit, followed by exposure to synthetic perspiration solution (23 °C, ambient aeration) over time expressed as ppm in solution. Synthetic perspiration solution was exposed to 0.8 cm² of copper of the copper alloy coupon, with a surface to volume ratio of 2.67 cm²/L. Data is the average of 3 replicates and error bars are one standard deviation. 148

Figure 2.47. Copper release from C11000 and Nordic Gold when freshly ground to 1200 grit and thermally oxidized at 170 °C for 60 minutes, followed by exposure to synthetic perspiration solution (23 °C, ambient aeration) over time expressed as ppm in solution. Synthetic perspiration solution was exposed to 0.8 cm² of copper of the copper alloy coupon, with a surface to volume ratio of 2.67 cm²/L. Data is the average of 3 replicates and error bars are one standard deviation. 148

Figure 2.48. Copper release from C11000 and Nordic Gold when freshly ground to 1200 grit and air oxidized at ambient lab conditions for 30 days, followed by exposure to

synthetic perspiration solution (23 °C, ambient aeration) over time expressed as ppm in solution. Synthetic perspiration solution was exposed to 0.8 cm² of copper of the copper alloy coupon, with a surface to volume ratio of 2.67 cm²/L. Data is the average of 3 replicates and error bars are one standard deviation. 149

Figure 2.49. Copper ion release from C11000 and Nordic Gold when freshly ground to 1200 grit, thermally oxidized at 170 °C for 60 minutes, or air oxidized at ambient lab conditions for 30 days, followed by exposure to synthetic perspiration solution (23 °C, ambient aeration) over time, expressed as ppm in solution. Synthetic perspiration solution was exposed to 0.8 cm² of copper of the copper alloy coupon, with a surface to volume ratio of 2.67 cm²/L. Data is the average of 3 replicates and error bars are one standard deviation. 149

Figure 2.50. Charge analysis of C11000 and Nordic Gold when freshly ground to 1200 grit, thermally oxidized at 170 °C for 60 minutes, or air oxidized at ambient lab conditions for 30 days, followed by exposure to synthetic perspiration solution (23 °C, ambient aeration) over time. Exposure area of working electrode (copper alloy) for EIS was 0.8 cm². Galvanostatic reductions were conducted at 0.02 mA/cm² on an area of 0.8 cm². Synthetic perspiration solution was exposed to 0.8 cm² of copper of the copper alloy coupon, with a surface to volume ratio of 2.67 cm²/L. 151

Figure 2.51. Charge comparison of Q_{corr} calculated from gravimetric mass loss, EIS, and ($Q_{\text{oxide}} + Q_{\text{solution}}$) of C11000 and Nordic Gold when freshly ground to 1200, followed by exposure to synthetic perspiration solution (23 °C, ambient aeration) over time. Exposure area of working electrode (copper alloy) for EIS was 0.8 cm². Galvanostatic reductions were conducted at 0.02 mA/cm² on an area of 0.8 cm². Synthetic perspiration solution was exposed to 0.8 cm² of copper of the copper alloy coupon, with a surface to volume ratio of 2.67 cm²/L. 152

Figure 2.52. University of Virginia disinfection studies of *E. coli* (HCB1) in solution of synthetic perspiration (0.5% NaCl, 0.1% CH₄N₂O, 0.1% C₃H₆O₃, pH 6.5) and Cu²⁺ ions from a CuCl₂ solution at 23 °C, enumerated by most probable number (MPN) method. 160

Figure 2.53. Correlation of constant copper release rates from copper alloys to time needed to achieve 1 ppm Cu²⁺ at a surface to volume ratio of 2.67 cm²/L. 161

Figure 3.1. Determination of deliquescence point and Conc_{equil} vs. RH relationship using OLI Analyzer Studio 9.0 software. 174

Figure 3.2. E-pH diagram of expected corrosion behavior in chlorinated medium (2 M Cl⁻, 10 μm Cu⁺ in H₂O at 25 °C) to represent concentrated synthetic perspiration constructed with Medusa software.. 175

Figure 3.3. Equivalent circuit used to model corrosion behavior of copper alloys 178

Figure 3.4. Reduction order of copper oxides CuO and Cu₂O.¹²⁵ However, other papers suggest CuO reduces to Cu₂O, rather than to CuO to Cu as reported here.^{126,127} 182

Figure 3.5. Galvanostatic reduction analysis corresponds time to completely reduce a corrosion species (t_i) to inflection points on the galvanostatic reduction spectra, and reduction potential (E_i) to the plateau preceding the inflection point. 184

Figure 3.6. Comparative calibration curves of Cu in deionized water and concentrated synthetic perspiration after 130 hours (no exposure to copper alloys) at 224.7 nm. 186

Figure 3.7. Procedural flow chart of converting signal obtained by ICP-OES to copper ion release (ions/cm²). 187

Figure 3.8. Open circuit potential (OCP) of C11000 and Nordic Gold freshly ground to 1200 grit and exposure to concentrated synthetic perspiration (23 °C, ambient aeration) for 1 hour. 190

Figure 3.9. Cyclic polarization (CP) of C11000 and Nordic Gold freshly ground to 1200 grit and exposure to concentrated synthetic perspiration (23 °C, ambient aeration) for 1 hour prior to CP. 190

Figure 3.10. Cyclic polarization (CP) of C11000 and Nordic Gold freshly ground to 1200 grit and exposure to concentrated synthetic perspiration (23 °C, ambient aeration) for 1 hour prior to CP. Figure b is a close-up of the red-outlined portion of figure a. 191

Figure 3.11. Nyquist plot of C11000 freshly ground to 1200 grit, then exposed to concentrated synthetic perspiration solution (23 °C, ambient aeration) for 130 hours, overlaid with model fit by the Simplex method. Exposure area was 0.8 cm². B₅ was bound to between 10 and 70 s^{1/2}/Ω, while the remaining parameters were left unbound to fit the data. Fit resulted in R₁ = 5.381 Ω, R₂ = 715.3 Ω, R₃ = 2.76 x 10⁻⁴ Ω, Y₀₄ = 5.58 x 10⁻³ s^{1/2}/Ω, B₅ = 23.45 s^{1/2}/Ω, Y₀₆ = 4.14 x 10⁻³ s^{1/2}/Ω, a₇ = 6.96 x 10⁻¹, Y₀₈ = 1.90 x 10⁻³ s^{1/2}/Ω, a₉ = 6.73 x 10⁻¹. 194

Figure 3.12. Nyquist plot of Nordic Gold freshly ground to 1200 grit, then exposed to concentrated synthetic perspiration solution (23 °C, ambient aeration) for 130 hours, overlaid with model fit by the Simplex method. Exposure area was 0.8 cm². B₅ was bound to between 10 and 70 s^{1/2}/Ω, while the remaining parameters were left unbound to fit the data. Fit resulted in R₁ = 4.517 Ω, R₂ = 1.45 x 10³ Ω, R₃ = 4.21 x 10⁻⁶ Ω, Y₀₄ = 6.64 x 10⁻³ s^{1/2}/Ω, B₅ = 29.25 s^{1/2}/Ω, Y₀₆ = 2.11 x 10⁻⁴ s^{1/2}/Ω, a₇ = 1.00, Y₀₈ = 1.42 x 10⁻³ s^{1/2}/Ω, a₉ = 6.44 x 10⁻¹. 195

Figure 3.13. Bode plots of C11000 freshly ground to 1200 grit, then exposed to concentrated synthetic perspiration solution (23 °C, ambient aeration) for various times indicated. 196

Figure 3.14. Bode plots of Nordic Gold freshly ground to 1200 grit, then exposed to concentrated synthetic perspiration solution (23° C, ambient aeration) for various times indicated. 196

Figure 3.15. Bode plots of C11000 and Nordic Gold freshly ground to 1200 grit, then exposed to concentrated synthetic perspiration solution (23° C, ambient aeration) for 0 and 130 hours. 197

Figure 3.16. Bode plots of C11000 and Nordic Gold freshly ground to 1200 grit, air oxidized at ambient lab conditions for 30 days, then exposed to concentrated synthetic perspiration solution (23 °C, ambient aeration) for 0 and 130 hours. 198

Figure 3.17. Instantaneous corrosion rate ($1/R_p$) over time for C11000 freshly ground to 1200 grit, or air oxidized at ambient lab conditions for 30 days, then exposed to concentrated synthetic perspiration solution (23 °C, ambient aeration). Data is the average of a minimum of 3 replicates and error bars are one standard deviation. 199

Figure 3.18. Instantaneous corrosion rate ($1/R_p$) over time for Nordic Gold when freshly ground to 1200 grit or air oxidized at ambient lab conditions for 30 days, then exposed to concentrated synthetic perspiration solution (23 °C, ambient aeration). Data is the average of a minimum of 3 replicates and error bars reflect one standard deviation. 199

Figure 3.19. Instantaneous corrosion rate ($1/R_p$) at 0 hours (left) and 130 hours (right) for C11000 and Nordic Gold when freshly ground to 1200 grit or air oxidized at ambient lab conditions for 30 days, then exposed to concentrated synthetic perspiration solution (23 °C, ambient aeration). Data is the average of a minimum of 3 replicates and error bars reflect one standard deviation. 200

Figure 3.20. Visual analysis of C11000 under freshly ground and air oxidized conditions after the indicated time exposure to concentrated synthetic perspiration at 23 °C and ambient aeration. 203

Figure 3.21. Visual analysis of Nordic Gold under freshly ground and air oxidized conditions after the indicated time exposure to concentrated synthetic perspiration at 23 °C and ambient aeration. 204

Figure 3.22. SEM micrographs of C11000 exposed to concentrated synthetic perspiration (23 C, ambient aeration) for 130 hours using backscattered electrons at 100x (a), 250x (b) and 1000x (c) 205

Figure 3.23. SEM micrographs of Nordic Gold exposed to concentrated synthetic perspiration (23 C, ambient aeration) for 130 hours using backscattered electrons at 100x (a), 250x (b) and 1000x (c) 206

Figure 3.24. Reflectivity of C11000 and Nordic Gold samples when freshly ground to 1200 grit, furnace oxidized at 170 °C for 60 minutes, or air oxidized at ambient lab

conditions for 30 days, then exposed to concentrated synthetic perspiration solution at 23 °C and ambient aeration for various times. 208

Figure 3.25. Visible light spectrum wavelengths with corresponding observed color.¹²⁹ 208

Figure 3.26. Reflectivity of C11000 and Nordic Gold samples when freshly ground to 1200 grit or air oxidized at ambient lab conditions for 30 days, then exposed to concentrated synthetic perspiration solution at 23 °C and ambient aeration for 0 hours (left) and 130 hours (right). 209

Figure 3.27. GIXRD of C11000 and Nordic Gold samples when freshly ground to 1200 grit, or air oxidized at ambient lab conditions for 30 days, prior to exposure to concentrated synthetic perspiration solution, where only FCC metallic Cu (PDF Card No. 00-004-0836) peaks are evident. Spectra are shown offset ($y=120$ on intensity scale) for ease of comparison. 210

Figure 3.28. GIXRD of C11000 (top) and Nordic Gold (bottom) samples when freshly ground to 1200 grit then exposed to concentrated synthetic perspiration solution at 23 °C and ambient aeration for various times indicated. 211

Figure 3.29. GIXRD of C11000 (top) and Nordic Gold (bottom) samples when freshly ground to 1200 grit and air oxidized at ambient lab conditions for 30 days, then exposed to concentrated synthetic perspiration solution at 23 °C and ambient aeration for various times indicated. 212

Figure 3.30. GIXRD of C11000 and Nordic Gold samples when freshly ground to 1200 grit or air oxidized at ambient lab conditions for 30 days, after exposure to concentrated synthetic perspiration solution (23 °C, ambient aeration) for 130 hours, with FCC metallic Cu, Cu_2O and CuO peaks highlighted. Spectra are shown offset ($y=150$) for ease of comparison. 213

Figure 3.31. GIXRD of C11000 and Nordic Gold samples when freshly ground to 1200 grit or air oxidized at ambient lab conditions for 30 days, after exposure to concentrated synthetic perspiration solution (23 °C, ambient aeration) for 130 hours, with FCC metallic Cu, CuCl , Cu_2Cl , and $\text{Cu}_2(\text{OH})_3\text{Cl}$ peaks highlighted. Spectra are shown offset ($y=150$) for ease of comparison. 214

Figure 3.32. Comparative GIXRD of C11000 and Nordic Gold when freshly ground to 1200 grit followed by exposure to concentrated synthetic perspiration solution (23 °C, ambient aeration) for 130 hours. Spectra are shown offset ($y=170$) for ease of comparison. 215

Figure 3.33. Comparative GIXRD of C11000 and Nordic Gold when freshly ground to 1200 grit, then air oxidized at ambient lab conditions, followed by exposure to

concentrated synthetic perspiration solution (23 °C, ambient aeration) for 130 hours. Spectra are shown offset (y=170) for ease of comparison. 216

Figure 3.34. Galvanostatic reduction of C11000 and Nordic Gold when freshly ground to 1200 grit or air oxidized at ambient lab conditions for 30 days, followed by exposure to concentrated synthetic perspiration solution (23 °C, ambient aeration) for the various times indicated. Galvanostatic reductions were conducted at 0.02 mA/cm² on an area of 0.8 cm². 220

Figure 3.35. Galvanostatic reduction of C11000 (left) and Nordic Gold (right) when freshly ground to 1200 grit followed by exposure to concentrated synthetic perspiration solution (23 °C, ambient aeration) for 0 and 130 hours. Galvanostatic reductions were conducted at 0.02 mA/cm² on an area of 0.8 cm². 221

Figure 3.36. Galvanostatic reduction of C11000 (left) and Nordic Gold (right) when freshly ground to 1200 grit, then air oxidized at ambient lab conditions for 30 days followed by exposure to concentrated synthetic perspiration solution (23 °C, ambient aeration) for 0 and 130 hours. Galvanostatic reductions were conducted at 0.02 mA/cm² on an area of 0.8 cm². 221

Figure 3.37. Galvanostatic reduction analysis to produce inflection points by taking the first derivative of C11000 and Nordic Gold when freshly ground to 1200 grit or air oxidized at ambient lab conditions for 30 days, followed by exposure to concentrated synthetic perspiration solution (23 °C, ambient aeration) for the various times indicated. Galvanostatic reductions were conducted at 0.02 mA/cm² on an area of 0.8 cm². 222

Figure 3.38. Galvanostatic reduction over laid with inflection analysis of C11000 and Nordic Gold when freshly ground to 1200 grit air oxidized at ambient lab conditions for 30 days, followed by exposure to concentrated synthetic perspiration solution (23 °C, ambient aeration) for various times. Galvanostatic reductions were conducted at 0.02 mA/cm² on an area of 0.8 cm². 223

Figure 3.39. Galvanostatic reduction with inflection points (t_i) and associated potentials (E_i) of C11000 (left) and Nordic Gold (right) when freshly ground to 1200 grit then air oxidized at ambient lab conditions for 30 days, followed by exposure to concentrated synthetic perspiration solution (23 °C, ambient aeration) for 130 hours. Galvanostatic reductions were conducted at 0.02 mA/cm² on an area of 0.8 cm². 223

Figure 3.40. Summary of galvanostatic reduction data on C11000 and Nordic Gold when freshly ground to 1200 grit or air oxidized at ambient lab conditions for 30 days, followed by exposure to concentrated synthetic perspiration solution (23 °C, ambient aeration) for various times. Galvanostatic reductions were conducted at 0.02 mA/cm² on an area of 0.8 cm². Data is the average of 3 replicates and error bars are one standard deviation. 224

Figure 3.41. Comparative galvanostatic reduction of C11000 (solid red line) and Nordic Gold (dotted blue line) when freshly ground to 1200 grit followed by exposure to

concentrated synthetic perspiration solution (23 °C, ambient aeration) for 130 hours. Galvanostatic reductions were conducted at 0.02 mA/cm² on an area of 0.8 cm². 225

Figure 3.42. Comparative galvanostatic reduction of C11000 (solid red line) and Nordic Gold (dotted blue line) when freshly ground to 1200 grit then air oxidized at ambient lab conditions for 30 days, followed by exposure to concentrated synthetic perspiration solution (23 °C, ambient aeration) for 130 hours. Galvanostatic reductions were conducted at 0.02 mA/cm² on an area of 0.8 cm². 225

Figure 3.43. Galvanostatic reduction points (t_i, E_i) of C11000 (left) and Nordic Gold (right) when freshly ground to 1200 grit or air oxidized at ambient lab conditions for 30 days, followed by exposure to concentrated synthetic perspiration solution (23 °C, ambient aeration) for 130 hours. Galvanostatic reductions were conducted at 0.02 mA/cm² on an area of 0.8 cm². Data is the average of 3 replicates and error bars are one standard deviation. 226

Figure 3.44. Galvanostatic reduction points (t_i, E_i) of C11000 and Nordic Gold when freshly ground to 1200 grit or air oxidized at ambient lab conditions for 30 days, followed by exposure to concentrated synthetic perspiration solution (23 °C, ambient aeration) for 130 hours. Galvanostatic reductions were conducted at 0.02 mA/cm² on an area of 0.8 cm². Data is the average of 3 replicates and error bars are one standard deviation. 226

Figure 3.45. Copper release of C11000 and Nordic Gold when freshly ground to 1200 grit or air oxidized at ambient lab conditions for 30 days, followed by exposure to concentrated synthetic perspiration solution (23 °C, ambient aeration) over time. Concentrated synthetic perspiration solution was exposed to 0.8 cm² of copper of the copper alloy coupon to 300 mL of solution, with a surface to volume ratio of 2.67 cm²/L. Data is the average of 3 replicates and error bars are one standard deviation. 228

Figure 3.46. Copper release from C11000 when freshly ground to 1200 grit or air oxidized at ambient lab conditions for 30 days, followed by exposure to concentrated synthetic perspiration solution (23 °C, ambient aeration) over time, expressed as ppm in solution (left) and amount Cu²⁺ in 300 mL divided by electrode area (0.8 cm²) (right) over time. Concentrated synthetic perspiration solution was exposed to 0.8 cm² of copper of the copper alloy coupon to 300 mL of solution, with a surface to volume ratio of 2.67 cm²/L. Data is the average of 3 replicates and error bars are one standard deviation. 229

Figure 3.47. Copper ion release from Nordic Gold when freshly ground to 1200 grit or air oxidized at ambient lab conditions for 30 days, followed by exposure to concentrated synthetic perspiration solution (23 °C, ambient aeration) over time, expressed as ppm in solution (left) and amount Cu²⁺ in 300 mL divided by electrode area (0.8 cm²) (right) over time. Concentrated synthetic perspiration solution was exposed to 0.8 cm² of copper of the copper alloy coupon to 300 mL of solution, with a surface to volume ratio of 2.67 cm²/L. Data is the average of 3 replicates and error bars are one standard deviation. 229

Figure 3.48. Copper release from C11000 and Nordic Gold when freshly ground to 1200 grit, followed by exposure to concentrated synthetic perspiration solution (23 °C, ambient aeration) over time expressed as ppm in solution. Concentrated synthetic perspiration solution was exposed to 0.8 cm² of the copper alloy coupon, with a surface to volume ratio of 2.67 cm²/L to 300 mL of solution, with a surface to volume ratio of 2.67 cm²/L. Data is the average of 3 replicates and error bars are one standard deviation. 230

Figure 3.49. Copper release from C11000 and Nordic Gold when freshly ground to 1200 grit and air oxidized at ambient lab conditions for 30 days, followed by exposure to concentrated synthetic perspiration solution (23 °C, ambient aeration) over time expressed as ppm in solution. Concentrated synthetic perspiration solution was exposed to 0.8 cm² of the copper alloy coupon to 300 mL of solution, with a surface to volume ratio of 2.67 cm²/L. Data is the average of 3 replicates and error bars are one standard deviation. 230

Figure 3.50. Copper ion release from C11000 and Nordic Gold when freshly ground to 1200 grit or air oxidized at ambient lab conditions for 30 days, followed by exposure to concentrated synthetic perspiration solution (23 °C, ambient aeration) over time, expressed as ppm in solution. Concentrated synthetic perspiration solution was exposed to 0.8 cm² of copper of the copper alloy coupon to 300 mL of solution, with a surface to volume ratio of 2.67 cm²/L. Data is the average of 3 replicates and error bars are one standard deviation. 231

Figure 3.51. Elemental release from Nordic Gold when freshly ground to 1200 grit or air oxidized at ambient lab conditions for 30 days, followed by exposure to concentrated synthetic perspiration solution (23 °C, ambient aeration) for various times, expressed as ppm in solution. No Al or Sn release was detected by ICP-OES from Nordic Gold. Data is the average of 3 replicates and error bars are one standard deviation. 231

Figure 3.52. Elemental release from C11000 and Nordic Gold when freshly ground to 1200 grit or air oxidized at ambient lab conditions for 30 days, followed by exposure to concentrated synthetic perspiration solution (23 °C, ambient aeration) for 130 hours, expressed as ppm in solution. No Al or Sn release was detected by ICP-OES from Nordic Gold. 232

Figure 3.53. Charge analysis of C11000 and Nordic Gold when freshly ground to 1200 grit air oxidized at ambient lab conditions for 30 days, followed by exposure to concentrated synthetic perspiration solution (23 °C, ambient aeration) over time. Exposure area of working electrode (copper alloy) for EIS was 0.8 cm². Galvanostatic reductions were conducted at 0.02 mA/cm² on an area of 0.8 cm². Concentrated synthetic perspiration solution was exposed to 0.8 cm² of copper of the copper alloy coupon, with a surface to volume ratio of 2.67 cm²/L. 234

Figure 3.54. Charge comparison of Q_{corr} calculated from EIS versus ($Q_{\text{oxide}} + Q_{\text{solution}}$) of C11000 and Nordic Gold when freshly ground to 1200 grit air oxidized at ambient lab conditions for 30 days, followed by exposure to concentrated synthetic perspiration

solution (23 °C, ambient aeration) over time. Exposure area of working electrode (copper alloy) for EIS was 0.8 cm². Galvanostatic reductions were conducted at 0.02 mA/cm² on an area of 0.8 cm². Concentrated synthetic perspiration solution was exposed to 0.8 cm² of copper of the copper alloy coupon, with a surface to volume ratio of 2.67 cm²/L. 235

Figure 3.55. Comparison of OCP (a) and cyclic polarization (b) from C11000 and Nordic Gold when freshly ground to 1200 grit followed by exposure solution (23 °C, ambient aeration). 236

Figure 3.56 Comparison of corrosion rate from C11000 and Nordic Gold when freshly ground to 1200 grit or air oxidized at ambient lab conditions for 30 days, followed by exposure solution (23 °C, ambient aeration) over time. Figure a is a complete comparison, whereas figure b compares C11000 and figure c compares Nordic Gold. Data is the average of 3 replicates and error bars are one standard deviation. 237

Figure 3.57 Comparison of galvanostatic reduction points (t_i, E_i) of C11000 and Nordic Gold when freshly ground to 1200 grit or air oxidized at ambient lab conditions for 30 days, followed by exposure to concentrated synthetic perspiration solution (23 °C, ambient aeration) for 130 hours. Galvanostatic reductions were conducted at 0.02 mA/cm² on an area of 0.8 cm². Figure a is a complete comparison, whereas figure b compares C11000 and figure c compares Nordic Gold. Data is the average of 3 replicates and error bars are one standard deviation. 238

Figure 3.58. Comparison of copper release from C11000 and Nordic Gold when freshly ground to 1200 grit or air oxidized at ambient lab conditions for 30 days, followed by exposure solution (23 °C, ambient aeration) over time, expressed as ppm in solution. Solution was exposed to 0.8 cm² of copper of the copper alloy coupon, with a surface to volume ratio of 2.67 cm²/L. Figure a is a complete comparison, whereas figure b compares C11000 and figure c compares Nordic Gold. Data is the average of 3 replicates and error bars are one standard deviation. 239

Figure 3.59. Correlation of constant copper release rates from copper alloys to time needed to achieve 1 and 10 ppm Cu²⁺ at a surface to volume ratio of 2.67 cm²/L. 243

Figure 3.60. University of Virginia disinfection studies of *E. coli* (HCB1) in solution of synthetic perspiration (0.5% NaCl, 0.1% CH₄N₂O, 0.1% C₃H₆O₃, pH 6.5) and Cu²⁺ ions from a CuCl₂ solution at 23 °C, enumerated by most probable number (MPN) method. 244

Figure 4.1. Change of oxygen reduction current with the change of the thickness of water layer indicated by the time spent to heat the iron sample.¹³⁴ 252

Figure 4.2. Schematic illustration of corrosion product layer formation during copper exposure to CO₂ at low (<1 ppm) and ambient (350 ppm) levels.¹⁵⁰ 254

Figure 4.3. Relative humidity and temperature was collected throughout drying and wetting cycles, and a sample portion is displayed here. As seen, temperature remains steady at 22 C, while RH varies depending on the cycle position. 257

Figure 4.4. Reduction order of copper oxides CuO and Cu₂O.¹²⁵ However, other papers suggest CuO reduces to Cu₂O, rather than to CuO to Cu as reported here.^{126,127} 261

Figure 4.5. Galvanostatic reduction analysis corresponds time to completely reduce a corrosion species (t_i) to inflection points on the galvanostatic reduction spectra, and reduction potential (E_i) to the plateau preceding the inflection point. 263

Figure 4.6. Comparative calibration curves of Cu in deionized water and synthetic perspiration after 130 hours (no exposure to copper alloys) at 224.7 nm. 265

Figure 4.7. Procedural flow chart of converting signal obtained by ICP-OES to copper ion release (ions/cm²). 265

Figure 4.8. Visual analysis of C11000 when freshly ground to 1200 grit, deposited with 100 μ L of synthetic perspiration solution (23 °C, ambient aeration) and exposed to 4 hour wetting-4 hour drying cycles. 269

Figure 4.9. Visual analysis of Nordic Gold when freshly ground to 1200 grit, exposed to 100 μ L of synthetic perspiration solution (23 °C, ambient aeration) and exposed to 4 hour wetting-4 hour drying cycles. 270

Figure 4.10. SEM micrographs of C11000 exposed to 100 μ L synthetic perspiration (23 °C, ambient aeration) for 12 dry-wet cycles and left uncleaned using SEI at 100x (a), 250x (b) and 1000x (c). 271

Figure 4.11. SEM micrographs of Nordic Gold exposed to 100 μ L synthetic perspiration (23 °C, ambient aeration) for 12 dry-wet cycles and left uncleaned using SEI at 100x (a), 250x (b) and 1000x (c) 272

Figure 4.12. SEM micrographs of C11000 exposed to 100 μ L synthetic perspiration (23 °C, ambient aeration) for 12 dry-wet cycles and cleaned with 6 M HCl for 3 minutes using SEI at 100x (a), 250x (b) and 1000x (c) 273

Figure 4.13. SEM micrographs of Nordic Gold exposed to 100 μ L synthetic perspiration (23 °C, ambient aeration) for 12 dry-wet cycles and cleaned with 6 M HCl for 3 minutes using SEI at 100x (a), 250x (b) and 1000x (c) 274

Figure 4.14. Reflectivity of C11000 when freshly ground to 1200 grit, deposited with 100 μ L of synthetic perspiration solution (23 °C, ambient aeration) and exposed to 4 hour wetting-4 hour drying cycles. Image a is the reflectivity of a visually blue edge, b is the reflectivity of a visually dark-black edge, and c is reflectivity of the center of the dried droplet area. 276

Figure 4.15. Reflectivity of Nordic Gold when freshly ground to 1200 grit, deposited with 100 μL of synthetic perspiration solution (23 $^{\circ}\text{C}$, ambient aeration) and exposed to 4 hour wetting-4 hour drying cycles. Image a is reflectivity of a visually blue edge, b is reflectivity of the center of the dried droplet area. 276

Figure 4.16. Visible light spectrum wavelengths with corresponding observed color.¹²⁹277

Figure 4.17. GIXRD of C11000 and Nordic Gold samples when to 1200 grit, deposited with 100 μL of synthetic perspiration solution (23 $^{\circ}\text{C}$, ambient aeration) and exposed a number of 4 hour drying-4 hour wetting cycles. 279

Figure 4.18. GIXRD of C11000 sample when to 1200 grit, deposited with 100 μL of synthetic perspiration solution (23 $^{\circ}\text{C}$, ambient aeration) and exposed to 4 hour wetting-4 hour drying cycles. Spectra highlights FCC metallic Cu, copper oxide, chloride and carbonate corrosion product peaks. 280

Figure 4.19. GIXRD of Nordic Gold sample when to 1200 grit, deposited with 100 μL of synthetic perspiration solution (23 $^{\circ}\text{C}$, ambient aeration) and exposed to 4 hour wetting-4 hour drying cycles. Spectra highlights FCC metallic Cu, copper oxide, chloride and carbonate corrosion product peaks. 281

Figure 4.20. Galvanostatic reduction of C11000 when freshly ground to 1200 grit, deposited with 100 μL of synthetic perspiration solution (23 $^{\circ}\text{C}$, ambient aeration) and exposed to 4 hour wetting-4 hour drying cycles. Galvanostatic reductions were conducted at 0.02 mA/cm^2 on an area of 0.8 cm^2 . Figure a shows the reduction waves, while figure b shows the inflection points used to determine time of complete reduction. 284

Figure 4.21. Galvanostatic reduction of Nordic Gold when freshly ground to 1200 grit, deposited with 100 μL of synthetic perspiration solution (23 $^{\circ}\text{C}$, ambient aeration) and exposed to 4 hour wetting-4 hour drying cycles. Galvanostatic reductions were conducted at 0.02 mA/cm^2 on an area of 0.8 cm^2 . Figure a shows the reduction waves, while figure b shows the inflection points used to determine time of complete reduction. 285

Figure 4.22. Galvanostatic reduction of C11000 and Nordic Gold when freshly ground to 1200 grit, followed by deposition of synthetic perspiration and expose for 1 and 9 dry-wet cycles. Galvanostatic reductions were conducted at 0.02 mA/cm^2 on an area of 0.8 cm^2 . Data is the average of 3 replicates and error bars are one standard deviation. 286

Figure 4.23. Comparative galvanostatic reduction of C11000 (solid red line) and Nordic Gold (dotted blue line) when freshly ground to 1200 grit followed by deposition of synthetic perspiration and 12 dry-wet cycles. Galvanostatic reductions were conducted at 0.02 mA/cm^2 on an area of 0.8 cm^2 . 286

Figure 4.24. Schematic representation of inner directly formed oxides and outer corrosion precipitates formed by homogeneous chemical reaction. 287

Figure 4.25. Copper release from C11000 and Nordic Gold when freshly ground to 1200 grit, deposited with 100 μL of synthetic perspiration solution (23 $^{\circ}\text{C}$, ambient aeration) and exposed to a number of 4 hour drying-4 hour wetting cycles, then washed with 10 mL of synthetic perspiration solution. Average area of droplet size is assumed to be 0.8 cm^2 . Data is the average of 3 replicates and error bars are one standard deviation. 288

Figure 4.26. Elemental release from Nordic Gold when freshly ground to 1200 grit, deposited with 100 μL of synthetic perspiration solution (23 $^{\circ}\text{C}$, ambient aeration) and exposed to a number of 4 hour drying-4 hour wetting cycles, then washed with 10 mL of synthetic perspiration solution. Average area of droplet size is assumed to be 0.8 cm^2 . Data is the average of 3 replicates and error bars are one standard deviation. 289

Figure 4.27. Charge analysis of C11000 and Nordic Gold when freshly ground to 1200 grit followed by deposition of 100 μL of synthetic perspiration solution (23 $^{\circ}\text{C}$, ambient aeration) and exposed to 12 dry-wet cycles. Galvanostatic reductions were conducted at 0.02 mA/cm^2 on an area of 0.8 cm^2 . Solution analysis was conducted on 10 mL of synthetic perspiration wash solution utilized to gather thin electrolyte layer <5 minutes before the end of the final dry cycle, with an average droplet area to be 0.8 cm^2 . Incongruent dissolution was determined by ICP-OES and factored into Q_{corr} calculations for Nordic Gold. Corrosion products are likely a mixture of Cu^+ and Cu^{2+} , and precipitate copper chloride products are likely not analyzed by galvanostatic reduction. Data is the average of 3 replicates and error bars are one standard deviation. 291

Figure 4.28. Charge analysis of C11000 and Nordic Gold when freshly ground to 1200 grit followed by deposition of 100 μL of synthetic perspiration solution (23 $^{\circ}\text{C}$, ambient aeration) and exposed to 12 dry-wet cycles. Galvanostatic reductions were conducted at 0.02 mA/cm^2 on an area of 0.8 cm^2 . Solution analysis was conducted on 10 mL of synthetic perspiration wash solution utilized to gather thin electrolyte layer <5 minutes before the end of the final dry cycle, with an average droplet area to be 0.8 cm^2 . Summation of Q_{solution} and Q_{oxide} were calculated from the average Q_{solution} and Q_{oxide} values. Incongruent dissolution was determined by ICP-OES and factored into Q_{corr} calculations for Nordic Gold. Corrosion products are likely a mixture of Cu^+ and Cu^{2+} , and precipitate copper chloride products are likely not analyzed by galvanostatic reduction. Data is the average of 3 replicates and error bars are one standard deviation. 292

Figure 4.29. University of Virginia disinfection studies of *E. coli* (HCB1) in solution of synthetic perspiration (0.5% NaCl , 0.1% $\text{CH}_4\text{N}_2\text{O}$, 0.1% $\text{C}_3\text{H}_6\text{O}_3$, pH 6.5) and Cu^{2+} ions from a CuCl_2 solution at 23 $^{\circ}\text{C}$, enumerated by most probable number (MPN) method. 295

Figure 4.30. A comparison of C11000 and Nordic Gold corrosion behavior exposed to different testing environments, when freshly ground to 1200 grit. Drying-wetting testing was conducted by the deposition of 100 L of synthetic perspiration, approximate area of 0.8 cm^2 . Full immersion testing was conducted by the exposure of 300 mL solution to a 0.8 cm^2 area of alloy. Mass loss and Q_{corr} are normalized by the number of hours testing

occurred over (130 hours for full immersion testing, 96 hours for drying-wetting testing). In the case of concentrated perspiration full immersion and synthetic perspiration drying-wetting testing, incongruent dissolution was determined by ICP-OES and factored into Q_{corr} calculations. Data is the average of 3 replicates and error bars are one standard deviation. 297

Figure 4.31. A comparison of C11000 and Nordic Gold corrosion behavior exposed to different testing environments, when freshly ground to 1200 grit. Drying-wetting testing was conducted by the deposition of 100 L of synthetic perspiration, approximate area of 0.8 cm^2 . Full immersion testing was conducted by the exposure of 300 mL solution to a 0.8 cm^2 area of alloy. Galvanostatic reduction waves were compared at 96 hours of exposure for full immersion testing, and 12 dry-wet cycles (96 total hours) for drying-wetting testing. 298

Figure 4.32. Copper release from C11000 (left) and Nordic Gold (right) when freshly ground to 1200 grit. Drying-wetting testing was conducted by the deposition of 100 μL of synthetic perspiration, approximate area of 0.8 cm^2 , and washing of the thin electrolyte layer with 10 mL of synthetic perspiration for ICP-OES analysis. Full immersion testing was conducted by the exposure of 300 mL solution to a 0.8 cm^2 area of alloy, and an aliquot of exposure solution was collected for ICP-OES analysis. Data is the average of 3 replicates and error bars are one standard deviation. 300

List of Tables

Table 1.1. Various growth mediums for the culture of <i>Staphylococcus aureus</i> demonstrate the wide variety of compositions utilized (see Appendix A).....	41
Table 1.2. Composition of alloys discussed in this literature review for antimicrobial efficacy in wt%.	46
Table 1.3. Hypothetical solubility products of copper compounds found experimentally assuming precipitation process occurred by homogeneous chemical reaction ⁶⁰	53
Table 1.4. Half-cell reactions of possible products formed in high chloride solution.....	59
Table 1.5. Composition of synthetic solutions used in previous sweat exposure studies.	66
Table 1.6. UNS designations and composition of wrought copper alloys. ⁹⁴	68
Table 1.7. Approximate cost of copper alloying elements. ⁹⁵	68
Table 1.8. Composition by weight percent of copper alloys tested by the University of Virginia.....	73
Table 2.1. Composition of synthetic perspiration solutions used in previous exposure studies	94
Table 2.2. Composition of synthetic perspiration solution in g/L and M.	96
Table 2.3. Calculation of equivalent weight of Nordic Gold using either Cu ⁺ or Cu ²⁺ ...	101
Table 2.4. Comparison of galvanostatic reduction methods utilized in ASTM standard, Nakayama's previous study and previously used in house method.....	103
Table 2.5. Possible corrosion products reduced by galvanostatic reduction at potentials below associated half-cell potentials. Assumptions were that [Cl ⁻] is 10 ⁻⁸ M, [H ⁺] is 3.98 x 10 ⁻⁹ M, and [OH ⁻] is 2.51 x 10 ⁻⁶ M for pH 8.4.....	105
Table 2.6. Solubility limits of copper corrosion products in 300 mL synthetic perspiration. Concentrations were assumed as [Cl ⁻] = 8.6 x 10 ⁻² M, [H ⁺] = 3.2 x 10 ⁻⁷ M, [OH ⁻] = 3.2 x 10 ⁻⁸ M.	108
Table 2.7. Charge analysis by EIS for C11000 and Nordic Gold when freshly ground to 1200 grit, furnace oxidized at 170 °C for 60 minutes, or air oxidized at ambient lab conditions for 30 days, then exposed to synthetic perspiration solution (23 °C, ambient aeration) for 130 hours. Q _{corr} /area by EIS were calculated as seen in Equations 2.5-2.8, where B= 0.057 V. ¹²³ Data is the average of a minimum of 3 replicates with standard deviation.....	114

Table 2.8. Charge (Q_{corr}) analysis based on mass loss after 130 hours exposure of 0.8 cm ² copper alloy to synthetic perspiration (23 °C, ambient aeration).	122
Table 2.9. Analysis of constant copper release rates to determine lengths of time needed to achieve antimicrobial copper concentration.	161
Table 3.1. Composition of synthetic perspiration solutions used in previous exposure studies.	166
Table 3.2. Composition of synthetic perspiration solutions based on human hand perspiration deposited on a metal surface, allowed to dry, and rewet at 93% RH.	174
Table 3.3. Calculation of equivalent weight of Nordic Gold using either Cu ⁺ or Cu ²⁺ . In each E.W. reported, all elements were considered to dissolve congruently or proportional to their mass fraction reported. Additionally, a case of incongruent dissolution is assumed, with 92.1 wt% Cu and 7.9 wt% Zn. The difference arises from Cu ⁺ vs. Cu ²⁺ assumption.	180
Table 3.4. Comparison of galvanostatic reduction methods utilized in ASTM standard, Nakayama's previous study and previously used in house method.....	183
Table 3.5. Possible corrosion products reduced by galvanostatic reduction at potentials below associated half-cell potentials. Assumptions were that [Cl ⁻] is 10 ⁻⁸ M, [H ⁺] is 3.98 x 10 ⁻⁹ M, and [OH ⁻] is 2.51 x 10 ⁻⁶ M for pH 8.4.....	184
Table 3.6. Solubility limit of copper corrosion products in 300 mL concentrated synthetic perspiration. Concentrations were assumed as [Cl ⁻] = 2 M, [H ⁺] = .005 M, [OH ⁻] = 1.9 x 10 ⁻¹² M.....	187
Table 3.7. Charge analysis by EIS for C11000 and Nordic Gold when freshly ground to 1200 grit or air oxidized at ambient lab conditions for 30 days, then exposed to concentrated synthetic perspiration solution (23 °C, ambient aeration) for 130 hours. $Q_{\text{corr}}/\text{area}$ by EIS were calculated as seen in Equations 3.12-3.14, where $B = 0.057 \text{ V}$. ¹²³ Data is the average of a minimum of 3 replicates with one standard deviation.	193
Table 3.8. Charge (Q_{corr}) analysis based on mass loss of 3 specimens with standard deviation after 130 hours exposure of 0.8 cm ² copper alloy freshly ground to 1200 grit to concentrated synthetic perspiration (23 °C, ambient aeration).	201
Table 3.9. Analysis of constant copper release rates to determine lengths of time needed to achieve antimicrobial copper concentration.	244
Table 4.1. Composition of synthetic perspiration solutions used in previous exposure studies	250
Table 4.2. Composition of synthetic perspiration solution in g/L and M.....	256

- Table 4.3. Calculation of equivalent weight of Nordic Gold using either Cu^+ or Cu^{2+} . In each E.W. reported, all elements were considered to dissolve congruently or proportional to their mass fraction reported. Additionally, a case of incongruent dissolution is assumed, with 94.7 wt% Cu and 5.3 wt% Zn. The difference arises from Cu^+ vs. Cu^{2+} assumption. 258
- Table 4.4. Comparison of galvanostatic reduction methods utilized in ASTM standard, Nakayama's previous study and previously used in house method..... 261
- Table 4.5. Possible corrosion products reduced by galvanostatic reduction at potentials below associated half-cell potentials. Assumptions were that $[\text{Cl}^-]$ is 10^{-8} M, $[\text{H}^+]$ is 3.98×10^{-9} M, and $[\text{OH}^-]$ is 2.51×10^{-6} M for pH 8.4..... 263
- Table 4.6. Charge (Q_{corr}) analysis based on mass loss of 3 specimens with standard deviation after exposure to 100 μL synthetic perspiration (droplet area= 0.8 cm^2) and 12 dry-wet cycles on copper alloy freshly ground to 1200 grit (23 °C, ambient aeration). 267
- Table 4.7. Solubility limits of copper corrosion products in 100 μL droplet of synthetic perspiration. $[\text{Cl}^-]$ is 8.6×10^{-2} M, $[\text{H}^+]$ is 3.2×10^{-7} M, and $[\text{OH}^-]$ is 3.2×10^{-8} M..... 290

1 Introduction

1.1 The Importance of Identifying Color Stable Antimicrobial Alloys

1.1.1 Hospital Acquired Infections

Hospital acquired infections (HAIs) have become a prevalent risk associated with our centers of health.⁴ Such environments are the breeding ground for “superbugs”, bacteria that has become resistant to existing drugs.⁵ Methicillin-resistant *Staphylococcus aureus* (MRSA) was reported at only 2% in the United Kingdom in 1990, and rose to over 40% in the early 2000s.⁶ In 2005, 94,650 American contracted MRSA, of which 18,650 died, exceeding deaths from AIDS.¹ MRSA is nearly always acquired in hospitals, and is spread by hand-to-surface contact, and often contracted in hospitals by patients with already weakened immune systems.⁷ High touch surfaces such as bed rails, IV stands and door push plates are currently constructed of stainless steel, which offers no antimicrobial benefits.⁸ The number of individuals coming in contact with these surfaces means that bacteria can be easily spread throughout a hospital ward due to the migration of staff, patients, and guests. The Center for Disease Control and Prevention’s National and State Healthcare-associated Infections Standardized Infection Ratio Reports for 2010 and 2011 show an overall increase in the number of HAI’s, despite increased awareness.⁹

1.1.2 Mitigating Approaches

One approach to mitigating MRSA epidemics is selective screening of patients at the time of admission, allowing the affected individuals to be isolated and treated to prevent disease transfer to other patients, known as the “search and destroy” method.¹⁰ This approach has been very successful in other countries, such as the Netherlands.

However, MRSA prevalence among *Staphylococcus aureus* (*S. aureus*) is only 1% in the Netherlands compared to 50% in the United States, primarily attributed to stringent antibiotic use elsewhere.¹⁰ While this method has been highly effective in countries with low MRSA prevalence, its success in settings with high MRSA prevalence remains controversial.¹¹ In studies conducted in hospital settings with higher MRSA prevalence such as the United Kingdom, this approach was unsuccessful due to inadequate isolation facilities and need to maximize bed usage.¹² Additional concerns regard the application of such an intensive method in large hospitals, where the entire patient population cannot be screened upon entry, and patient selection processes have not been well defined.¹³ While screening methods will likely identify a number of MRSA contaminated patients, it is impossible to detect all on a large-scale operation.

A second approach involves mitigating the hospital environment, either through improved cleaning methods or the development of materials that are antimicrobial in nature. While hospitals have attempted to improve their cleaning methods, research has shown the presence of MRSA to subsist even directly after a standard room cleaning.¹⁴ An example of terminal cleaning procedure following discharge of an infectious patient involves the cleaning of surfaces with a solution of detergent sanitizer (GWP 4L, containing 5-15% non-ionic surfactant and 5-15% cationic surfactant, diluted 1:500) (GWP Group, Elland, W. Yorkshire, UK) followed by drying with a disposable cloth.⁵ Additionally, bed curtains and linens are laundered, all horizontal surfaces are damp dusted, walls are damp-mopped, and floors are dust mopped using disposable mop heads with detergent sanitizer.⁵ While terminal cleaning between patients are very thorough and time intensive, additional daily cleaning aim to prevent biofilm development caused by

transferred contaminants by cleaning high touch surfaces, dusting all horizontal surfaces above shoulder level, and dust mopping floors with sanitizer.¹⁵ Utilization of alternative cleaning methods such as hydrogen peroxide vapor decontamination have proven highly effective at eliminating MRSA, but is limited to smaller, vacated areas.⁵ Separate studies provide definitive evidence that MRSA was contracted by a patient while in hospital care, despite pre-screening and adherence to hand hygiene and contact precautions.¹⁶

Significant research has explored replacing high touch surfaces (i.e. bed rail, IV stand, door handle, computer mouse) with materials with intrinsic antimicrobial properties.¹⁷ Stainless steel, which is commonly used for these high touch surfaces is easily cleaned, but has no intrinsic antimicrobial properties, and as discussed earlier, daily or terminal cleaning is not sufficient to prevent nosocomial MRSA.¹⁸ A clinical case study at Selly Oak Hospital, Birmingham by the Copper Development Association, NYC, determined that by replacing plastic and stainless steel surfaces with “copperized” items, bacterial “load” expressed as colony forming unit (cfu)/cm² was reduced by 90% compared to non-copper surfaces.¹⁷ Unfortunately, pure copper’s propensity to tarnish rapidly leads to the appearance of a dirty or brown discolored hospital environment, and the apparent level of cleanliness is important for patient confidence, even if strictly cosmetic.¹⁹ While pure copper’s high tarnishing rate and low corrosion resistances makes it unsuitable for the healthcare environment due to aesthetics, copper alloys containing greater than 70 wt% copper display antimicrobial properties in addition to providing corrosion resistance¹⁸. In fact, strategically selected surfaces can reduce 90% of bacterial load.² While regular cleaning methods are not sufficient to prevent the spread of nosocomial MRSA, the utilization of copper alloys in combination with cleaning methods

would significantly reduce bacterial load on high touch surfaces where they can otherwise be transferred between patients.

1.2 A Brief Review of Antimicrobial Copper Alloys

1.2.1 EPA-Approved Alloy Systems

As of November 2011, 479 copper alloys have been designated by the Environmental Protection Agency (EPA) as antimicrobial materials.²⁰ This indicates that when regularly cleaned (daily cleaning and terminal cleaning between patients), a copper alloy will demonstrate antibacterial activity against *Staphylococcus aureus*, *Escherichia coli* O157:H7, *Pseudomonas aeruginosa*, *Enterobacter aerogenes*, Vancomycin-resistant *Enterococcus faecalis* (VRE), and methicillin-resistant *Staphylococcus aureus* (MRSA), by the following.²¹

1. Continuously reduce bacterialⁱcontaminationⁱⁱ, achieving 99.9% reduction of bacteria from initial level within two hours of exposure.
2. Kill greater than 99.9% of Gram-negativeⁱⁱⁱ and Gram-positive^{iv} bacteria within two hours of exposure.
3. Deliver continuous and ongoing antibacterial action, remaining effective in killing 99.9% bacteria within two hours.
4. Kill greater than 99.9% of bacteria within two hours and continue to kill 99% of bacteria even after repeated re-contamination.

ⁱ*Staphylococcus aureus*, *Escherichiacoli* O157:H7, *Pseudomonasaeruginosa*, *Enterobacteraerogenes*, Vancomycin-resistant *Enterococcusfaecalis* (VRE), or methicillin-resistant *Staphylococcus aureus* (MRSA)

ⁱⁱ Contamination is defined by the Environmental Protection Agency as the introduction of harmful or hazardous matter into the environment.

ⁱⁱⁱ Gram-negative bacteria are characterized by a thin peptidoglycan layer²²

^{iv} Gram-positive bacteria are characterized by a, a thick peptidoglycan layer²²

5. Help inhibit the buildup and growth of bacteria within two hours of exposure between routine cleaning and sanitizing steps. Routine cleaning is termed as daily cleaning while patients are occupying rooms, and terminal cleaning when preparing a room for new patients.

These criteria pertain to the use of exposing copper to bacteria and recording bacteria load in the number of CFUs remaining on the surface following a given time. Reduced CFUs indicate efficacy, but no data regarding Cu ion release.

1.2.2 Antimicrobial Mechanisms

The use of copper for medical purposes has been well known since ancient Egypt, where the Smith Papyrus describes the use of copper for wound and water sterilization.²³ Later civilizations, such as the Greeks, Romans and Aztecs utilized copper to treat various skin infections, burns, intestinal worms, and headaches.²⁴ In the 19th century, it was noted that copper workers appeared immune to cholera during the 1832 outbreak in Paris, France.²³ From the late 19th to early 20th century, inorganic copper preparations became a common medical treatment for ailments such as lupus, eczema, tubercular infections, anemia, syphilis and chorea.²³ While it has continued to be utilized for a variety of medical applications, the exact mechanism by which metallic copper kills microorganisms is disputed. It is known that higher copper content in alloys²⁵, higher temperature²⁶ and higher relative humidity¹ all contribute to an increased efficacy of bacterial death due to contact with a copper surface (contact killing). These tendencies all point to a role of corrosion in copper release as they are all factors which promote corrosion. Many studies support the role of free copper ions in the contact killing, though the exact mechanism by which copper surfaces are capable of killing bacteria is still

unclear. One possible cause is the production of reactive oxygen species (ROS) such as hydroxyl radicals (OH^\bullet) and superoxide due to redox cycling between different copper species.²⁴

1. $\text{H}_2\text{O}_2 + \text{O}_2^- \rightarrow \text{O}_2 + \text{OH}^- + \text{OH}^\bullet$
2. $\text{Cu(II)} + \text{O}_2^- \rightarrow \text{Cu(I)} + \text{O}_2$
3. $\text{Cu(I)} + \text{H}_2\text{O}_2 \rightarrow \text{Cu(II)} + \text{O}_2 + \text{OH}^- + \text{OH}^\bullet$

Another hypothesis is the rapid accumulation of copper ions into the cells, which leads to structural damage and permeability of the cell membrane, resulting in the release of low-molecular weight substances from the cytosolic compartment.^{25,26} It is unknown whether it is cupric (Cu^{2+}) or cuprous (Cu^+) ions that mediate this effect, as both have been reported in separate studies.^{27,28} The final hypothesis proposes that cell death is primarily due to DNA degradation. Cu(II) ions bind to DNA bases in mammalian cells, causing the double helix to unwind.²⁹ ROS then cause double and single-strand breaks, as well as intrastrand cross-linking, which leads to replication arrest and cell death if not repaired.³⁰ Cell death could be attributed to one or a combination of the methods listed above.

1.2.3 Alternative Antimicrobial Metallic Materials

In 1893, Karl Wilhelm von Nageli determined a number of metallic ions to exhibit toxic behavior on living cells. Among these are silver, copper and zinc.³¹ The antimicrobial effect of their ions (Ag^+ , Cu^{2+} , Zn^{2+}) have been widely studied in the scientific community.³²⁻³⁵ Significant research has explored use of elementary silver, silver oxides and silver nanoparticles in medical devices as well as water treatment.³⁶⁻⁴¹ Comparative studies between copper and silver nanofilms reveal better antimicrobial

efficacy for copper nanofilms, and more variability in bacterial response between strains on silver nanofilms.⁴² A comparative study on the effectiveness of copper and silver nanoparticles conclude a concentration of 70 µg/mL of silver nanoparticles and 60 µg/mL of copper nanoparticles were necessary for complete inhibition of *E. coli* and *Bacillus subtilis*(*B. subtilis*).⁴³ Additional studies utilizing silver and copper nanoparticles as antimicrobial agents against *E. coli*, *B. subtilis*, and *S. aureus* support copper's greater antibacterial affect over silver against *B. subtilis*, attributed to a greater affinity to surface active groups such as the abundance of amines and carboxyl groups on the cell surface compared to *E. coli* and *S. aureus*.⁴⁴ Zinc oxide nanoparticles have also been studied for their antimicrobial efficacy, but have been found to require a 100x minimum inhibitory concentration compared to silver nanoparticles (i.e. 500 µg/mL compared to 4.86 µg/mL) in order to affect *Streptococcus mutans*.⁴⁵ Zinc complexes also formed smaller inhibition zones compared to copper complexes against *E. coli*, *B. subtilis* and *C. albicans*.⁴⁶ The concentration of metal ions required to inhibit bacterial growth or provide bactericidal behavior is a complex mixture of multiple factors, including test organism and test solution. The large variety of bacteria includes metal ion sensitize and tolerant species, as well as chemical composition and structure of individual species⁴⁷, as discussed in the different behavior between *E. coli*, *B. subtilis* and *S. aureus* to copper nanoparticles.⁴⁴ Testing solutions result in variation of cell survivability, as well as free metal ion availability due to binding to growth media.⁴⁷ The addition of yeast extract and cysteine were attributed to the reduced toxic effect of copper on *Aerobacter aerogenes* due to the compounds binding to copper.⁴⁸ Therefore, free metal ions must be available for antimicrobial behavior to occur.

1.3 Antimicrobial Efficiency Testing

1.3.1 EPA Testing Procedures

Three EPA antimicrobial test methods have been published to ensure proper categorizing regarding antimicrobial efficacy and registration of antimicrobial copper alloys.⁴⁹⁻⁵¹ Label claims define what manufacturer can claim the antimicrobial benefits of a product are to the general public. Registration as an antimicrobial copper alloy requires every test to be successful, as specified in the following sections. Each test is conducted utilizing a copper alloy test surface and a stainless steel control, cleaned with alcohol and rinsed with deionized water then allowed to air dry. Test organisms were prepared by inoculation of appropriate broth with organism and incubation for 24±2 hours at 35-37 °C. Inoculation of all surfaces occurs by the deposition of bacteria culture suspended in 10 mL of undefined nutrient broth medium, measuring 10⁷ colony forming units (CFU) per coupon.² Bacteria is enumerated by standard spread plate technique on tryptic soy agar (TSA) plates (5% sheep blood agar plates), and visually enumerated on plates by stain or biochemical assay.⁴⁹⁻⁵¹ Broth medium varies by test organism, and many tests broths can be appropriate for a single test organism, though they vary in chemical composition and amount of dissolved solids. This is potentially significant in that it could affect corrosion rates. Table 1.1 shows the compositions of several common broth mediums for the culture of *Staphylococcus aureus*.^{50,52} No designated broth mediums can be found for EPA antimicrobial copper testing procedures, where test methods indicate only “appropriate broth” to be used, without defining appropriate. The lack of specific test broth results in varying amounts of dissolved solids, dissolved oxygen, pH, and

fraction of metal ion binding to proteins, all of which can affect antimicrobial behavior.⁴⁹⁻

51

Table 1.1. Various growth mediums for the culture of <i>Staphylococcus aureus</i> demonstrate the wide variety of compositions utilized (see Appendix A).		
Media	Dissolved Solids (g/L)	pH
Baird-Parker Medium	60	7.0 (± 0.2)
Tryptic Soy Agar	40	7.0 (± 0.2)
Brain Heart Infusion Broth	37	7.4 (± 0.2)
Mannitol Salt Agar	111	7.4 (± 0.2)
Tryptic Soy Broth	30	7.3 (± 0.2)
Vogel and Johnson Agar	60	7.2 (± 0.2)

1.3.1.1 Efficacy of Copper Alloy Surfaces as Sanitizers

The test method for efficacy of copper alloy surface as a sanitizer requires the deposition of a fixed amount of test organism on a sterilized copper alloy surface (carrier) for 120 minutes, followed by washing of the carrier with neutralizer solution.⁴⁹ A standard spread plate technique is utilized to observe the number of colonies formed after incubation.⁵³ A 99.9% reduction of test organisms must be met after 120 minutes at 25 °C. In order to submit claims for residual self-sanitizing activity or continuous reduction capability, sanitizing efficacy testing must be conducted utilizing *Staphylococcus aureus* and *Enterobacter aerogenes*.⁴⁹ If successful, the following claim is made.

Label Claims: This surface kills greater than 99.9% of bacteria within two hours.

1.3.1.2 Residual Self-Sanitizing Activity of Copper Alloy Surfaces

The test method for residual self-sanitizing activity of copper alloy surfaces requires the simulated “wearing” of a sanitized copper alloy surface during both wet and dry conditions, followed by inoculations of the surface with a “sanitizer” organism suspension after each wear cycle, defined as one pass of an abrasion tester to the left and

return pass to the right (Figure 1.1).⁵⁰ For wet cycles, the setup includes a dry cotton cloth sprayed with sterile deionized water from a Preval sprayer from a distance of 75 ± 1 cm for no more than 1 second.⁵⁰ Wearing occurs due to the abrasive nature of skin during regular handling, or by cleaning clothes during cleaning.¹⁵ A total of 12 wearing cycles are conducted, alternating wet and dry cycles over a 24 hour period at standard laboratory temperature and relative humidity. For wet cycles, abrasion clothes are sprayed with deionized water.⁵⁰ Following 24 hours, a final inoculation with the “sanitizer” organism is dried on the surface and exposed at ambient temperature for 120 minutes before removal using a neutralizer solution. A standard spread plate technique is utilized to observe the number of colonies formed after incubation. The surface must reduce the total number of organisms by a minimum of 99.9% within the 24 hour period. If successful, the following claim is made.

Label Claims: This surface kills greater than 99.9% of bacteria for 24 hours.

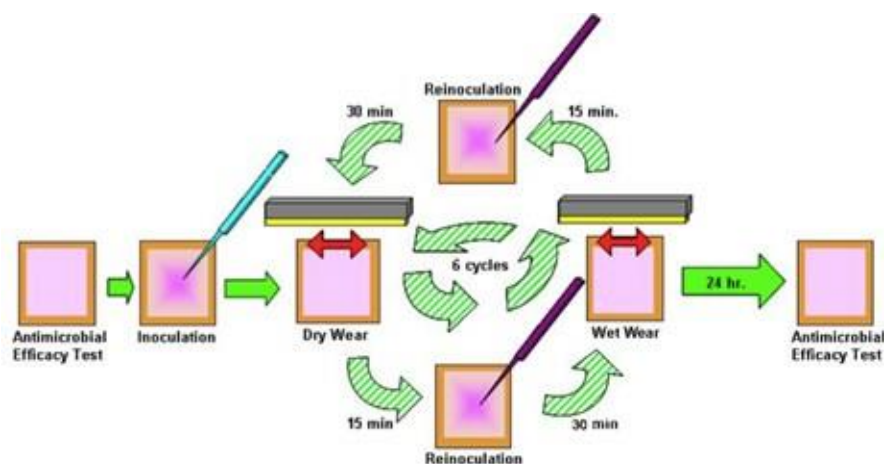


Figure 1.1. Residual self-sanitizing test protocol schematic.⁵⁴

1.3.1.3 Continuous Reduction of Bacterial Contamination on Copper Alloy Surfaces

The test method for continuous reduction of bacterial contamination on copper alloy surfaces requires the initial inoculation of a five sanitized copper alloy coupons (Time= 0 hours), followed by the re-inoculation of the surface at 3, 6, 9, 12, 15, 18, and 21 hours.⁵¹ One copper alloy coupon is removed at 2, 6, 12, 18, and 24 hours, corresponding to 1, 2, 4, 6, and 8 inoculations of bacteria. Coupons are washed with a neutralizer solution, and the standard spread plate technique utilized to observe the number of colonies formed after incubation. The surface must reduce the number of organisms on the surface by 90% compared to the stainless steel control over the 24 hour inoculation/exposure period.

Label Claims:

1. This surface continuously reduces bacterial contamination
2. This surface provides continuous/ongoing/persistent antimicrobial action even with repeated exposures.
3. This surface continuously kills over 90% of bacteria after repeated exposures during a day.
4. This surface prevents the buildup of disease-causing bacteria
5. This surface delivers continuous, long-lasting antibacterial activity.

1.3.2 Copper Development Association Antimicrobial Copper Results

The Copper Development Association (CDA) has conducted numerous studies comparing the effectiveness of stainless steel to copper alloys as antimicrobial touch surfaces at various conditions.^{1,55,56} Composition of the alloys tested for antimicrobial efficacy can be found in (Table 1.2). A study conducted to compare the relative

effectiveness of copper (C19700), brass (C24000) and stainless steel (S320400) at ambient room temperature (22 °C) on MRSA bacterial contamination demonstrated a significant reduction of bacteria on both copper and brass surfaces with no reduction on stainless steel (Figure 1.2).⁵⁵ The CDA has successfully identified a variety of factors that affect the necessary kill time on a copper surface. Most critically, antimicrobial behavior is strongly dependent on alloy composition. In general, reduction in the copper content of an alloy reduces the antimicrobial behavior (Figure 1.3).⁵⁶ This is not always the case, however, as secondary and ternary alloying elements can either promote or inhibit copper ion release necessary for antimicrobial behavior, which will be discussed more in detail.

The condition of the copper surface also plays a key role in antimicrobial behavior. On identical copper alloys, a tarnished surface resulting from a year of outdoor exposure in suburban New York City is “more antimicrobial” than when the tarnish film was removed with an abrasive cloth to restore a bright condition for high copper content alloys (Figure 1.4).⁵⁷ This effect is diminished as copper content decreases. As expected, larger inoculation size, leading to higher concentration of bacteria load, requires longer times for complete kill of bacteria.⁵⁵ Lower temperatures also depress antimicrobial response, as seen in a study on the viability of *E. coli* on C11000 surfaces at 4° compared to 20 °C.⁵⁷ However, relative humidity has demonstrated no effect on antimicrobial efficacy on copper alloys, where conducted at 20, 24 and 90% RH result in a log reduction of >5.5-6.4 on all alloys, meaning 500,000 – 4,000,000 microorganisms can be reduced to 1 organism within the test period.¹ However, these tests do not quantify copper ion release rates or corrosion rate as they relate to antimicrobial efficacy, and rely only on log reduction of microorganism studies. By only evaluating bacterial

survivability, critical information regarding the behavior of the metal is overlooked.

Evaluating corrosion rate and copper ion release of alloys as they relate to antimicrobial efficacy is a valuable avenue of investigation that could screen copper alloys prior to antimicrobial testing to determine their potential benefit as an antimicrobial material.

Table 1.2. Composition of alloys discussed in this literature review for antimicrobial efficacy in wt%.

Alloy	Cu	O	Pb	Sn	Zn	Fe	P	Ni	Co	Mg	Mn	Al	Si	C	S	N	Cr
C10200	100	0.001															
C11000	99.99	0.01															
C19700	97.6		0.05	0.20	0.20	1.20	0.40	0.05	0.05	0.20	0.05						
C22000	91.00		0.05		8.90	0.05											
C24000	81.50		0.05		18.4	0.05											
C63800	92.90		0.05		.8	0.20		0.20	0.55	0.10	2.10	3.10					
C65000	91.95		0.05		1.5	0.80		0.60			1.30		3.80				
C70600	85.15		0.05		1	1.80		11.00			1.00						
C75200	66.50		0.05		13.64	0.26		19.5			0.05						
C77000	56.60		0.05		23.1	0.25		19.50			0.50						
S30400						66.5		10.5			2.0		0.8	0.0	0.0	0.1	20.00

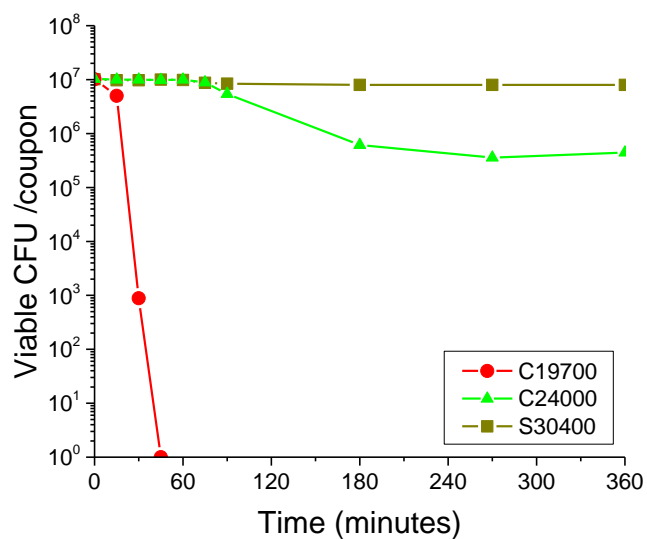


Figure 1.2. Viability of methicillin-resistant *staphylococcus aureus* (NTC10442) (MRSA) at 22 °C on copper (C19700, 97.6% Cu), brass (C24000, 81.5% Cu) or stainless steel (S30400) over 360 minutes tested in tryptone soy broth.⁵⁵

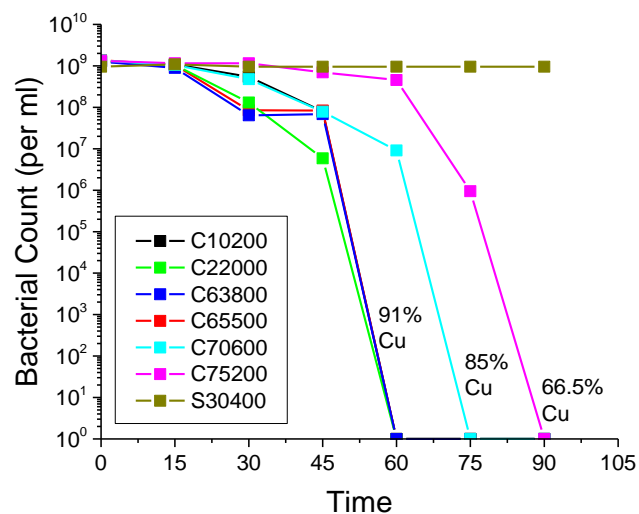


Figure 1.3. Viability of *L. monocytogenes* at 20 °C on various copper alloy surfaces, where antimicrobial efficiency follows copper content in Brain Heart Infusion Broth.⁵⁷

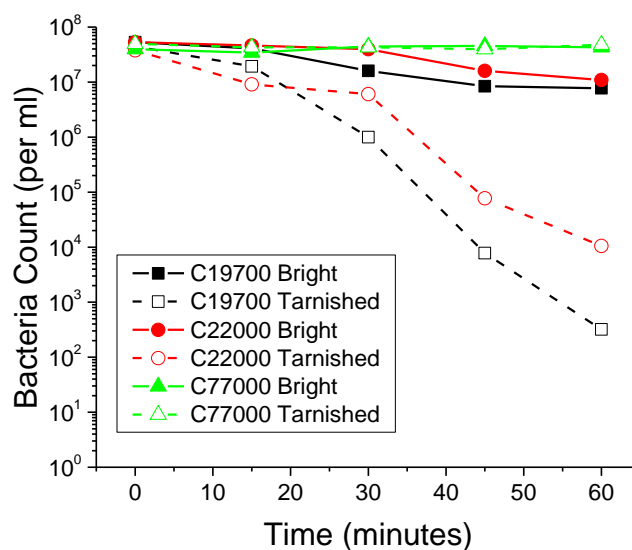


Figure 1.4. The effects of tarnishing on *E. coli* 20 °C viability on various copper alloy surfaces in tryptone soy broth.⁵⁷

1.3.3 In House Disinfection Studies

In house studies of disinfection “kill curves” were performed at the University of Virginia to observe the relative effectiveness of copper ions (Cu^{2+}) at varying concentrations on killing *E. coli* (HCB1) in synthetic perspiration (0.5% NaCl, 0.1% $\text{CH}_4\text{N}_2\text{O}$, 0.1% $\text{C}_3\text{H}_6\text{O}_3$, adjusted to pH 6.5 using NH_4OH), and enumerated by the most probable number (MPN) method. *E. coli* (HCB1) was obtained from Howard C. Berg at Harvard University. Batch disinfection experiments were conducted by introducing approximately 1.25×10^6 MPN of *E. coli* to a solution of 250 mL synthetic perspiration and CuCl_2 to achieve 0, 0.1, 1, 10, or 100 ppm Cu^{2+} solutions. Solutions were stirred at room temperature. At fixed intervals, 1 mL of solution was removed from the batch and mixed with 1 mL of phosphate buffered saline (PBS) in order to precipitate the Cu^{2+} and prevent bacteria death during incubation due to extended contact with Cu^{2+} beyond the

period specified. An aliquot of 0.2 mL of PBS/batch solution was diluted in 100 mL of autoclaved, deionized water and Colilert® (Idexx). Solutions were sealed in Quanti-Trays® (Idexx) and incubated for 24 hours at 35° C. Following incubation, Quanti-Tray® wells appear yellow if positive for total coliforms^v, and fluorescent under ultraviolet light if positive for *E. coli*. positive wells are counted and compared to Quanti-Tray® MPN table to determine the most probable number (MPN) of total *E. coli*.

These in house disinfection studies established the viability of microorganisms in synthetic perspiration for extended periods of time, as well as a investigation of the effect of Cu²⁺ concentration on *E. coli* cell viability. *E. coli* survived in excess of 3 days in synthetic perspiration containing no added nutrients or metal ions. Copper ions were effective at killing *E. coli* at rates greater than the natural die-off in synthetic perspiration solution at concentrations above 0.1 ppm (Figure 1.5). At greater Cu concentrations, a faster rate of bacterial decay is observed. This study supports the notion that a critical concentration of copper ions is necessary in solution for antimicrobial efficacy, and the use of synthetic perspiration as a possible test medium for microorganism viability studies in the future. Of significant interest is the rate of release of Cu ions from copper alloys given these benchmarks.

^v Coliforms are defined as rod-shaped Gram-negative non-spore forming bacteria, and are common bacterial indicators for sanitary quality in food and water.

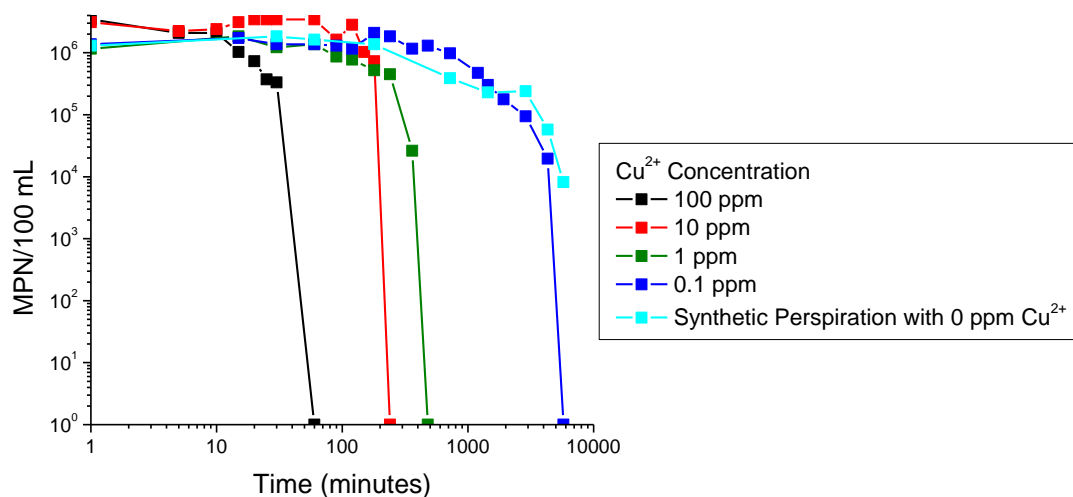


Figure 1.5. In house disinfection studies of *E. coli* (HCB1) in solution so synthetic perspiration (0.5% NaCl, 0.1% CH₄N₂O, 0.1% C₃H₆O₃) and Cu²⁺ ions from a CuCl₂ solution at 23 °C, enumerated by most probable number method.

1.4 The Need to Understand the Fate of Oxidized Copper in Copper and Copper Alloys

The critical issue with CDA kill-curves as an evaluation of antimicrobial efficacy is that the findings are empirical and lack understanding of the alloy behavior, particularly copper ion release responsible for antimicrobial behavior. As determined from CDA kill rates, the alloy composition is a critical factor affecting antimicrobial behavior, suggesting that most copper ions are released from the bulk alloy as opposed to due to the chemical dissolution of corrosion products. In order to be able to better understand the corrosion mechanisms at work during antimicrobial behavior, it is necessary to first perform a review of copper corrosion in atmospheric, saline, and perspiration environments.

1.4.1 Atmospheric Corrosion and Tarnishing of High Purity Copper

Atmospheric corrosion of copper has been both exploited for its stunning visual effects in architecture and condemned for its detrimental effects on electrical connections.⁵⁸ A large variety of factors influence atmospheric corrosion processes including pollution, temperature, and relative humidity.⁵⁸ In atmospheric corrosion, surface hydroxylation occurs very rapidly, where water (H_2O) dissociation is driven by the formation of metal oxide (MO) or metal hydroxide (MOH) bonds, where dissociation increases with the number of lattice defects in the surface.⁵⁸ Atmospheric H_2O is then adsorbed onto the surfaces to various degrees dependent on the hydrophobic/hydrophilic nature of the substrate and density of defects. The first layer of adsorbed H_2O is highly ordered, and subsequent layers become more random and mobile. H_2O layers will include adsorbed aerosol particles from the environment, which result in a greater amount of adsorbed H_2O at a given relative humidity (RH). Additionally, the aqueous phase acts as solvent for atmospheric constituents that influence corrosion rate, such as hydrogen sulfide and sulfur dioxide.^{58,59} The relatively slow deposition rate of atmospheric constituents leads to non-equilibrium conditions on the surface of the metal, resulting in chemical activities that are not proportional to the partial pressures.⁵⁸ Unfortunately, metals are naturally heterogeneous, leading to heterogeneous surface adsorption to form water clusters at specific sites. Therefore, reaction products may vary substantially across the surface. While certain sites may be more conducive to anodic or cathodic reactions, ready access to atmospheric oxygen often leads to the anodic reaction to be rate limiting. One of the most important processes in atmospheric corrosion occurs when hydrogen ions undergo exchange, causing bonds between surface metal ions and their immediate

neighbors to weaken and promote dissolution of the metal into solution.⁵⁸ Once the concentration of ion pairs within the liquid layer reaches super saturation, solid phase precipitation will occur. The formation rate may be limited by the rate of growth along the surface as opposed to the rate of precipitation. Therefore, it is more likely that a small number of large precipitation sites are formed as opposed to many small sites.⁵⁸

Precipitated nuclei grow in size and number, resulting in a complete layer of cuprite (Cu_2O) to form. Further growth must occur by transport through the corrosion product (Cu_2O), either by species of the liquid layer (Cl^- , O^{2-} , SO_4^{2-}) penetrating inward or metal ions outward.⁵⁸ So long as the film remains thin and porous, the atmospheric corrosion remains rate limited by the anodic reaction as transport of ions is not hindered.⁵⁸ The layer will thicken by the dissolution of ions into the aqueous layer, where ions coordinate into ion pairs and precipitate on the metal surface.⁵⁸ Several precipitation reactions and solubility of corrosion products are listed in Table 1.3. The formation sequence of corrosion products may vary during atmospheric corrosion over time due to concentration of atmospheric constituents. Figure 1.6 diagrams the typical phase transformation as a function of Cl^- versus $\text{SO}_2/\text{SO}_4^{2-}$. Figures 1.17-1.19 represent simplified schematic representations of the formation of sulfate, chloride, and carboxylic acid corrosion products on a copper patina. For simplicity, the schematics represent a depression on the metal surface which could be produced by heavy dew or rain, though the patina is spatially homogeneous.

Chemical Formula	Reaction	Solubility (K_{sp})
$\text{Cu}_4(\text{OH})_6\text{SO}_4$ (brochantite)	$4\text{Cu}^{2+} + 6\text{OH}^- + \text{SO}_4^{2-} = \text{Cu}_4(\text{OH})_6\text{SO}_4$	2.52×10^{-69}
$\text{Cu}_2(\text{OH})_2\text{CO}_3$ (malachite)	$2\text{Cu}^{2+} + 2\text{OH}^- + \text{CO}_3^{2-} = \text{Cu}_2(\text{OH})_2\text{CO}_3$	4.38×10^{-34}
$\text{Cu}_2(\text{OH})_3\text{Cl}$ (atacamite)	$2\text{Cu}^{2+} + 3\text{OH}^- + \text{Cl}^- = \text{Cu}_2(\text{OH})_3\text{Cl}$	1.72×10^{-35}
Cu_2O (cuprite)	$2\text{Cu}^+ + \text{OH}^- = \text{Cu}_2\text{O} + \text{H}^+$	2.6×10^{-2}
CuCl (nantokite)	$\text{Cu}^+ + \text{Cl}^- = \text{CuCl}$	1.86×10^{-7}

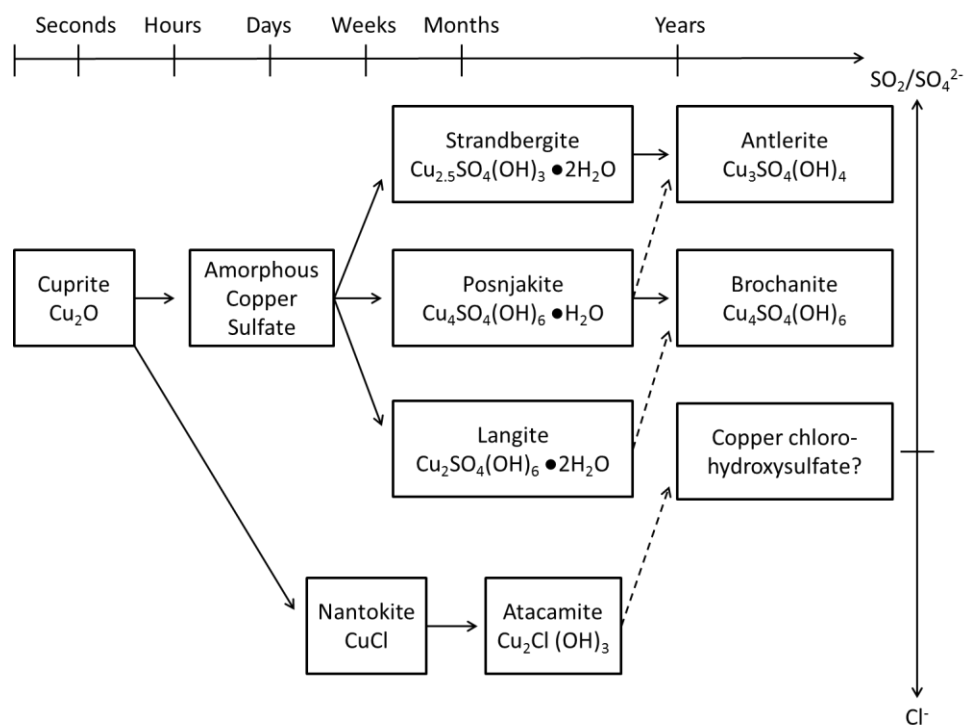


Figure 1.6. Formation sequence for compounds in copper corrosion products formed under sheltered conditions for varying degrees of atmospheric constituents.⁵⁸

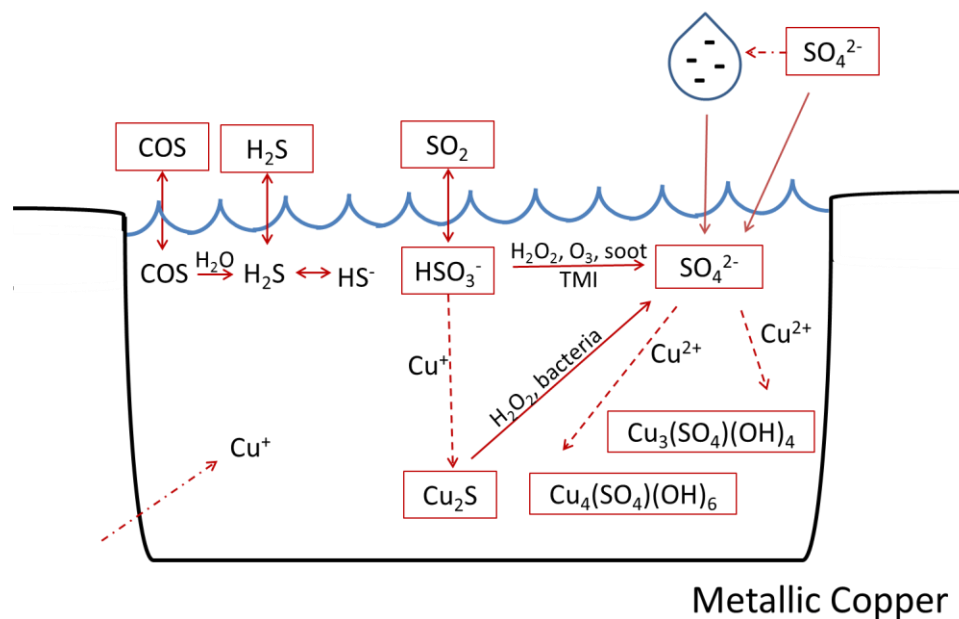


Figure 1.7. Schematic representation of the processes involved in the formation of sulfate components in copper patinas.⁵⁸

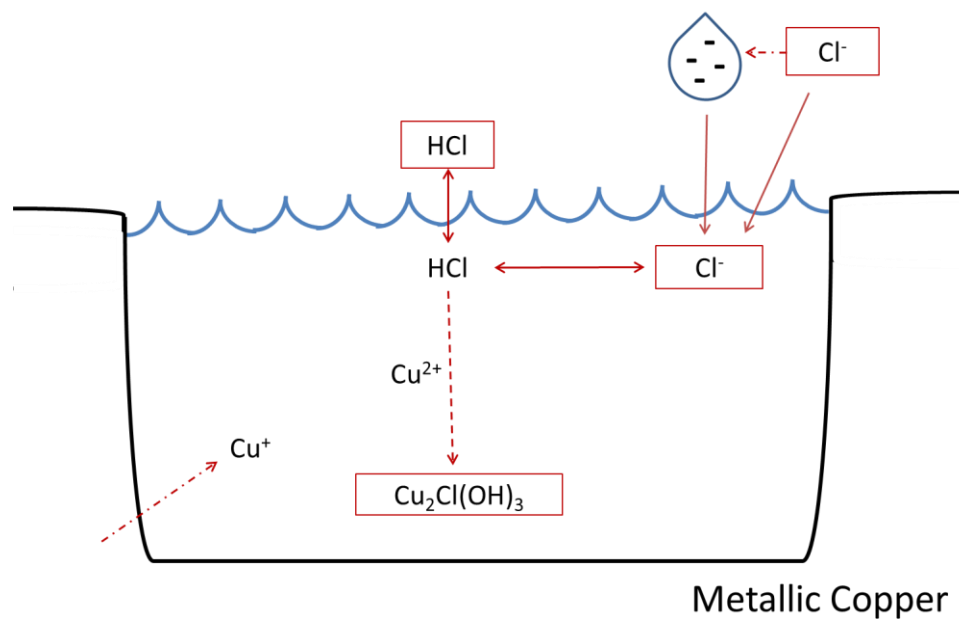


Figure 1.8. Schematic representation of the processes involved in the formation of chloride components of copper patinas.⁵⁸

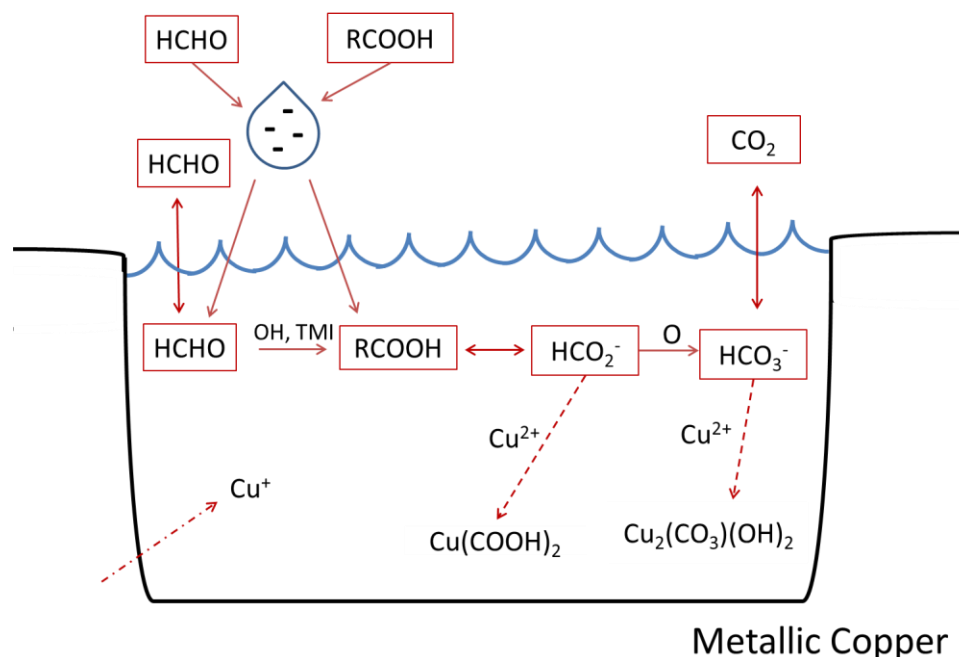


Figure 1.9. Schematic representation of the processes involved in the formation of the carboxylic acid components of copper patinas.⁵⁸

In outdoor environments, exposure to precipitation results in a portion of the corrosion products dislodging from the metal surface and washing away with soluble species, known as runoff. Studies by Leygraf and Wallinder have explored the relationship between corrosion rate and runoff rate of copper alloys, altering previous thoughts that runoff rate was only related to the amount of corroded metal. A field exposure in 1996 in Stockholm, Sweden, determined that copper alloys exposed to precipitation for 48 weeks determined predominantly cuprite (Cu_2O) corrosion products formed, with varying thickness between 5-12 μm .⁶¹ Only 20% of mass loss over 48 weeks was metal runoff, indicating large fractions of corrosion products are retained on the surface.⁶¹ Another complimentary study found that though corrosion rate decreases over time, no such time dependence exist in runoff rate.⁶² Runoff rate was only related to

environmental characteristics and precipitation (rain) intensity, where more less intense precipitation causes greater copper release.⁶¹ Another study comparing annual release rates of copper and zinc from brass (Cu-Zn), bronze (Cu-Sn) and pure copper found comparable copper release between pure copper sheets and bronze (Figure 1.10).³ Copper alloys containing secondary elements, such as zinc (Zn) and nickel (Ni), can form products that result from the secondary element corrosion, and suppress copper ion release. Nickel rich alloys are prone to forming nickel hydroxide ($\text{Ni}(\text{OH})_2$) and nickel oxide (NiO), which consequently makes passivation of the surface easier to achieve.⁶³ Zinc-based products are not detected on the alloy's surface, however, despite the known process of dezincification. The passive zinc product layer breaks down in the presence of chloride ions, resulting in a faster dissolution than formation of zinc products.⁶³ A schematic of the fate of a copper alloy in a solution droplet akin to atmospheric corrosion, shown in Figure 1.11, demonstrates the possible fates of copper and alloying elements in the corrosion process. Possible fates include dissolution of copper or secondary alloying elements (Zn, Al, Ni, Mn) into the solution, incorporation of copper or secondary alloying element into an electrochemically connected surface oxide, dissolution of copper or secondary alloying element into solution before precipitation to the surface of the oxide, or incongruent dissolution to generate a partially dealloyed zone.

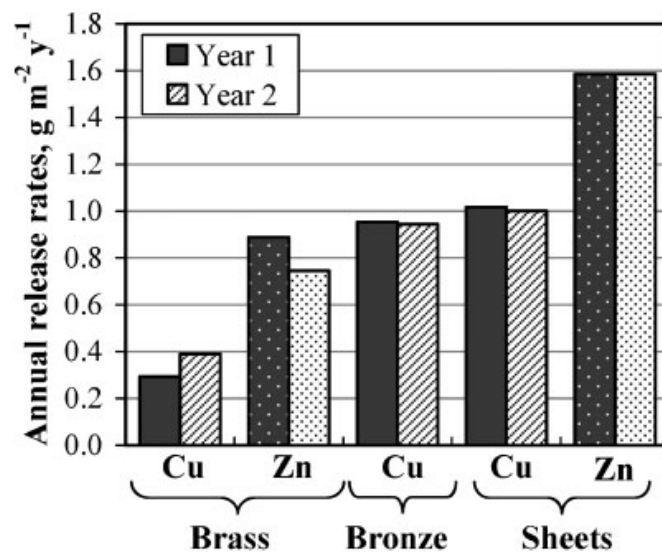


Figure 1.10. Annual release rate of copper and zinc from brass (Cu-Zn), bronze (Cu-Sn), and separate pure metal constituents exposed to identical conditions during 2 years of urban exposure.³

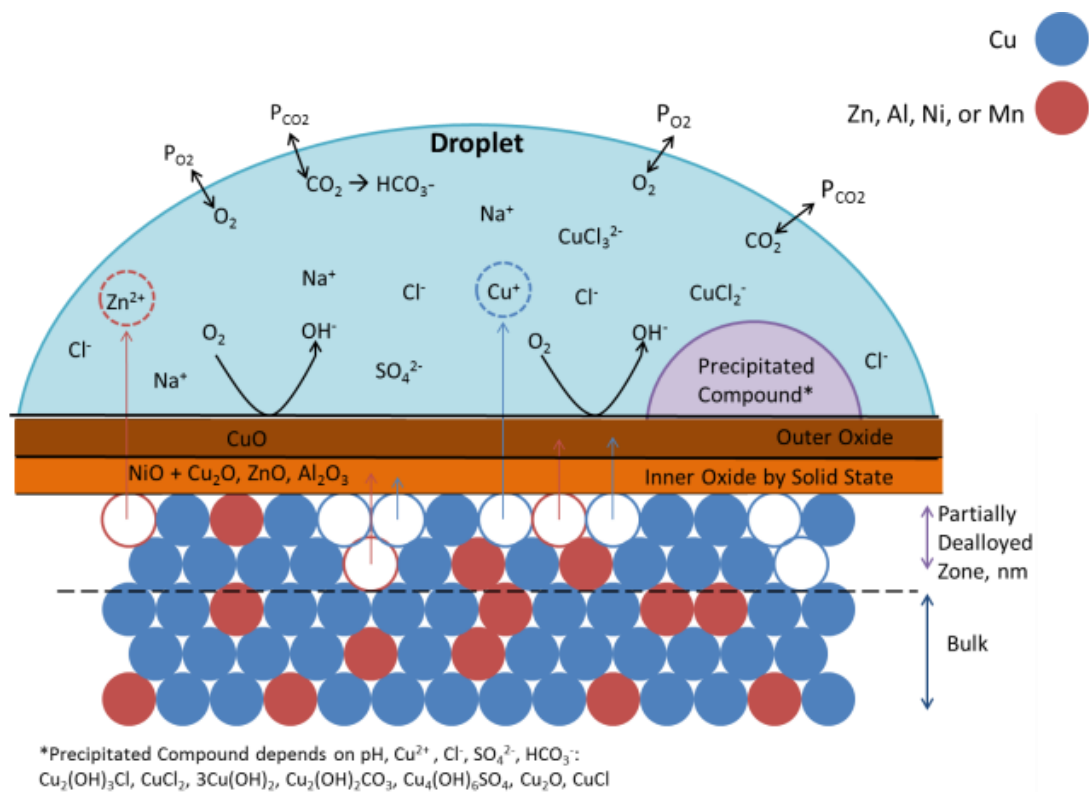


Figure 1.11. Schematic of copper alloy corrosion in solution droplet akin to atmospheric corrosion at normal relative humidity.

Indoor environments are characterized by relatively constant temperature, %RH, and airflow conditions, with a broad spectrum of gaseous and particulate constituents at constant levels.⁶⁴ While numerous studies have explored copper corrosion in outdoor, marine and industrial environment^{59,65-67}, significantly fewer have studied copper corrosion exposed to indoor environments.⁶⁷⁻⁶⁹ In 1990, Schubert and Egidio performed a comprehensive study that evaluated the surface composition of copper exposed to an indoor environment from between 3 and 49 years.⁶⁷ Copper surfaces had a significant carbon layer, consistent with large amount of organic constituents in indoor atmospheres. Beneath the carbon layer were copper oxides, primarily Cu_2O , and significantly less copper sulfide and copper chloride products. Compositions were similar for all periods of time, varying only in thickness and ratio of carbon to copper content. Another study conducted by Cano et al in 2001, examined the effect of various levels of relative humidity on copper tarnish products over a period of 21 days.⁷⁰ Tarnish layers were thicker (17 nm) at a lower relative humidity (40% RH), but composed of 34% copper hydroxide ($\text{Cu}(\text{OH})_2$) and 66% cuprite (Cu_2O). At higher relative humidity (80% RH), tarnish layers were thinner and composed of 84% $\text{Cu}(\text{OH})_2$ and 16% Cu_2O . Bastidas and Simancas evaluated the corrosion products of a copper-containing intrauterine device at 40 °C and 35% RH for 30 months by XPS and determined that a two layer oxide layer formed adjacent to the copper surface, with an inner layer of Cu_2O and an outer layer of tenorite (CuO).⁷¹ Relative amounts were 27% Cu_2O and 73% CuO . The porous nature of Cu_2O enables outward copper ion diffusion, while CuO obstructs diffusion. The total thickness of this oxide layer was estimated by sputter rate to be 1-1.2 nm. While the composition of copper tarnish in indoor environments is generally agreed to be primarily

cuprous and cupric oxides with minor chloride, sulfide, and hydrocarbon products, the relative humidity plays a significant role in the determination of the thickness of the tarnish layer. Table 1.4 lists possible reactions of corrosion products formed in high chloride solution such as a surface frequently touched by hand perspiration and allowed to undergo atmospheric corrosion.

Table 1.4. Half-cell reactions of possible products formed in high chloride solution		
Chemical Formula	Half Cell Reactions	Potential (V _{MMSE})
CuO (tenorite)	$\text{Cu}_2\text{O} + 2\text{OH}^- + \text{H}_2\text{O} \rightarrow 2\text{CuO} \cdot \text{H}_2\text{O} + 2\text{e}^-$	E = -0.399
$\text{Cu}_2(\text{OH})_3\text{Cl}$	$2\text{Cu} + \text{Cl}^- + 3\text{OH}^- \rightarrow \text{Cu}_2(\text{OH})_3\text{Cl} + 4\text{e}^-$	E = -0.548
CuCl_2	$4\text{Cu} + 2\text{Cl}^- + 6\text{OH}^- \rightarrow \text{CuCl}_2 \cdot 3\text{Cu}(\text{OH})_2 + 8\text{e}^-$	E = -0.560
Cu_2O (cuprite)	$2\text{Cu} + 2\text{OH}^- \rightarrow \text{Cu}_2\text{O} + \text{H}_2\text{O} + 2\text{e}^-$	E = -0.675

The fate of copper depends strongly on environment, including temperature, relative humidity, pH, and pollutant concentrations (Cl^- , O^{2-} , SO_4^{2-}). The higher the relative humidity, the more likely atmospheric constituents can become incorporated into the tarnish layer as it forms.⁵⁸ However, high relative humidity results in comparably thinner tarnish layers.⁶⁴ As seen in Figure 1.12, the pH of the solution and potential of the metallic surface are factors in determining the fate of copper through the corrosion process. At oxidizing potentials, acidic pH conditions generate ionic products in the form of Cu^{2+} or CuCl_2^- , and at neutral pH form either $\text{CuCl}_2 \cdot 3\text{Cu}(\text{OH})_2$ or CuO , at strong oxidizing potentials. As corrosion occurs, the solution becomes more alkaline, shifting the corrosion products to copper oxides, including Cu_2O , $\text{Cu}(\text{OH})_2$, and CuO . The concentration of pollutant species (Cl^- , O^{2-} , SO_4^{2-}) determine the formation sequence and composition of corrosion layer. Additionally, concentrations of pollutant species (Cl^- , O^{2-} , SO_4^{2-}) and pH determine the identity of insoluble corrosion precipitates, as seen in Figure 1.6. Atmospheric corrosion always generates a layer of cuprite (Cu_2O), followed by

hydroxide, chloride or sulfate corrosion products depending on their environmental availability.

Despite a well-defined understanding of copper's behavior in atmospheric exposure, the effects of wetting and drying cycles due to frequent handling and cleaning are not well understood. The closest study found that mimics conditions copper would experience in a hospital environment was conducted by researchers at the New Mexico Institute of Mining and Technology, who explored the effects of synthetic perspiration on copper and copper alloys by the use of a "baton" test where samples were passed between different people for varying periods of time and exposed to indoor air overnight.⁷² The fate of copper was determined only as corrosion product formation and corrosion rate, but no study was conducted on the release of copper ions into solution that would facilitate antimicrobial efficacy.

$$[\text{Cl}^-]_{\text{TOT}} = 86.00 \text{ mM}$$

$$[\text{Cu}^+]_{\text{TOT}} = 10.00 \text{ } \mu\text{M}$$

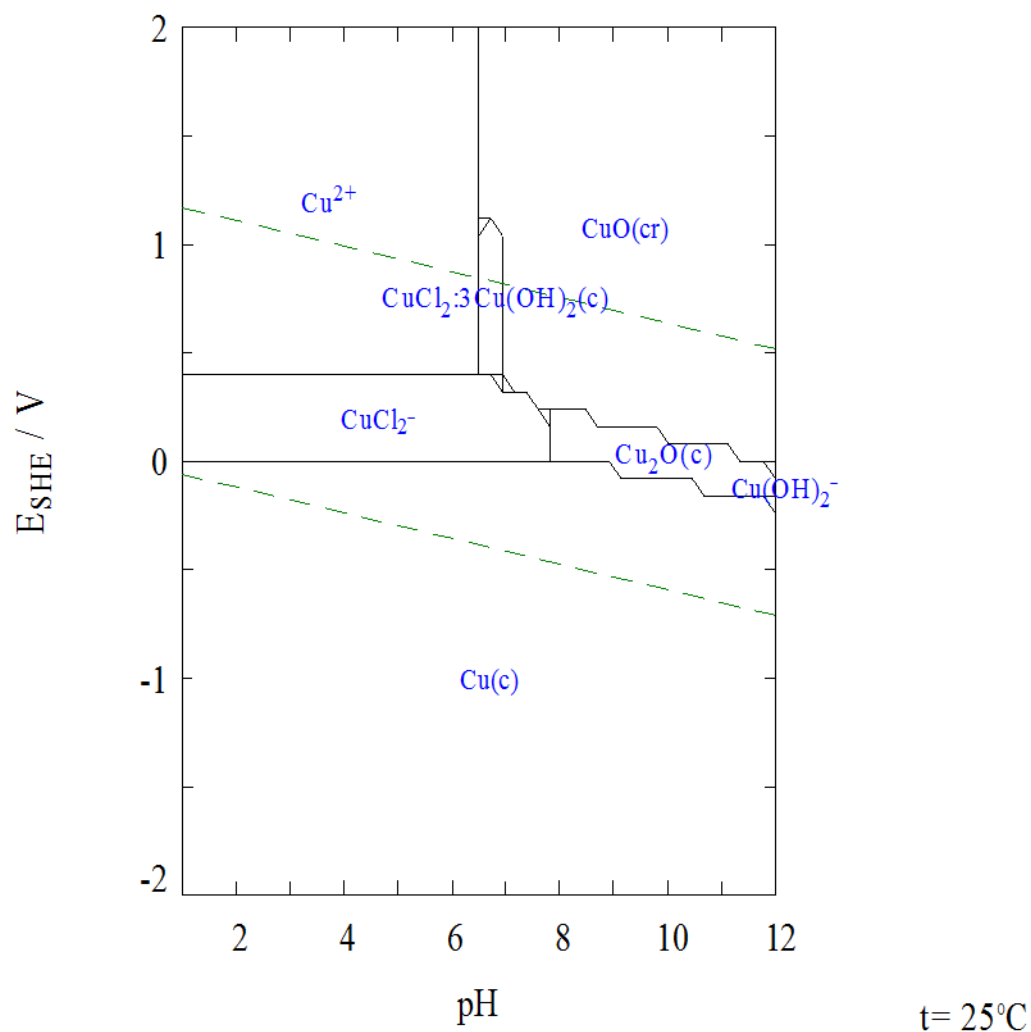


Figure 1.12. E-pH diagram of expected corrosion behavior in chlorinated medium (86 mM Cl^- , 10 μM Cu^+ in H_2O at 25 °C) to represent concentrated synthetic perspiration constructed with Medusa software, courtesy of Michael Hutchison

1.4.2 Copper Corrosion by Seawater in Full Immersion

The utilization of copper for condenser-tubes and other marine applications has made the study of corrosion in submerged marine conditions particularly important.⁷³ A variety of factors affect copper and copper alloy's performance in seawater⁷⁴, particularly film formation, oxygen content, temperature, velocity, and metal-ion concentration.⁷⁵

Copper films in submerged seawater differ depending on the level of pollution, just as in atmospheric corrosion. Typically, a protective film of cupric oxychloride ($\text{CuCl}_2 \bullet 3\text{Cu}(\text{OH})_2$), cupric hydroxide ($\text{Cu}(\text{OH})_2$) or copper carbonate (CuCO_3) will form on the surface⁷⁶, but in the presence of sulfides, copper sulfide can also form in sulfide polluted seawater.⁷⁵ This copper sulfide is cathodic compared to other corrosion products, and in the case of a break in the protective films will lead to localized corrosion.⁷⁵

Dissolved oxygen content plays a critical role in copper corrosion where increased dissolved oxygen leads to increased corrosion rate, simultaneously depolarizing cathodic areas, oxidizing cuprous ions to cupric ions, and promoting the formation of a protective film.⁷⁵ After the formation of a protective film, oxygen must first diffuse through this layer, slowing the corrosion rate considerably. In a study to determine the impedance behavior of copper and copper-nickel alloys in aerated salt water, copper specimens formed cupric hydroxyl-chloride ($\text{Cu}_2(\text{OH})_3\text{Cl}$) corrosion product over Cu_2O , where improved corrosion resistance over time was due to firmly adhered Cu_2O rather than $\text{Cu}_2(\text{OH})_3\text{Cl}$.⁷⁷ At normal working conditions, warm water accelerates copper corrosion, but as temperatures are heated significantly, reduced dissolved oxygen and increased tendency for mineral scale (CaCO_3) production decrease the corrosion rate.⁷⁵ Metal-ion concentrations are likely to be higher under crevices on the copper or copper alloy, leading to localized attack directly around but outside the crevice area. This is due to the conversion of release cuprous ions to cupric ions by dissolved oxygen in the seawater, which in turn attack the copper to produce more cuprous ions, causing a cyclic phenomenon. While increased salinity is known to accelerate corrosion⁷⁵, it simultaneously reduces the amount of possible dissolved oxygen, the most critical

element to the copper corrosion process.⁷⁸ Ions formed by the dissociated salts attract polar water molecules, reducing the water molecule's affinity for non-polar oxygen molecules.

Corrosion of copper due to full immersion in seawater depends primarily on the composition of the solution. While temperature affects the rate of corrosion, the concentration of Cl^- , SO_4^{2-} , and O^{2-} affect the species of corrosion products formed, as is similar to atmospheric corrosion. The formation of an inner layer of Cu_2O reduces corrosion rate over time due to the oxide layer passivating the surface, followed by the formation of cupric oxychloride ($\text{CuCl}_2 \bullet 3\text{Cu}(\text{OH})_2$), cupric hydroxide ($\text{Cu}(\text{OH})_2$) or copper carbonate (CuCO_3) depending on seawater chemistry. However, the composition of seawater is dramatically different than perspiration, containing not only chloride and sodium at greater concentrations than perspiration, but also magnesium, sulfur, calcium, potassium, and bromine.⁷⁴ The higher concentrations of these constituents can cause different electrochemical behavior that does not accurately reflect their behavior when in frequent contact with perspiration, including corrosion rate, corrosion product formation, and copper ion release.

While copper corrosion in seawater is well understood due to the marine application of copper alloys, the composition of seawater varies drastically from the composition of human perspiration despite both being saline solutions. Seawater contains a larger variety of salts and metal ions that can result in different corrosion behavior, versus perspiration which contains more small organic molecules. Seawater also contains significant microbial organisms that can lead to bio-corrosion, while perspiration does not naturally contain microorganisms.

1.4.3 Copper Corrosion by Human Perspiration in Full Immersion

While a wide range of studies have been conducted for copper corrosion in seawater due to its prevalence for marine applications, significantly fewer have been conducted utilizing perspiration. Many of the tests that have been conducted on copper and copper alloys in synthetic perspiration have been limited to copper-nickel alloys, with a focus on contact sensitization by nickel.^{63,79,80} The composition of mammalian perspiration varies depending on physical, pharmacological and environmental conditions, but is generally characterized by a saline medium with lactic acid ($C_3H_6O_3$) and urea (CH_4N_2O).⁸¹ A variety of synthetic perspirations have been utilized in studies, varying between acidic and neutral pH, as well as total composition (Table 1.5). In comparison to the multiple compounds that can make up the protective layer in a seawater environment, studies have shown that corrosion products following exposure to perspiration are primarily Cu_2O with minor Cu, O and Cl based compounds depending on the composition of the alloy.⁶³ In copper rich alloys, chloride ions behave as dopants for Cu_2O defect structures, and the thickness of the corrosion film depends on the copper content.⁶³ The hand baton study by Fredj, Prichard and Burleigh agree with these findings when the perspiration is alternatively wet and dry by passing between different individuals for various times over a 2 year period (Figure 1.13), where thickness of Cu_2O trends with copper content.⁷² Additionally, EDS analysis of a copper alloy surface (C70600, 88.5% Cu-10.2% Ni) immersed in synthetic perspiration (0.8 NaCl-3.0% $C_2H_4O_2$) for one month showed that the surface was rich in chloride precipitates, with significantly fewer oxide and carbon precipitates.⁷² Corrosion rate obtained by electrochemical impedance spectroscopy indicates copper and copper alloys were similar

between 4 and 32 days in synthetic perspiration, likely due to the formation of a passive oxide layer.⁷² Nickel containing alloys (C70600 and C57200) corroded 40 times faster than C11000 in synthetic sweat over 32 days, due to the degradation of the protective barrier in nickel containing alloys. C11000, followed by C26000, maintained the greatest corrosion resistance over time likely due to their passive film stability. However, this study did not establish corrosion behavior during the formation of a passive film, as corrosion resistance is only measured when passivation has already occurred in most alloys. Daily cleaning may also have an effect on the formation of oxides prior to 4 days, and terminal cleaning would likely occur over the 32 day window studied, which could result in the stripping of the passive layer. CDA kill rates are conducted on freshly ground samples that have not fully air passivated, with a maximum testing period of 24 hours, well below the time period of this study. The differing conditions of the copper alloys means that no correlation can be drawn between corrosion behavior and antimicrobial efficacy. Additionally, no testing has been conducted on the influence of thin oxides formed by air on corrosion and ion release in perspiration, as they would naturally occur in hospital environments. A study on corrosion and ion release comparing the results of freshly ground samples and those that have been possibly passivated by air is necessary in order to determine the growth behavior of the passive layer over time when exposed to human perspiration.

Composition (by mass percentage)	pH
0.87% NaCl, 0.16% CH ₄ N ₂ O, 10.92% C ₃ H ₅ NaO ₃ (60% w/w), 0.016% Na ₂ HPO ₄	7.5 ⁸²
1.96% NaCl, 0.49% CH ₄ N ₂ O, 1.39% C ₃ H ₆ O ₃ , 0.25% C ₂ H ₄ O ₂ , 1.71% NH ₄ Cl	4.7 ⁸³
0.5% NaCl, 0.1% CH ₄ N ₂ O, 0.1% C ₃ H ₆ O ₃	6.5 ^{63,84,85}
0.3% NaCl, 0.1% Na ₂ SO ₄ , 0.2% CH ₄ N ₂ O, 0.2% C ₃ H ₆ O ₃	6.6 or 4.5 ⁸⁶
0.5% NaCl, 0.1% CH ₄ N ₂ O, 0.5% C ₃ H ₆ O ₃	5 ⁸⁷
0.5% NaCl, 0.1% CH ₄ N ₂ O, 0.1% C ₃ H ₆ O ₃	4.5 ⁸⁸

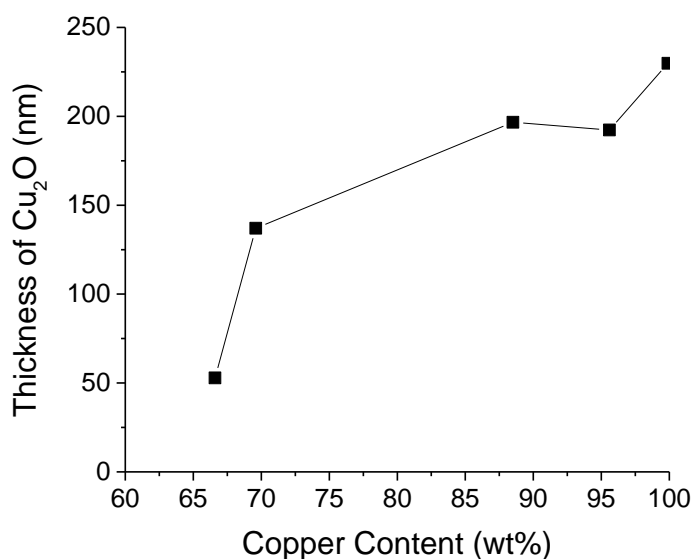


Figure 1.13. Evolution of thickness of cuprous oxide (Cu₂O) vs. copper content after hand contact test, corroded by passing between different individuals for various times over a 2 year period.⁷²

While full immersion testing in perspiration does not accurately represent the wetting and drying cycles copper is likely to encounter in a hospital application, they offer valuable insight as a first step on the possible corrosion products and corrosion rates. Exposure to perspiration generates a layer of protective Cu₂O of varying thickness depending on copper content, which serves to passivate the surface against further corrosion. Additionally, copper chloride and possible oxide corrosion products precipitate

on the surface of Cu_2O . Based on this research, it is expected that copper exposed to perspiration due to frequent handling will have similar corrosion product formation, though corrosion rate variations due to wetting and drying rather than constant contact to perspiration.⁷² However, previous work only examines the effect of alloying on discoloration and corrosion rate after a passive layer has already formed. Alloying content is not examined for copper ion release, as it relates to antimicrobial efficacy, or corrosion behavior during the formation of passive oxides. Additionally, no studies outside of the University of Virginia explore copper ion release correlated to antimicrobial efficacy as a factor of corrosion behavior.

1.5 Effects of Alloying Composition

1.5.1 Copper Content

While copper alloys range from greater than 95% copper to as low as 42% copper in select copper-nickel-zinc (nickel silver) alloys, only those with copper content above 65% exhibit antimicrobial efficiency.^{18,55,56,89-92} As discussed earlier, antimicrobial efficiency generally increases with copper content.²⁵ However, as seen in previous studies, the composition of an alloy matters beyond copper composition, as secondary alloying elements can affect corrosion rate and corrosion products formed.⁷² Copper alloys are sub-divided based on alloying composition and classified either as coppers, high-copper alloys, brasses, bronzes, copper-nickels and copper silvers.⁹³ Table 1.6 .lists UNS numbers and compositions for possible copper alloys.

Generic Name	UNS Numbers	Composition
Coppers	C10100-C15999	99.9% Cu
High-copper alloy	C16200-C19999	>95% Cu
Brasses	C20000-C28580	<35% Zn, Remaining Cu
Leaded brasses	C31200-C38590	62% Cu, 0.5-3.5% Pb, Remaining Zn
Tin brasses	C40400-C49080	2-40% Zn, 0.2-3% Sn, Remaining Cu
Phosphor bronzes	C50100-C52400	0.5-11% Sn, 0.01-.35% P, Remaining Cu
Aluminum bronzes	C60600-C64400	9-12% Al, <6% Fe and Ni, Remaining Cu
Silicon bronzes	C64700-C66100	<20% Zn, <6% Si, Remaining Cu
Copper-nickels	C70000-C73499	2-30% Ni, Remaining Cu
Nickel silvers	C73500-C79999	7-20% Ni, 14-46% Zn, Remaining Cu

1.5.1 Major Alloying Elements

While copper naturally possesses a range of highly desirable behaviors (corrosion resistance, easy fabrication, electric and thermal conductivity), incorporation of alloying elements can improve specific behaviors with minimal negative impacts to copper's natural properties. The most prominent alloying elements are nickel (Ni), zinc (Zn), aluminum (Al), and tin (Sn), as seen in Table 1.6. Not only do these elements affect the behavior of the copper alloy, but they can significantly alter the price as well (Table 1.7). As seen in Figures 1.14-1.17, all binary alloys containing over the necessary 65% Cu for antimicrobial behavior are FCC solid solutions with alloying elements contained in solid solution at the levels reported, except for high Sn and Al content when considered as binary alloys.

Primary Metals	Approximate Relative Cost
Copper (Cu)	1
Tin (Sn)	7.8
Nickel (Ni)	4
Zinc (Zn)	0.5
Aluminum (Al)	0.9

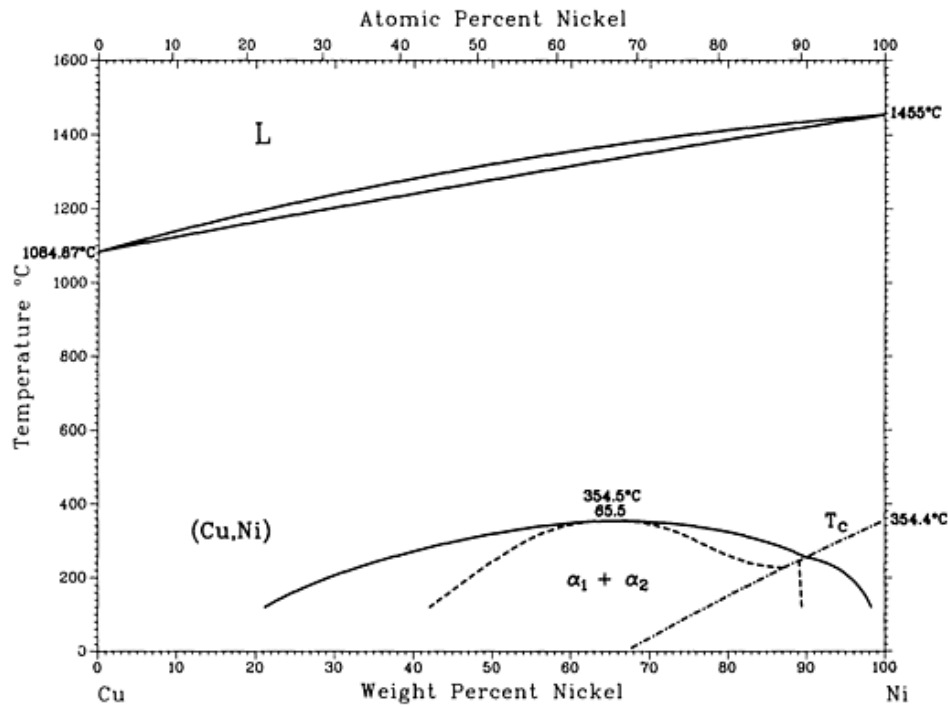


Figure 1.14. Binary phase diagram of Cu-Ni.⁹⁶

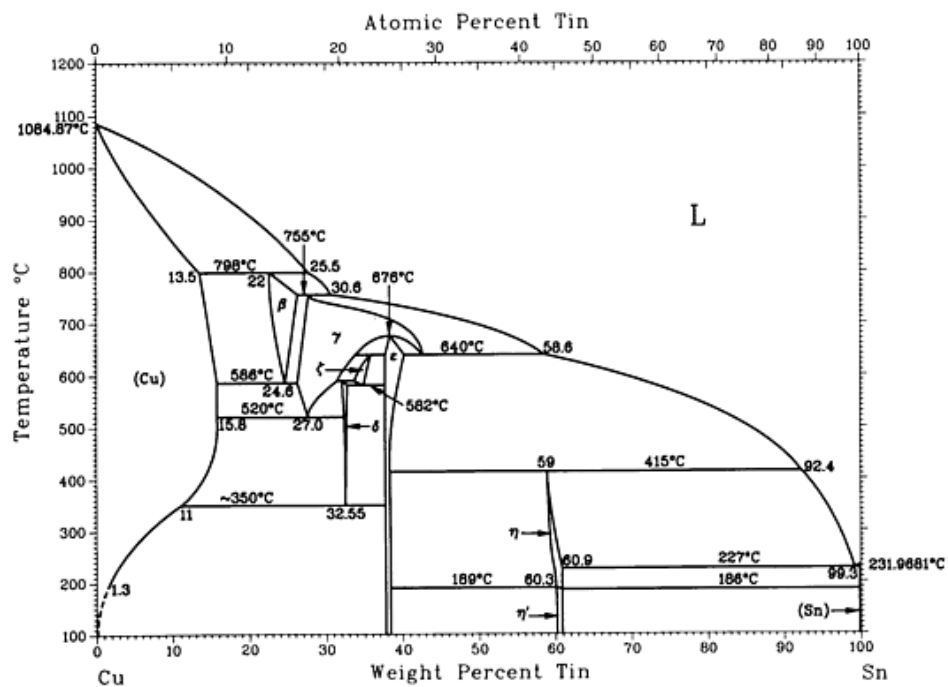


Figure 1.15. Binary phase diagram of Cu-Sn.⁹⁶

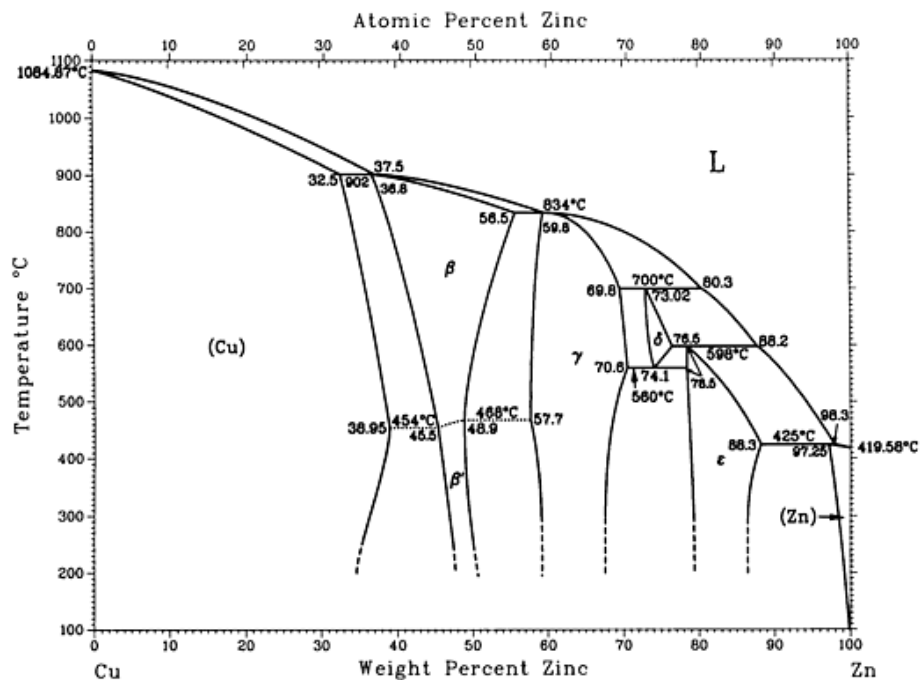


Figure 1.16. Binary phase diagram of Cu-Zn.⁹⁶

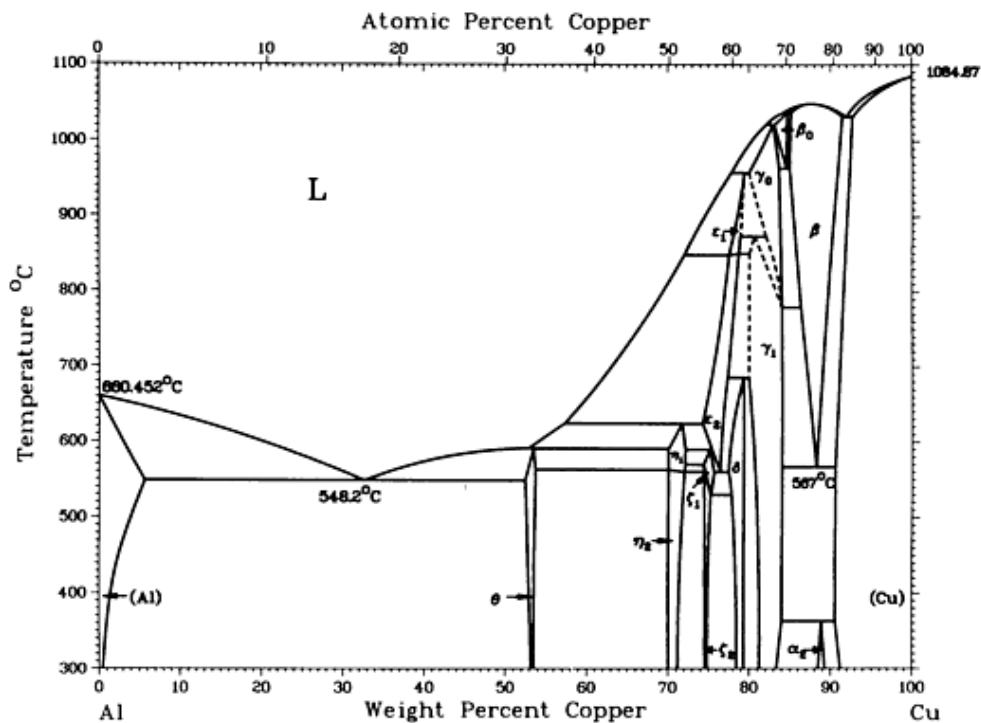


Figure 1.17. Binary phase diagram of Cu-Al.⁹⁶

Nickel is known to improve the tarnish resistance of copper alloys in excess of 1%, and their addition modifies the natural salmon color of pure copper to silver.⁹⁷ Cu-Ni alloys containing 10% Ni performed favorably in both touch and cleaning testing evaluations for anti-tarnish, antimicrobial copper alloys, showing very little discoloration over 21 days of regular handling.⁹⁸ Previous testing has indicated that alloys containing significant amounts of Ni inhibit copper ion release, thereby inhibiting antimicrobial activity based on bacterial interaction with copper ions.⁹⁹ Antimicrobial tests by the CDA indicate that despite the depressed ion release, Cu-Ni alloys are effective antimicrobial surfaces.⁵⁷ However, due to copper-nickel's prominence as a coinage metal, extensive research has been conducted related to contact dermatitis due to nickel sensitization. In industrialized countries, 10% of females and 2-4% of males are nickel-sensitive¹⁰⁰, resulting in eczema, and efforts have been made to minimize nickel inclusions to prevent primary sensitization and further exposure.¹⁰¹⁻¹⁰³

The addition of zinc to copper is primarily utilized for color modification, resulting in a bright gold appearance.⁹⁷ Cu-Zn alloys, also known as brasses, are regularly used for doorknobs, locks, and other aesthetic fixtures. When Zn is added to Cu-Ni alloys, it improves tarnish resistances, with additions of Zn between 6.8% up to 15%⁹⁷. Above 15% Zn, selective leaching of Zn from the alloy results in dezincification, leaving a copper-rich sponge due to the substitution alloying. This sponge has poor mechanical properties.⁹⁷ Additionally, Cu-Zn alloys above 15% Zn can suffer from stress corrosion cracking. Cu-Zn alloys performed reasonable well in touch testing, demonstrating less than 75% of "not deep" discoloration, though when cleaned by wiping a cloth saturated with cleaner (i.e. Pro Bowl: phosphoric acid (8%), Wex-All, Proxi®: Hydrogen peroxide

(<8%), Dawn® Dish soap: diluted 1:10 in water) become darkly discolored.⁹⁸ Previous studies conducted by Leygraf and Wallinder indicate significant amounts of Zn inhibit copper ion release.⁹⁹ Brightly polished Cu-Zn alloys had minimal antimicrobial activity in CDA testing, though were markedly more efficient when tarnished.⁵⁷

Aluminum additions to copper result in better corrosion resistance and wear resistance, with little color modification.⁹⁷ Cu-Al alloys contain 0.6-3% Al to improve hand tarnish resistance⁹⁸, with additions between 8-11% negatively effecting antimicrobial activity.⁵⁶ Previous tests indicate significant amounts of Al in Cu alloys inhibit copper ion release.⁹⁹

Tin is added to improve corrosion resistance and strength of the alloy, and is often found as a ternary alloying element with zinc or nickel.⁹⁷ Sn additions range from 1-10%. Cu-Sn alloys with iron and Ni performed similarly to Cu-Zn alloys in both touch and cleaning testing.⁹⁸ Previous studies indicate Sn additions promote copper ion release, suggesting better antimicrobial activity for alloys containing Sn as a ternary alloying element.⁹⁹

1.5.2 Ranking of Alloys

Previous studies at the University of Virginia performed by Derek Horton, Hung Ha and Hannah Bindig have examined the corrosion product formation, copper ion release and corrosion rate by electric impedance spectroscopy (EIS) of 7 copper alloys, whose compositions are listed in Table 1.8. Composition by weight percent of copper alloys tested by the University of Virginia. Following 130 hour exposure to synthetic perspiration, C11000 and C26000 were the least reflective in the visible light spectrum (370-730 nm), and Nordic Gold the most. Characterization of the surface oxide by

galvanostic reduction and charge per reduction wave analysis indicate thickest oxides formed on C75200 and EcoBrass reduced 3 corrosion products^{vi}. All other alloys only indicate the presence of 2 corrosion products, varying in thickness of individual corrosion species, but similar total oxide thickness between C11000, C26000, C51000, and C70600. The thinnest oxides formed on Nordic Gold, with a thin layer of outer oxide and thicker layer of inner oxide (Figure 1.18). Surface oxide characterization by grazing incidence x-ray diffraction (GIXRD) indicate the presence of copper oxides on the surface of several freshly ground copper samples, and a mixture of copper oxides and copper chlorides on the copper samples following 130 hour exposure to synthetic perspiration (Figure 1.19). Similar results were observed by Raman spectroscopy (Figure 1.20)

Alloy	Cu	P	Sn	Zn	Fe	Al	Mn	Pb	Ni	Si
C11000	>99.9									
C26000	68.5-71.0			28.88-31.38	0.05			0.07		
C51000	93.41-95.32	0.03-0.35	4.2-5.8	0.3	0.1			0.05		
C70600	85.55-88.35			1.0	1.0-1.8		0.6	0.05	9.0-11.0	
C75200	63.0-66.5			13.1-19.6	0.25		1.0	0.05	16.5-19.5	
C87850 Eco-Brass	74.4-78.0	0.05-0.2	0.3	17.76-22.06	0.1		0.1	< 0.09	0.2	2.7-3.4
Nordic Gold	89		1	5		5				

^{vi} Based on reduction waves at distinct differential potentials

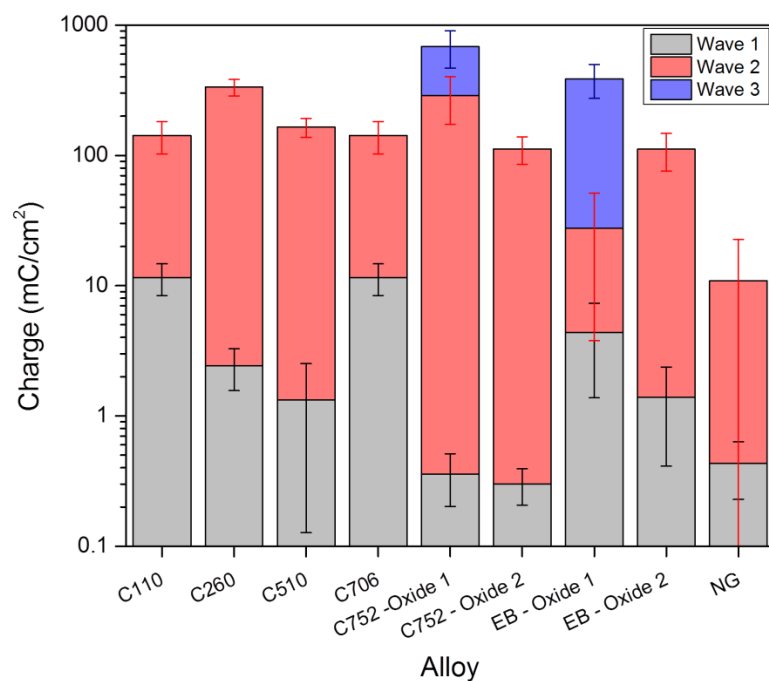


Figure 1.18. Total charge per reduction wave found by galvanostatic reduction analysis of copper alloys exposed to 130 hours of synthetic perspiration. Some alloys had two regions of distinct oxide coloration and were tested separately, labeled oxide 1 and oxide 2. Nordic Gold has the thinnest total oxide layer.

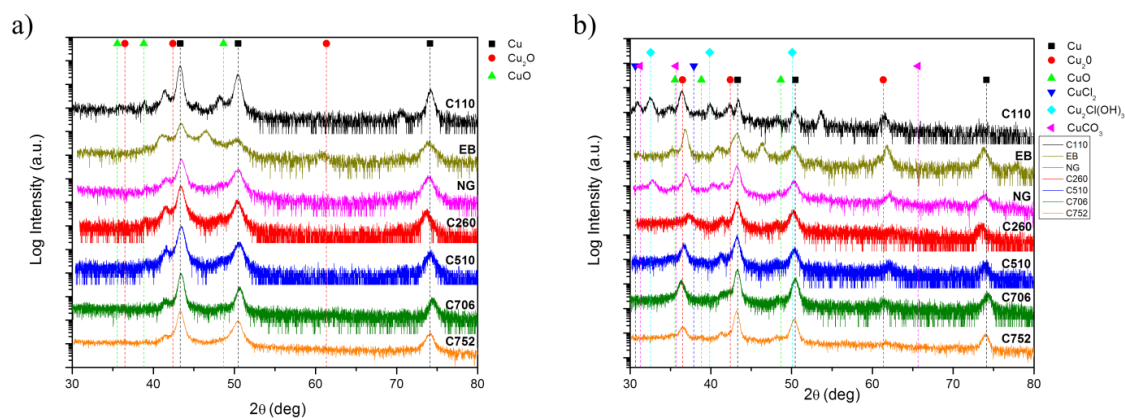


Figure 1.19. Grazing incidence x-ray diffraction (GIXRD) of copper alloys freshly ground (a) and after 130 hours of exposure to synthetic perspiration (b).

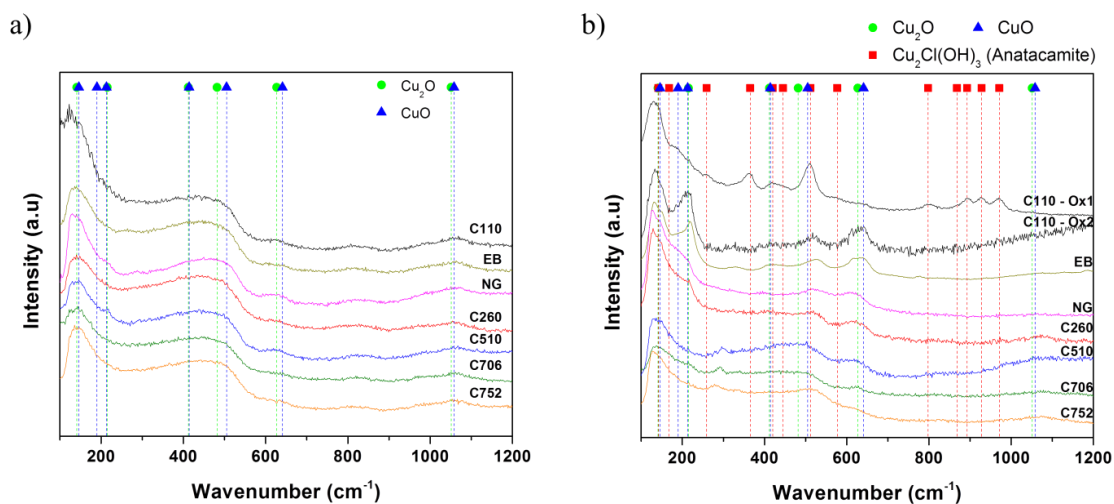


Figure 1.20. Raman spectroscopy of copper alloys freshly ground (a) and after 130 hours of exposure to synthetic perspiration (b).

Following exposure to synthetic perspiration for 130 hours, copper ion concentration was determined by atomic absorption spectroscopy (AAS). AAS cannot distinguish between the ionic state of copper ions (Cu^{2+} or Cu^{+}), and the total concentration is expected to be a mixture of both ionic states. After 130 hours, alloys containing Zn and Ni released less Cu compared to C11000, where the alloy containing the greatest Zn content (C26000) exhibits the lowest copper ion release. Additionally, copper alloy containing only Sn as a major alloying element released copper ions in excess of C11000, as seen in C51000 (Figure 1.21).

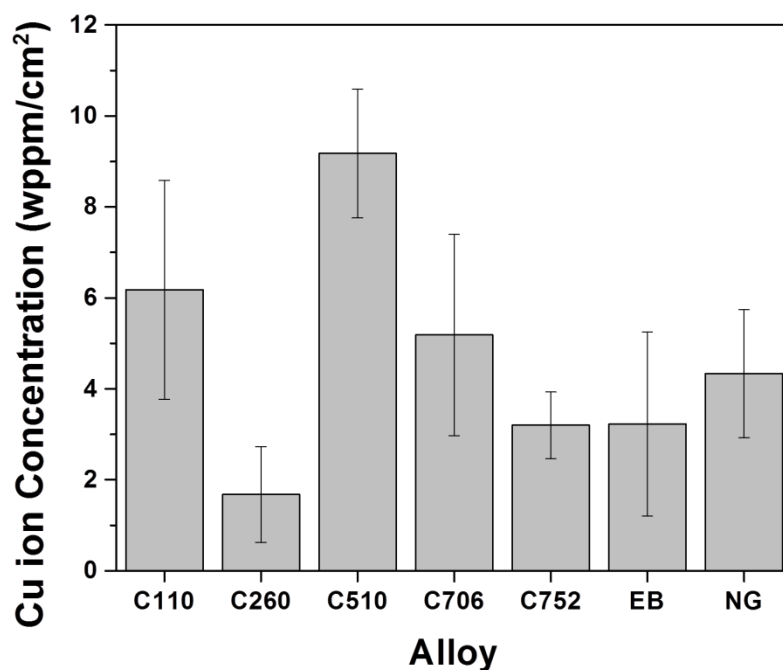


Figure 1.21. Copper ion concentration after copper alloys exposed to 130 hours in synthetic perspiration.

During exposure to synthetic perspiration for 130 hours, instantaneous corrosion rate was characterized by electrochemical impedance spectroscopy, defined as the inverse polarization resistance of a material. Corrosion rate of freshly ground copper alloys indicated low corrosion rate on C26000 due to the greatest percentage of zinc, and the highest corrosion rate on C70600. Following exposure to synthetic perspiration for 130 hours, most alloys exhibited a lower corrosion rate, with the exception of C51000, matching data of the high copper ion release

While copper alloys high in copper content release significant amounts of copper ions and are therefore most antimicrobial, these alloys are also the most prone to tarnish. They would therefore be undesirable in hospital applications where aesthetics are important for the perception of cleanliness. Nordic gold, however, releases moderate

amounts of copper ions, and forms thinner oxides than other copper alloys studied.

Because Nordic Gold was developed to be a tarnish resistant, nickel-free copper alloy, it poses a unique alloy for studies as a possible color-stable, antimicrobial alloy for hospital applications.

1.6 Nordic Gold

Nordic Gold's composition is characterized by 89% copper, 5% aluminum, 5% zinc, and 1% tin.¹⁰⁴ No material density is available, though calculations through weight average density result in 8.49 g/cm³. Nordic Gold answered the need for a tarnish resistant, non-allergenic coinage material in the presence of human perspiration, due to the prevalence of nickel allergy in the majority of industrialized countries.¹⁰⁵ The alloy was developed in the 1980's by Outokumpu Copper in Västerås, Sweden. In 2002, Nordic Gold was introduced as the material for the 10, 20, and 50 Euro cent coins, the primary currency of Europe. Since then, research has continued on the properties of Nordic Gold, specifically interested in its application as an antimicrobial alloy due to its high copper content.¹⁰⁶⁻¹⁰⁸ The combination of antimicrobial properties and tarnish resistance lends itself to applications such as high touch surfaces, where color stability is important. While zinc is known to reduce copper ion release, and aluminum is suspected to passivate the alloy surface, the addition of tin, known to enhance copper ion release, may result in a copper alloy with sufficient copper ion release to be antimicrobial, with minimal tarnishing.

1.6.1 Color Stability

In accordance with the goals leading to Nordic Gold's development as an alloy, testing indicates partial color stability to both thermal oxidation and perspiration.⁹⁹ In a

hand-contact tarnish test performed at the New Mexico Institute of Mining and Technology, Nordic Gold still appeared bright and highly reflective after 55 days of regular handling, compared to significant darkening of C11000 in the same test.¹⁰⁹ Differences in reflectivity were attributed to surface roughening due to continuous pits in C11000 compared to bright surfaces that had few small pits.⁷² Work at the University of Virginia has observed that Nordic Gold develops thinner oxides than other copper alloys tested, supporting that Nordic Gold demonstrates the color stability desired for hospital applications.

1.6.2 Antimicrobial Activity and Passivation

The utilization of antimicrobial copper alloys as conformal layers over high touch surfaces, through the use of a PVD coating, was patented in late 2013.¹⁰⁶ This patent specifies that Nordic Gold is particularly preferred for coatings of thickness 1-7 μm , as at this thickness the alloy can provide necessary amount of copper while also being easily mounted on a substrate.¹⁰⁶ Not only does Nordic Gold provide an antimicrobial surface ideal for surfaces likely to come in contact with multiple people, high abrasion resistance is ideal for frequent handling such as on door handles, window handles, sanitary fittings, and light switches.¹⁰⁶

The Copper Development Association has observed that Nordic Gold when freshly cleaned by vortexing with acetone and 2 mm diameter glass beads is capable of killing initial concentrations of MRSA above 1.0×10^7 CFU in 6 hours at 20 °C (Figure 1.22) utilizing EPA testing procedures, with an antimicrobial efficacy (log reduction) of 1.² However, samples tested in an as received condition or tested 7 days after polishing demonstrated no significant antimicrobial activity (Figure 1.23).

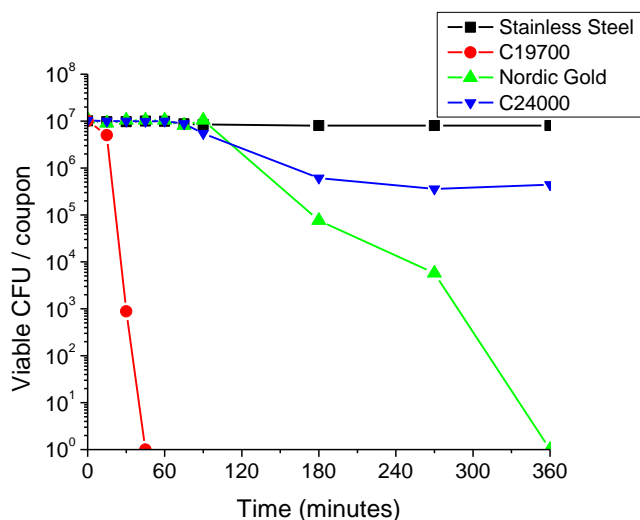


Figure 1.22. Viability of methicillin resistant *staphylococcus aureus* over 6 hours on a freshly cleaned (by alcohol and deionized water) stainless steel, C19700, C24000, and Nordic Gold sample in tryptone soy broth (C19700, C24000, and stainless steel) and unknown broth (Nordic Gold).²

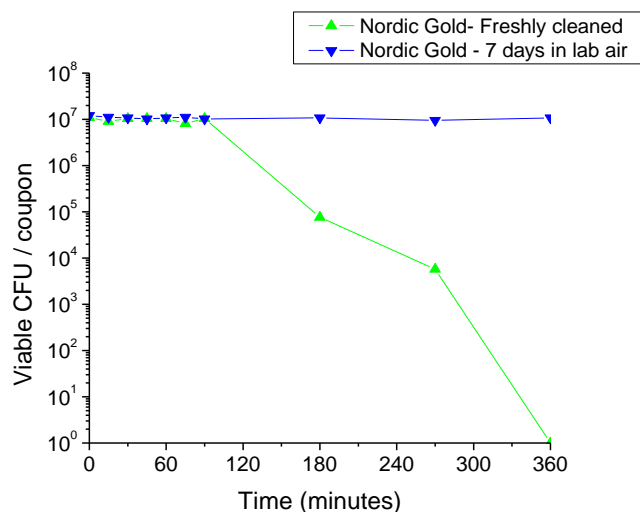


Figure 1.23. Viability of methicillin resistant *staphylococcus aureus* over 6 hours on freshly cleaned Nordic Gold compared to Nordic Gold samples cleaned (by alcohol and deionized water), then exposed to ambient lab conditions for 7 days in unknown broth.²

A study conducted utilizing a “dry” copper surface (opposed to a thinly spread broth medium as used in EPA testing) to study the mechanisms of contact-mediated microbe killing was conducted by streaking cultures concentrated in phosphate buffered

saline over copper coupons and drying in the laboratory environment. This study observed that Nordic Gold killed initial concentrations of *C. albicans* cells above 1.0×10^6 CFU in 60 minutes at 23 °C, compared to pure copper which killed within 5 minutes (Figure 1.24).¹⁰⁷ An important note is though these studies are quantified as “dry” copper surfaces, in laboratory conditions above 65% RH, monolayers of water begin to accumulate on the copper surface.¹¹⁰ Under these conditions, even “dry” copper surfaces have a thin layer of solution to facilitate copper ion release. No %RH is specified for these tests.

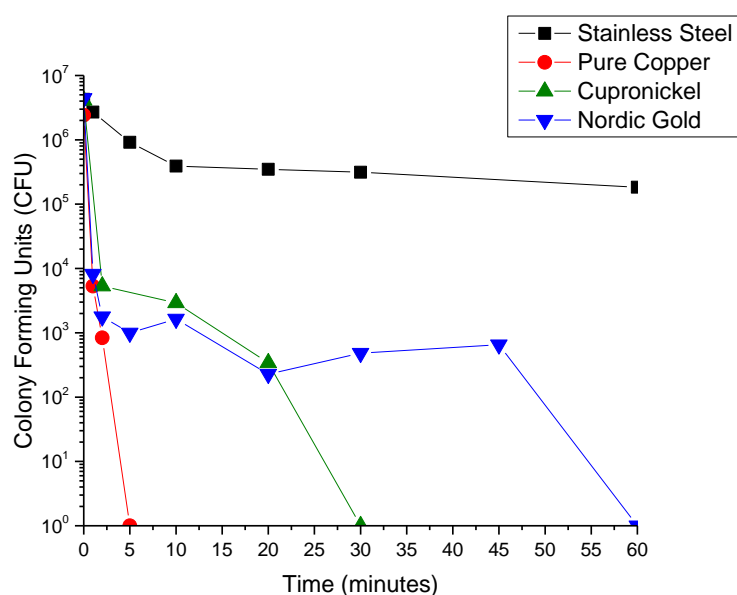


Figure 1.24. Viability of *C. albicans* on dry metallic surfaces at 23 °C.¹⁰⁷

A study examining the bacterial diversity on Moroccan Dirham and Euro coins, including coins composed on Nordic Gold, found several *Staphylococcus* strains surviving on the coinage surfaces despite metallic copper’s contact killing efficiency, attributed to moisture and dirt deposits (Figure 1.25).¹⁰⁸ Coins tested included 0.01 € (copper-covered steel), 0.1 € (Nordic Gold), 1 € (center: 75% Cu-25% Ni clad on Ni

core, outer ring: 75% Cu-5%Ni-20% Zn), and 2 € (center: 75% Cu-25% Ni clad on Ni core, outer ring: 75% Cu-25% Ni). Examination of unwashed and washed 0.1 € coins resulted in varied cell viability between strains. Washed and chemically sterilized 0.1 € coins were highly effective at killing all strains within 360 minutes. Unwashed 0.1 € coins, which will contain salt and dust deposits, reduced *Micrococcus luteus* and *S. epidermidis* by approximately 10%, *S. hominis* spp. *hominis* by 50%, and *S. aureus* by 90% within 360 minutes.

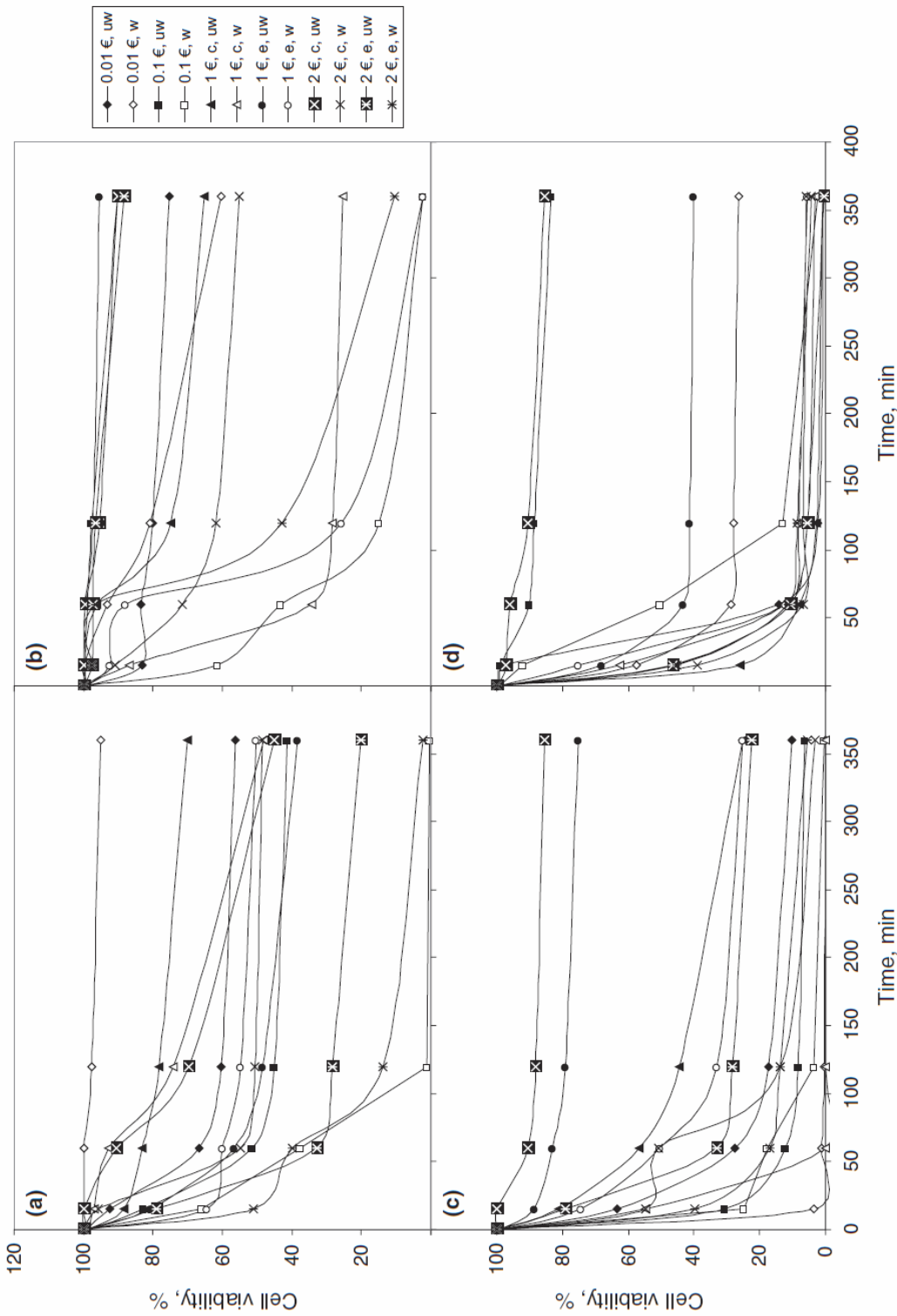


Figure 1.25. Cell viability of *Staphylococcus hominis* spp. *hominis* (a), *Micrococcus luteus* (b), *S. aureus* (c), and *S. epidermidis* (d) on unwashed (uw) and washed (w) Euro coins, tested on the center (c) or edge (e) of the coin.¹⁰⁸ 0.1 € is Nordic Gold.

There are conflicting results regarding Nordic Gold's antimicrobial properties, likely due to the wide variety of testing procedures used to obtain kill rates and a variety of surface conditions. Variations between testing solution (broth or "dry"), treatment of the alloy prior to testing (freshly ground, sterilized, soiled, air oxidized) do not allow a clear picture of Nordic Gold's antimicrobial efficacy. Because the only data collected has been purely empirical and based only on kill rate data, there is a lack of electrochemical and surface science information regarding what factors affect the alloys antimicrobial efficacy through the corrosion process.

1.7 Critical Unresolved Issues

According to the CDA, Nordic Gold's antimicrobial efficiency decreases dramatically after exposure to lab air for 7 days, due to the development of a passive tarnish layers as seen in Figure 1.23.² This is contrary to CDA's previous studies on other CU alloys that indicate the formation of a tarnish layer increases antimicrobial efficiency.⁵⁷ This would indicate that the amount of tarnish and composition of the passive tarnish layer is different or results in functionally different behavior towards copper ion release compared to C19700 or C22000, which contain 99 and 90% copper respectively, and are suspected to have tarnish layers composed of primarily Cu_2O and CuO .⁵⁷

Nordic Gold has been sparsely tested in the scientific community, and those studies that have been conducted have focused on its antimicrobial potential.^{2,107,108} No studies were found to analyze the corrosion rate or corrosion products formed by Nordic Gold, outside of previous studies at the University of Virginia.⁹⁹ Those studies that did examine Nordic Gold with respects to its antimicrobial potential utilized either a growth

medium or buffer solutions on the surface of the alloy. Neither of these solutions properly reflects the composition of the solution that facilitates corrosion on high touch surfaces in 30-60 RH%, standard hospital ward conditions. Corrosion would naturally occur by the transfer of perspiration from a human to the alloy's surface, which subsequently dries and is rewet by additional hand contact. It is suspected that antimicrobial testing solutions are either too mild in the case of buffer solutions, or too highly saturated in salts in the case of growth mediums to properly mimic the realistic scenario of copper ion release due to tarnish by hand perspiration. If the broth medium used was over saturated with salts, this would result in a significant reduction of the amount of dissolved oxygen and could inhibit copper ion release. Disinfection studies as a part of this project have established microorganism viability is reasonable in synthetic perspiration to allow corrosion testing, and the existence of a critical copper ion concentration in solution necessary for microorganism death, though this concentration will vary depending on organism. However, no studies were found that relate copper ion released from copper alloy surfaces to microorganism viability on the copper alloy surface.

Copper ion release is essential for antimicrobial behavior, and the greater copper ion release correlates to greater antimicrobial efficacy. However, high Cu alloys are also typically those most prone to tarnish, making them undesirable in hospital applications where aesthetics are important for the perception of cleanliness.¹¹¹ Because Nordic Gold was developed to be a tarnish resistant, nickel-free copper alloy, it poses a unique alloy for studies as a possible color-stable, antimicrobial alloy for hospital applications. However, this issue of passivation and loss of antimicrobial function must be further understood.

1.8 Thesis Objectives

1.8.1 The Fate of Copper

The purpose of this Master's thesis will be to track the fate of copper in Nordic Gold (89% Cu, 5% Zn, 5% Al, 1% Sn) compared to commercial copper C11000 (>99.9% Cu) throughout the corrosion process in synthetic perspiration compared to a broth solution, and determine the influence of the thin oxides formed on the fate of copper. Thin oxide effects will be explored by comparing the fate of copper between freshly ground, air oxidized and thermally oxidized samples of C11000 and Nordic Gold. For this study, the fate of copper refers to the path and end product of copper ions involved in the corrosion process. Possible "fates" are dissolution into the solution as Cu^+ or Cu^{2+} , incorporation into the oxide, dissolution into solution and then precipitated on the surface of the oxide in the form of insoluble corrosion products, or incongruent dissolution to generate a partially dealloyed surface zone. While the exact mechanism by which copper kills organisms is complex and still debated, sources agree that copper ions play a critical role.^{24,27-30} Therefore, alloys that release significant amounts of Cu^{2+} are likely most antimicrobial.

1.8.2 Approach

This master's thesis will focus on determining the effects of three separate variables on the fate of copper in Nordic Gold compared to commercial copper C11000: degree of surface oxidation before testing on copper ion release, alloy composition, and the corrosion environment. Alloys will be either freshly ground, furnace oxidized or air oxidized before being exposed to a test solution. Test solutions will be either a synthetic sweat solution similar to those in literature or a concentrated synthetic sweat solution that

will simulate the contact of perspiration prior to drying on an alloy's surface. Lastly, a wet-dry test regimen will be undertaken. Copper alloy samples will be exposed to full immersion conditions in a selected solution. The use of electrochemical impedance spectroscopy will attempt to correlate corrosion rate to the alloys resistance to ion release. Following exposure, alloys will be analyzed for their oxide composition by optical microscopy, grazing incidence x-ray diffraction, reflectivity, and galvanostatic reduction. The solution used in the exposure will be analyzed for copper ion content by inductively coupled plasma-optical emission spectrometry. Auger spectroscopy will be used to study alloying elements at the metal-oxide interface. Through the combination of these methods, the fate of the copper ion through the corrosion process can be tracked. The comparison of Nordic Gold to C11000 under both fresh and oxidized conditions will provide insight in the question of why and how air oxidation changes the antimicrobial efficacy, and determine whether Nordic Gold could be used as a color stable, antimicrobial surface, even after an air formed tarnish layer has been formed.

1.8.3 Thesis Organization

Chapter 1 provides an introduction to antimicrobial materials, with a focus on antimicrobial copper and its corrosion mechanisms associated with antimicrobial efficacy. A review of current EPA standards for the evaluation of antimicrobial copper is included, as well as information obtained from the Copper Development Association regarding factors that affect antimicrobial behavior in copper alloys. An in house disinfection study establishes the effect of copper ions on *E. coli*, as well as *E. coli*'s viability in a synthetic perspiration solution which serves as proof of concept for this study. A literature review of copper corrosion mechanisms and corrosion products by

atmospheric corrosion, and full immersion corrosion in saline solutions (seawater and perspiration) provides necessary background to investigate copper corrosion as a mechanism for antimicrobial efficacy. The effects of alloying composition on corrosion behavior are reviewed to determine the effect of alloying composition on antimicrobial efficacy, beyond the effect of copper content. Finally, a literature review of Nordic Gold examines the shortcomings of previous studies pertaining to Nordic Gold's antimicrobial efficacy and the need to establish an understanding of the relationship between antimicrobial efficacy and corrosion behavior.

Chapter 2 will explore the effects of full immersion in synthetic perspiration on corrosion behavior of Nordic Gold and C11000, with a focus on the effect of thin oxides formed by air oxidation, as well as thermal oxidation compared to freshly ground samples. The methods of corrosion behavior analysis are discussed. The results of this section should provide insight into the corrosion behavior of human perspiration on alloys following the formation of a passive film. Such results will be beneficial in predicting the antimicrobial efficacy of Nordic Gold as an antimicrobial high touch surface for extended periods of time in hospital applications.

Due to the drying process that perspiration transferred to surfaces undergo at the moderate humidity found in hospital environments, Chapter 3 will look at the effects of a concentrated synthetic perspiration on Nordic Gold and C11000. This concentrated synthetic perspiration will mimic the repeated transfer of perspiration to a surface over time. The increased salt load of the surface is suspected to effect corrosion behavior, and therefore likely antimicrobial efficacy. Utilization of concentrated perspiration will enable a full immersion study, where results can be compared between earlier synthetic

perspiration and broth studies to determine the effect of solution on the corrosion mechanism, including the salt and organic matter concentrations.

In order to compare to better understand the corrosion behavior of copper alloys exposed to perspiration and subsequently dried, Chapter 4 will determine the corrosion behavior of Nordic Gold and C11000 in droplets of synthetic perspiration solution during drying and re-wetting cycles. The results of drying-wetting experiments will be compared to both full immersion in synthetic perspiration and full immersion in concentrated perspiration to determine their effectiveness of predicting corrosion behavior likely to occur in hospital applications.

2 The Fate of Copper during Corrosion of Nordic Gold (89% Cu, 5% Zn, 5% Al, 1% Sn) vs. C11000 (>99.9% Cu) in Synthetic Perspiration Solution (0.5% NaCl, 0.1% CH₄N₂O, 0.1% C₃H₆O₃)

2.1 Abstract

Methicillin-resistant *staphylococcus aureus* (MRSA) is highly contagious and is spread mainly by hand-to-surface contact. In 2005, 94,650 patients in the United States contracted MRSA, and 18,650 of these patients died.¹ MRSA is especially prevalent in hospitals, where patients are infected with MRSA by touching surfaces that will, in turn, be touched by other patients whose immune systems may be compromised. This research is related to the goal of minimizing the spread of antibiotic-resistant diseases in hospitals enabled by corrosive release of Cu⁺ and Cu²⁺ from copper alloys in solutions such as human perspiration. At the same time it is desirable to maintain color stability on hospital surfaces by minimizing tarnishing. This creates a clearly contradictory situation. Unfortunately, the copper alloys with the best antimicrobial efficacy are often those that tarnish more readily. Conversely, the most corrosion resistant copper alloys in human perspiration often do not exhibit very good antimicrobial efficacy especially after long periods after abrasion. Nordic Gold (89% Cu, 5% Zn, 5% Al, 1% Sn) was reported to kill MRSA after freshly abraded, but when exposed to ambient lab conditions for 7 days, Nordic Gold passivates.² However, kill rate studies were not conducted in a solution that mimics hospital condition corrosion mechanism (i.e. salt transfer from hand perspiration due to frequent skin contact).

The goals of this study is to understand tarnishing, copper release and color stability of a Cu-Al-Zn-Sn alloy (Nordic Gold) in synthetic perspiration compared to C11000, and

the role of thin oxides such as those formed by air oxidation. This was done by tracking the “fate of copper” through the corrosion process by analysis of total copper oxidation, electrochemical analysis of the oxide layer formed, and solution analysis for dissolved copper.

Following exposure to synthetic perspiration, Nordic Gold exhibited decreased instantaneous corrosion rates and a lesser degree of tarnishing while maintaining comparable copper release rates to C11000. Additionally, the presence of thin oxides had minimal effect on C11000, but more noticeable effects on the behavior of Nordic Gold. Air oxidized Nordic Gold exhibited a decreased instantaneous corrosion rate compared to the freshly ground alloy, a thinner corrosion layer, but comparable copper release to the freshly ground sample. This behavior is attributed to the complex effect of Nordic Gold’s alloying elements.

2.2 Introduction

Due to the rising number of hospital acquired infections in recent years, significant research has explored exploiting copper alloys for their inherent antimicrobial nature to replace high touch surfaces. Antimicrobial copper alloys are evaluated based on EPA protocol “Efficacy of Copper Alloy Surfaces as Sanitizers”, guaranteeing the alloy kills 99.9% of bacteria within two hours.⁴⁹ However, this protocol only empirically evaluates the alloys antimicrobial efficacy, and offers no insight into the exact role of corrosion on copper ion release responsible for antimicrobial behavior nor the critical Cu^+ or Cu^{2+} concentration required to serve in this function. Additionally, EPA qualifications for antimicrobial copper alloys are based on the corrosion of the copper alloy in a nutrient broth ideal for growing bacteria⁴⁹⁻⁵¹, rather than on the medium that would naturally

facilitate the alloys corrosion in a hospital environment. The likely relevant environment on high touch surfaces is hand perspiration.^{112,113}

Antimicrobial behavior in copper alloys has been established as a result of microorganism's interaction with copper ions, there is a direct correlation between antimicrobial efficacy and corrosion behavior. During the corrosion process, copper ions can become part of one of several "fates" as a result of metal oxidation: retention of the metal oxide at the interface¹¹⁴, dissolution into the solution¹¹⁵, selective leaching or dealloying of other elements¹¹⁶, or dissolution into the solution followed by precipitation on the surface of the oxide as an insoluble corrosion product¹¹⁷, or complexation with species in the environment. Only those copper ions that are dissolved into the solution are responsible for antimicrobial behavior. Moreover, those ions that become part of an oxide may be sequestered.

Nordic Gold (89% Cu, 5% Zn, 5% Al, 1% Sn) is an fcc solid solution alloy that has been examined by several research groups as a possible antimicrobial material due to its high copper content.¹⁰⁶⁻¹⁰⁸ Additionally, due to its development as an alloy for European coinage, Nordic Gold is also tarnish resistant¹⁰⁵, which in combination with its high copper content makes it an attractive prospect for hospital applications where both antimicrobial efficacy and visual appeal are desired.¹¹¹ EPA testing by the Copper Development Association (CDA) indicates that Nordic Gold (89% Cu, 5% Zn, 5% Al, 1% Sn) is antimicrobial when freshly cleaned², but when exposed to ambient lab temperature and relative humidity for 7 days, it passivates completely.² When freshly cleaned, Nordic Gold is capable of reducing 10^7 colony forming units (CFU/6.4516 cm² coupon) of methicillin resistant *S. aureus* within 6 hours.² However, following exposure

to ambient lab conditions for 7 days, there is no reduction in CFU within the same 6 hour period, the same as is observed for stainless steel which is known to have no antimicrobial properties.^{1,55,56,118} EPA antimicrobial testing on Nordic Gold suggests that thin oxides are sufficient to impede the release of copper ions from the bulk alloy to the surface in order to kill bacteria, which is undesirable for longer term applications as high touch surfaces.² This exposes the lack of evaluation that has been conducted on the effect of thin oxides on corrosion rate, copper ion release, and subsequently antimicrobial activity. Other sources have also reported Nordic Gold's antimicrobial ability on a variety of microorganisms. *C. albicans* suspended in phosphate buffers solution and subsequently allowed to dry on Nordic Gold was observed to achieve full reduction from 10^6 CFU within 60 minutes on a 6.25 cm^2 area.¹⁰⁷ *S. hominis* and *S. aureus* on Nordic Gold were completely killed within 6 hours on washed and chemically sterilized European coins, and partial reductions (10% and 90%) on unwashed European coins that likely contained salt and dust deposits.¹⁰⁸ There are conflicting results regarding Nordic Gold's antimicrobial properties, likely due to the wide variety of testing procedures used to obtain kill rates. Variations between testing solution (broth or "dry"), treatment of the alloy prior to testing (freshly ground, sterilized, soiled, air oxidized) do not allow a clear picture of Nordic Gold's antimicrobial efficacy. Because the only data collected has been purely empirical and based only on kill rate data, there is a lack of information regarding what factors affect the alloys antimicrobial efficacy through the corrosion process.

Previous electrochemical studies at the University of Virginia that included Nordic Gold (89% Cu, 5% Zn, 5% Al, 1% Sn) as an alloy of interest determined that the unique combination of alloying elements resulted in unexpected corrosion behavior.¹¹⁹

Alloys containing zinc were observed to have a lower corrosion rate compared to other zinc-free alloys examined¹¹⁹, and studies by Goidanich indicate that the presence of zinc in an alloy decreases the copper ion release.³ Nordic Gold was observed to have moderate corrosion rate when exposed to synthetic perspiration compared to other alloys studied, but remained remarkably color stable following 130 hours of exposure to synthetic perspiration.¹¹⁹ Despite its moderate corrosion rate, Nordic Gold had the thinnest oxide layer, below the thickness of the copper alloy with the lowest corrosion rate studied (C75200).¹¹⁹ Additionally, it was observed to have released moderate amounts of Cu ions compared to other alloys studied following 130 exposed to synthetic perspiration.¹¹⁹ Goidanich reported that copper alloys containing Sn released similar amounts of Cu to pure copper sheets, despite having stoichiometrically less copper content, indicating additions of Sn enhance copper release from an alloy.³ The unique combination of both alloying additions that suppress corrosion rate (Zn) and enhance copper release (Sn) result in a unique alloy that may have the ability to both be antimicrobial while maintaining relatively low corrosion over time.

Corrosion behavior is a factor of both alloy composition and environment. In applications as antimicrobial high touch surfaces, copper alloys will rely on the perspiration transferred by handling to facilitate the copper ion release necessary for antimicrobial activity.^{112,113} Therefore, corrosion behavior should mimic this solution as closely as possible. The utilization of a solution that reflects the basic composition and pH of human perspiration is necessary to achieve results that can predict practical application of the alloy for its intended purpose. A variety of synthetic perspiration solutions have been utilized in research, varying in composition and pH (Table 2.1). Full

immersion testing, while not reflective of the atmospheric corrosion that would occur in hospitals, is the first step in the examination of electrochemical behavior and quantitative analysis of copper ion release into solution. The ability to determine copper ion release from a copper alloy is critical in determining a relationship between corrosion behavior and antimicrobial efficacy.

Table 2.1. Composition of synthetic perspiration solutions used in previous exposure studies	
Composition (by mass percentage)	pH
0.87% NaCl, 0.16% CH ₄ N ₂ O, 10.92% C ₃ H ₅ NaO ₃ (60% w/w), 0.016% Na ₂ HPO ₄	7.5 ⁸²
1.96% NaCl, 0.49% CH ₄ N ₂ O, 1.39% C ₃ H ₆ O ₃ , 0.25% C ₂ H ₄ O ₂ , 1.71% NH ₄ Cl	4.7 ⁸³
0.5% NaCl, 0.1% CH ₄ N ₂ O, 0.1% C ₃ H ₆ O ₃	6.5 ^{63,84,85}
0.3% NaCl, 0.1% Na ₂ SO ₄ , 0.2% CH ₄ N ₂ O, 0.2% C ₃ H ₆ O ₃	6.6 or 4.5 ⁸⁶
0.5% NaCl, 0.1% CH ₄ N ₂ O, 0.5% C ₃ H ₆ O ₃	5 ⁸⁷
0.5% NaCl, 0.1% CH ₄ N ₂ O, 0.1% C ₃ H ₆ O ₃	4.5 ⁸⁸

The objective of this study is to determine the effect of thin, air formed oxides on the corrosion of Nordic Gold (89% Cu, 5% Zn, 5% Al, 1% Sn) and on the fate of copper during corrosion in order to gain a fundamental understanding of their effect on antimicrobial activity. The behavior of Nordic Gold when freshly ground, air oxidized for 30 days in ambient lab conditions, or thermally oxidized will be compared to that of C11000, a commercially pure copper alloy, under identical conditions. Instantaneous corrosion rates will be compared to determine the effect of oxides on corrosion rate over time exposed to a synthetic perspiration solution by electrochemical impedance spectroscopy.⁸⁴ Mass loss by gravimetric analysis will also provide insight on integrated corrosion damage. The fate of copper through the corrosion process in perspiration will be tracked through analysis of oxides (optical spectrophotometry, grazing incidence x-ray diffraction, galvanostatic reduction) and copper ion release (inductively coupled plasma-

optical emission spectrometry). This study will ultimately provide a link between corrosion behavior and antimicrobial efficacy in an applications based situation, where thin oxides will form as a result of long-term use.

2.3 Experimental Procedure

C11000 (>99.9% Cu) and Nordic Gold (89% Cu, 5% Zn, 5% Al, 1% Sn) were obtained as sheets from the Copper Development association and cut in house into 2.5 x 2.5 cm coupons of varying thickness. All C11000 and Nordic Gold (89% Cu, 5% Zn, 5% Al, 1% Sn) coupons were ground using silicon carbide (SiC) metallography paper to successively finer grits up to 1200 grit. Immediately following grinding, coupons were placed in methanol to minimize oxidation until before testing. Samples were dried of methanol by compress air. Samples left in this condition for testing are designated as freshly ground (abbreviated Fresh).

2.3.1 Pre-Oxidation Conditions

Following grinding to 1200 grit, select samples were oxidized prior to immersion studies to simulate oxides that would be found in hospital environments after long term air exposure. Select alloys were left in lab air, averaging 23°C and 34% RH, for 30 days prior to immersion testing. Typical hospital conditions range from 21-24 °C and 30-60% RH.¹²⁰ These samples are here after designated air oxidized (abbreviated AirO).

Additional select samples were furnace oxidized at 170 °C for 60 minutes in attempts to accelerate oxide thickness formation without dealloying. These samples are here after designated furnace oxidized (abbreviated FurO).

2.3.2 Exposure Experiments

A synthetic perspiration solution was made based on standard BS EN 1811:2011.⁸⁴ Synthetic perspiration was prepared using purified water (resistivity 18.2 M Ω -cm) produced by an Academic MilliQ filtration system (MilliPore) and reagent grade chemicals were used to dissolve 5 g/L NaCl (Sigma-Aldrich), 1 g/L Urea (CH₄N₂O) (Fisher Scientific), and 1 g/L Lactic Acid (C₃H₆O₃) (90%, Acros Organics), and the pH adjusted by addition of ammonium hydroxide (NH₄OH) (Fisher Scientific) to 6.5 (\pm .05) (Table 2.2). Synthetic perspiration solution was used at ambient aeration at 23 °C within 24 hours of preparation, stable at pH 6.5.

Table 2.2. Composition of synthetic perspiration solution in g/L and M.			
Chemical	Molecular Weight	Concentration (g/L)	Molarity (M)
NaCl	58.44	5	0.08556
CH ₄ N ₂ O	60.06	1	0.01665
C ₃ H ₆ O ₃	90.08	1	0.00999

Samples were placed in individual electrochemical flat cell with a 1 cm diameter circular aperture and an area of 0.8 cm². Cells were filled with 300 mL of synthetic perspiration and allowed to sit unstirred at ambient lab temperature (23 °C) and ambient aeration for 12, 48, 96, or 130 hours before samples were removed and dried by compressed air. Between each exposure, cells were washed with 0.1 M HCl to remove synthetic perspiration buildup and possible copper product precipitates along the cell walls.

2.3.3 E-I Behavior and Open Circuit Potential of C11000 and Nordic Gold

Cyclic voltammetry (CV) experiments were conducted on Princeton Applied Research Model 273A potentiostats with CorrWare software. Experiments were conducted in chloride free electrochemical flat cells utilizing a conventional 3-electrode

setup. This utilized a mercury-mercury sulfate electrode (MSSE), a platinum-mesh counter electrode, and the sample as a working electrode with an area of 0.8 cm^2 . Tests were conducted at 0.02 mA/cm^2 in deaerated borate buffer solution ($\text{Na}_2\text{B}_4\text{O}_7 + \text{H}_3\text{BO}_3$), pH 8.4. Experiments cycled potentials between -1.4 and 0 V versus the reference for a total of 5 cycles, with a collection rate of 1 mV/s.

Open circuit potential (OCP) experiments were conducted in electrochemical flat cells utilizing a conventional 3-electrode setup. This utilized a saturated calomel reference (SCE) electrode with a luggin probe to minimize solution resistance, a platinum-mesh counter electrode, and the sample as a working electrode. OCP-EIS was conducted in 300 mL synthetic perspiration solution at 23 °C and ambient aeration. OCP was conducted on a combination of Gamry Reference 600, Gamry PCI4, and Gamry Femtostat potentiostats controlled by Gamry Framework software. Cyclic polarization (CP) experiments were conducted following 1 hour held at OCP, beginning from 10 mV below OCP, and potential ranges from $0.085 \text{ V}_{\text{SCE}}$ to $-0.04915 \text{ V}_{\text{SCE}}$ with a collection rate of 1 mV/sec and 1 point/mV.

2.3.4 Corrosion Rate by OCP-EIS and Mass Loss

2.3.4.1 Open Circuit Potential-Electrical Impedance Spectroscopy

Open circuit potential-Electrical Impedance Spectroscopy (OCP-EIS) tests were conducted in electrochemical flat cells utilizing a conventional 3-electrode setup. This utilized a saturated calomel reference (SCE) electrode with a luggin probe to minimize solution resistance, a platinum-mesh counter electrode, and the sample as a working electrode. OCP-EIS was conducted in 300 mL synthetic perspiration solution at 23 °C and ambient aeration.

OCP-EIS was conducted on a combination of Gamry Reference 600, Gamry PCI4, and Gamry Femtostat potentiostats controlled by Gamry Framework software. OCP was held for 30 minutes at designated time increments prior to EIS. EIS was conducted from $1 \times 10^5 - 1 \times 10^{-3}$ Hz at an amplitude of 10 mV RMS, with data collection occurring at 8 points/decade. A minimum of 3 replicates per corresponding sample and exposure time were obtained. Error was determined by standard deviation of the sample set.

Data was analyzed using Gamry EChem Analyst (Version 6.11) and with the equivalent circuit shown in Figure 2.1 with associated variables.^{121,122} R_1 is the solution resistance, R_2 is the resistance to charge transfer, R_3 is the resistance of the oxide, and Z_D is responsible for finite, porous diffusion impedance likely due to the oxygen reduction reaction in pores of the oxide¹²². Equations 2.1-2.4 define the relationship between the variables such as the constant phase elements (CPE) and the finite porous diffusion impedance (Z_D) in terms of their complex impedances. The polarization resistance (R_P) is defined in Equation 2.5. The instantaneous corrosion rate is taken to be proportional to inverse polarization resistance ($1/R_P$) and taken as B/R_P , where $B = \left(\frac{1}{2.303} \right) \left(\frac{\beta_a \beta_c}{\beta_a + \beta_c} \right)$. B^* is a term used to define the quotient of the diffusion layer thickness and the square-root of the average diffusion coefficient (Equation 2.3) Data was fit using the Simplex Method, with B_5 limited to $10-70 \text{ s}^{1/2}$, according to sample calculations of typical diffusion rates and boundary layer thickness. The remaining variables were left unbounded. Corrosion rate ($1/R_P$) was related to charge (Q_{corr}) through the Stern-Geary approach and integration of charge utilizing Equations 2.6-2.8. B is a function of the anodic (β_a) and cathodic (β_c) Tafel slopes, and fixed at 0.057 V (Equation 2.7).¹²³

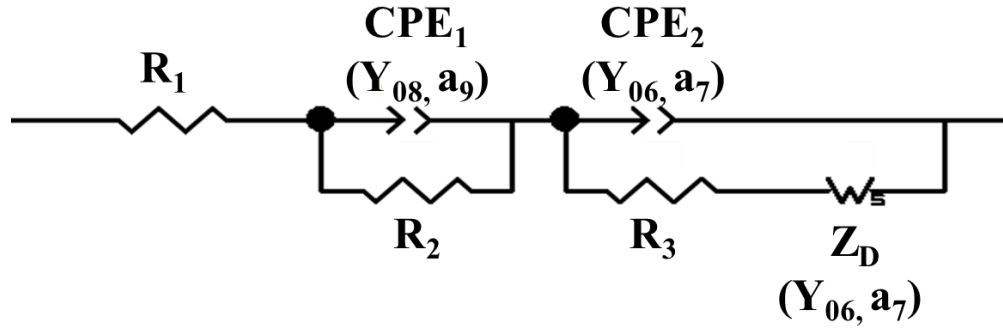


Figure 2.1. Equivalent circuit used to model corrosion behavior of copper alloys.

$$\text{CPE:} \quad Z = \frac{1}{j\omega^a} \quad \text{Equation 2.1}$$

$$\text{W:} \quad Z_D = R_D \frac{\tanh\{B\sqrt{j\omega}\}}{B\sqrt{j\omega}} \quad \text{Equation 2.2}$$

$$B * = \frac{\delta}{D^{1/2}} \quad \text{Equation 2.3}$$

$$R_D = \frac{B_5}{Y_{04}} \quad \text{Equation 2.4}$$

$$\text{Polarization Resistance:} \quad R_p = R_2 + R_3 + R_D \quad \text{Equation 2.5}$$

$$\text{Q}_{corr}: \quad i_{corr} = \frac{B}{R_p} = \frac{1}{R_p} \left(\frac{1}{2.303} \right) \left(\frac{\beta_a * \beta_c}{\beta_a + \beta_c} \right) \quad \text{Equation 2.6}$$

$$B = \left(\frac{1}{2.303} \right) \left(\frac{\beta_a * \beta_c}{\beta_a + \beta_c} \right) \quad \text{Equation 2.7}$$

$$Q_{corr} = \int i_{corr} * A * dt \quad \text{Equation 2.8}$$

2.3.4.2 Mass Loss by Gravimetric Analysis

Mass loss was conducted in accordance to ASTM G1-03. Baseline mass loss was conducted on freshly ground (1200 grit) copper alloy samples, preserved in methanol.

Copper alloys masses were obtained after freshly ground (1200 grit, preserved in methanol) and after 130 hour exposure to synthetic perspiration by an analytical balance (M-220D, Denver Instrument). Copper alloys were cleaned by exposing the corroded

surface to 6 M HCl for 3 minutes at ambient lab temperature, washing with Millipore water and drying by compressed air. Mass changes were obtained after cleaning on the same instrument. Freshly ground copper alloy mass loss was utilized as a baseline measurement to determine the effect of corrosion product removal on the bare metal. The effect of cleaning was established to cause negligible dissolution of the metallic alloy, with no mass loss occurring in Nordic Gold before and after cleaning, and 0.1 mg mass loss occurring in C11000. Mass loss (Δm) was equated to charge (Q_{corr}) utilizing Equation 2.9, where F is Faraday's constant (96500 Coulombs/equivalent), and $E.W.$ is equivalent weight (grams/equivalent) Equivalent weights were calculated for both Cu^+ and Cu^{2+} for comparison, as shown in Equation 2.10, where f is the weight fraction of alloying elements, n is the number of equivalent electrons exchanged (equiv./mol), and a is atomic weight. $E.W.$ for C11000 was defined as 63.546 g/equiv. (Cu^+) or 31.773 g/equiv. (Cu^{2+}). Table 2.3 defines calculations for $E.W.$ for an alloy such as Nordic Gold. Congruent dissolution was assumed in all cases. Additionally, a B value was calculated based on Q_{corr} obtained by mass loss in order to compare to the assumed value of $B=0.057$ V utilized in electrochemical impedance spectroscopy calculations.

$$Q_{corr} \text{ by Mass Loss} = \Delta m F / (E.W.) \quad \text{Equation 2.9}$$

$$E.W. = \sum \frac{f_i n_i}{a_i} \quad \text{Equation 2.10}$$

Table 2.3. Calculation of equivalent weight of Nordic Gold using either Cu^+ or Cu^{2+} .

Reaction	Nernst Potential (E°/V) (SHE)	Equivalent Electrons (equiv./mol)	Atomic weight (g/mol)	Weight Fraction (wt%)	Equivalent Weight (E.W) (g/equiv.)
$\text{Cu}^+ + e^- = \text{Cu}$	0.521	1	63.546	89	47.03036
$\text{Cu}^{2+} + 2e^- = \text{Cu}$	0.342	2	63.546	89	28.35394
$\text{Al}^{3+} + 3e^- = \text{Al}$	-1.662	3	26.982	5	
$\text{Zn}^{2+} + 2e^- = \text{Zn}$	-0.762	2	65.38	5	
$\text{Sn}^{2+} + 2e^- = \text{Sn}$	-0.138	2	118.71	1	

2.3.5 Corrosion Product Analysis

2.3.5.1 Optical Spectrophotometry

Reflectivity was used as a means to determine the degree of tarnish, and thus aesthetic appeal, of the tarnished surfaces. Optical reflectance as a function of wavelength was determined by using a tungsten halogen lamp (LS-1, Ocean Optics), reflection probe (R400-7-VIS/NIR, Ocean Optics) and coupled optical spectrometer (Jaz, Ocean Optics) using SpectraSuite software. The light source was held at a fixed distance perpendicular (90°) to the sample surface using a RPH-1 reflection probe holder. A STAN-SSH High-reflectivity specular reflectance standard was used for calibration of the light reference (100%) which guarantees 85-90% reflectance across 250-800 nm and 85-98% reflectance across 800-2500 nm. Integration time was set automatically using SpectraSuite software, and measurements were conducted using 10 scans to average, with a boxcar width of 5 to increase signal to noise ratio. Particular interest was paid to the visible light region, wavelengths 370-730 nm. One sample per alloy, pre-exposure treatment, and time was conducted as a representative of the 3 samples exposed. The test area was determined as an area where visual composition matched the majority composition of the surface.

2.3.5.2 Grazing Incidence X-Ray Diffraction

Grazing incidence X-ray diffraction measurements were carried out on a Panalytical X'Pert Pro MPD diffractometer applying the associated software (DataCollector). Cu-K α radiation ($\lambda = 1.5406 \text{ \AA}$) was used in all experiments. The incident beam was conditioned using a parallel beam X-ray mirror for Cu radiation with a $1/32^\circ$ divergent slit and 20 mm mask. The use of a 20 mm mask ensured that signal was measured from a line across the entire sample, resulting in the averaging of potentially heterogeneous sections of the oxide. A beam attenuator with 0.125 mm Ni foil was employed for the alignment of the sample following standard alignment procedures. Samples were placed in the center of an Eulerian cradle mounting stage, and an incident angle of 0.5° was used for measurements, limiting depth of interaction to $0.2 \text{ }\mu\text{m}$.¹²⁴ The diffracted beam was conditioned with a parallel plate collimator, parallel plate collimator slit (with alignment only), and 0.04 radians Soller slits, then recorded using a proportional Xe detector. The 2θ scan range was $20\text{-}100^\circ$.

2.3.5.3 Galvanostatic Reduction to Analyze Oxides

Galvanostatic reduction operates on the principle of electrochemically reducing corrosion products sequentially through the application of constant current. The corrosion products with the highest reduction potentials are reduced first. Based on work by Nakayama, Kaji, Shibata, Notoya, and Osakai, galvanostatic reduction can be used to identify the order of reduction in copper oxides (CuO, Cu₂O) that was previously debated.¹²⁵ As seen in Figure 2.2, CuO is known to reduce first, followed by the reduction of Cu₂O, a result of the oxides sandwich like structure where Cu₂O is contained by CuO and metallic Cu.

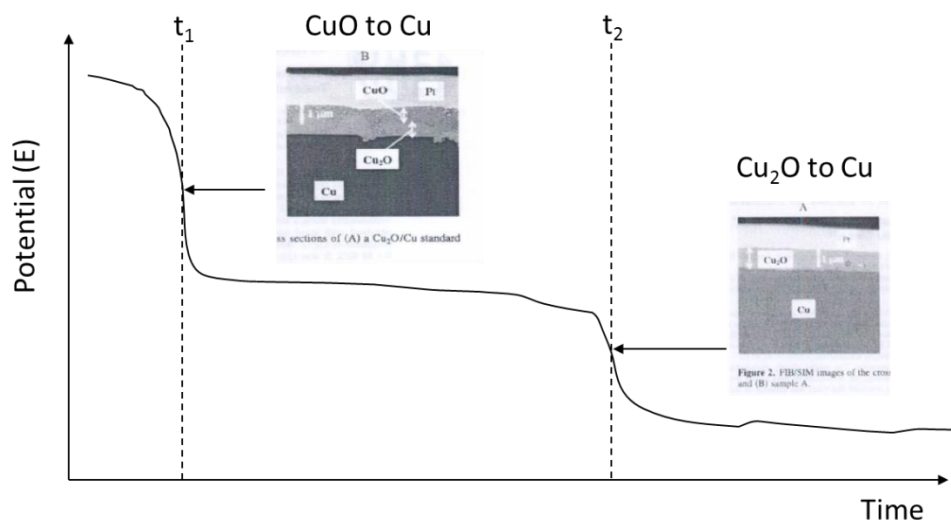


Figure 2.2. Reduction order of copper oxides CuO and Cu₂O.¹²⁵ However, other papers suggest CuO reduces to Cu₂O, rather than to CuO to Cu as reported here.^{126,127}

Galvanostatic reduction experiments were conducted on Princeton Applied Research Model 273A potentiostats with CorrWare software. Experiments were conducted in chloride free electrochemical flat cells utilizing a conventional 3-electrode setup. This utilized a mercury-mercury sulfate electrode (MSSE), a platinum-mesh counter electrode, and the sample as a working electrode. Tests were conducted at 0.02 mA/cm² in deaerated borate buffer solution (Na₂B₄O₇+H₃BO₃), pH 8.4, with a collection rate of 1 point/sec. A minimum of 3 replicates per corresponding sample and exposure time were obtained. Table 2.4 compares the galvanostatic reduction method utilized against methods used in ASTM B825¹²⁸ and Nakayama, et al.¹²⁵

Table 2.4. Comparison of galvanostatic reduction methods utilized in ASTM standard, Nakayama's previous study and previously used in house method.			
Method	Solution	pH	i _{corr}
ASTM B825 ¹²⁸	1 M KCl	7	1.0 mA/cm ²
Nakayama ¹²⁵	0.1 M KCl	7	0.5 mA/cm ²
	1 M KOH	14	
	6 M KOH + 1 M LiOH	14	
Experimental Procedure	0.019 M Na ₂ B ₄ O ₇ + 0.131 M H ₃ BO ₃	8.4	0.02 mA/cm ²

ASTM B825 was utilized to determine the precise time associated with reduction peak characteristics by determination of differential inflection points (Figure 2.3).¹²⁸ Derivatives were manually calculated as the difference of potential between 15 consecutive seconds, and inflection points determined by visual evaluation. Inflection peaks correspond to times when a full reduction of a species occurred. For example, Figure 2.3 shows the reduction of CuO and Cu₂O, where t_1 corresponds to the time at which the full reduction of CuO is achieved, and t_2 corresponds to the time at which the full reduction of Cu₂O is achieved. Potentials that correspond to the inflection point time were determined by the peak preceding the inflection point, by the average of the first 15 seconds in the case of the first reduction peak and visual evaluation for those following. In Figure 2.3, E_1 corresponds to the potential at which CuO is reduced, and E_2 corresponds to the potential at which Cu₂O is reduced. Data is often represented as inflection point-reduction potential pairs (t_i, E_i), indicated by circles in Figure 2.3. Table 2.5 lists the half-cell reactions for possible corrosion products that could be reduced by galvanostatic reduction. Chloride concentration ($[Cl^-]$) was assumed to be 10^{-8} M as reductions were conducted in Cl^- free cells. Hydrogen concentrations ($[H^+]$) were derived from pH (8.4). The exposure spot size (0.8 cm^2) was matched precisely to the reduction spot size (0.8 cm^2), so that all corrosion products were reduced simultaneously.

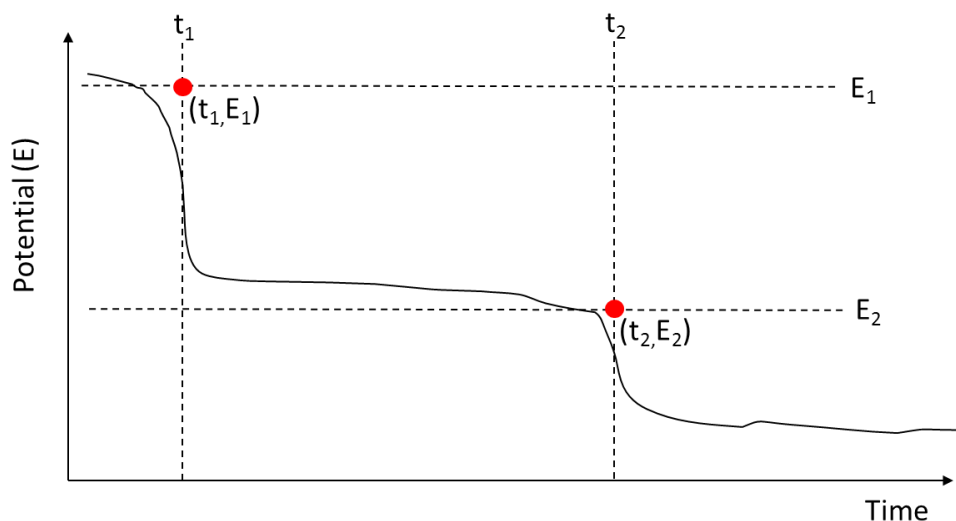


Figure 2.3. Galvanostatic reduction analysis corresponds time to completely reduce a corrosion species (t_i) to inflection points on the galvanostatic reduction spectra, and reduction potential (E_i) to the plateau preceding the inflection point.

Table 2.5. Possible corrosion products reduced by galvanostatic reduction at potentials below associated half-cell potentials. Assumptions were that $[Cl^-]$ is 10^{-8} M, $[H^+]$ is 3.98×10^{-9} M, and $[OH^-]$ is 2.51×10^{-6} M for pH 8.4.			
Half Cell Reaction	V_{SHE}	V_{SCE}^{vii}	V_{MMSE}^{viii}
$2CuO \bullet H_2O + 2e^- \rightarrow Cu_2O + 2OH^- + H_2O$	0.25056	0.00956	-0.39944
$Cu_2(OH)_3Cl + 4e^- \rightarrow 2Cu + Cl^- + 3OH^-$	0.24588	0.00488	-0.40412
$CuCl_2 \bullet 3Cu(OH)_2 + 8e^- \rightarrow 4Cu + 2Cl^- + 6OH^-$	0.19228	-0.04872	-0.45772
$Cu_2O + H_2O + 2e^- \rightarrow 2Cu + 2OH^-$	-0.02544	-0.26644	-0.67544
$Sn(O)^* + 2H^+ + 2e^- \rightarrow Sn + H_2O$	-0.58744	-0.82844	-1.23744
$Zn(O)^{**} + 2H^+ + 2e^- \rightarrow Zn + H_2O$	-0.89644	-1.13744	-1.54644

* Assumed to be hydroxylated $Sn(OH)_2$
 ** Assumed to be amorphous hydroxylated $Zn(OH)_2$

2.3.6 Solution Analysis by ICP-OES

Inductively coupled plasma-optical emission spectrometry (ICP-OES) was utilized to determine copper ions released from alloys. ICP-OES samples were collected at times corresponding to the removal of copper alloy samples for surface analysis of

^{vii} $V_{SCE} = V_{SHE} - 0.241$

^{viii} $V_{MMSE} = V_{SHE} - 0.650$

corrosion products at 12, 48, 96 and 130 hours, and were not acidified. Copper alloy samples had a surface to volume ratio of $2.67 \text{ cm}^2/\text{L}$ during the exposure time. A 300 mL aliquot of 0.1 M HCL was used to wash the cell following exposure, where the sample hole was covered with inert parafilm wax to prevent leakage. This wash solution was initially analyzed in addition to the exposure solution to determine possible corrosion product precipitation along the walls of the cell during exposure. Early measurements indicated that levels of Cu, Zn, Al, and Sn were all below calibration limits, and it was surmised that no measurable precipitation along the cell walls occurred. Note that while ICP-OES can detect elements in solution regardless of complexation with other matter in the solution, it cannot differentiate between oxidation states (Cu^+ or Cu^{2+}).

Measurements were conducted using a Thermo Scientific iCAP 6200 with a HF-compatible sample introduction system. A yttrium (Y) internal standard was utilized to account for instrumental fluctuations, and observed a wavelengths 230.6 and 325.6 nm, which were determined to have no interference with elements possible in sample solutions (Cu, Al, Zn, or Sn). Calibration was conducted in Millipore water and synthetic perspiration after 130 hours (with no exposure to copper alloys) with additions of 0.1-100 ppm Cu using single element ICP-OES standards (Agilent Technologies). Figure 2.4 compares the calibration of the two solutions at 224.7 nm. A calibration of signal intensity versus copper content was used to determine copper content (ppm) in test solutions. A minimum of 3 replicates per corresponding sample and exposure time were analyzed, each analyzed at 224.7 nm in triplicate. Raw concentrations were manipulated as seen in Figure 2.5 to achieve concentration in $\text{Cu ions}/\text{cm}^2$. Table 2.6 lists possible copper precipitates, associated solubility constants (K_{sp}) and maximum concentration of

Cu^{2+} or Cu^+ as ions possible in solution 300 mL solution before a product may precipitate. Concentrations for solubility concentrations were taken as $[\text{Cl}^-] = 8.6 \times 10^{-2}$ M, $[\text{H}^+] = 3.2 \times 10^{-7}$ M, $[\text{OH}^-] = 3.2 \times 10^{-8}$ M. Copper ion release rates (m) are calculated linearly ($mx+b$) from 12 to 130 hours, and initial 12 hour release rate determined by y-intercept (b).

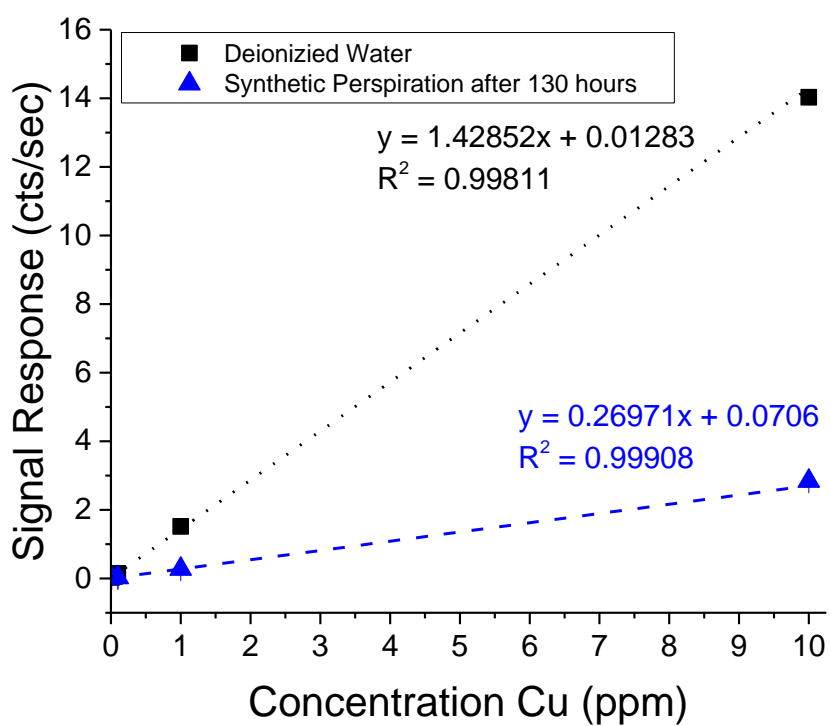


Figure 2.4. Comparative calibration curves of Cu in deionized water and synthetic perspiration after 130 hours (no exposure to copper alloys) at 224.7 nm.

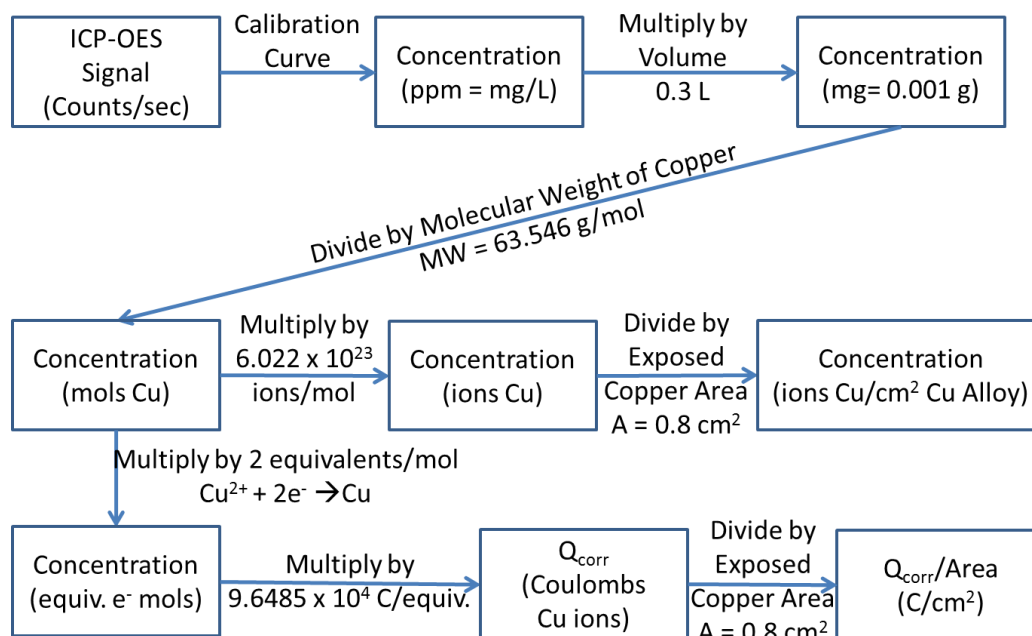


Figure 2.5. Procedural flow chart of converting signal obtained by ICP-OES to copper ion release (ions/cm²).

Chemical Formula	Reaction	K_{sp}	Solubility of Cu^+ or Cu^{2+} (ions/300 mL)
$Cu_2(OH)_3Cl$ (atacamite)	$2Cu^{2+} + 3 OH^- + Cl^- = Cu_2(OH)_3Cl$	1.72×10^{-35}	8.18×10^{15}
Cu_2O (cuprite)	$2Cu^+ + OH^- = Cu_2O + H^+$	2.6×10^{-2}	6.74×10^{22}
$CuCl$ (nantokite)	$Cu^+ + Cl^- = CuCl$	1.86×10^{-7}	1.81×10^{17}

2.4 Results

2.4.1 E-I Behavior and Open Circuit Potential of C11000 and Nordic Gold

It is well known that alloy composition affects corrosion behavior. The addition of Zn is routinely seen to lower the corrosion rate of copper alloys, correlating well with the reports of poor antimicrobial behavior in Cu-Zn alloys.¹¹⁹ While Al successfully enhances the tarnish resistance of copper alloys^{97,98}, this effect does not lead to poor

antimicrobial behavior except when in excess of 8%.⁵⁶ The observation Cu- Sn do not result in the expected stoichiometric reduction of Cu ion release compared to pure Cu indicates a mechanism in which Sn enhances the ion release from the bulk alloy.³ While these effects have been observed independently, the interaction of these effects in an alloy are not well understood. Comparing the corrosion behavior of Nordic Gold to the well-known corrosion behavior of pure copper (C11000) will offer valuable insight regarding the complex effect of secondary alloying elements.

The presence of Zn, Al, and Sn on electrochemical behavior was observed to affect electrochemical behavior during the corrosion process. The formation and reduction of corrosion products on C11000 and Nordic Gold were observed through cyclic voltammetry in deaerated borate buffer solution (pH 8.4) to complement galvanostatic reduction. As seen in Figure 2.6, the formation of Cu_2O (a_1) occurs at a slightly higher potential on Nordic Gold compared to C11000, and results in a higher peak. CuO (a_2) is shifted to a lower potential and results in a lower peak in Nordic Gold compared to C11000. The reduction of CuO (c_2) and Cu_2O (c_1) on Nordic Gold both occur at slightly more negative potentials compared to C11000. This is consistent with observations made during the galvanostatic reduction of Nordic Gold consistently having lower reduction potentials prior and following exposure to synthetic perspiration, indicating that there is some minor effect of Zn, Al or Sn specifically on Cu peak position. Despite the presence of Zn, Al and Sn, the only oxidation and reduction peaks observed were CuO and Cu_2O . As seen in Figure 2.7, the open circuit potential of Nordic Gold is initially significantly lower than C11000, but rises steadily with time compared to the relatively stable OCP of C11000. This is likely due to the dealloying of Zn or Al early

in the corrosion process, and is suspected to stabilize below the OCP of C11000 at longer times.¹¹⁹ While the anodic behavior of Nordic Gold and C11000 in synthetic perspiration is similar, cathodic behavior varies (Figure 2.8). Both alloys reduce the primary corrosion product near $-0.2 V_{SCE}$, presumed to be Cu_2O , with Nordic Gold having slightly lower reduction potentials. C11000 reduces a second corrosion product near $-0.4 V_{SCE}$, presumed to be CuO . Nordic Gold reduces two lesser corrosion products near -0.35 and $-0.425 V_{SCE}$, possibly a Zn, Al or Sn oxide and CuO respectively. It is possible that ions released into the solution are reduced as well.

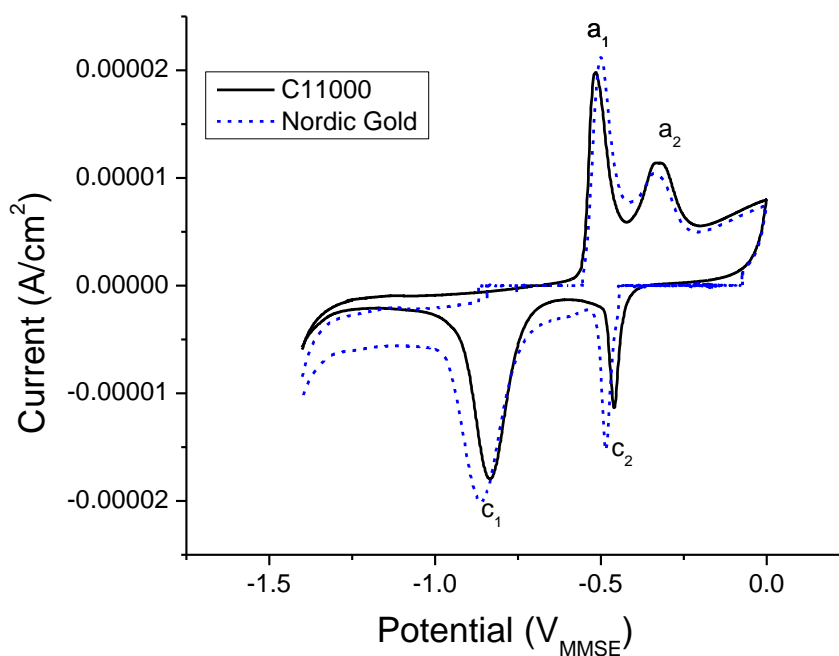


Figure 2.6. Cyclic voltammetry of C11000 and Nordic Gold freshly ground to 1200 grit, exposed to deaerated borate buffer (pH 8.4).

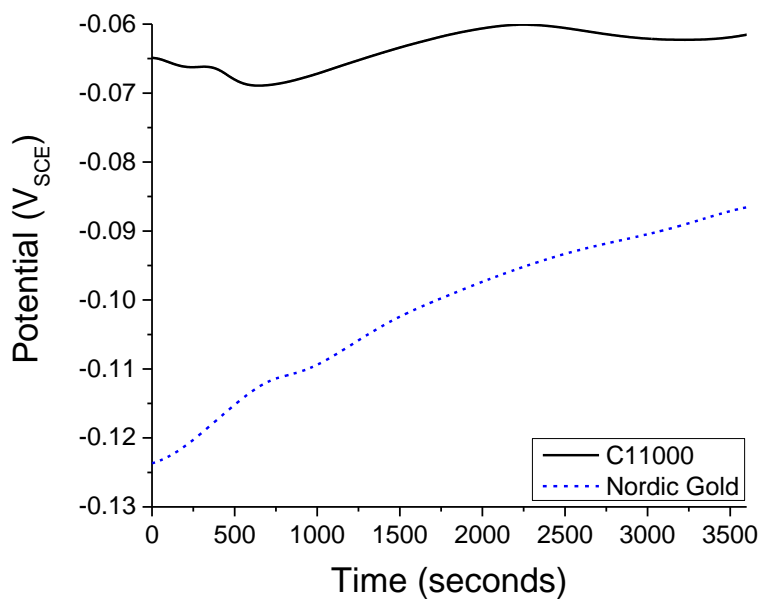


Figure 2.7. Open circuit potential (OCP) of C11000 and Nordic Gold freshly ground to 1200 grit and exposure to synthetic perspiration (23 °C, ambient aeration) for 1 hour.

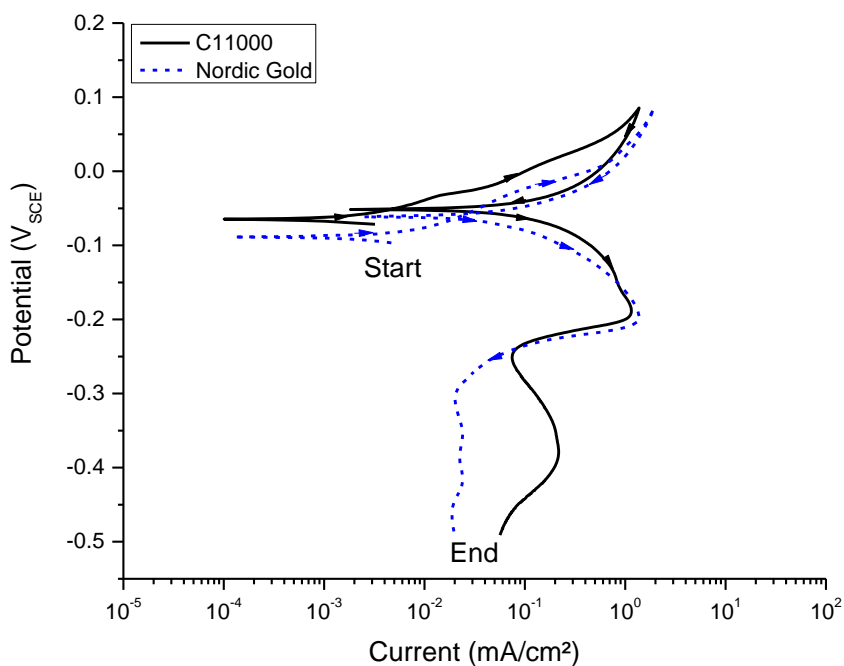


Figure 2.8. Cyclic polarization (CP) of C11000 and Nordic Gold freshly ground to 1200 grit and exposure to synthetic perspiration (23 °C, ambient aeration) for 1 hour prior to CP.

2.4.2 Corrosion Rate by OCP-EIS and Mass Loss

2.4.2.1 Instantaneous Corrosion Rate by EIS

Open circuit potential was held for 30 minutes prior to electrochemical impedance spectroscopy. After exposure to perspiration for 30 minutes, all alloys demonstrated complex EIS behavior consistent with diffusional impedance likely due to the occurrence of oxygen reduction reactions.¹²² EIS behavior was dependent on time exposed to synthetic perspiration, alloy composition, and pre-treatment conditions (freshly ground, thermally oxidized or air oxidized). Figures 2.9-2.10 show example Nyquist fits using the fitting method described in experimental procedure, which shows good agreement between data and model fit. The data used in the model is shown.

Over time, the instantaneous corrosion rate of both C110000 and Nordic Gold decrease. Figures 2.11-2.12 demonstrate example progression of EIS behavior over time for freshly ground C11000 and Nordic Gold. Over time, low frequency impedance values increase and the peak phase shifts to lower frequencies. A comparison of the exposure time dependence of instantaneous corrosion rate can be seen in Figures 2.13-2.15, where the comparison between 0 and 130 hours in synthetic perspiration solution support that regardless of alloy composition whether samples were freshly ground or air oxidized under ambient lab conditions for 30 days, the instantaneous corrosion rate decreases with exposure time. At low frequencies ($10^{-3} - 10^{-2}$ Hz) at 0 hours exposure to synthetic perspiration (23 °C, ambient aeration) after thermally oxidation at 170 °C for 60 minutes, samples exhibited complex behavior that did not fit the model utilized. These were attributed to the sensitivity of low frequency EIS to convection, particularly when diffusional impedance is involved. For comparative analysis, Nordic Gold and C11000

when thermally oxidized at 170 °C for 60 minutes at 0 hours of exposure were only analyzed to frequencies as low as 10^{-2} Hz. When this limitation is applied, thermally oxidized samples also exhibited decreased corrosion rates over time.

Alloy composition also affected EIS behavior, as seen in Figures 2.13-2.15. When freshly ground to 1200 grit (Figure 2.13) and first exposed to synthetic perspiration solution (23° C, ambient aeration), Nordic Gold produces a lower corrosion rate compared to C11000, and the phase angle is shifted towards higher frequencies in Nordic Gold compared to C11000. After exposure to synthetic perspiration (23° C, ambient aeration) for 130 hours, Nordic Gold continues to produce a lower corrosion rate compared to C11000, but the Nordic Gold phase angle shifts to higher frequencies, while the C11000 phase angle shifts to lower frequencies. These behaviors are also consistent when both alloys have been thermally oxidized at 170 °C for 60 minutes (Figure 2.14) and air oxidized at ambient lab conditions for 30 days (Figure 2.15). Charge analysis by EIS of C11000 and Nordic Gold utilizing the average instantaneous corrosion rate ($1/R_p$) at 0 and 130 hours of exposure to synthetic perspiration (23 °C, ambient aeration) are listed in Table 2.7.

Table 2.7. Charge analysis by EIS for C11000 and Nordic Gold when freshly ground to 1200 grit, furnace oxidized at 170 °C for 60 minutes, or air oxidized at ambient lab conditions for 30 days, then exposed to synthetic perspiration solution (23 °C, ambient aeration) for 130 hours. $Q_{\text{corr}}/\text{area}$ by EIS were calculated as seen in Equations 2.5-2.8, where $B= 0.057 \text{ V}$.¹²³ Data is the average of a minimum of 3 replicates with standard deviation.

	0 Hours Exposure Synthetic Perspiration	130 Hours Exposure Synthetic Perspiration	
Alloy: Treatment	$1/R_p$ (ohms ⁻¹ /cm ²)	$1/R_p$ (ohms ⁻¹ /cm ²)	$Q_{\text{corr}}/\text{area}$ (C/cm ²)
C11000: Freshly Ground	1.76×10^{-4} ($\pm 8.89 \times 10^{-5}$)	7.81×10^{-5} ($\pm 5.23 \times 10^{-5}$)	3.38 C/cm ²
C11000: Furnace Oxidized	2.36×10^{-4} ($\pm 5.08 \times 10^{-5}$)	8.83×10^{-5} ($\pm 1.55 \times 10^{-5}$)	4.31 C/cm ²
C11000: Air Oxidized	2.04×10^{-4} ($\pm 1.16 \times 10^{-5}$)	4.46×10^{-5} ($\pm 1.37 \times 10^{-5}$)	3.30 C/cm ²
Nordic Gold: Freshly Ground	1.84×10^{-4} ($\pm 7.34 \times 10^{-5}$)	4.05×10^{-5} ($\pm 2.12 \times 10^{-5}$)	2.98 C/cm ²
Nordic Gold: Furnace Oxidized	1.55×10^{-4} ($\pm 9.28 \times 10^{-5}$)	6.58×10^{-5} ($\pm 4.94 \times 10^{-5}$)	2.93 C/cm ²
Nordic Gold: Air Oxidized	9.22×10^{-5} ($\pm 3.77 \times 10^{-5}$)	6.10×10^{-5} ($\pm 1.09 \times 10^{-5}$)	2.04 C/cm ²

The presences of thin oxides on the surface of copper alloys were also observed to affect EIS behavior. At 0 hours exposure to synthetic perspiration (23 °C, ambient aeration), the presences of thin oxides by thermal oxidation and air oxidation increased the instantaneous corrosion rates of C11000, but decreased the instantaneous corrosion rate on Nordic Gold. Following exposure to synthetic perspiration (23 °C, ambient aeration) for 130 hours, thin oxides formed by thermal oxidation continued to result in a slightly higher instantaneous corrosion rate of C11000 and Nordic Gold compared to freshly ground samples, though within one standard deviation (Figure 2.16). Thin oxides formed by natural air oxidation at room temperature continued to result in slightly lower instantaneous corrosion rates of C11000 and Nordic Gold compared to freshly ground samples, though also within one standard deviation (Figure 2.17). Figure 2.18 provides a summary of instantaneous corrosion rate ($1/R_p$) following exposure to synthetic perspiration (23 °C, ambient aeration) for 130 hours.

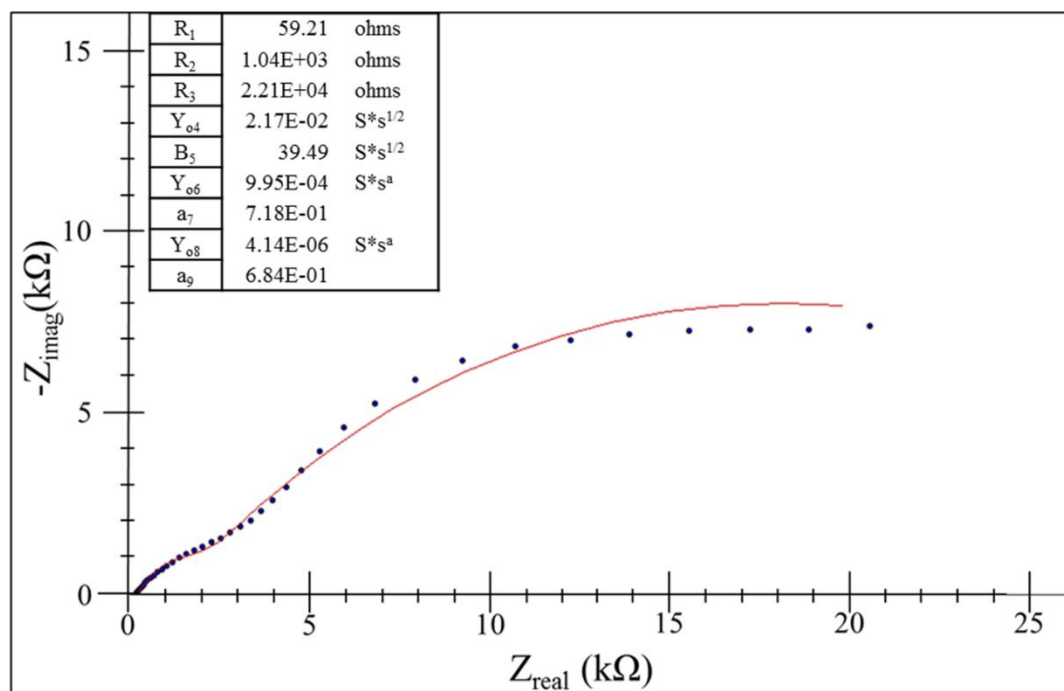


Figure 2.9. Nyquist plot of C11000 freshly ground to 1200 grit, then exposed to synthetic perspiration solution (23 °C, ambient aeration) for 130 hours, overlaid with model fit by the Simplex method. The exposure area was 0.8 cm².

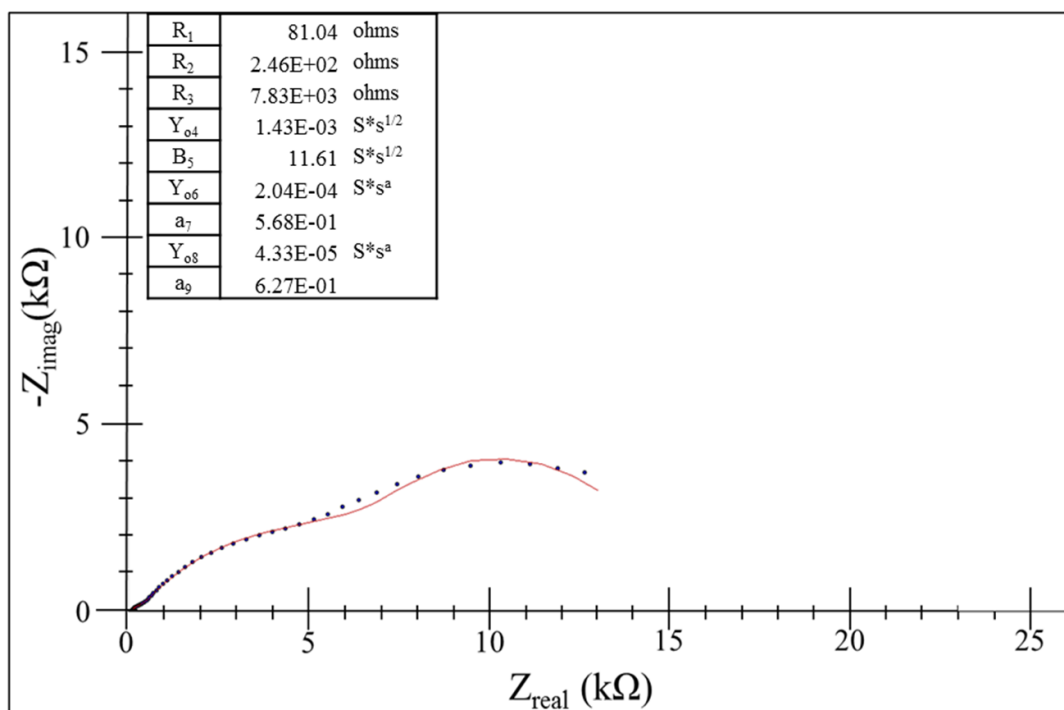


Figure 2.10. Nyquist plot of Nordic Gold freshly ground to 1200 grit, then exposed to synthetic perspiration solution (23 °C, ambient aeration) for 130 hours, overlaid with model fit by the Simplex method. The exposure area was 0.8 cm².

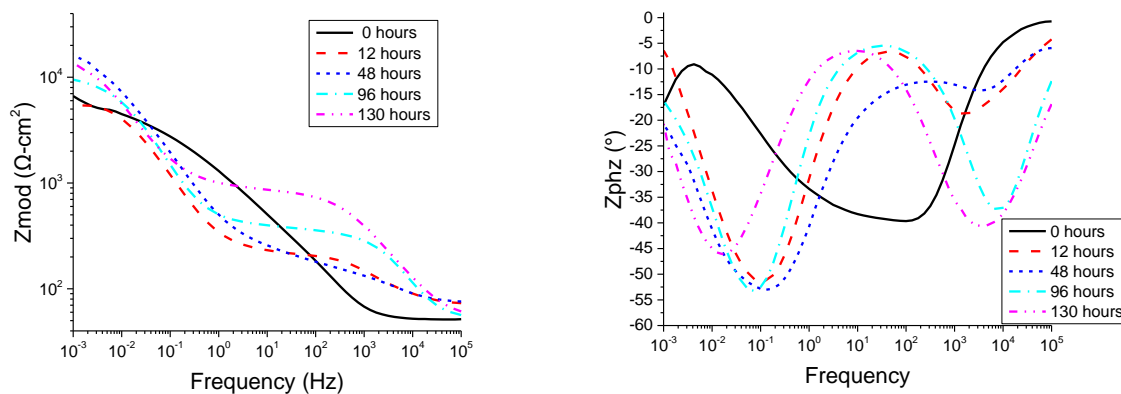


Figure 2.11. Bode plots of C11000 freshly ground to 1200 grit, then exposed to synthetic perspiration solution (23 °C, ambient aeration) for various times indicated.

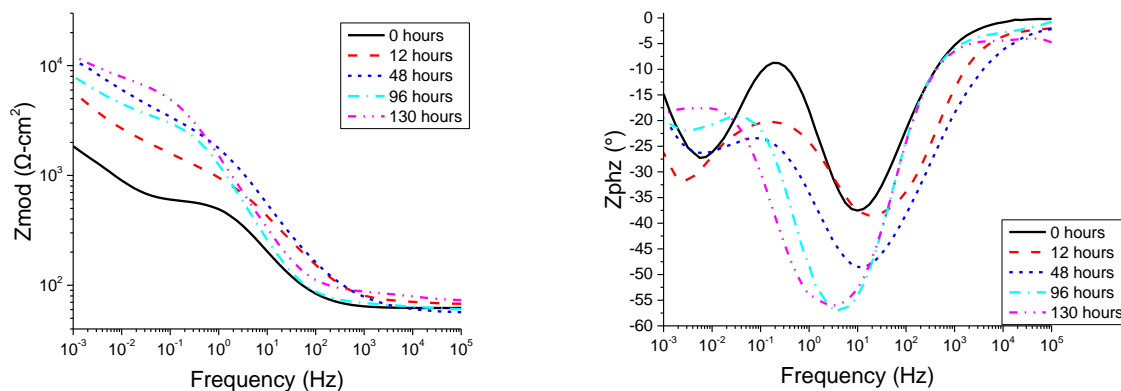


Figure 2.12. Bode plots of Nordic Gold freshly ground to 1200 grit, then exposed to synthetic perspiration solution (23° C, ambient aeration) for various times indicated.

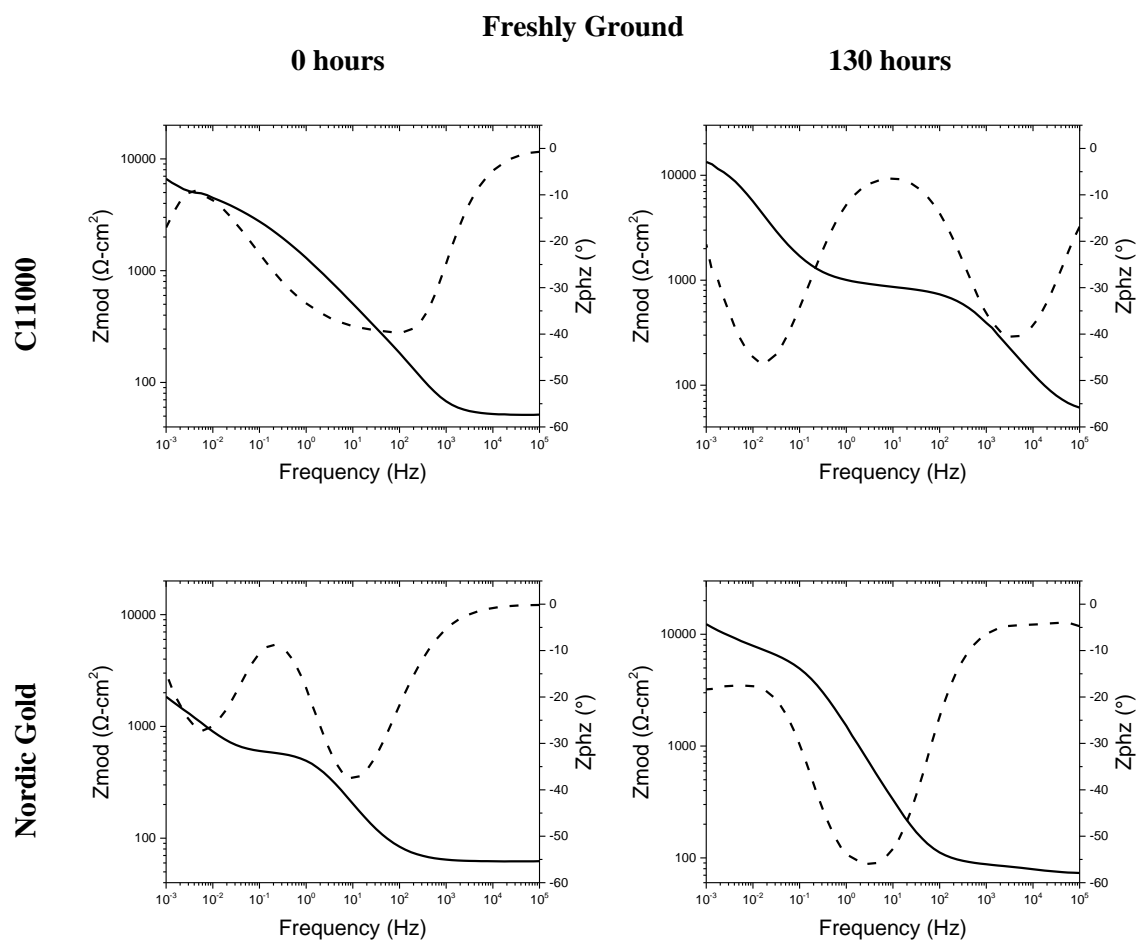


Figure 2.13. Bode plots of C11000 and Nordic Gold freshly ground to 1200 grit, then exposed to synthetic perspiration solution (23° C, ambient aeration) for 0 and 130 hours.

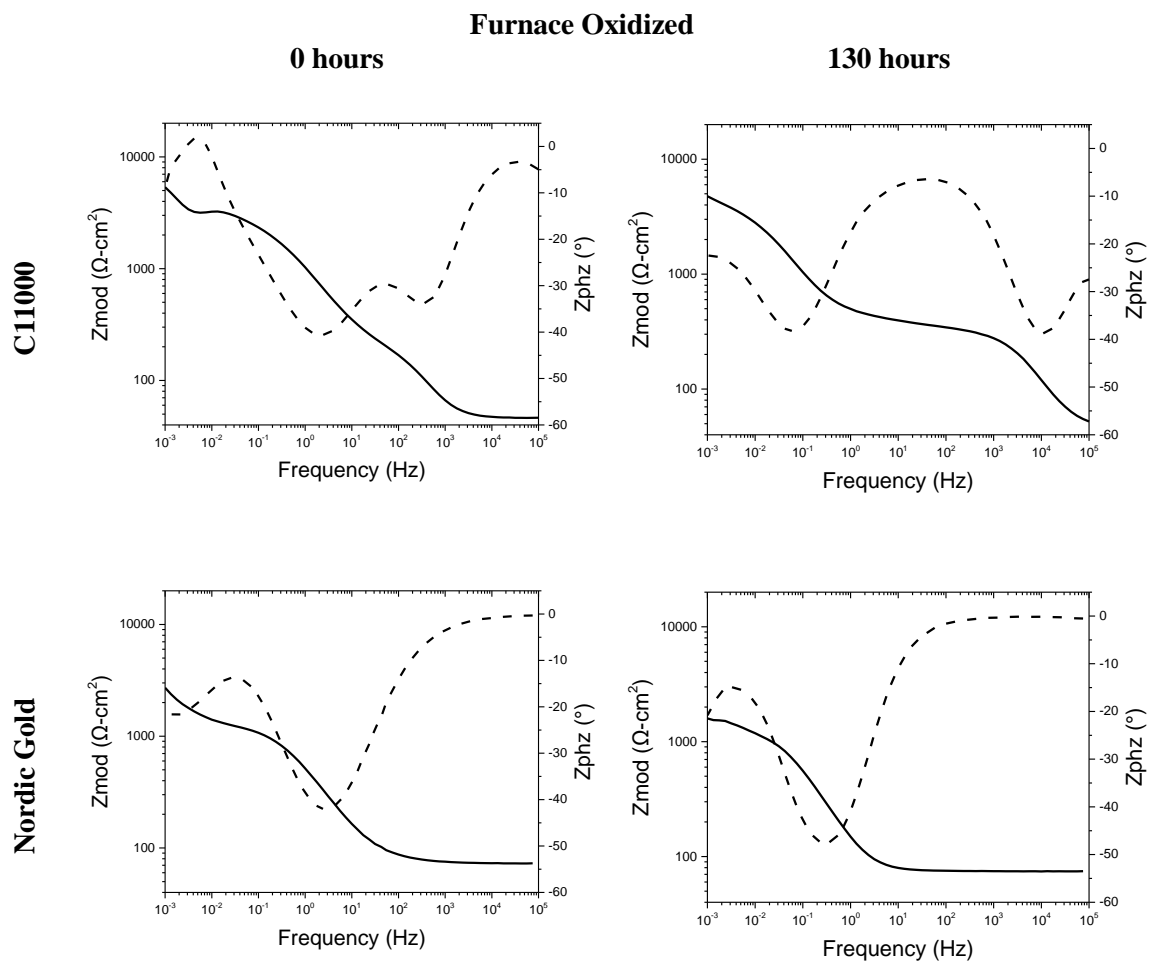


Figure 2.14. Bode plots of C11000 and Nordic Gold freshly ground to 1200 grit, furnace oxidized at 170 °C for 60 minutes, then exposed to synthetic perspiration solution (23° C, ambient aeration) for 0 and 130 hours.

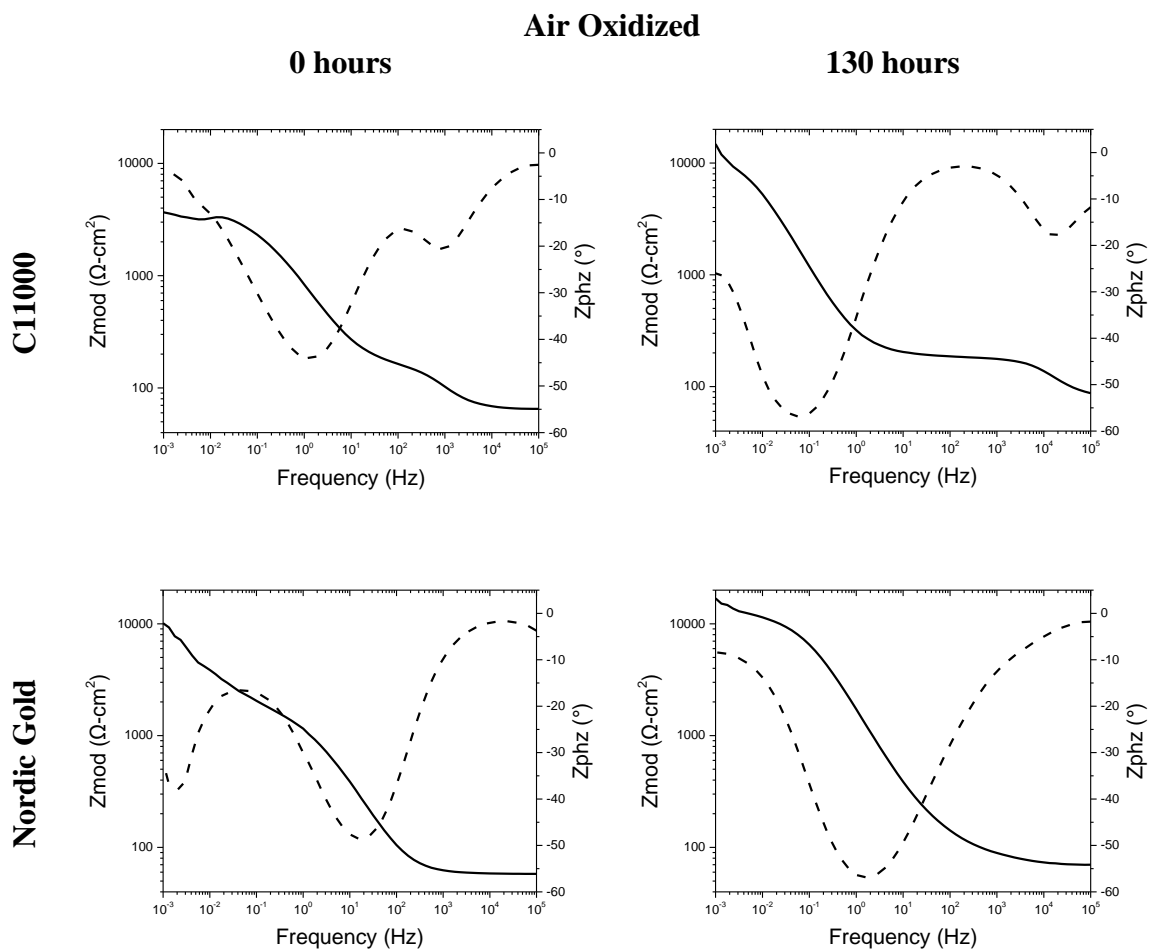


Figure 2.15. Bode plots of C11000 and Nordic Gold freshly ground to 1200 grit, air oxidized at ambient lab conditions for 30 days, then exposed to synthetic perspiration solution (23 °C, ambient aeration) for various times.

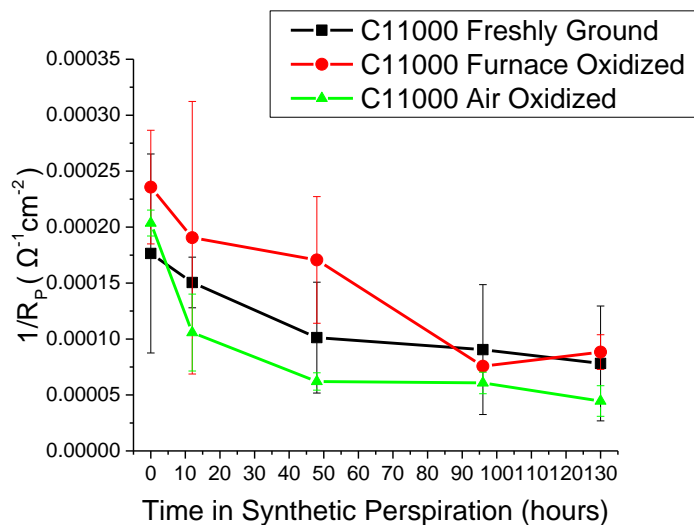


Figure 2.16. Instantaneous corrosion rate ($1/R_p$) over time for C11000 freshly ground to 1200 grit, furnace oxidized at 170 °C for 60 minutes, or air oxidized at ambient lab conditions for 30 days, then exposed to synthetic perspiration solution (23 °C, ambient aeration). Data is the average of 3 replicates and error bars are one standard deviation.

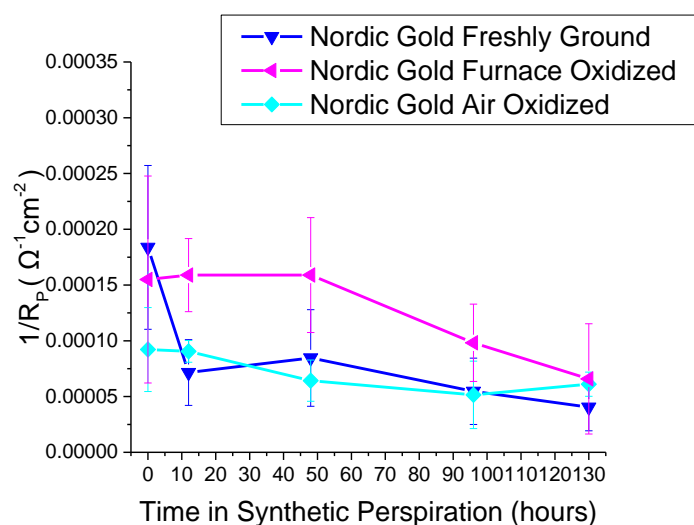


Figure 2.17. Instantaneous corrosion rate ($1/R_p$) over time for Nordic Gold when freshly ground to 1200 grit, furnace oxidized at 170 °C for 60 minutes, or air oxidized at ambient lab conditions for 30 days, then exposed to synthetic perspiration solution (23 °C, ambient aeration) for various times. Data is the average of 3 replicates and error bars are one standard deviation.

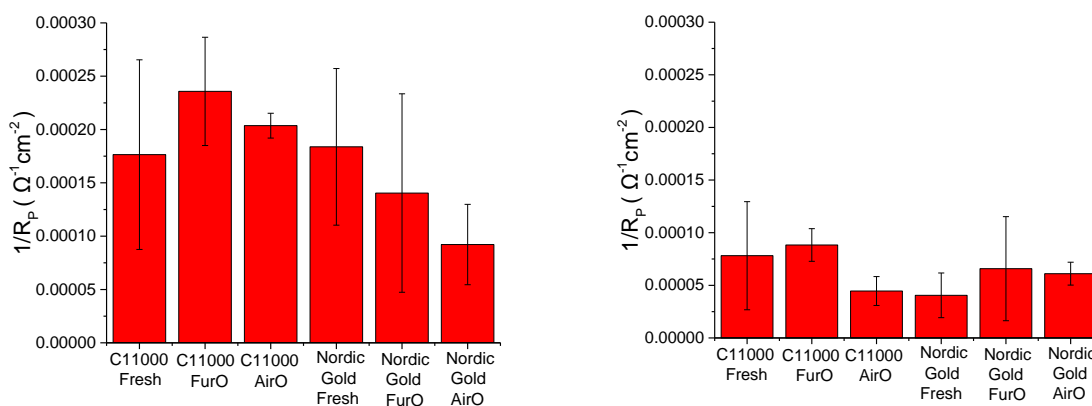


Figure 2.18. Instantaneous corrosion rate ($1/R_p$) at 0 hours (left) and 130 hours (right) for C11000 and Nordic Gold when freshly ground to 1200 grit, furnace oxidized at 170 °C for 60 minutes, or air oxidized at ambient lab conditions for 30 days, then exposed to synthetic perspiration solution (23 °C, ambient aeration). Data is the average of a minimum of 3 replicates and error bars reflect one standard deviation.

2.4.2.2 Mass Loss by Gravimetric Analysis

Mass loss by gravimetric analysis was conducted on freshly ground C10000 and Nordic Gold just after polishing and after being exposed to synthetic perspiration for 130 hours. This study serves as a qualitative confirmation of corrosion rate dependency on the alloys composition. Mass loss following 130 hours in synthetic perspiration was determined to be 0.77 (± 0.06) mg in Nordic Gold, and 1.1 (± 0.1) mg in C11000 in an exposure area of 0.8 cm². Table 2.8 lists mass loss (Δm) and associated charge (Q_{corr}) for Nordic Gold and C11000 adjusted for area and depending on Cu⁺ or Cu²⁺. These results are consistent with instantaneous corrosion rates observed by EIS, where Nordic Gold consistently exhibits lower corrosion rate than C11000. A B value was calculated for C11000 and Nordic Gold based on Q_{corr} calculated by mass loss, as seen in Equation 2.11, utilizing average $1/R_p$ values obtained at 0 and 130 hours. Note t_0 is 0.5 hours, accounting for the OCP period prior to EIS measurements.

$$B = \frac{\left(\frac{Q_{\text{corr by Mass Loss}^*2}}{(t_{130 \text{ hours}} - t_0 \text{ hours})} \right)}{\left(\left(\frac{1}{R_{P_{130 \text{ hours}}}} \right) + \left(\frac{1}{R_{P_0 \text{ hours}}} \right) \right)} \quad \text{Equation 2.11}$$

Table 2.8. Charge (Q_{corr}) analysis based on mass loss after 130 hours exposure of 0.8 cm^2 copper alloy to synthetic perspiration ($23 \text{ }^\circ\text{C}$, ambient aeration).					
Alloy	Mass Loss (Δm) (mg)	Mass Loss (mg/cm^2)	$Q_{\text{corr/area}}$ (C/cm^2) $\text{Cu}^+ + e^- = \text{Cu}$	$Q_{\text{corr/area}}$ (C/cm^2) $\text{Cu}^{2+} + 2e^- = \text{Cu}$	B (V) Calculated by Q_{corr} (Cu^{2+})
C11000	1.1 (± 1)	1.4 (± 1)	2.1 (± 2) ^{ix}	4.2 (± 4) ^x	0.07
Nordic Gold	0.77 (± 0.06)	0.96 (± 0.07)	2.0 (± 1) ^{xi}	3.3 (± 2) ^{xii}	0.06

2.4.3 Surface Analysis of Corrosion Products

2.4.3.1 Tarnishing in Synthetic Perspiration

Optical images of C11000 and Nordic Gold under freshly ground, furnace oxidized, and air oxidized conditions were collected at each exposure time in triplicate. The results are shown in Figures 2.19-2.20. After both furnace and air oxidation, a darker red-brown tone was observed in C11000 and a darker gold-brown tone observed in Nordic Gold. After exposure to synthetic perspiration, all samples showed significant tarnishing. However, at times after 12 hours, Nordic Gold did not continue to discolor significantly. This is in contrast to C11000, which continued to discolor to a bright salmon-pink color between 48 and 130 hours.

^{ix} Equivalent weight, $\text{Cu}^+ = 63.55 \text{ equiv./g}$

^x Equivalent weight, $\text{Cu}^{2+} = 31.77 \text{ equiv./g}$

^{xi} Equivalent weight, congruent $\text{Cu}^+ = 47.03 \text{ equiv./g}$

^{xii} Equivalent weight, congruent $\text{Cu}^{2+} = 28.35 \text{ equiv./g}$

Scale 0.5 cm	Freshly Ground			Furnace Oxidized			Air Oxidized		
	1	2	3	1	2	3	1	2	3
0 Hours									
12 Hours									
48 Hours									
96 Hours									
130 Hours									

Figure 2.19. Visual analysis of C11000 under freshly ground, furnace oxidized and air oxidized conditions after the indicated time exposure to synthetic perspiration at 23 °C and ambient aeration.

Scale 0.5 cm	Freshly Ground			Furnace Oxidized			Air Oxidized		
	1	2	3	1	2	3	1	2	3
0 Hours									
12 Hours									
48 Hours									
96 Hours									
130 Hours									

Figure 2.20. Visual analysis Nordic Gold under freshly ground, furnace oxidized and air oxidized conditions after the indicated time exposure to synthetic perspiration at 23 °C and ambient aeration.

2.4.3.2 Tarnish Analysis by Optical Spectrophotometry

Reflectivity was utilized as a qualitative comparison for the degree of tarnish acquired on samples over time exposed to synthetic perspiration. In all samples, exposure to synthetic perspiration caused a significant decrease in reflectivity after only 12 hours of exposure (Figure 2.21). The greatest degree of reflectivity was observed at 630-730 nm on both materials, corresponding orange to dark red light as was visually observed (Figure 2.22). After 130 hours of exposure to synthetic perspiration, all alloys have a <15% reflectivity (Figure 2.23). When air oxidized, Nordic Gold had a lower level of reflectivity before being exposed to synthetic perspiration, but tarnished to the same degree as Nordic Gold when freshly ground. Therefore, there is an overall slightly lesser degree of tarnishing occurring when Nordic Gold is air oxidized before being exposed to synthetic perspiration, likely due to the presence of a stable thin surface oxide.

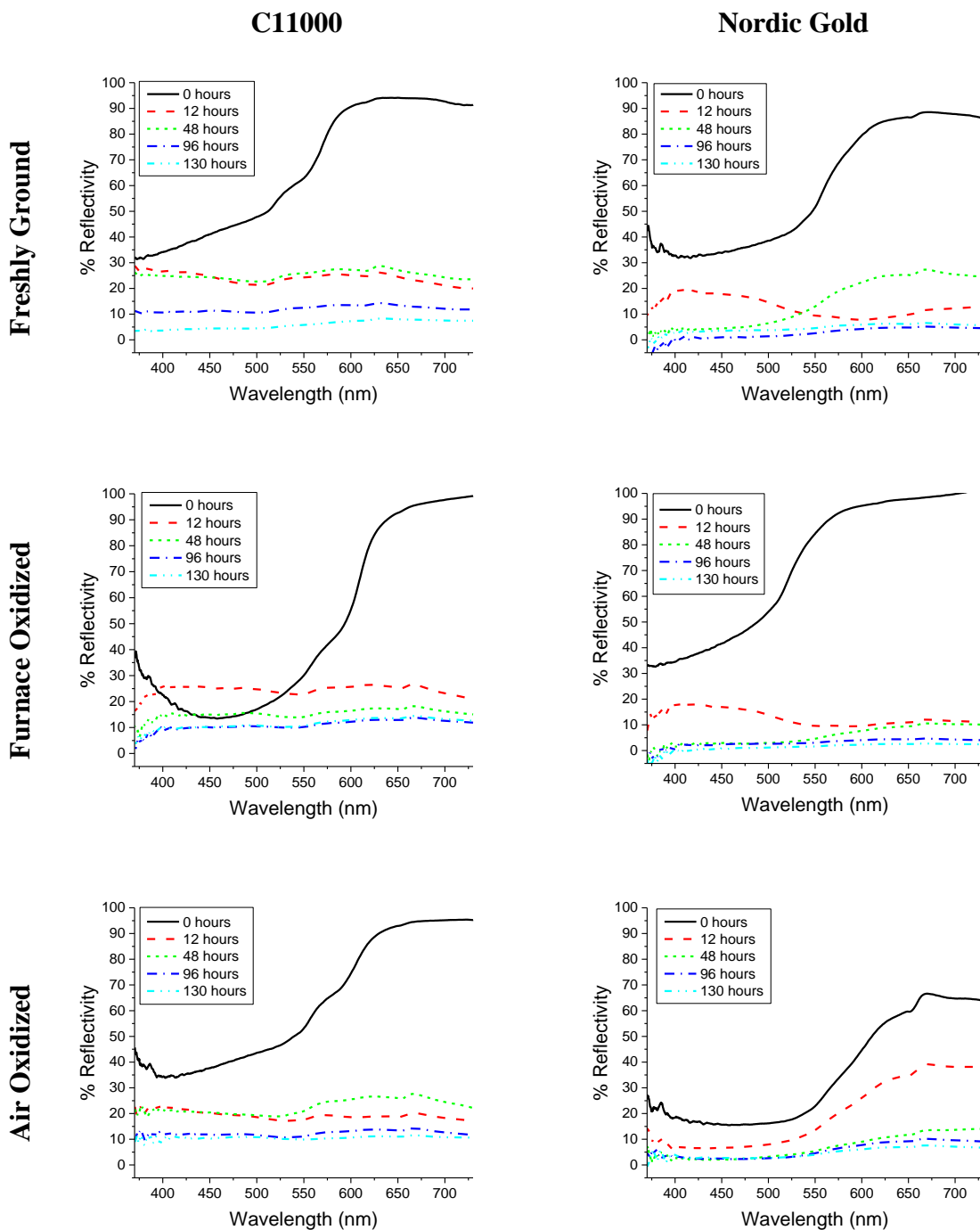


Figure 2.21. Reflectivity of C11000 and Nordic Gold samples when freshly ground to 1200 grit, furnace oxidized at 170 °C for 60 minutes, or air oxidized at ambient lab conditions for 30 days, then exposed to synthetic perspiration solution at 23 °C and ambient aeration for various times.

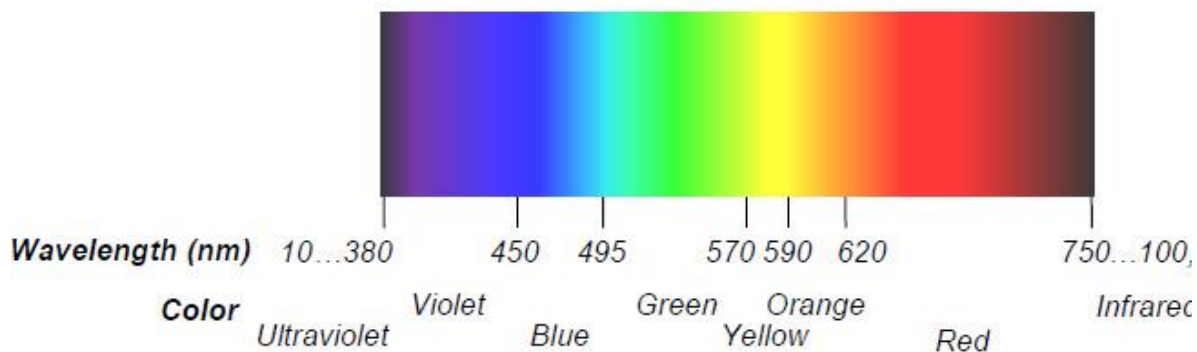


Figure 2.22. Visible light spectrum wavelengths with corresponding observed color.¹²⁹

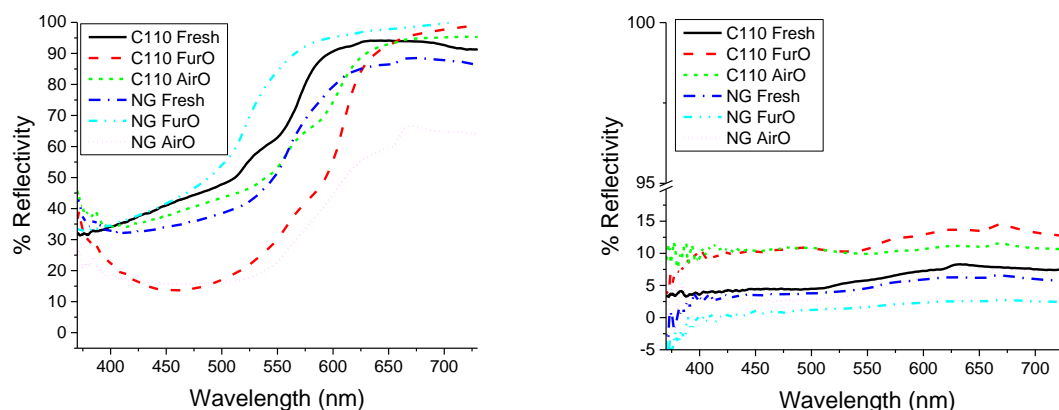


Figure 2.23. Reflectivity of C11000 and Nordic Gold samples when freshly ground to 1200 grit, furnace oxidized at 170 °C for 60 minutes, or air oxidized at ambient lab conditions for 30 days, then exposed to synthetic perspiration solution at 23 °C and ambient aeration for 0 hours (left) and 130 hours (right).

2.4.3.3 Corrosion Product Analysis by GIXRD

Prior to exposure to synthetic perspiration, all samples exhibited only peaks consistent with fcc copper and no corrosion products, despite the pre-treatment of furnace and air oxidation (Figure 2.24). GIXRD peaks in Nordic Gold before exposure to synthetic perspiration were shifted to lower angles, consistent with substitution alloying effects on the Cu fcc lattice parameter (Figure 2.25). Following exposure to synthetic perspiration, all samples developed crystalline corrosion products, regardless of pretreatment, as seen in Figure 2.26. Peaks were identified based on International Centre

for Diffraction Data (ICDD) PDF cards. In all samples, exposure to synthetic perspiration results in peaks consistent with Cu_2O , most noticeably in C11000 freshly ground or furnace oxidized conditions, where peak intensity of the primary Cu_2O peak ($2\theta = 36.4$) exceeds the primary Cu peak ($2\theta = 43.3$) after 130 hours. After 130 hours, all Nordic Gold samples indicate a small amount of Cu_2O on the surface, while C11000 samples contain Cu_2O and CuO (Figure 2.26). Figures 2.27-2.29 shows comparative GIXRD of C11000 and Nordic Gold after identical pre-treatments to highlight the effect of alloy composition on corrosion behavior.

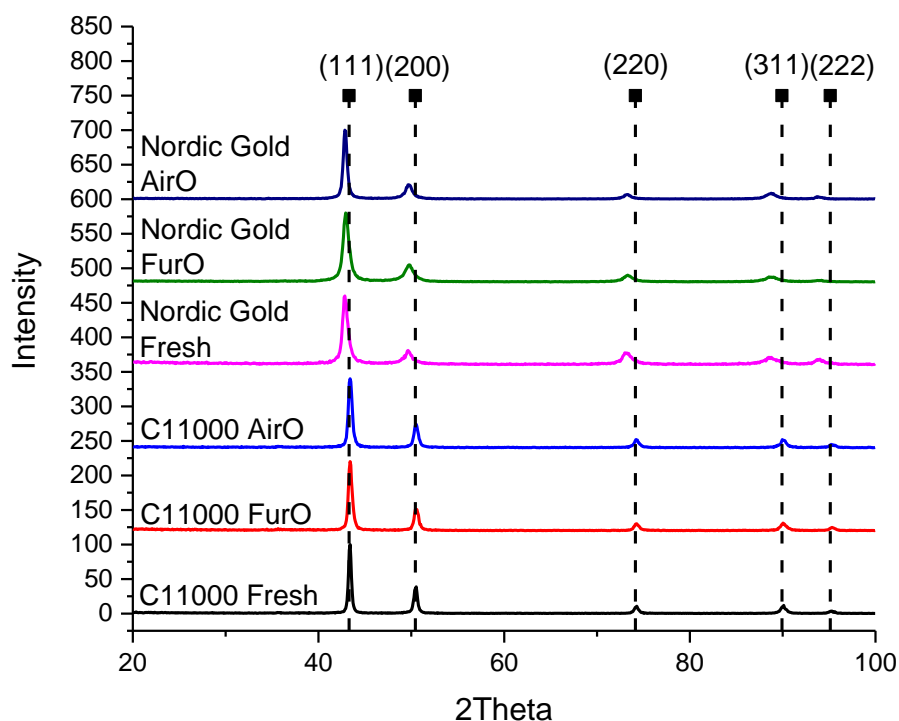


Figure 2.24. GIXRD of C11000 and Nordic Gold samples when freshly ground to 1200 grit, furnace oxidized at 170 °C for 60 minutes, or air oxidized at ambient lab conditions for 30 days, prior to exposure to synthetic perspiration solution, where only FCC metallic Cu (PDF Card No. 00-004-0836) peaks are evident. Spectra are shown offset ($y=120$) for ease of comparison.

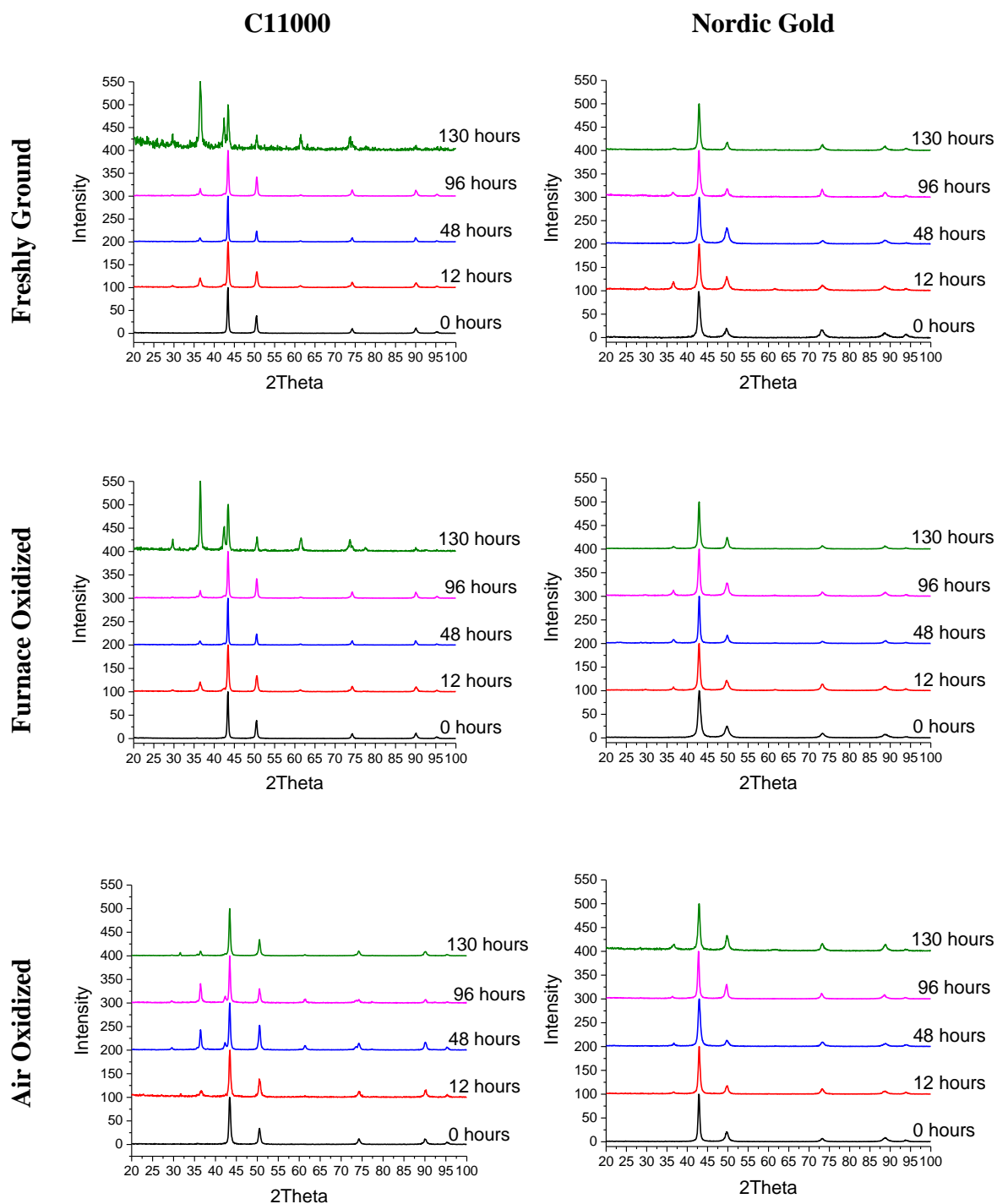


Figure 2.25. GIXRD of C11000 and Nordic Gold samples when freshly ground to 1200 grit, furnace oxidized at 170 °C for 60 minutes, or air oxidized at ambient lab conditions for 30 days, then exposed to synthetic perspiration solution (23 °C, ambient aeration) for various times indicated. The development of Cu₂O is evident in all samples, regardless of composition or pretreatment. Spectra are shown offset ($y=100$) for ease of comparison.

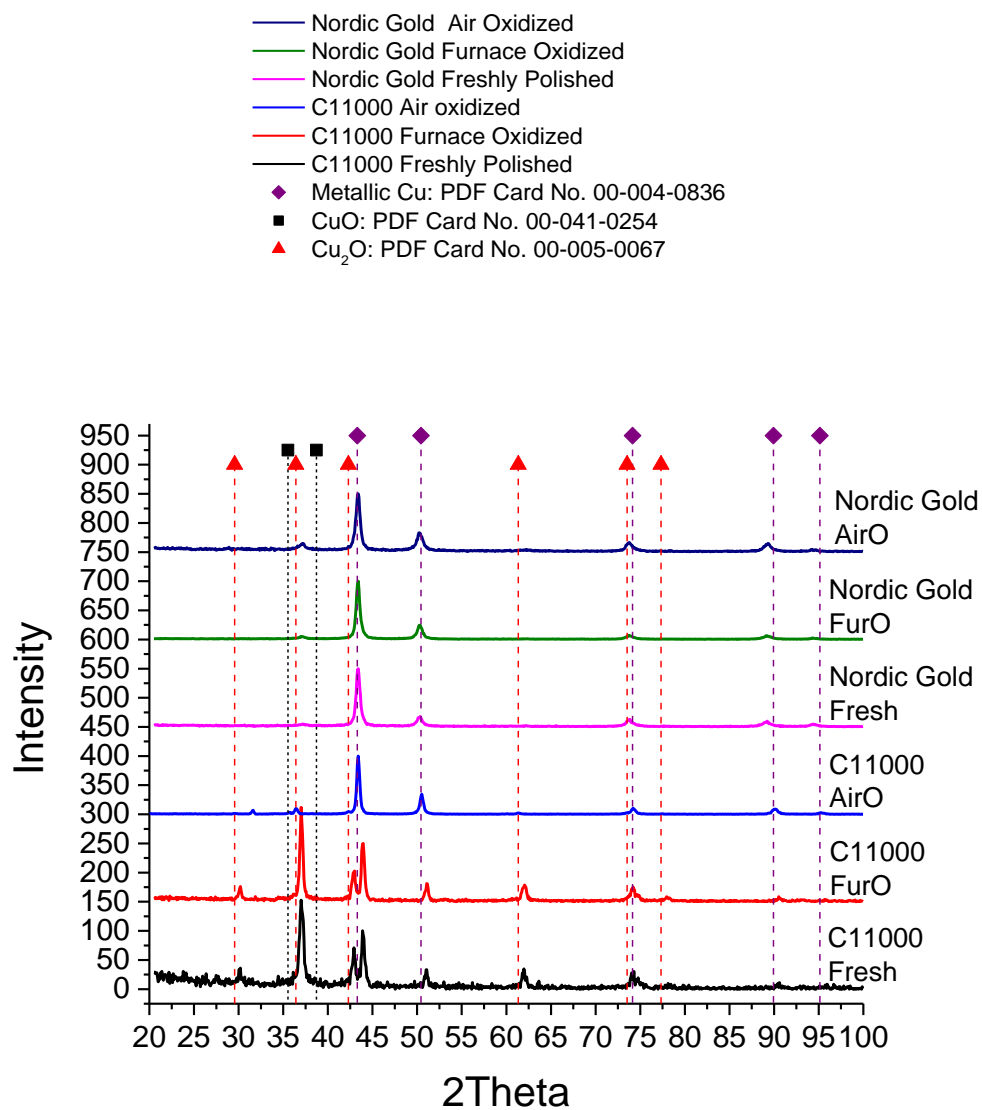


Figure 2.26. GIXRD of C11000 and Nordic Gold samples when freshly ground to 1200 grit, furnace oxidized at 170 °C for 60 minutes, or air oxidized at ambient lab conditions for 30 days, after exposure to synthetic perspiration solution (23 °C, ambient aeration) for 130 hours, where only FCC metallic Cu peaks, Cu₂O and CuO peaks are evident. Spectra are shown offset ($y=150$) for ease of comparison.

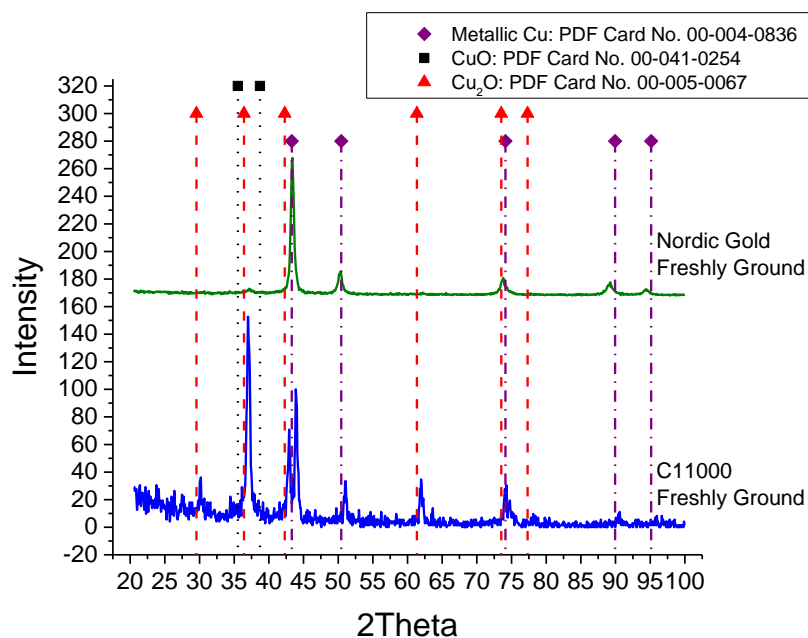


Figure 2.27. Comparative GIXRD of C11000 and Nordic Gold when freshly ground to 1200 grit followed by exposure to synthetic perspiration solution (23 °C, ambient aeration) for 130 hours. Spectra are shown offset ($y=170$) for ease of comparison.

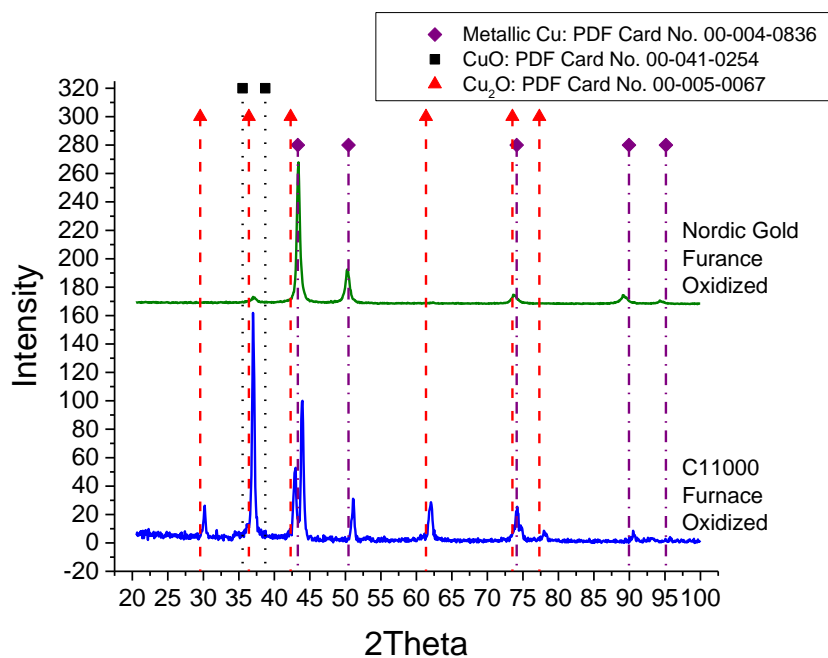


Figure 2.28. Comparative GIXRD of C11000 and Nordic Gold when freshly ground to 1200 grit, then thermally oxidized at 170 °C for 60 minutes, followed by exposure to synthetic perspiration solution (23 °C, ambient aeration) for 130 hours. Spectra are shown offset ($y=170$) for ease of comparison.

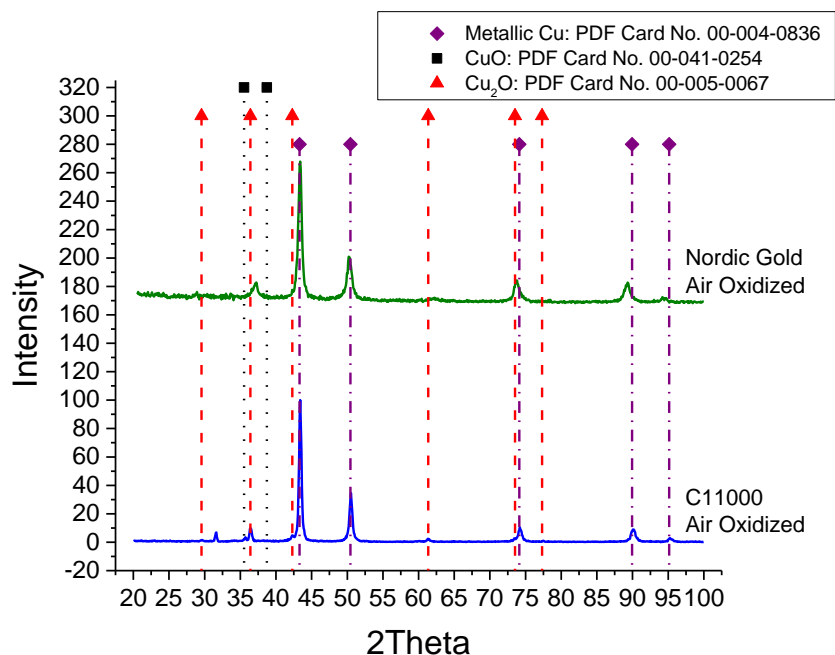


Figure 2.29. Comparative GIXRD of C11000 and Nordic Gold when freshly ground to 1200 grit, then air oxidized at ambient lab conditions, followed by exposure to synthetic perspiration solution (23 °C, ambient aeration) for 130 hours. Spectra are shown offset ($y=170$) for ease of comparison.

2.4.3.4 Corrosion Product Analysis by Galvanostatic Reduction

Samples were analyzed prior to exposure to synthetic perspiration to determine composition of oxides formed by thermal or air oxidation (Figure 2.30). Before exposure to synthetic perspiration (23 °C, ambient aeration), thermally and air oxidized C11000 experienced longer reduction times near $-0.8 V_{MMSE}$ compared to freshly ground C11000 and similar reduction times near $-1.2 V_{MMSE}$, but no additional reduction waves were present. Prior to exposure to synthetic perspiration (23 °C, ambient aeration), thermally oxidized Nordic Gold had similar length times near $-0.75 V_{MMSE}$, but longer reduction times near $-1.05 V_{MMSE}$. Air oxidized Nordic Gold experienced a longer reduction times near $-0.75 V_{MMSE}$, similar reductions waves near $-1.05 V_{MMSE}$, and an additional

reduction at $-1.3 V_{\text{MMSE}}$. The change in reduction behavior between freshly ground samples and thermally or air oxidized samples confirms the presences of thin oxides following pre-treatment. The identity of C11000 thin oxides following thermal or air oxidation have similar identity judging from reduction potential as the corrosion product ($-0.8 V_{\text{MMSE}}$) that forms on C11000 after only minutes of exposure to air during the transfer from methanol to the reaction cell.^{xiii} The identity of Nordic Gold thin oxides when thermally oxidized have similar identity as the corrosion product on freshly ground Nordic Gold judging from reduction potentials ($-0.75 V_{\text{MMSE}}$ and $-1.05 V_{\text{MMSE}}$), but the corrosion product formed by air oxidation contains an additional species ($-1.3 V_{\text{MMSE}}$).

Figures 2.30-2.33 demonstrate the dependence of exposure time of the sample to synthetic perspiration on reduction behavior. In cases where the reduction of a species begins at a more negative potentials and increases over time, the corrosion product is likely becoming easier to reduce. Over time, C11000's outer most corrosion layer ($-0.8 V_{\text{MMSE}}$) decreases slightly in thickness, while the inner corrosion layer, seen at longer reduction times, thickens. Following 130 hours, the presences of a third species is noticeable. Nordic Gold experiences a similar behavior, with the outer layer thinning slightly while the inner layer thickens. However, following 130 hours the identity of the corrosion species are difficult to determine and could contain small amounts of copper chloride corrosion products or Sn oxides, as plateaus and inflection points are unclear (Figures 2.30-2.35). Figure 2.36 demonstrates example inflection points determined by differentiation (t_i) and potentials (E_i) associated of C11000 and Nordic Gold that are used to define Figure 2.37.

^{xiii} Outer layer of corrosion layer was taken as the highest oxidation state

Figures 2.38-2.40 demonstrate the effect of additional alloying elements on corrosion products by comparing C11000 and Nordic Gold at identical pretreatment conditions, as well as attempts to identify corrosion products based on electrochemical reduction potentials. Nordic Gold is consistently reduced at lower potentials and shorter times compared to C11000, indicating composition of the alloy which the oxide is being reduced affects the reduction-oxidation reaction. The composition of C11000's corrosion layer following 130 hours of exposure to synthetic perspiration (23 °C, ambient aeration), especially when corroded in the thin oxides, is suspected to be composed to CuO, $\text{Cu}_2(\text{OH})_3\text{Cl}$ and Cu_2O with well-defined plateaus and inflection points below these reduction potentials. The composition of Nordic Gold's corrosion product following 130 hours of exposure to synthetic perspiration (23 °C, ambient aeration) are more difficult to discern, containing both CuO and Cu_2O as well as possible thin layers of $\text{Cu}_2(\text{OH})_3\text{Cl}$ and $\text{Sn}(\text{OH})_2$.^{xiv} Despite the possible presence of more corrosion species compared to C11000, the overall reduction time for Nordic Gold is consistently much less than C11000 (Figures 2.41-2.42). This is indicative that a thinner corrosion layer forms on Nordic Gold while exposed to synthetic perspiration (23 °C, ambient aeration) for identical periods of time and under the same pre-treatment conditions as a result of alloy composition.

^{xiv} $\text{Cu}_2(\text{OH})_3\text{Cl}$ and $\text{Sn}(\text{OH})_2$ were not detected by XRD, and detection by Raman spectroscopy was precluded due to formation as an inner corrosion layer.

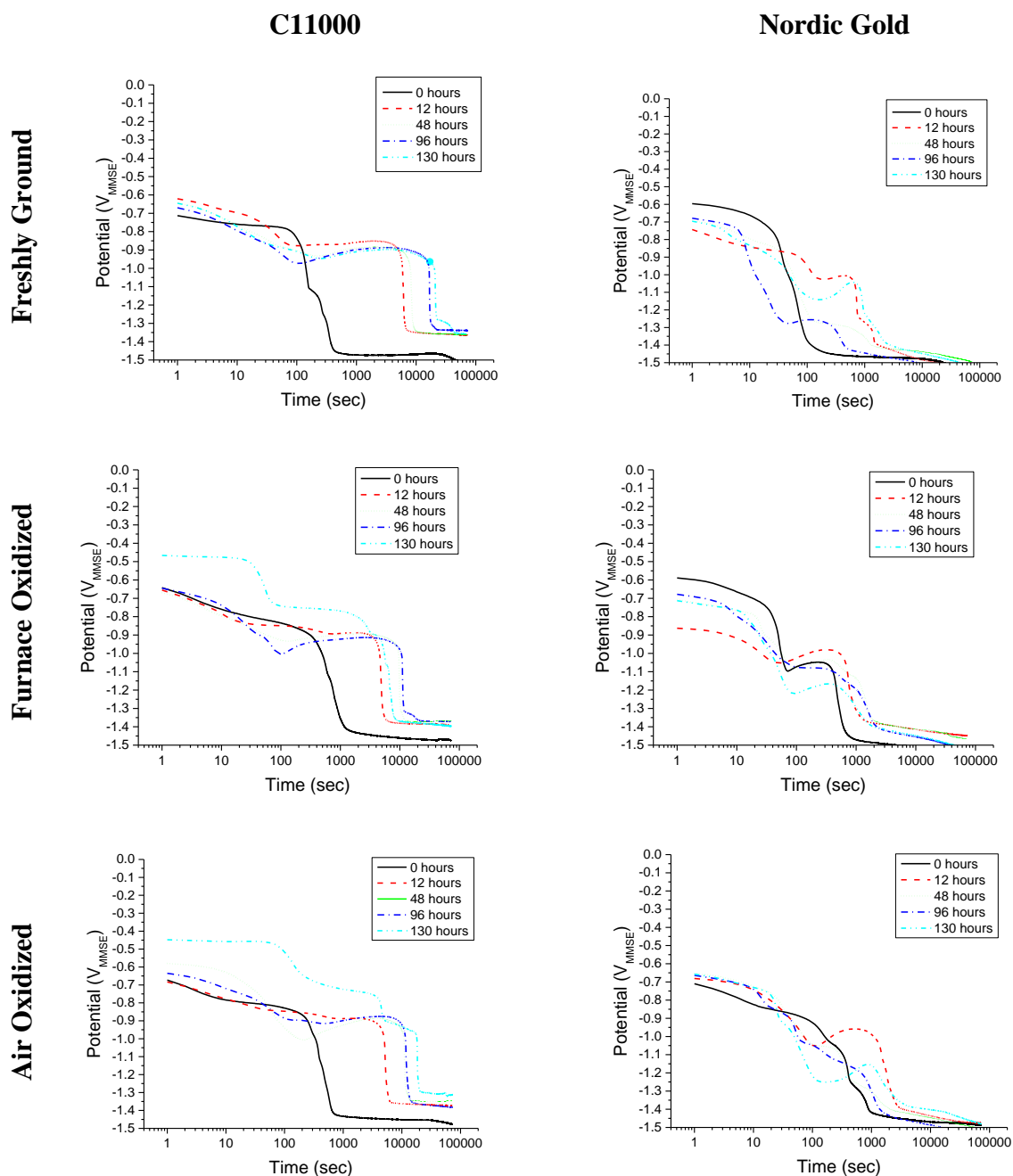


Figure 2.30. Galvanostatic reduction of C11000 and Nordic Gold when freshly ground to 1200 grit, thermally oxidized at 170 °C for 60 minutes, or air oxidized at ambient lab conditions for 30 days, followed by exposure to synthetic perspiration solution (23 °C, ambient aeration) for various times indicated. Galvanostatic reductions were conducted at 0.02 mA/cm² on an area of 0.8 cm².

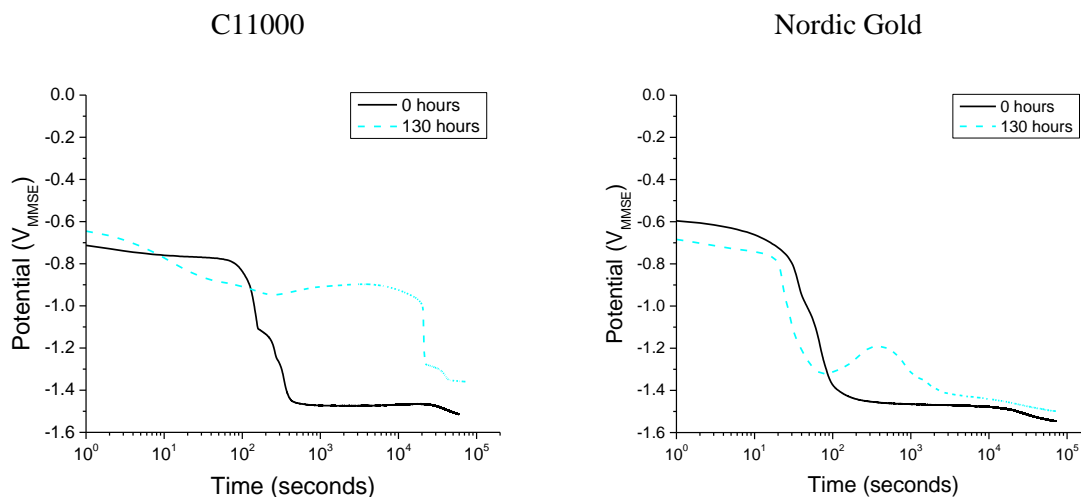


Figure 2.31. Galvanostatic reduction of C11000 (left) and Nordic Gold (right) when freshly ground to 1200 grit followed by exposure to synthetic perspiration solution (23 °C, ambient aeration) for 0 and 130 hours. Galvanostatic reductions were conducted at 0.02 mA/cm² on an area of 0.8 cm².

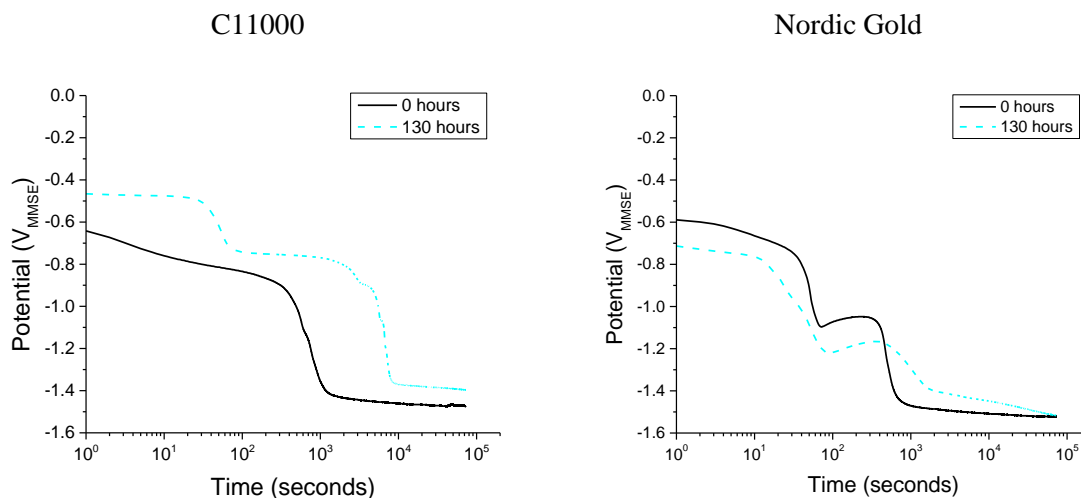


Figure 2.32. Galvanostatic reduction of C11000 (left) and Nordic Gold (right) when freshly ground to 1200 grit, thermally oxidized at 170 °C for 60 minutes followed by exposure to synthetic perspiration solution (23 °C, ambient aeration) for 0 and 130 hours. Galvanostatic reductions were conducted at 0.02 mA/cm² on an area of 0.8 cm².

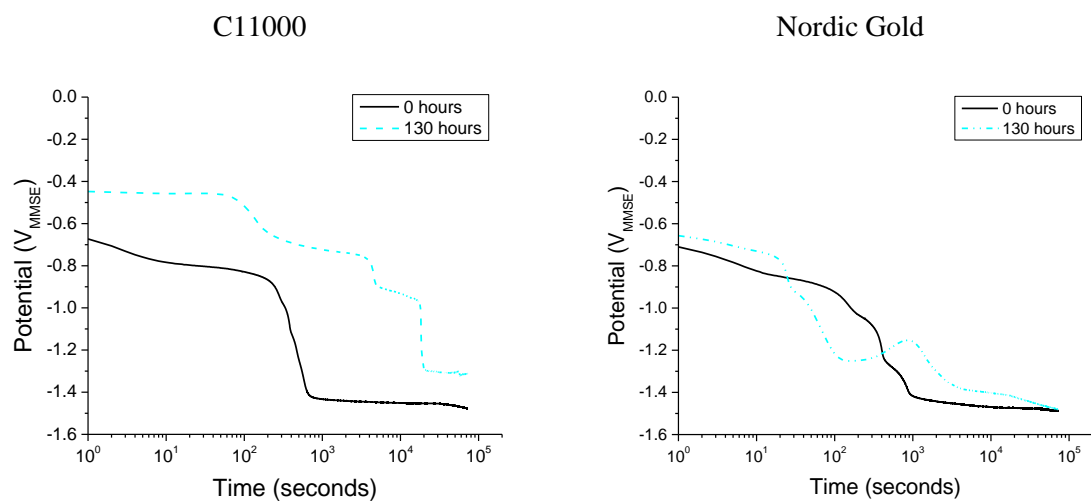


Figure 2.33. Galvanostatic reduction of C11000 (left) and Nordic Gold (right) when freshly ground to 1200 grit, air oxidized at ambient lab conditions for 30 days followed by exposure to synthetic perspiration solution (23 °C, ambient aeration) for 0 and 130 hours. Galvanostatic reductions were conducted at 0.02 mA/cm² on an area of 0.8 cm².

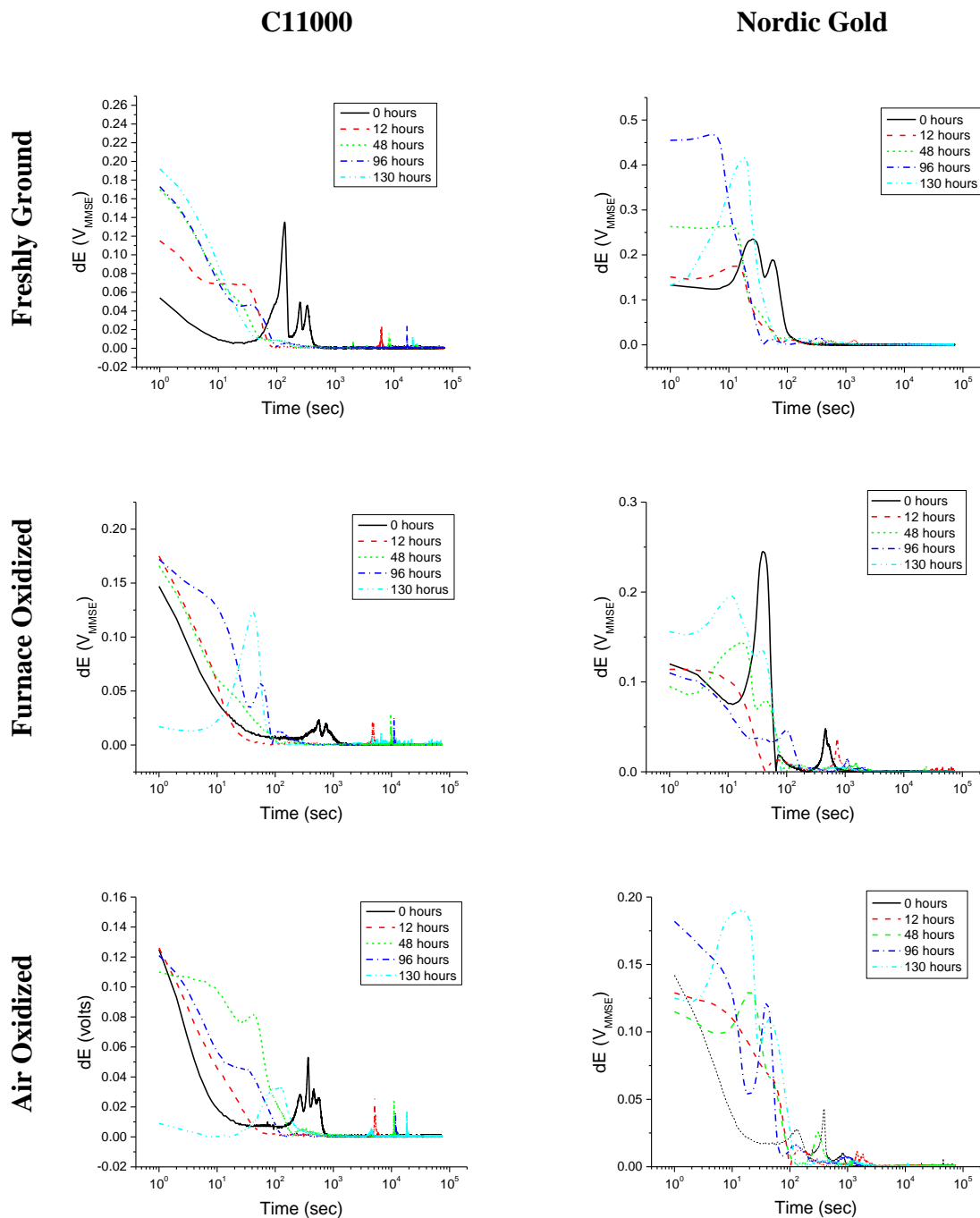


Figure 2.34. Galvanostatic reduction analysis of inflection points by taking the first derivative of C11000 and Nordic Gold when freshly ground to 1200 grit, thermally oxidized at 170 °C for 60 minutes, or air oxidized at ambient lab conditions for 30 days, followed by exposure to synthetic perspiration solution (23 °C, ambient aeration) for various times indicated. Galvanostatic reductions were conducted at 0.02 mA/cm² on an area of 0.8 cm².

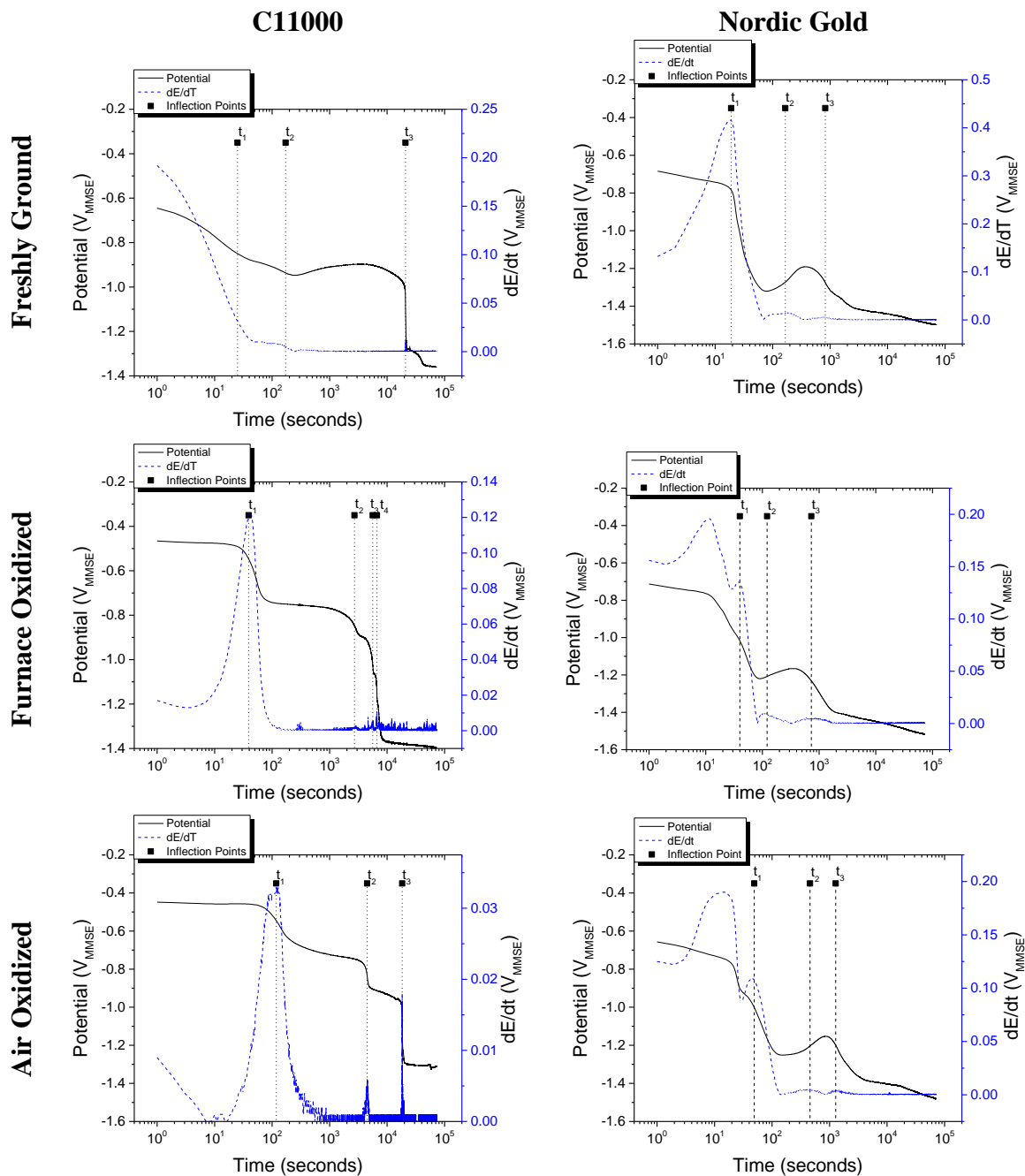


Figure 2.35. Galvanostatic reduction over laid with inflection analysis of C11000 and Nordic Gold when freshly ground to 1200 grit, thermally oxidized at 170 °C for 60 minutes, or air oxidized at ambient lab conditions for 30 days, followed by exposure to synthetic perspiration solution (23 °C, ambient aeration) for 130 hours. Galvanostatic reductions were conducted at 0.02 mA/cm² on an area of 0.8 cm².

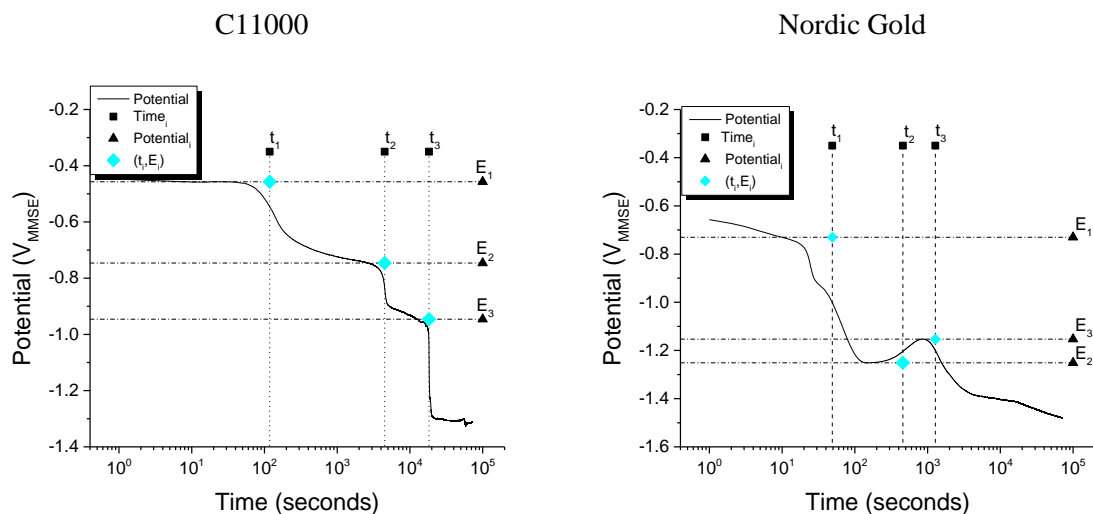


Figure 2.36. Galvanostatic reduction with inflection points (t_i) and associated potentials (E_i) of C11000 (left) and Nordic Gold (right) when freshly ground to 1200 grit then air oxidized at ambient lab conditions for 30 days, followed by exposure to synthetic perspiration solution (23 °C, ambient aeration) for 130 hours. Galvanostatic reductions were conducted at 0.02 mA/cm² on an area of 0.8 cm².

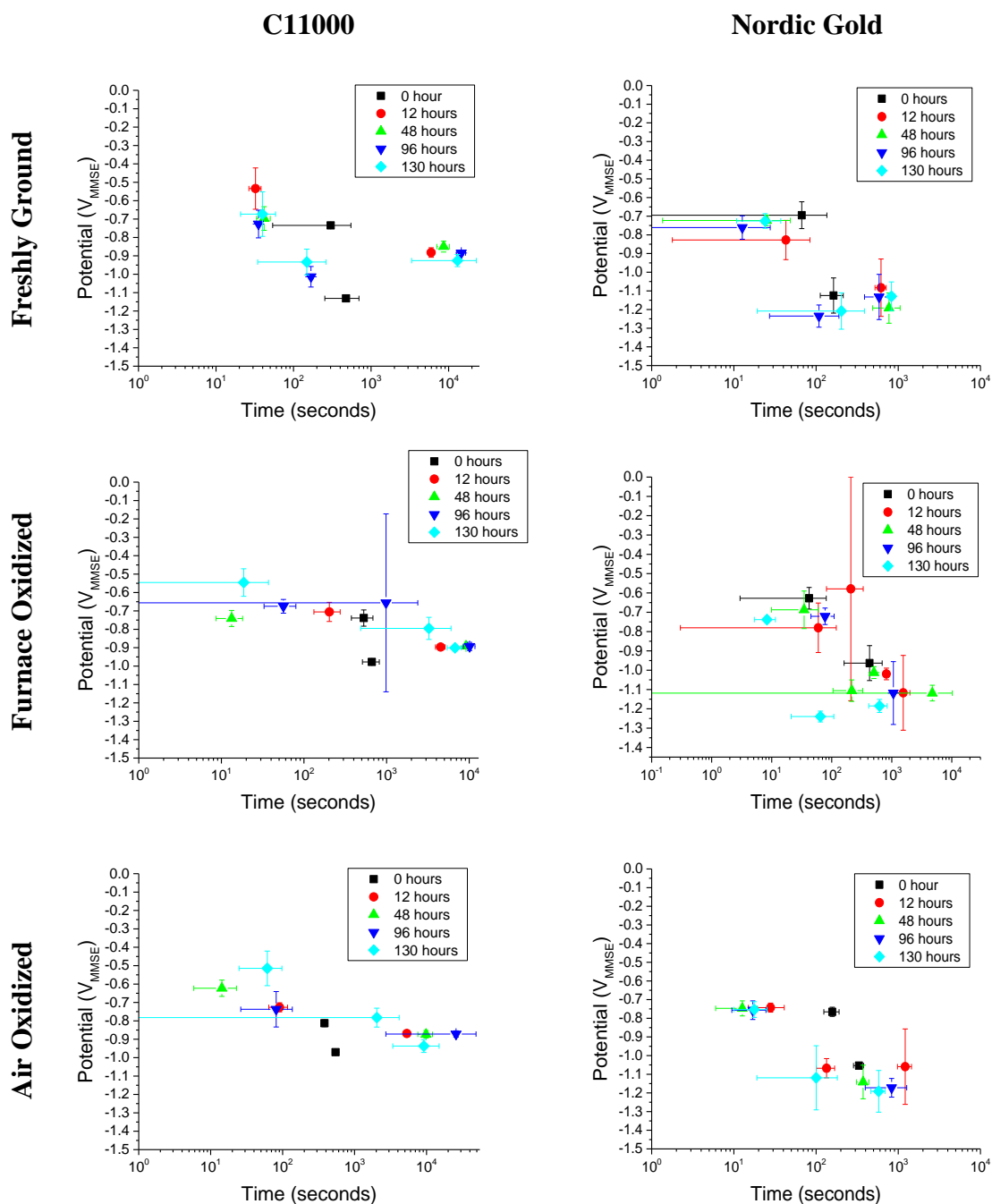


Figure 2.37. Galvanostatic reduction of C11000 and Nordic Gold when freshly ground to 1200 grit, thermally oxidized at 170 °C for 60 minutes, or air oxidized at ambient lab conditions for 30 days, followed by exposure to synthetic perspiration solution (23 °C, ambient aeration) for various times indicated. Galvanostatic reductions were conducted at 0.02 mA/cm² on an area of 0.8 cm². Data is the average of 3 replicates and error bars are one standard deviation.

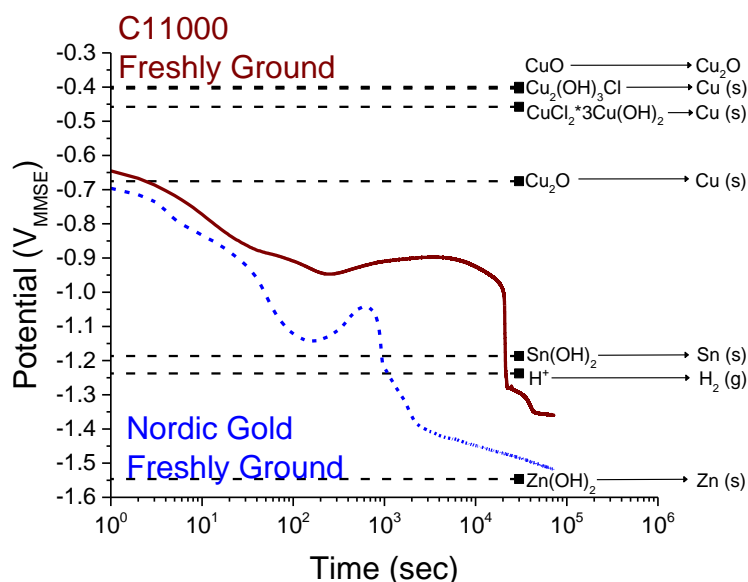


Figure 2.38. Comparative galvanostatic reduction of C11000 and Nordic Gold when freshly ground to 1200 grit followed by exposure to synthetic perspiration solution (23 °C, ambient aeration) for 130 hours. Galvanostatic reductions were conducted at 0.02 mA/cm² on an area of 0.8 cm².

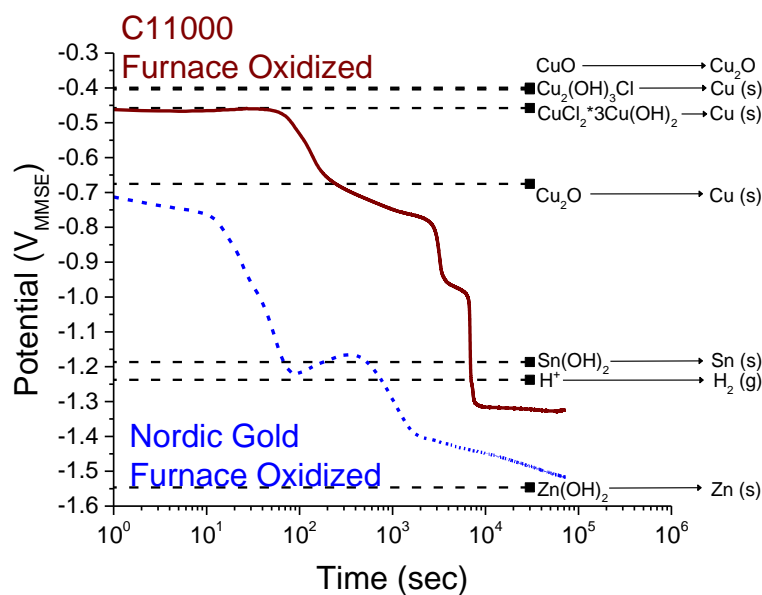


Figure 2.39. Comparative galvanostatic reduction of C11000 and Nordic Gold when freshly ground to 1200 grit then thermally oxidized at 170 °C for 60 minutes, followed by exposure to synthetic perspiration solution (23 °C, ambient aeration) for 130 hours. Galvanostatic reductions were conducted at 0.02 mA/cm² on an area of 0.8 cm².

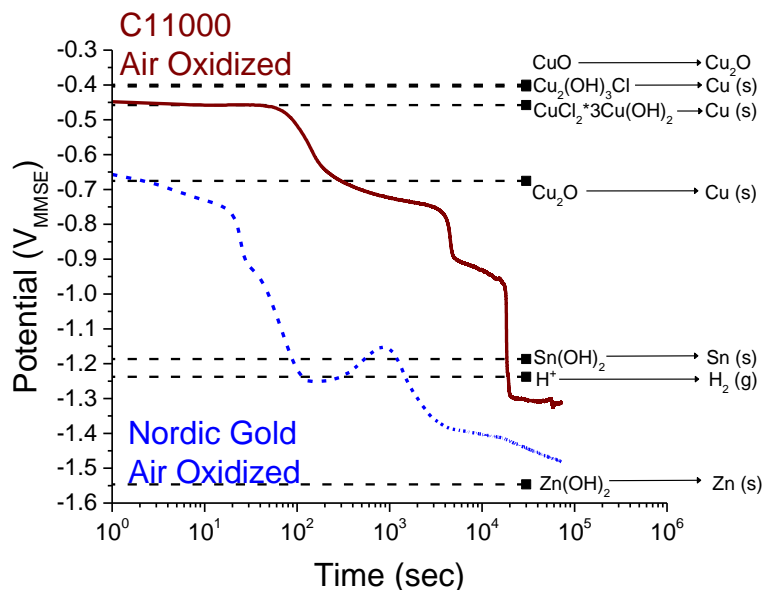


Figure 2.40. Comparative galvanostatic reduction of C11000 and Nordic Gold when freshly ground to 1200 grit then air oxidized at ambient lab conditions for 30 days, followed by exposure to synthetic perspiration solution (23 °C, ambient aeration) for 130 hours. Galvanostatic reductions were conducted at 0.02 mA/cm² on an area of 0.8 cm².

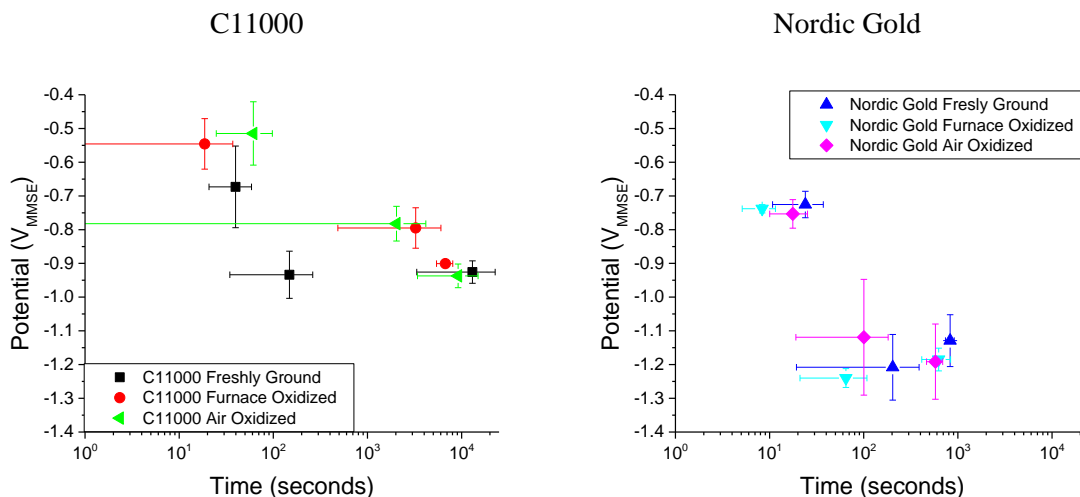


Figure 2.41. Galvanostatic reduction points (t_i, E_i) of C11000 (left) and Nordic Gold (right) when freshly ground to 1200 grit, thermally oxidized at 170 °C for 60 minutes, or air oxidized at ambient lab conditions for 30 days, followed by exposure to synthetic perspiration solution (23 °C, ambient aeration) for 130 hours. Galvanostatic reductions were conducted at 0.02 mA/cm² on an area of 0.8 cm². Data is the average of 3 replicates and error bars are one standard deviation.

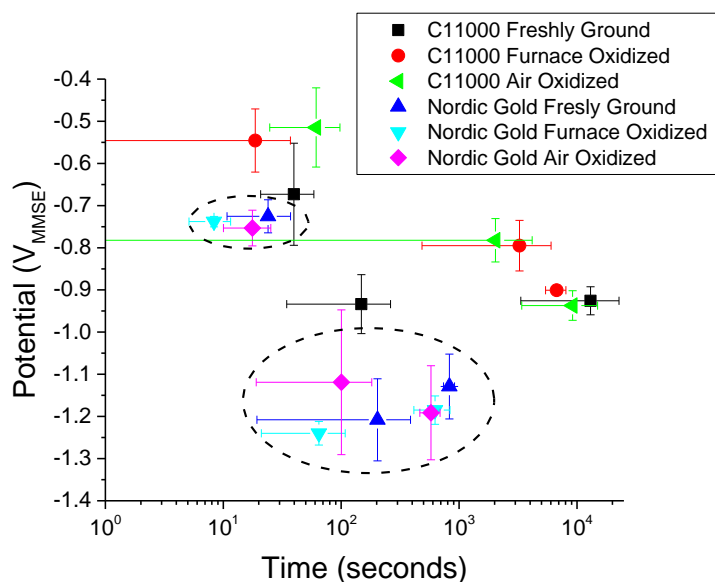


Figure 2.42. Galvanostatic reduction points (t_i, E_i) of C11000 and Nordic Gold when freshly ground to 1200 grit, thermally oxidized at 170 °C for 60 minutes, or air oxidized at ambient lab conditions for 30 days, followed by exposure to synthetic perspiration solution (23 °C, ambient aeration) for 130 hours. Galvanostatic reductions were conducted at 0.02 mA/cm² on an area of 0.8 cm². Data is the average of 3 replicates and error bars are one standard deviation.

2.4.4 Copper Ion Release by ICP-OES

Copper ion release was analyzed in synthetic perspiration solution by inductively coupled plasma-optical emission spectrometry (ICP-OES). Copper release was assumed to be a factor of time exposure to synthetic perspiration, pre-treatment condition, and alloy composition. As seen in Figure 2.43, the first 12 hours a higher initial copper release before and during the formation of protective tarnish layers and does not follow a linear trend with the remaining sampling times. However, once a protective layer has formed following 12 hours of exposure, copper release increased over time in a nearly linear manner.

The presence of thin oxides has both an effect on initial copper release (<12 hour exposure) and the rate of copper release between 12 and 130 hours of exposure. As seen

in Figure 2.43, the presence of thin oxides on C11000 formed by both thermal and air oxidation decreases initial copper ion release compared to freshly ground C11000. The opposite is true in Nordic Gold, where the presence of thin oxides increases initial copper ion release compared to freshly ground Nordic Gold. Thin oxides formed by air oxidation on C11000 also decrease the rate of copper release (0.0019 ppm/hour for 0.8 cm² area) compared to the freshly ground alloy (0.0021 ppm/hour for 0.8 cm² area), while those formed by thermal oxidation increase the rate of copper release (0.0031 ppm/hour for 0.8 cm² area). Both thermally formed and air formed oxides on Nordic Gold result in a decreased rate of copper release (0.0027 and 0.025 ppm/hour for 0.8 cm² area respectively) compared to freshly ground Nordic Gold (0.0034 ppm/hour for 0.8 cm² area). Figures 2.44-2.45 compare copper release from C11000 and Nordic Gold under pre-treatment conditions.

Figures 2.46-2.48 demonstrate the dependence of alloy composition on copper release over time. When freshly ground, Nordic Gold release less copper within the first 12 hours compared to C11000, the average copper release following 130 hours is nearly identical. In the presence of thin oxides, initial copper ion release from Nordic Gold and C11000 are very similar, and continue to be similar within statistical error through 130 hours of exposure to synthetic perspiration. As seen in Figure 2.49, copper release from C11000 and Nordic Gold following 130 hours of exposure to synthetic perspiration are remarkably similar despite both alloy composition differences, and the presences of thin oxides.

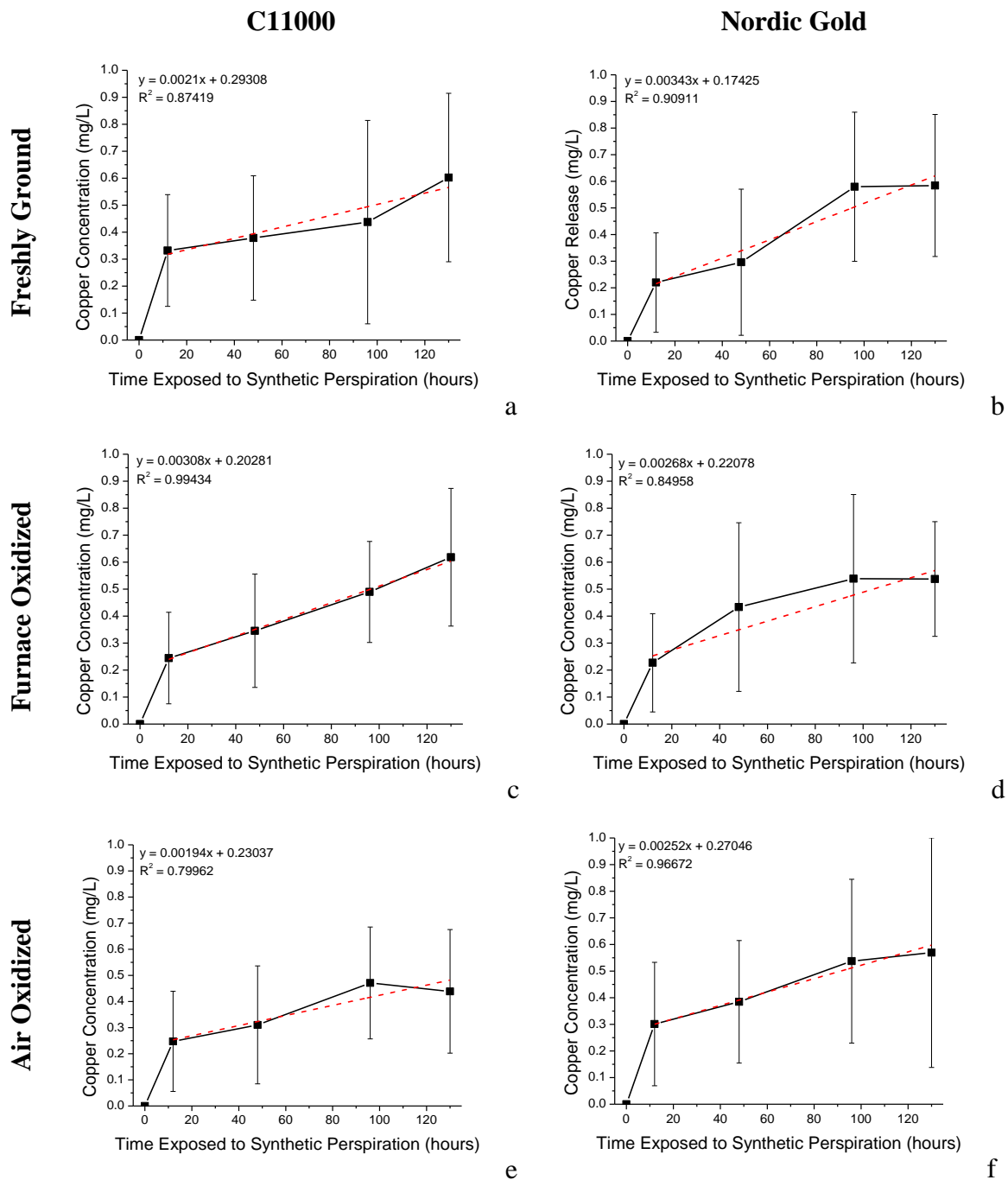
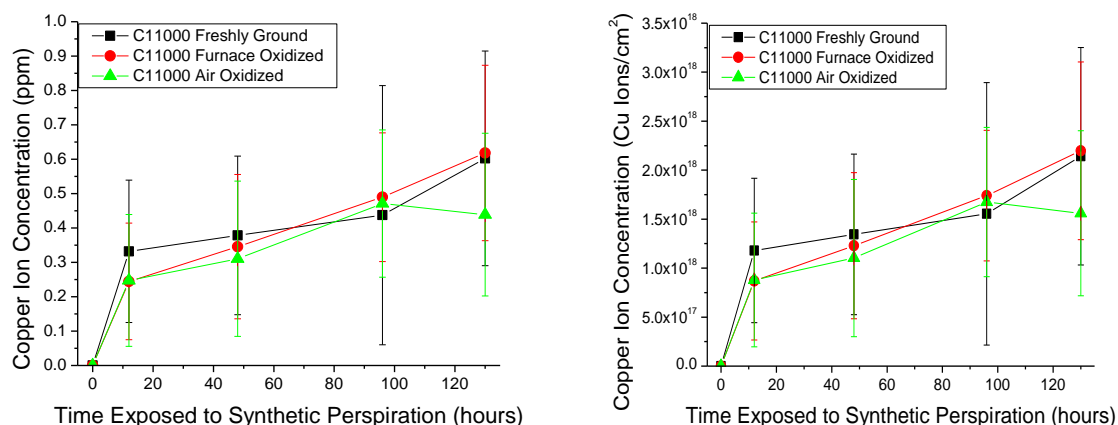


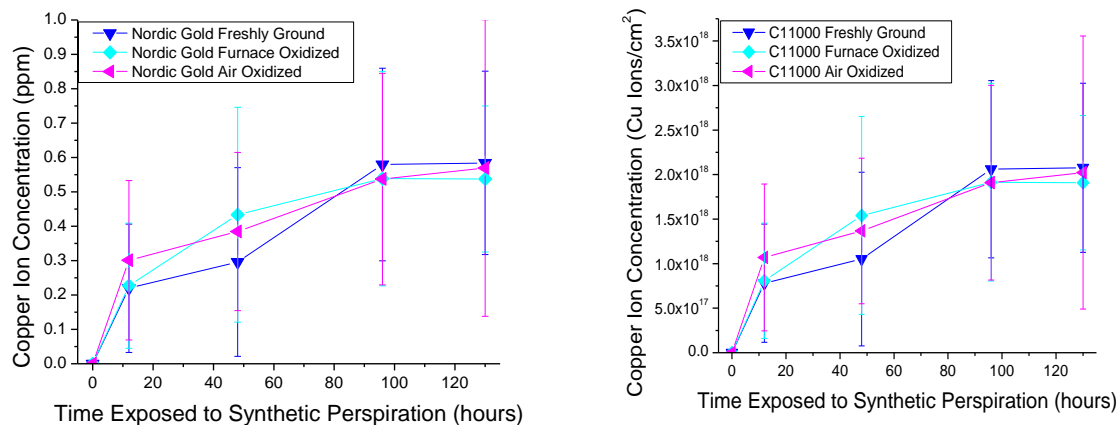
Figure 2.43. Copper concentration as a factor of time for C11000 and Nordic Gold when freshly ground to 1200 grit, thermally oxidized at 170 °C for 60 minutes, or air oxidized at ambient lab conditions for 30 days, followed by exposure to synthetic perspiration solution (23 °C, ambient aeration) over time. Synthetic perspiration solution was exposed to 0.8 cm² of copper of the copper alloy coupon, with a surface to volume ratio of 2.67 cm²/L. Data is the average of 3 replicates and error bars are one standard deviation. The dashed line indicates a linear fit of the data.



a

b

Figure 2.44. Copper concentration as a factor of time for C11000 when freshly ground to 1200 grit, thermally oxidized at 170 °C for 60 minutes, or air oxidized at ambient lab conditions for 30 days, followed by exposure to synthetic perspiration solution (23 °C, ambient aeration) over time, expressed as ppm in solution (a) and amount Cu^{2+} in 300 mL divided by electrode area (0.8 cm^2) (b) over time. Synthetic perspiration solution was exposed to 0.8 cm^2 of copper of the copper alloy coupon, with a surface to volume ratio of $2.67 \text{ cm}^2/\text{L}$. Data is the average of 3 replicates and error bars are one standard deviation.



a

b

Figure 2.45. Copper concentration as a factor of time for Nordic Gold when freshly ground to 1200 grit, thermally oxidized at 170 °C for 60 minutes, or air oxidized at ambient lab conditions for 30 days, followed by exposure to synthetic perspiration solution (23 °C, ambient aeration) over time, expressed as ppm in solution (a) and amount Cu^{2+} in 300 mL divided by electrode area (0.8 cm^2) (b) over time. Synthetic perspiration solution was exposed to 0.8 cm^2 of copper of the copper alloy coupon, with a surface to volume ratio of $2.67 \text{ cm}^2/\text{L}$. Data is the average of 3 replicates and error bars are one standard deviation.

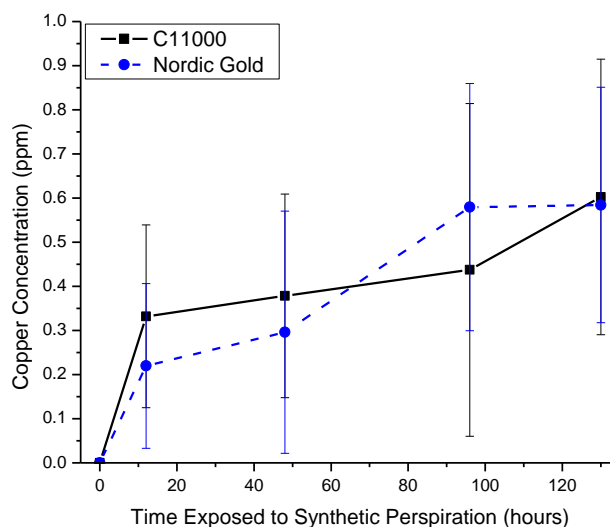


Figure 2.46. Copper concentration as a factor of time for C11000 and Nordic Gold when freshly ground to 1200 grit, followed by exposure to synthetic perspiration solution (23 °C, ambient aeration) over time expressed as ppm in solution. Synthetic perspiration solution was exposed to 0.8 cm² of copper of the copper alloy coupon, with a surface to volume ratio of 2.67 cm²/L. Data is the average of 3 replicates and error bars are one standard deviation.

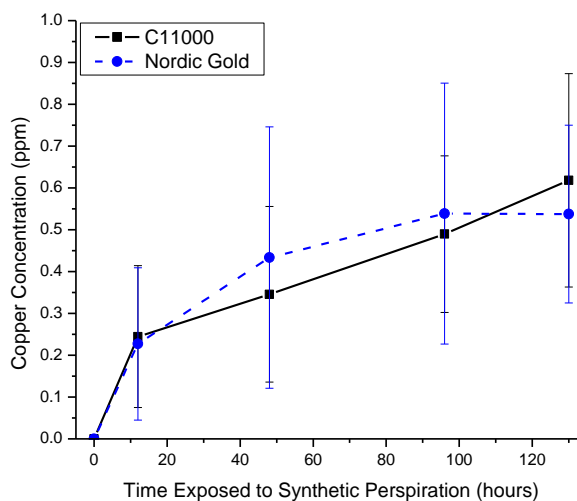


Figure 2.47. Copper concentration as a factor of time for C11000 and Nordic Gold when freshly ground to 1200 grit and thermally oxidized at 170 °C for 60 minutes, followed by exposure to synthetic perspiration solution (23 °C, ambient aeration) over time expressed as ppm in solution. Synthetic perspiration solution was exposed to 0.8 cm² of copper of the copper alloy coupon, with a surface to volume ratio of 2.67 cm²/L. Data is the average of 3 replicates and error bars are one standard deviation.

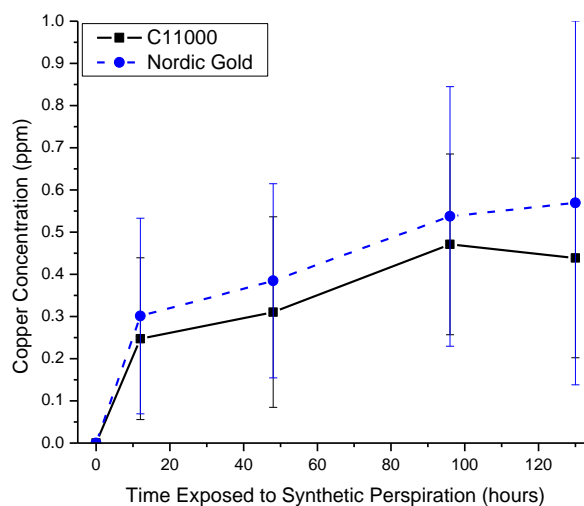


Figure 2.48. Copper concentration as a factor of time for C11000 and Nordic Gold when freshly ground to 1200 grit and air oxidized at ambient lab conditions for 30 days, followed by exposure to synthetic perspiration solution (23 °C, ambient aeration) over time expressed as ppm in solution. Synthetic perspiration solution was exposed to 0.8 cm² of copper of the copper alloy coupon, with a surface to volume ratio of 2.67 cm²/L. Data is the average of 3 replicates and error bars are one standard deviation.

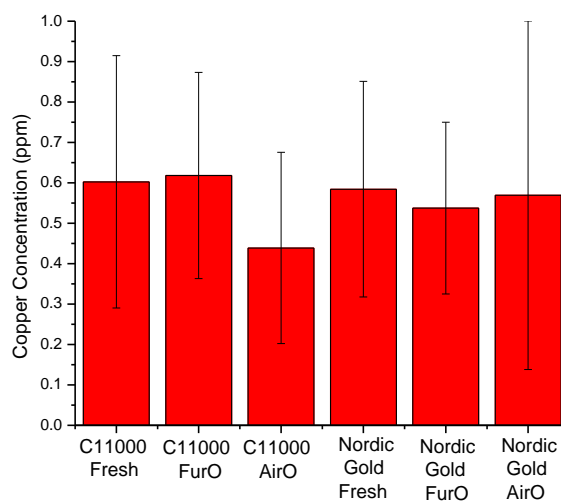


Figure 2.49 Copper concentration as a factor of time for C11000 and Nordic Gold when freshly ground to 1200 grit, thermally oxidized at 170 °C for 60 minutes, or air oxidized at ambient lab conditions for 30 days, followed by exposure to synthetic perspiration solution (23 °C, ambient aeration) over time, expressed as ppm in solution. Synthetic perspiration solution was exposed to 0.8 cm² of copper of the copper alloy coupon, with a surface to volume ratio of 2.67 cm²/L. Data is the average of 3 replicates and error bars are one standard deviation.

2.5 Discussion

2.5.1 Summary of Results and Findings

Ideally, the fate of copper can be tracked through the corrosion process of a copper alloy through charge transfer to the oxide, evaluated by galvanostatic reduction, and charge transfer to the solution, evaluated by ICP-OES, compared to total oxidation rate monitored by EIS and total oxidation charge based on mass loss analysis with Cu^+ and Cu^{2+} . Figure 2.50a-b shows that charge analysis by EIS agree with charge by mass loss. It is likely that corrosion products are a mix of Cu^+ and Cu^{2+} , as seen by GIXRD, rather than purely Cu^+ or Cu^{2+} as represented in Table 2.8. Initially, it appears the majority of charge is transferred to the solution at 12 hours of exposure to synthetic perspiration, consistent with the high initial copper release into solution seen in Figure 2.43. This study additionally demonstrates that there is consistently more charge transfer by oxidation to the solution than by direct formation of the oxide, indicating that a greater percent of copper tends to undergo dissolution into solution than incorporation into the oxide layer. While charge transfer associated with Cu oxidization in solution are similar between C11000 and Nordic Gold, charge transfer to the oxide varies significantly with alloy composition (Figures 2.50-2.51). Additionally, charge transfer to the oxide in Nordic Gold is more affected by the presence of thin oxides compared to C11000 (Figure 2.50). It is evident, therefore, that both alloy composition and the presence of thin oxides affect the fate of copper. Even though the corrosion rate is slightly lower for Nordic Gold and the oxide layer thinner compared to C11000, copper release is occurring through the oxide layers.

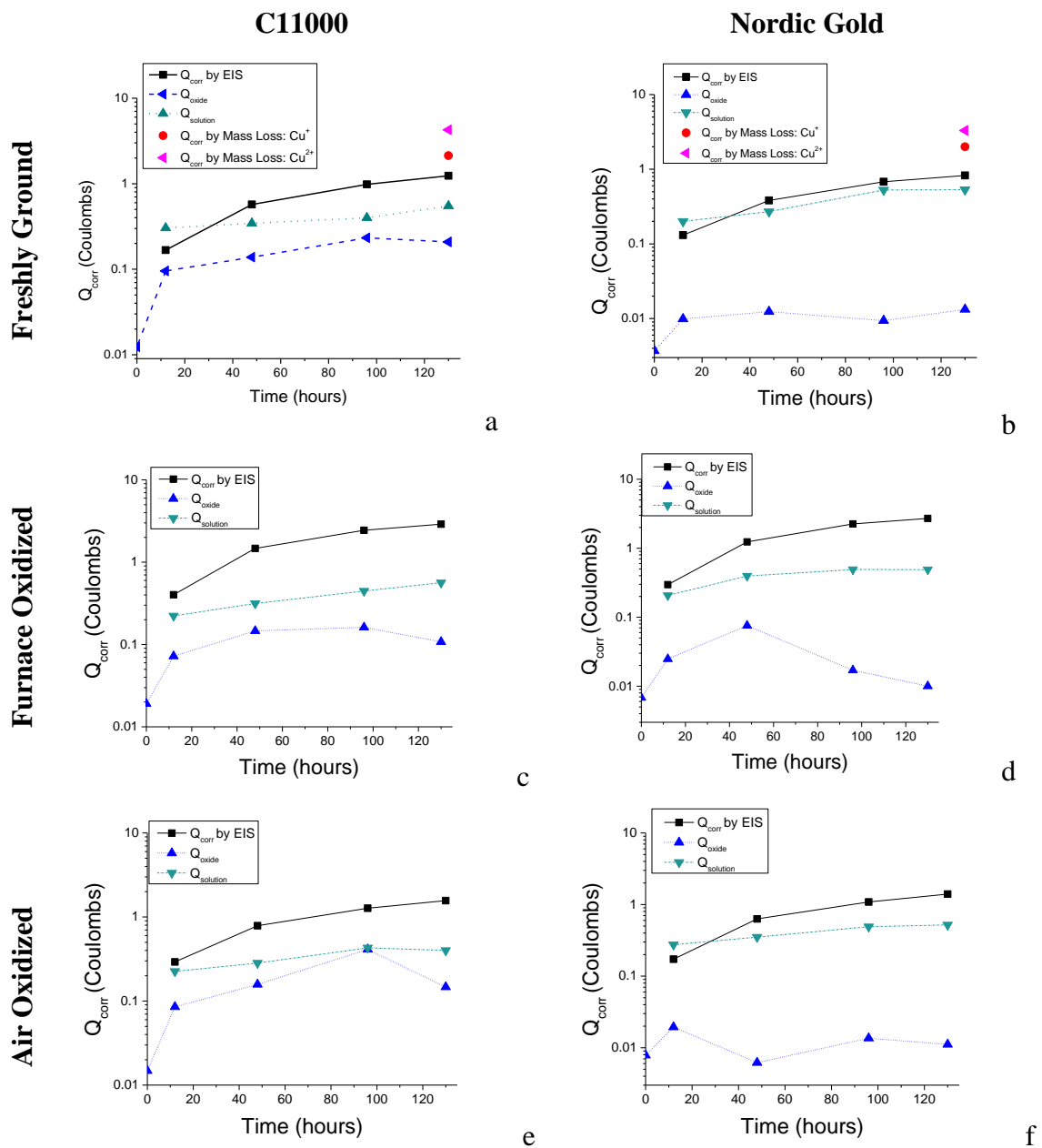


Figure 2.50. Charge analysis of C11000 and Nordic Gold when freshly ground to 1200 grit, thermally oxidized at 170 °C for 60 minutes, or air oxidized at ambient lab conditions for 30 days, followed by exposure to synthetic perspiration solution (23 °C, ambient aeration) over time. Exposure area of working electrode (copper alloy) for EIS was 0.8 cm². Galvanostatic reductions were conducted at 0.02 mA/cm² on an area of 0.8 cm². Synthetic perspiration solution was exposed to 0.8 cm² of copper of the copper alloy coupon, with a surface to volume ratio of 2.67 cm²/L.

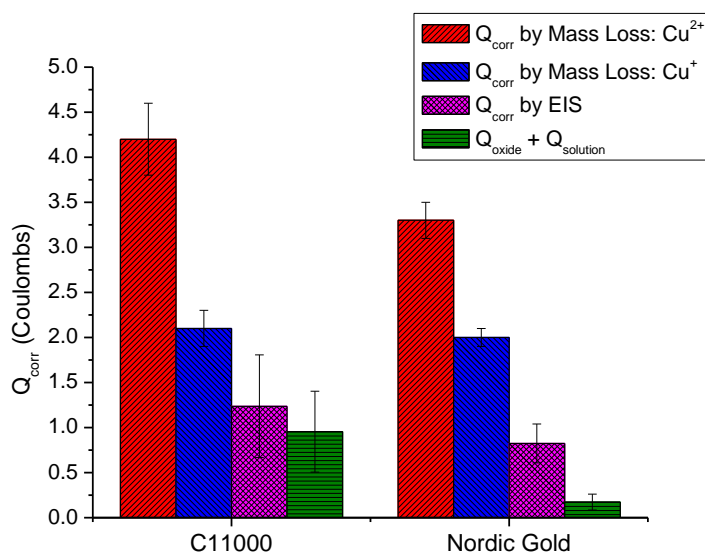


Figure 2.51. Charge comparison of Q_{corr} calculated from gravimetric mass loss, EIS, and ($Q_{\text{oxide}} + Q_{\text{solution}}$) of C11000 and Nordic Gold when freshly ground to 1200, followed by exposure to synthetic perspiration solution (23 °C, ambient aeration) over time. Exposure area of working electrode (copper alloy) for EIS was 0.8 cm². Galvanostatic reductions were conducted at 0.02 mA/cm² on an area of 0.8 cm². Synthetic perspiration solution was exposed to 0.8 cm² of copper of the copper alloy coupon, with a surface to volume ratio of 2.67 cm²/L.

Studies by the CDA indicate that when a thin oxide forms on the surface of Nordic Gold, the copper alloy lacks antimicrobial efficacy.² The difference of antimicrobial behavior between freshly ground and air oxidized samples therefore must stem from a difference in corrosion behavior due to the presence of a thin air formed oxide. This thin, air formed oxide layer and a thermally generated oxide layer were characterized prior to exposure to synthetic perspiration by galvanostatic reduction and GIXRD on both C11000 and Nordic Gold (Figures 2.24 and 2.30). The air formed and thermally formed oxide layers proved too thin to be evaluated by GIXRD, as no corrosion product peaks appeared in the spectrum prior to exposure to synthetic

perspiration (Figure 2.24). While not seen in GIXRD, galvanostatic reduction concluded that a thickening of both CuO and Cu₂O occurs on C11000 when air or thermally oxidized (Figure 2.30). Air and thermally oxidized Nordic Gold also experienced a thickening of Cu₂O. However, only air oxidized Nordic Gold contained a third species, which based on potential is attributed to either amorphous Zn(OH)₂ or Sn(OH)₂. These oxides have not been previously detected by GIXRD, galvanostatic reduction or Raman spectroscopy to appear on Nordic Gold following exposure to synthetic perspiration.¹¹⁹

The corrosion of C11000 in synthetic perspiration is minimally affected by the presence of thin oxides (Figure 2.18). Because instantaneous corrosion rate was unaffected by the presence of thin oxides in the case of C11000 at any exposure from 0-130 hours to synthetic perspiration, this suggests that C11000 is not strongly affected by the presence of a thin passive layer such as formed by air oxidation. This observation is consistent with observations from the CDA that C19700 (a similar high copper alloy, 97.6% Cu) maintains antimicrobial behavior when tarnished.⁵⁷ The thin oxide (CuO and Cu₂O) formed by either thermal oxidation or air oxidation is insufficient to act as a protective barrier against further corrosion. With such a high copper content, the positive open circuit potential (OCP) enables Cu⁺/Cu²⁺ corrosion. Precipitation may enable the darker corrosion layers that form and become more discolored over time (Figure 2.19).

The presence of thin, air or thermally formed oxides on C11000 neither changes the progression of discoloration, or the degree to which reflectivity is lost over time (Figures 2.19 and 2.21). Additionally, the presence of thin oxides prior to exposure to synthetic perspiration did not alter the species of corrosion products formed on the surface after exposure to synthetic perspiration (Figures 2.26 and 2.30). Thin oxides did

not inhibit the further development of Cu_2O and CuO on the surface of C11000. However, as evident in both GIXRD (Figure 2.26) and galvanostatic reduction (Figure 2.30), the presence of a thin film formed by air oxidation did hinder the growth of further film on C11000, resulting in a thinner oxide layer compared to either the thermally oxidized counterpart, or the freshly ground variant. This suggests that while air passivation of C11000 does not have a significant effect on the rate of corrosion in synthetic perspiration, it does affect the rate at which oxides subsequently form on the bulk alloy. An examination of copper ion release reveals similar ion release between 0 and 96 hours for all pre-treatment conditions for C11000, indicating thin oxides on C11000 do not inhibit the dissolution of copper into solution. This result corresponds to the lower instantaneous corrosion rate of air oxidized C11000 following exposure to synthetic perspiration for 130 hours, where the corrosion rate was lower than either thermally oxidized or freshly ground alloys.

The corrosion of Nordic Gold is more significantly affected by the presence of thin oxides. The instantaneous corrosion rate of Nordic Gold when air oxidized was lower than furnace oxidized or freshly ground samples (Figure 2.17). While all instantaneous corrosion rates decrease with time exposed to the synthetic perspiration, the small degree to which Nordic Gold corrodes when air oxidized indicates the presence of a stable, protective layer formed during exposure to lab air that affected subsequent exposure to synthetic perspiration. While this layer thickens to enhance protection, the coloration darkens to a matte yellow-brown, which occurs regardless of the presence of thin oxides (Figure 2.20). As seen in C11000, the presence of thin oxides did not alter the continued development of Cu_2O and CuO (Figure 2.30). However, as

was seen in air oxidized Nordic Gold, thin oxides did result in the development of thinner oxide layers for both thermally and air oxidized samples (Figure 2.30). While thin oxides resulted in a thinner corrosion layer after exposure to synthetic perspiration, the thinner corrosion layer did not have a significant effect on copper ion release in synthetic perspiration (Figure 2.43). Throughout all times observed, freshly ground Nordic Gold and Nordic Gold with thin air formed oxides maintained similar levels of copper ion release (Figure 2.49). The presence of thin oxides resulting in a thinner corrosion layer may also enable easier transfer of ions from the bulk metal into solution. The relative color stability of Nordic Gold following initial discoloration was attributed to Al additions, known to help maintain color stability in alloys.⁹⁸ While Zn is reported to decrease copper release and Sn to increase copper release³, the combined effect in Nordic Gold resulted in similar copper release to C11000, indicating the enhancing effect of Sn is stronger than the suppressing effect of Zn. It is evident that the effect of alloy composition remains a critical factor in corrosion behavior.

2.5.2 Effect of Zn, Al, and Sn Alloying Additions and Thin Oxides on Copper Corrosion Electrochemistry in Synthetic Perspiration

The findings of this study shed light onto the role of Zn, Al and Sn as alloying additions in copper alloys compared to pure copper. Nordic Gold exhibits a lower corrosion rate than C11000, observed in instantaneous rate and confirmed by total mass loss (Figures 2.16-2.17, Table 2.7). The instantaneous corrosion rate of Nordic Gold is consistently slightly less than that of C11000, and over 130 hours, results in 30% less mass lost to the corrosion layer or solution (Figure 2.18). As there is stoichiometrically less copper to participate in the corrosion process, and Zn is known to reduce the

corrosion rate, this result corresponds well to the previously observed behavior.¹¹⁹

However, since the OCP suggests the initial dealloying of Zn or Al at OCP, some mass loss and charge transfer may also be due to these elements participating in alloy oxidation as well prior to EIS measurements began, which were not accounted for in Figure 2.50.

The formation of tarnish and corrosion layers was also significantly affected by the alloys composition. A visual inspection of Nordic Gold reveals that, while C11000 continues to discolor over time exposed to synthetic perspiration (Figure 2.19), Nordic Gold's optical properties change initially after 12 hours of exposure, but do not continue to discolor with time (Figure 2.20). This is likely a result of Al, which enables Nordic Gold to maintain color stability following initial tarnish, and attests the alloys success as a tarnish-resistant coinage metal. This lack of continued discoloration is supported by the observation that Nordic Gold consistently produces a thinner oxide layer compared to C11000 (Figure 2.42). While corrosion layers on C11000 continue to thicken over time exposed to synthetic perspiration, Nordic Gold maintains a similar oxide thickness following 12 hours of exposure. This stability is likely the reason that $\text{Cu}_2(\text{OH})_3\text{Cl}$ is only observed to form in C11000. $\text{Cu}_2(\text{OH})_3\text{Cl}$ was only observed after 96 hours of exposure to synthetic perspiration, and was not detected on Nordic Gold.

While it clear that alloying additions affect electrochemical behavior, the effect of thin oxides is less clear. Additionally, the manner in which the oxides are generated effect electrochemical behavior. Based on galvanostatic reduction of non-exposed alloys (Figure 2.30), it is evident that thermally generated oxides and air generated oxides are not identical. While the presence of thin oxides minimally affected i_{corr} of C11000, Nordic Gold experienced a decrease in i_{corr} even in the presence of thermally generated

oxides, but to the greatest extent in the presence of air generated oxides (Figures 2.16-2.17). When exposed, i_{corr} of air oxidized Nordic Gold was statistically lower when first exposed to perspiration than either the freshly ground or thermally oxidized alloy. This electrochemical behavior suggests that a joint effect of thin oxides and alloying additions.

2.5.3 Effect of Zn, Al, and Sn Alloying Additions and Thin Oxides on Metal Release Rate in Synthetic Perspiration

An evaluation of copper release enables the correlation between corrosion behavior and antimicrobial function of copper alloy surfaces. While individual and/or selected alloying elements (Zn, Sn) have been examined for their effect on copper release³, the complex effects of multiple alloying additions that have opposing suppressing and enhancing effects has not. Charge analysis indicates that during the first 12 hours of exposure to synthetic perspiration, the majority of charge is transferred to the solution as opposed to the oxide (Figure 2.50). This observation is consistent with alloys lacking a sufficient protective layer (freshly ground samples) or having only a very thin protective layer that is ineffective at limiting release when exposed to harsh environments such as synthetic perspiration. Even once a thicker oxide begins to form, its protective ability is limited given the corrosivity of perspiration, resulting in a consistently larger charge transfer to the solution as compared to the oxide (Figure 2.50).

In an examination of copper release on freshly ground alloys, Nordic Gold has a lower copper release compared to C11000 in the first 12 hours of exposure to synthetic perspiration (Figure 2.43). This is consistent with lower OCP (Figure 2.7). This could be the result of dealloying of Zn or Al early in the corrosion process with limited dissolution of Cu by oxidation. If selective leaching of Zn or Al at OCP occurred prior to the

dissolution of Cu into solution, this would account for a decreased Cu concentration in this initial period. Qualitative evaluation revealed both the presence of Zn and Al in solution at all times of exposure. This suggests that alloying additions initially depress Cu release due to dealloying and OCP suppression below Cu/Cu^+ , Cu/Cu^{2+} , and $\text{Cu}/\text{Cu}_2\text{O}$ equilibria. However, Cu release from both alloys remains steady, despite decreasing i_{corr} , and total Cu release between alloys is similar following 12 hours of exposure. A steady copper release from the alloy despite decreasing i_{corr} suggests that Cu preferentially undergoes dissolution into solution as opposed to incorporation into the oxide, or that Cu dissolution from the oxide occurs simultaneously. This appears especially true of Nordic Gold, where copper release is steady, but oxide thickness does not change significantly following 12 hours (Figure 2.30). Additionally, despite Nordic Gold's lower copper content, copper release following 12 hours of exposure to synthetic perspiration solution remains similar to C11000 across all times. This suggests that the alloying element that enhances copper release (Sn^3) is capable of overcoming effects of elements suppressing copper release (Zn^3). Particularly, additions of Zn and Al cause suppressed copper release at short time periods (<12 hours), but are counteracted by Sn at longer times (>12 hours) to result in similar copper release between Nordic Gold and C11000 despite differing copper content.

As seen in Figures 2.44-2.45, the presence of thin air formed oxides did not affect copper release from either Nordic Gold or C11000. This behavior is attributed to the fact that while these thin oxides may be suitable to protect the alloy from atmospheric corrosion, they are not capable of protecting them from full immersion corrosion in a harsh perspiration solution. While galvanostatic reduction confirmed the presence of

oxides generated by either thermal or air oxidation, they are apparently sufficiently thin and porous as to not impede copper dissolution. In the case of air oxidized Nordic Gold, where i_{corr} was lower compared to freshly ground alloy and attributed to the presence of Zn or Sn oxide, this air formed layer does not appear to impede the steady dissolution of copper into solution over time in synthetic perspiration. Thus the observation of limited antimicrobial function in Nordic Gold is a function not only of environment but environmental specificity.

The concentration of copper dissolved into solution is critical to determine possible precipitates that would form on the surface of the oxide layer, and to relate copper concentration to antimicrobial efficacy. Based on Table 2.6, the concentration of copper ions in solution following 12 hours of exposure of the copper alloy to synthetic perspiration exceeds the solubility limit of $\text{Cu}_2(\text{OH})_3\text{Cl}$ and CuCl , but remains well below the solubility limit of Cu_2O (Figures 2.44-2.45). The utilization of a mild HCl rinse solution to dissolve any corrosion products formed along the walls to the exposure cell revealed that no quantifiable amount of Cu was precipitated in the cell. However, the possible presence of $\text{Cu}_2(\text{OH})_3\text{Cl}$ on C11000 following exposure to synthetic perspiration as was determined by galvanostatic reduction suggests that $\text{Cu}_2(\text{OH})_3\text{Cl}$ precipitated back onto the copper alloy during corrosion (Figure 2.30).

In order to relate copper release to antimicrobial efficacy, an evaluation of total copper release from alloys compared to copper content necessary to kill microorganisms is necessary. Figure 2.52 shows the results disinfection “kill curves” performed at the University of Virginia to observe the relative effectiveness of copper ions (Cu^{2+}) at varying concentrations on killing *E. coli* (HCB1) in synthetic perspiration, and

enumerated by the most probable number (MPN) method utilizing Colilert® and Quanti-Trays® (Idexx). *E. coli* (HCB1) was obtained from Howard C. Berg at Harvard University. At concentrations above 0.1 ppm Cu^{2+} , such as 1, 10, or 100 ppm, *E. coli* (HCB1) populations dropped faster than natural die off, indicating antimicrobial activity. Therefore, by relating the necessary quantity of Cu^{2+} to kill *E. coli* (HCB1) to copper release from Nordic Gold and C11000, it is evident that both alloys release sufficient copper within just the first 12 hours to kill *E. coli* (HCB1), as both levels are in excess of 0.2 ppm Cu^{2+} (Figure 2.43). Based on *E. coli* (HCB1) in synthetic perspiration, data suggests that both C11000 and Nordic Gold should have similar antimicrobial efficacy, and those antimicrobial efficacies are unaffected by the presence of thin oxides. Based on average release rates from Figure 2.43 and assuming unchanging corrosion behavior over time, Figure 2.53 and Table 2.9 define the times necessary to achieve 1, 10, and 100 ppm copper release from copper alloys.

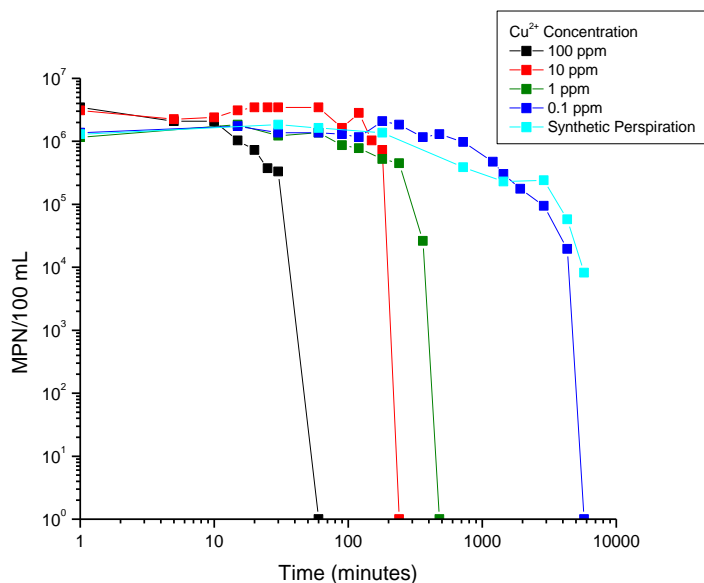


Figure 2.52. University of Virginia disinfection studies of *E. coli* (HCB1) in solution of synthetic perspiration (0.5% NaCl, 0.1% $\text{CH}_4\text{N}_2\text{O}$, 0.1% $\text{C}_3\text{H}_6\text{O}_3$, pH 6.5) and Cu^{2+} ions from a CuCl_2 solution at 23 °C, enumerated by most probable number (MPN) method.

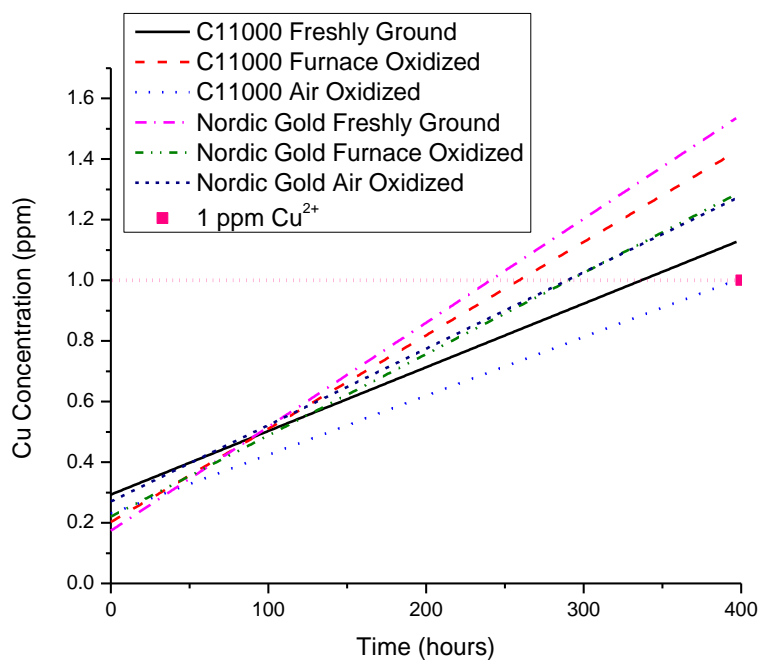


Figure 2.53. Correlation of constant copper release rates from copper alloys to time needed to achieve 1 ppm Cu^{2+} at a surface to volume ratio of $2.67 \text{ cm}^2/\text{L}$.

Table 2.9. Analysis of constant copper release rates to determine lengths of time needed to achieve antimicrobial copper concentration.

Alloy: Treatment	Concentration (ppm)		
	1	10	100
	Days Needed to Achieve Concentration Based on Constant Release Rates		
C11000: Freshly Ground	14	193	1978
C11000: Furnace Oxidized	11	133	1350
C11000: Air Oxidized	16	210	2143
Nordic Gold: Freshly Ground	10	119	1213
Nordic Gold :Furnace Oxidized	12	152	1551
Nordic Gold: Air Oxidized	12	161	1649

2.6 Conclusions

For use as hospital high touch surfaces, copper alloys must exhibit an antimicrobial robustness against passivation due to long term air exposure. While previous studies by the CDA have only analyzed the empirical survivability of bacteria

on the alloy surface in a nutrient broth solution, this study successfully identified the effects of thin air formed oxides versus freshly abraded surfaces on corrosion behavior in a perspiration solution. Corrosion behavior is a factor of alloy composition, the presence or lack of thin oxides and environment. C11000 was minimally affected by the presence of thin oxides, with no statistical difference between the corrosion rate (i_{corr}) and copper release from freshly ground alloy and either thermally or air generated oxides. Thin oxides did, however, limit the corrosion layers that accumulated on C11000 compared to the freshly ground alloy. Nordic Gold was affected to a greater extent by the presence of thin oxides, particularly formed by natural air oxidation. However a similar copper release to the freshly ground alloy was seen in synthetic perspiration solution. Based on the relationship of comparable copper release from both C11000 and Nordic Gold in synthetic perspiration, regardless of the presence of thin oxides, to concentrations of Cu^{2+} necessary to kill *E. coli* (HCB1), both alloys should provide similar antimicrobial behavior regardless of air oxidation.

3 The Fate of Copper during Corrosion of Nordic Gold (89% Cu, 5% Zn, 5% Al, 1% Sn) vs. C11000 (>99.9% Cu) in Concentrated Synthetic Perspiration Solution (2 M NaCl, 1 M CH₄N₂O, 0.11 M C₃H₆O₃)

3.1 Abstract

Methicillin-resistant *staphylococcus aureus* (MRSA) is highly contagious and is spread mainly by hand-to-surface contact. In 2005, 94,650 patients in the United States contracted MRSA, and 18,650 of these patients died.¹ MRSA is especially prevalent in hospitals, where patients are infected with MRSA by touching surfaces that will, in turn, be touched by other patients whose immune systems may be compromised. This research is related to the goal of minimizing the spread of antibiotic-resistant diseases in hospitals enabled by corrosive release of Cu⁺ and Cu²⁺ from copper alloys in solutions such as human perspiration. At the same time it is desirable to maintain color stability on hospital surfaces by minimizing tarnishing. This creates a clearly contradictory situation. Unfortunately, the copper alloys with the best antimicrobial efficacy are often those that tarnish more readily. Conversely, the most corrosion resistant copper alloys in human perspiration often do not exhibit very good antimicrobial efficacy especially after long periods after abrasion. Nordic Gold (89% Cu, 5% Zn, 5% Al, 1% Sn) was reported to kill MRSA after freshly abraded, but when exposed to ambient lab conditions for 7 days, Nordic Gold passivates.² However, MRSA kill rates studies were not conducted in a solution that mimics hospital condition corrosion mechanism (i.e. salt transfer from hand perspiration due to frequent skin contact). Additionally, no studies have examined the effect of concentration build-up during drying or repeated perspiration contamination on the alloy surface on corrosion behavior, as it relates to antimicrobial efficacy.

The goals of this study is to understand tarnishing, copper release and color stability of a Cu-Al-Zn-Sn alloy (Nordic Gold) in a concentrated synthetic perspiration designed to mimic the effects of a harsh environment just before drying following the initial deposit of salts from hand perspiration and subsequent drying on a copper surface are investigated as a part of this study. The chapter compares Nordic Gold to C11000, and the role of thin oxides such as those formed by air oxidation. This was accomplished by tracking the “fate of copper” through the corrosion process by analysis of total copper oxidation, electrochemical analysis of the oxide layer formed, and solution analysis of dissolved copper.

Concentrated perspirations solution resulted in a stronger thermodynamic driving force and rate of oxidation of copper alloys compared to normal concentration synthetic perspiration. Both alloys exhibited increasing instantaneous corrosion rates over the time exposed to the solution, with Nordic Gold exhibiting a larger rate compared to C11000. Thin air formed oxides increased corrosion rate compared to freshly ground counterparts. Additionally, Nordic Gold was observed to have a thinner oxide layer after exposure to concentrated synthetic perspiration, release less Cu into solution over time, and release less total metal ions into solution compared to C11000. The presence of thin oxides resulted in an increase in Cu release from the alloy, and a greater variety of corrosion products, including $\text{Cu}_2(\text{OH})_3\text{Cl}$ due to precipitation by homogeneous chemical reaction compared to freshly ground alloys where only CuO and Cu_2O were detected.

3.2 Introduction

Due to the rising number of hospital acquired infections in recent years, significant research has explored exploiting copper alloys for their inherent antimicrobial

nature to replace high touch surfaces. Current standards to evaluate antimicrobial copper rely only on empirically bacteria viability, and offers no insight into the exact role of corrosion on copper ion release responsible for antimicrobial behavior nor the critical Cu^+ or Cu^{2+} concentration required to serve in this function. Additionally, Environmental Protection Agency qualifications for antimicrobial copper alloys are based on the corrosion of the copper alloy in a nutrient broth ideal for growing bacteria⁴⁹⁻⁵¹, rather than on the medium that would naturally facilitate the alloys corrosion in a hospital environment. The likely relevant environment on high touch surfaces is hand perspiration.^{112,113} Additionally, the result of wetting and drying cycles on the chemistry of surfaces containing perspiration that would naturally occur in the environment have not been studied to establish a link between this type of corrosive environment and antimicrobial behavior.

These results likely depend on environmental severity and environment composition. In applications as antimicrobial high touch surfaces, copper alloys will rely on the perspiration transferred by handling to facilitate the copper ion release necessary for antimicrobial activity.^{112,113} Studies have reported that primary constituents of human perspiration to be salt (NaCl), potassium (K), lactic acid ($\text{C}_3\text{H}_6\text{O}_3$), and nitrogen containing compounds such as urea ($\text{CH}_4\text{N}_2\text{O}$), ammonia (NH_3), amino acids, uric acid ($\text{C}_5\text{H}_4\text{N}_4\text{O}_3$), and creatinine ($\text{C}_4\text{H}_7\text{N}_3\text{O}$).¹³⁰ Additionally, calcium (Ca) and magnesium (Mg) are present, and phosphorous (P), copper (Cu) and manganese (Mn), iron (Fe), iodine (I), fluorine (F) and bromine (Br) in trace amounts have been reported.¹³⁰ Typical pH values range 4-6.8.¹³⁰ The exact composition is highly dependent on the individual, including gender, environmental heat stress, and diet. A variety of synthetic perspiration

solutions have been utilized in research, varying in composition and pH (Table 3.1).

Based on the chemistry of perspiration, a handled object will be deposited with the full chemical composition of the perspiration, but over time will retain only those chemicals whose vapor pressure less than water, such as NaCl, urea and lactic acid, while those with a greater vapor pressure will be evaporated, such as ammonia. Therefore, the composition of the dried perspiration droplet can differ from the composition of the initially deposited perspiration droplet.

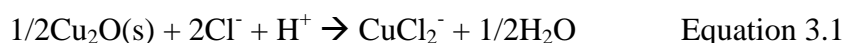
Table 3.1. Composition of synthetic perspiration solutions used in previous exposure studies.	
Composition (by mass percentage)	pH
0.87% NaCl, 0.16% CH ₄ N ₂ O, 10.92% C ₃ H ₅ NaO ₃ (60%), 0.016% Na ₂ HPO ₄	7.5 ⁸²
1.96% NaCl, 0.49% CH ₄ N ₂ O, 1.39% C ₃ H ₆ O ₃ , 0.25% C ₂ H ₄ O ₂ , 1.71% NH ₄ Cl	4.7 ⁸³
0.5% NaCl, 0.1% CH ₄ N ₂ O, 0.1% C ₃ H ₆ O ₃	6.5 ^{63,84,85}
0.3% NaCl, 0.1% Na ₂ SO ₄ , 0.2% CH ₄ N ₂ O, 0.2% C ₃ H ₆ O ₃	6.6 or 4.5 ⁸⁶
0.5% NaCl, 0.1% CH ₄ N ₂ O, 0.5% C ₃ H ₆ O ₃	5 ⁸⁷
0.5% NaCl, 0.1% CH ₄ N ₂ O, 0.1% C ₃ H ₆ O ₃	4.5 ⁸⁸

At 20% relative humidity (RH), one monolayer of water forms along clean surfaces, increasing at 75% RH to ~5 monolayers.¹³¹ The behavior of atmospheric corrosion above 3 monolayers of water are similar to those of bulk water.¹³² In high RH circumstances, invisible water clusters and water film develop along the surface, resulting in local anode and cathodes that enhance the corrosion process.¹³³ However, if salt particles exist along the metallic surface, a thicker water film can form compared to a clean surface.¹³³ The thickening of the water film results in the creation of passages for the migration of cations.¹³³ Thicker water films will exist at the points of wetting and connected by thinner layers across the surface.¹³² When perspiration is deposited on a surface, the RH of the environment determines whether the area continues to wet the

surface in the case of high RH, or begins to evaporate in the case of low RH.¹³² The critical RH, called the deliquescence point, determines the behavior of the solution due to its constituents. At the deliquescence point, the salt fully saturates the water droplets formed due to RH. At RH above the deliquescence point, the compound is considered in solution, due to the accumulation of water from the atmosphere.¹³² At RHs below the deliquescence point, the. If the compounds are in solution and the RH drops below the deliquescence point, the water evaporates from the solution and resulting in the droplet becoming super saturated with salt, and the salt consequently precipitates and dries, as well as in electrolyte thinning.^{134,135} This electrolyte thinning phenomenon has several effects on metal corrosion, including concentration build-up, increase in metal ion concentration and passivation.¹³⁶ Concentration build-up causes reduced solubility of oxygen and corrosion products in the electrolyte layer.^{136,137} It has been observed that concentration build-up by drying on carbon steel results in a reduced corrosion rate when the corrosion reaction is controlled by cathodic oxygen reduction, but increases corrosion rate when the corrosion reaction is controlled by anodic dissolution processes.¹³⁶

Atmospheric corrosion of copper in field and laboratory studies has been well researched.^{110,138-140} The fate of copper during atmospheric corrosion depends strongly on environment, including temperature, relative humidity, pH, and pollution concentrations (Cl^- , O^{2-} , SO_4^{2-}).⁵⁸ The higher the relative humidity, the more likely atmospheric constituents can become incorporated into the tarnish layer as it forms.⁵⁸ However, high relative humidity results in comparably thinner tarnish layers.⁶⁴ RH also determines the amount of adsorbed and absorbed water on the copper surface, thus determining its corrosion behavior.¹⁴¹ Additionally, the presence of salts on the surface of copper has

been observed to alter copper's corrosion behavior.^{132,141} A copper surface in contact with NaCl at 55% RH, well below its deliquescence point (75% RH) results in significant corrosion and mass gain caused by the formation of corrosion products, specifically Cu₂O.^{132,141} As corrosion takes place, chloride ions diffuse away from the NaCl particle along the electrolyte, and results in the decrease stability of copper's passive film.¹⁴² The mechanism of chloride-induced breakdown can be seen in Equation 3.1, where the products formed are either Cu₂O or CuCl depending on the electrolyte conditions.¹³² With a thickening water layer, the outward diffusion of chloride ions from the NaCl particle is enhanced.¹³² Additionally, the formation of other copper-chloride corrosion products such as CuCl₂*nH₂O (68.4% RH) that have lower deliquescence than NaCl (75% RH) will result in increasing the amount of absorbed water on the surface.¹⁴¹ Several studies have confirmed that the presence of NaCl on the surface of copper in a humid environment results in an increased corrosion rate.^{141,143} Depending on the pH and [Cl⁻] of the electrolyte, Cu ions either form nantokite (CuCl) or cuprite (Cu₂O), or form copper (I) chloride complexes.¹⁴¹ Additionally, in the presence of humidity, nantokite can form atacamite (Cu₂Cl(OH)₃) and paratacamite (Cu₂(OH)₃Cl).¹⁴¹



As antimicrobial behavior in copper alloys has been established to a result of microorganism's interaction with copper ions, there is a direct correlation between antimicrobial efficacy and corrosion behavior. During the corrosion process in wetting or drying, copper ions can become part of one of several "fates" as a result of metal oxidation: retention of the metal oxide at the interface¹¹⁴, a metal salt¹⁴¹, dissolution into the solution¹¹⁵, selective leaching or dealloying of Cu or other elements¹¹⁶, dissolution

into the solution followed by precipitation on the surface of the oxide as an insoluble corrosion product,¹¹⁷ or complexation with species in the environment. It is assumed that only those copper ions that are dissolved into the solution are responsible for antimicrobial behavior. Only those copper ions that are dissolved into the solution are responsible for antimicrobial behavior. Moreover, those ions that become part of an oxide may be sequestered.

Nordic Gold (89% Cu, 5% Zn, 5% Al, 1% Sn) is an fcc solid solution alloy that has been examined by several research groups as a possible antimicrobial material due to its high copper content.¹⁰⁶⁻¹⁰⁸ Additionally, due to its development as an alloy for European coinage, Nordic Gold is also tarnish resistant¹⁰⁵, which in combination with its high copper content makes it an attractive prospect for hospital applications where both antimicrobial efficacy and non-tarnishing visual appeal are desired.¹¹¹ EPA testing by the Copper Development Association (CDA) indicates that Nordic Gold (89% Cu, 5% Zn, 5% Al, 1% Sn) is antimicrobial when freshly cleaned², but when exposed to ambient lab temperature and relative humidity for 7 days, it passivates completely when tested for antimicrobial efficacy in bacteria growth medium.² When freshly cleaned, Nordic Gold is capable of reducing 10^7 colony forming units (CFU) of methicillin resistant *S. aureus* within 6 hours in bacteria growth medium.² However, following exposure to ambient lab conditions for 7 days, there is no reduction in CFU within the same 6 hour period when tested in bacteria growth medium, the same as is observed for stainless steel which is known to have no antimicrobial properties.^{1,55,56,118} EPA antimicrobial testing on Nordic Gold suggests that thin yet protective oxides are sufficient to impede the release of copper ions from the bulk alloy to the surface in order to kill bacteria, which is

undesirable for longer term applications as high touch surfaces.² This exposes the lack of evaluation that has been conducted on the effect of thin oxides on corrosion rate, copper ion release, and subsequently antimicrobial activity. Other sources have also reported Nordic Gold's antimicrobial ability on a variety of microorganisms. *C. albicans* suspended in phosphate buffers solution and subsequently allowed to dry on Nordic Gold was observed to achieve full reduction from 10^6 CFU within 60 minutes.¹⁰⁷ *S. hominis* and *S. aureus* on Nordic Gold were completely killed within 360 minutes on washed and chemically sterilized European coins, and partial reductions (10% and 90%) on unwashed European coins that likely contained salt and dust deposits.¹⁰⁸ Thus in summary, there are conflicting results regarding Nordic Gold's antimicrobial properties, likely due to the wide variety of testing procedures and testing environments used to obtain kill rates. Variations between testing solution (broth or "dry"), treatment of the alloy prior to testing (freshly ground, sterilized, soiled, air oxidized) do not allow Nordic Gold's antimicrobial efficacy to be clearly established. Because the only data collected has been purely empirical and based only on kill rate data without direct assessment of Cu ion release, there is a lack of information regarding what factors affect the alloys antimicrobial efficacy through the corrosion process.

The objective of this study is to determine the effect of thin, air formed oxides on the corrosion of Nordic Gold (89% Cu, 5% Zn, 5% Al, 1% Sn) compared to a freshly abraded version and on the fate of copper during corrosion in a concentrated perspiration solution mimicking conditions seen just before drying. The use of a concentrated synthetic perspiration solution is designed to mimic the effects of corrosion following the initial deposit of salts from hand perspiration and subsequent drying on a copper surface.

The behavior of Nordic Gold when freshly ground or air oxidized for 30 days in ambient lab conditions will be compared to that of C11000 (>99.9% Cu), a commercially pure copper alloy, under identical conditions. Instantaneous corrosion rates will be compared to determine the effect of the air formed oxide on corrosion rate over time exposed to a concentrated synthetic perspiration solution by electrochemical impedance spectroscopy.⁸⁴ Mass loss by gravimetric analysis will also provide insight on integrated corrosion damage. The fate of copper through the corrosion process in perspiration will be tracked through analysis of oxides as formed by air oxidation as well as those formed during exposure to concentrated synthetic perspiration solution, assessed by optical spectrophotometry, grazing incidence x-ray diffraction, galvanostatic reduction, and copper ion release assessed by inductively coupled plasma-optical emission spectrometry. This study will ultimately provide a link between corrosion behavior and antimicrobial efficacy in an applications based situation, where thin oxides will form as a result of long-term use and perspiration may become concentrated by before drying during wet/dry cycling.

3.3 Experimental Procedure

C11000 (>99.9% Cu) and Nordic Gold (89% Cu, 5% Zn, 5% Al, 1% Sn) were obtained as sheets from the Copper Development association and cut in house into 2.5 x 2.5 cm coupons. All C11000 (>99.9% Cu) and Nordic Gold (89% Cu, 5% Zn, 5% Al, 1% Sn) coupons were ground using silicon carbide (SiC) metallography paper to successively finer grits up to 1200 grit. Immediately following grinding, coupons were placed in methanol to minimize oxidation until just before testing. Samples were dried of

methanol by compress air. Samples left in this condition for testing are designated as freshly ground (abbreviated Fresh).

3.3.1 Pre-Oxidation Conditions

Following grinding to 1200 grit, select samples were oxidized prior to immersion studies to simulate oxides that would be found in hospital environments after long term air exposure. Select alloys were left in lab air, averaging 23°C and 34% RH, for 30 days prior to immersion testing. Typical hospital conditions range from 21-24 °C and 30-60% RH.¹²⁰ These samples are here after designated air oxidized (abbreviated AirO).

3.3.2 Exposure Experiments

A concentrated synthetic perspiration solution was generated to be representative of the rewetting or just before drying of a surface having been exposed to hand perspiration. Concentrated synthetic perspiration composition was based on synthetic perspiration solution based on standard BS EN 1811:2011.⁸⁴ OLI Analyzer Studio 9.0 software was used to construct plots of concentration (M) versus relative humidity for the individual constituents of the solution (Figure 3.1). A relative humidity of 93% was selected to correspond to conditions maintained in intensive care unit burn centers, where patients are highly susceptible to HAIs due to prolonged stays and open wound area.¹⁴⁴ A RH of 93% is above the critical RH of both NaCl (75% RH) and urea (72% RH). This enables a high solubility of both NaCl and urea, where the maximum solubility of NaCl at 93% RH is 45% of max solubility in pure H₂O at 23 °C, and maximum solubility of urea at 93% RH is 75% of max solubility in pure H₂O at 23 °C. In order to maintain a fully soluble composition and single-phase liquid, concentrations of urea and lactic acid were lowered from maximum concentrations at 93%. The composition of lactic acid was

determined by its maximum solubility (10 g/L) in pure H₂O at 23 °C, compared to the C vs. RH diagram which indicates a deliquescent point of >99% RH, in contrast to its observed state as a 90% liquid solution with H₂O at ~30% RH. The concentration of urea was chosen to reflect both the lower initial urea concentration in synthetic perspiration and the more severe concentration change with relative humidity. Table 3.2. lists the composition of synthetic perspiration based on to standard BS EN 1811:2011⁸⁴ and concentrated synthetic perspiration utilized for exposure experiments.

Concentrated synthetic perspiration was prepared using purified water (resistivity 18.2 MΩ-cm) produced by an Academic MilliQ filtration system (MilliPore) and reagent grade chemicals in order to generate a 2 M NaCl (Sigma-Aldrich), 1 M Urea (CH₄N₂O) (Fisher Scientific), and 0.11 M Lactic Acid (C₃H₆O₃) (90%, Acros Organics) solution of ambient pH. Concentrated synthetic perspiration solution was used at ambient aeration at 23 °C within 24 hours of preparation, stable at pH 2.28. Figure 3.2 shows the E-pH diagram for a chloride containing aqueous solution of 2 M concentration similar to concentrated synthetic perspiration without lactic acid or urea, with ambient pH noted in this solution. Experiments conducted by Michael Hutchison where droplets of unconcentrated synthetic perspiration solution (pH=6.5) were dried and rewet indicate that during drying, pH becomes more acidic, where smaller droplets become more acidic at a faster rate.¹⁴⁵

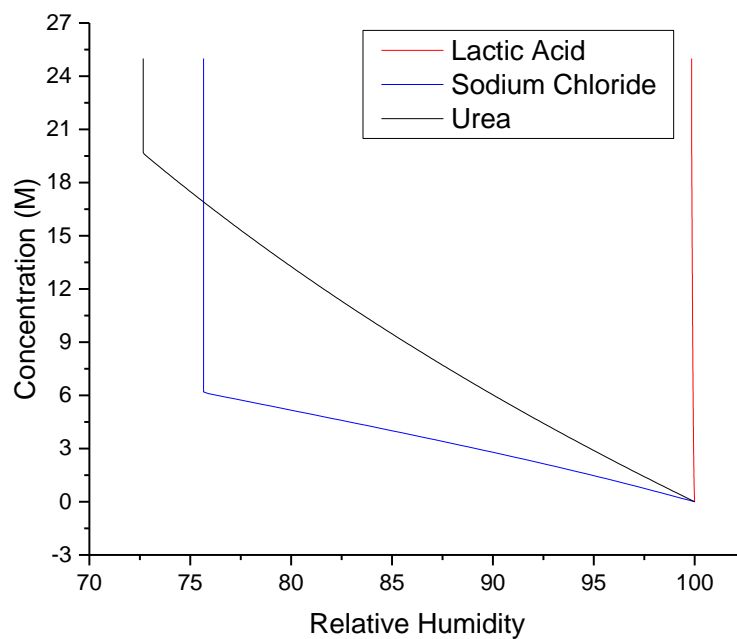


Figure 3.1. Determination of deliquescence point and $\text{Conc}_{\text{equil}}$ vs. RH relationship using OLI Analyzer Studio 9.0 software.

Table 3.2. Composition of synthetic perspiration solutions based on human hand perspiration deposited on a metal surface, allowed to dry, and rewet at 93% RH.									
Name	Formula	Solubility (g/L) in H ₂ O at 23 °C	Molecular Weight (g/mol)	Synthetic Perspiration* BS EN 1811:2011 ⁸⁴		Conc _{equil} at 93% RH Concentrated Perspiration		Concentrated Perspiration** <i>Solution Utilized in This Study</i>	
				g/L	M	g/L	M	g/L	M
Sodium Chloride	NaCl	357	58.44	5	0.086	163.6 3	2.8	116.88	2
Urea	CH ₄ N ₂ O	480	60.06	1	0.017	360.3 6	6	60.06	1
L(+)-Lactic Acid	C ₃ H ₆ O ₃	10	90.08	1	0.011			10	0.11

*Adjusted to pH 6.5 with ammonium hydroxide
 **Unadjusted pH =2.28

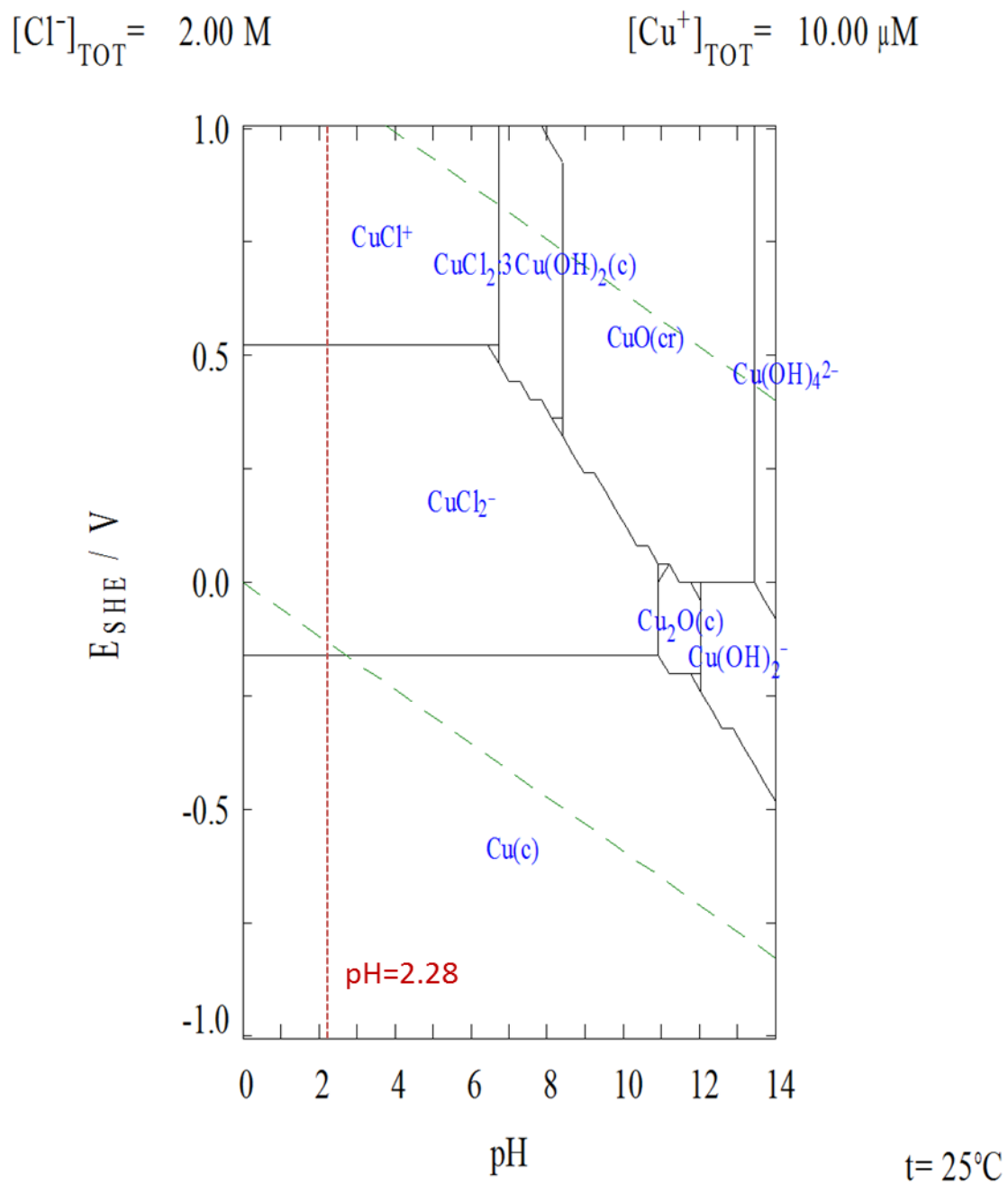


Figure 3.2. E-pH diagram of expected corrosion behavior in chlorinated medium (2 M Cl^- , $10 \mu\text{M}$ Cu^+ in H_2O at 25°C) to represent concentrated synthetic perspiration constructed with Medusa software, courtesy of Michael Hutchison.

Samples were placed in individual electrochemical flat cell with a 1 cm diameter circular aperture and an area of 0.8 cm². Cells were filled with 300 mL of concentrated synthetic perspiration and allowed to sit unstirred at ambient lab temperature (23 °C) and ambient aeration for 12, 48, 96, or 130 hours before samples were removed and dried by compressed air. Between each exposure, cells were washed 10 minutes with 0.1 M HCl to remove synthetic perspiration buildup and possible copper product precipitates along the cell walls.

3.3.3 E-I Behavior and Open Circuit Potential of C11000 and Nordic Gold

Open circuit potential (OCP) experiments were conducted in electrochemical flat cells utilizing a conventional 3-electrode setup. This utilized a saturated calomel reference (SCE) electrode with a luggin probe to minimize solution resistance, a platinum-mesh counter electrode, and the sample as a working electrode. OCP-EIS was conducted in 300 mL synthetic perspiration solution at 23 °C and ambient aeration. OCP was conducted on a combination of Gamry Reference 600, Gamry PCI4, and Gamry Femtostat potentiostats controlled by Gamry Framework software. Cyclic polarization (CP) experiments were conducted following 1 hour held at OCP, beginning from 10 mV below OCP, and potential ranges from 0.085 V_{SCE} to -0.04915 V_{SCE} with a collection rate of 1 mV/sec and 1 point/mV.

3.3.1 Corrosion Rate by OCP-EIS and Mass Loss

3.3.1.1 *Open Circuit Potential-Electrical Impedance Spectroscopy*

Open circuit potential-Electrical Impedance Spectroscopy (OCP-EIS) tests were conducted in electrochemical flat cells utilizing a conventional 3-electrode setup. This

utilized a saturated calomel reference (SCE) electrode with a luggin probe to minimize solution resistance, a platinum-mesh counter electrode, and the sample as a working electrode. OCP-EIS was conducted in 300 mL concentrated synthetic perspiration solution at 23 °C and ambient aeration.

OCP-EIS was conducted on a combination of Gamry Reference 600 and Gamry PCI4 potentiostats controlled by Gamry Framework software. OCP was held for 30 minutes at designated time increments prior to EIS. EIS was conducted from 1×10^5 – 1×10^{-3} Hz at an amplitude of 10 mV RMS, with data collection occurring at 8 points/decade. A minimum of 3 replicates per corresponding sample and exposure time were obtained. Error was determined by standard deviation of the sample set.

Data was analyzed using Gamry EChem Analyst (Version 6.11) and with the equivalent circuit shown in Figure 3.3 with associated variables.^{121,122} R_1 is the solution resistance, R_2 is the resistance to charge transfer, R_3 is the resistance of the oxide, and Z_D is responsible for finite, porous diffusion impedance likely due to the oxygen reduction reaction (ORR) in pores of the oxide.¹²² Figure 3.2 confirms that ORR is a dominant cathodic reaction. Equations 3.2-3.5 define the relationship between the variables such as the constant phase elements (CPE) and the finite porous diffusion impedance (Z_D) in terms of their complex impedances. The polarization resistance (R_P) is defined in Equation 3.6. The instantaneous corrosion rate is taken to be proportional to inverse polarization resistance ($1/R_P$) and taken as B/R_P , where $B = \left(\frac{1}{2.303} \right) \left(\frac{\beta_a \beta_c}{\beta_a + \beta_c} \right)$. B^* is a term used to define the quotient of the diffusion layer thickness and the square-root of the average diffusion coefficient (Equation 3.4). Data was fit using the Simplex Method, with B_5 limited to $10\text{-}70 \text{ s}^{1/2}$, according to sample calculations of typical diffusion rates and

boundary layer thickness. The remaining variables were left unbounded. Corrosion rate ($1/R_p$) was related to charge (Q_{corr}) through the Stern-Geary approach and integration of charge utilizing Equations 3.7-3.9. B is a function of the anodic (β_a) and cathodic (β_c) Tafel slopes, and fixed at 0.057 V (Equation 3.8).¹²³

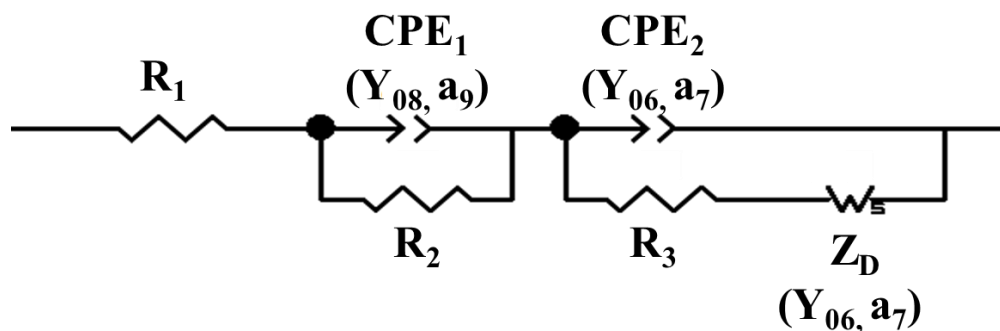


Figure 3.3. Equivalent circuit used to model corrosion behavior of copper alloys

$$\text{CPE:} \quad Z = \frac{1}{j\omega^a Y_0} \quad \text{Equation 3.2}$$

$$\text{W:} \quad Z_D = R_D \frac{\tanh\{B\sqrt{j\omega}\}}{B\sqrt{j\omega}} \quad \text{Equation 3.3}$$

$$B^* = \frac{\delta}{D^{1/2}} \quad \text{Equation 3.4}$$

$$R_D = \frac{B_5}{Y_{04}} \quad \text{Equation 3.5}$$

$$\text{Polarization Resistance:} \quad R_p = R_2 + R_3 + R_D \quad \text{Equation 3.6}$$

$$Q_{corr} \text{ by EIS:} \quad i_{corr} = \frac{B}{R_p} = \frac{1}{R_p} \left(\frac{1}{2.303} \right) \left(\frac{\beta_a^* \beta_c}{\beta_a + \beta_c} \right) \quad \text{Equation 3.7}$$

$$B = \left(\frac{1}{2.303} \right) \left(\frac{\beta_a^* \beta_c}{\beta_a + \beta_c} \right) \quad \text{Equation 3.8}$$

$$Q_{corr} = \int i_{corr} * A * dt \quad \text{Equation 3.9}$$

3.3.1.2 *Mass Loss by Gravimetric Analysis*

Mass loss was conducted in accordance with ASTM G1-03. Baseline mass loss was conducted on freshly ground (1200 grit) copper alloy samples, preserved in methanol. Copper alloys masses were obtained by an analytical balance (M-220D, Denver Instrument) after freshly ground (1200 grit, preserved in methanol) and after 130 hours exposed to a concentrated synthetic perspiration droplet and dried with compressed air. Corrosion products were removed by exposing the corroded surface to 6 M HCl for 3 minutes at ambient lab temperature, washing with Millipore water and drying with compressed air. Mass changes were obtained after cleaning on the same instrument. Freshly ground copper alloy mass loss was utilized as a baseline measurement to determine the effect of corrosion product removal on the bare metal. The effect of cleaning was established to cause negligible dissolution of the metallic alloy, with no mass loss occurring in Nordic Gold before and after cleaning, and 0.1 mg/cm² mass loss occurring in C11000. Mass loss (Δm) was equated to charge (Q_{corr}) utilizing Equation 3.10, where F is Faraday's constant (96500 Coulombs/equivalent), and E.W. is equivalent weight (grams/equivalent). Equivalent weights were calculated for both Cu^+ and Cu^{2+} for comparison, as shown in Equation 3.11, where f is the weight fraction of alloying elements, n is the number of equivalent electrons exchanged (equiv./mol), and a is atomic weight of each element in the alloy. The E.W. for C11000 was defined as 63.546 g/equiv. (Cu^+) or 31.773 g/equiv. (Cu^{2+}). Table 3.3 defines calculations for E.W. for an alloy such as Nordic Gold. Congruent dissolution was first assumed in all cases involving all elements. The E.W. for an alloy such as Nordic Gold is also reported assuming incongruent dissolution consisting of 92.1% Cu and 7.9% Zn.

$$Q_{corr} \text{ by Mass Loss} = \Delta mF / (E.W.) \quad \text{Equation 3.10}$$

$$E.W. = \sum \frac{f_i n_i}{a_i} \quad \text{Equation 3.11}$$

Table 3.3. Calculation of equivalent weight of Nordic Gold using either Cu^+ or Cu^{2+} . In each E.W. reported, all elements were considered to dissolve congruently or proportional to their mass fraction reported. Additionally, a case of incongruent dissolution is assumed, with 92.1 wt% Cu and 7.9 wt% Zn. The difference arises from Cu^+ vs. Cu^{2+} assumption.

Reaction	Nernst Potential (E°/V) (SHE)	Equivalent Electrons (equiv./mol)	Atomic Weight (g/mol)	Weight Fraction (wt%)	Equivalent Weight (E.W): Congruent (g/equiv.)	Equivalent Weight (E.W): Incongruent (g/equiv.)
$\text{Cu}^+ + e^- = \text{Cu}$	0.521	1	63.546	89	47.03	60.52
$\text{Cu}^{2+} + 2e^- = \text{Cu}$	0.342	2	63.546	89	31.84	59.14
$\text{Al}^{3+} + 3e^- = \text{Al}$	-1.662	3	26.982	5		
$\text{Zn}^{2+} + 2e^- = \text{Zn}$	-0.762	2	65.38	5		
$\text{Sn}^{2+} + 2e^- = \text{Sn}$	-0.138	2	118.71	1		

3.3.2 Corrosion Product Analysis

3.3.2.1 Optical Spectrophotometry

Reflectivity was used as a means to determine the degree of tarnish, and thus aesthetic appeal, of the tarnished surfaces. Optical reflectance as a function of wavelength was determined by using a tungsten halogen lamp (LS-1, Ocean Optics), reflection probe (R400-7-VIS/NIR, Ocean Optics) and coupled optical spectrometer (Jaz, Ocean Optics) using SpectraSuite software. The light source was held at a fixed distance perpendicular (90°) to the sample surface using a RPH-1 reflection probe holder. A STAN-SSH High-reflectivity specular reflectance standard was used for calibration of the light reference (100%) which guarantees 85-90% reflectance across 250-800 nm and 85-98% reflectance across 800-2500 nm. Integration time was set automatically using SpectraSuite software,

and measurements were conducted using 10 scans to average, with a boxcar width of 5 to increase signal to noise ratio. Particular interest was paid to the visible light region, with wavelengths from 370-730 nm. One sample per alloy, pre-exposure treatment, and time was conducted as a representative of the 3 samples exposed. The test area was a 11.16 mm² circle at the center, and color distinct regions of the corroded area.

3.3.2.2 Grazing Incidence X-Ray Diffraction

Grazing incidence X-ray diffraction measurements were carried out on a PanalyticalX'Pert Pro MPD diffractometer applying the associated software (DataCollector). Cu-K α radiation ($\lambda = 1.5406 \text{ \AA}$) was used in all experiments. The incident beam was conditioned using a parallel beam X-ray mirror for Cu radiation with a 1/32 $^\circ$ divergent slit and 20 mm mask. The use of a 20 mm mask ensured that signal was measured from a line across the entire sample, resulting in the averaging of potentially heterogeneous sections of the oxide. A beam attenuator with 0.125 mm Ni foil was employed for the alignment of the sample following standard alignment procedures. Samples were placed in the center of an Eulerian cradle mounting stage, and an incident angle of 0.5 $^\circ$ was used for measurements, limiting depth of interaction to 0.2 μm ¹²⁴. The diffracted beam was conditioned with a parallel plate collimator, parallel plate collimator slit (with alignment only), and 0.04 radians Soller slits, then recorder using a proportional Xe detector. The 2θ scan range was 20-100 $^\circ$.

3.3.2.3 Galvanostatic Reduction to Analyze Oxides

Galvanostatic reduction operates on the principle of electrochemically reducing corrosion products sequentially through the application of constant current. The corrosion products with the highest reduction potentials are reduced first. Based on worked by

Nakayama, Kaji, Shibata, Notoya, and Osakai, galvanostatic reduction can be used to identify the order of reduction in copper oxides (CuO, Cu₂O) that was previously debated.¹²⁵ As seen in Figure 3.4, CuO is known to reduce first, followed by the reduction of Cu₂O, a result of the oxides sandwich like oxide layer arrangement where Cu₂O is contained by CuO and metallic Cu.

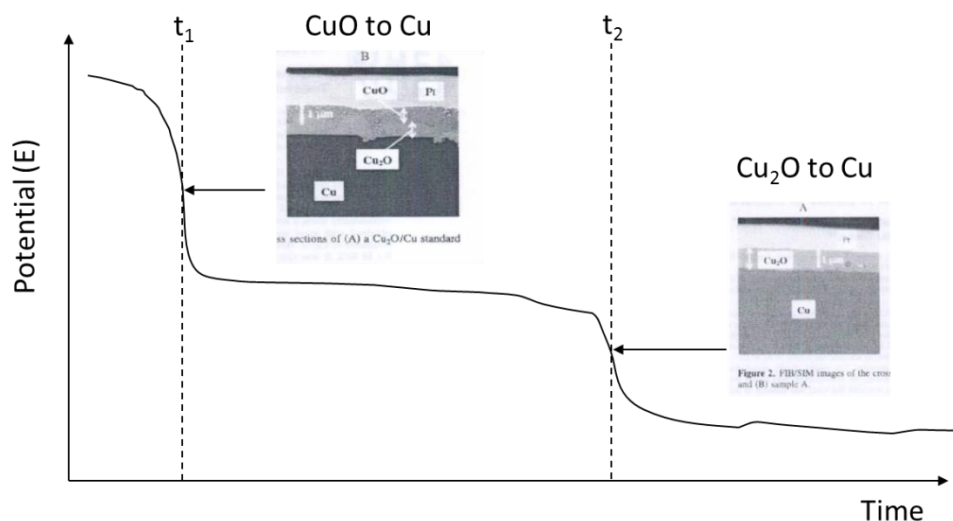


Figure 3.4. Reduction order of copper oxides CuO and Cu₂O.¹²⁵ However, other papers suggest CuO reduces to Cu₂O, rather than to CuO to Cu as reported here.^{126,127}

Galvanostatic reduction experiments were conducted on Princeton Applied Research Model 273A potentiostats with CorrWare software. Experiments were conducted in chloride free electrochemical flat cells utilizing a conventional 3-electrode setup. This utilized a mercury-mercury sulfate electrode (MSSE), a platinum-mesh counter electrode, and the sample as a working electrode. Tests were conducted at 0.02 mA/cm² in deaerated borate buffer solution (Na₂B₄O₇+H₃BO₃), pH 8.4, with a collection rate of 1 point/sec. A minimum of 3 replicates per corresponding sample and exposure time were obtained. Table 3.4 compares the galvanostatic reduction method utilized against methods used in ASTM B825¹²⁸ and Nakayama, et al.¹²⁵

Table 3.4. Comparison of galvanostatic reduction methods utilized in ASTM standard, Nakayama's previous study and previously used in house method.			
Method	Solution	pH	i_{corr}
ASTM B825 ¹²⁸	1 M KCl	7	1.0 mA/cm ²
Nakayama ¹²⁵	0.1 M KCl	7	0.5 mA/cm ²
	1 M KOH	14	
	6 M KOH + 1 M LiOH	14	
Experimental Procedure	0.019 M Na ₂ B ₄ O ₇ + 0.131 M H ₃ BO ₃	8.4	0.02 mA/cm ²

ASTM B825 was utilized to determine the precise time associated with reduction peak characteristics by determination of differential inflection points (Figure 3.5).¹²⁸ Derivatives were manually calculated as the difference of potential between 15 consecutive seconds, and inflection points determined by visual evaluation. Inflection peaks were taken to represent times when a full reduction of a species occurred. For example, Figure 3.5 shows the reduction of CuO and Cu₂O, where t_1 corresponds to the time at which the full reduction of CuO is achieved, and t_2 corresponds to the time at which the full reduction of Cu₂O is achieved. Potentials that correspond to the inflection point time were determined by the peak preceding the inflection point, by the average of the first 15 seconds in the case of the first reduction peak and visual evaluation for those following. In Figure 3.5, E_1 corresponds to the potential at which CuO is reduced, and E_2 corresponds to the potential at which Cu₂O is reduced. Data is often represented as inflection point-reduction potential pairs (t_i , E_i), indicated by circles in Figure 3.5. Table 3.5 lists the half-cell reactions for possible corrosion products that could be reduced by galvanostatic reduction. Chloride concentration ($[Cl^-]$) was assumed to be 10^{-8} M as reductions were conducted in Cl^- free cells. Hydrogen concentrations ($[H^+]$) were derived from pH (8.4). The exposure spot size (0.8 cm²) was matched precisely to the reduction spot size (0.8 cm²).

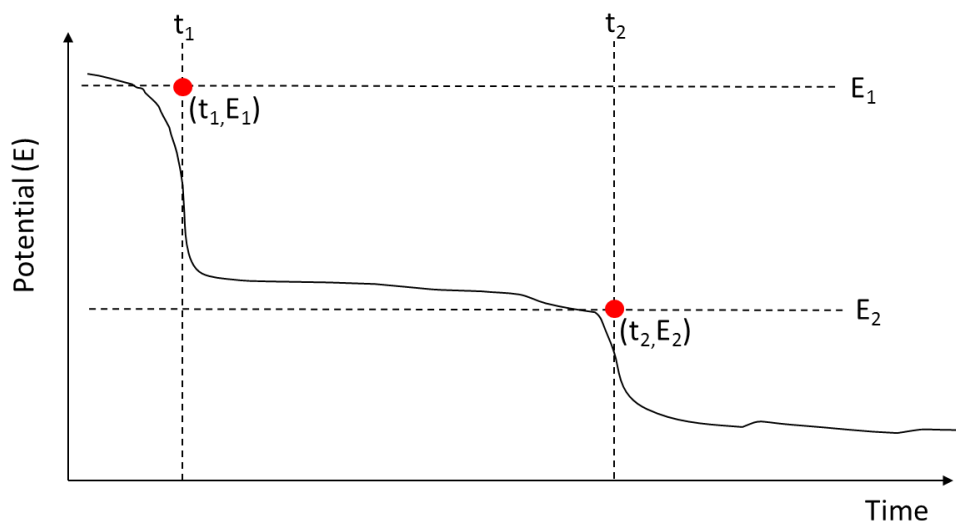


Figure 3.5. Galvanostatic reduction analysis corresponds time to completely reduce a corrosion species (t_i) to inflection points on the galvanostatic reduction spectra, and reduction potential (E_i) to the plateau preceding the inflection point.

Half-Cell Reaction	V_{SHE}	V_{SCE}^{xv}	V_{MMSE}^{xvi}
$2CuO \bullet H_2O + 2e^- \rightarrow Cu_2O + 2OH^- + H_2O$	0.25056	0.00956	-0.39944
$Cu_2(OH)_3Cl + 4e^- \rightarrow 2Cu + Cl^- + 3OH^-$	0.24588	0.00488	-0.40412
$CuCl_2 \bullet 3Cu(OH)_2 + 8e^- \rightarrow 4Cu + 2Cl^- + 6OH^-$	0.19228	-0.04872	-0.45772
$Cu_2O + H_2O + 2e^- \rightarrow 2Cu + 2OH^-$	-0.02544	-0.26644	-0.67544
$Sn(O)^* + 2H^+ + 2e^- \rightarrow Sn + H_2O$	-0.58744	-0.82844	-1.23744
$Zn(O)^{**} + 2H^+ + 2e^- \rightarrow Zn + H_2O$	-0.89644	-1.13744	-1.54644

* Assumed to be hydroxylated $Sn(OH)_2$
 ** Assumed to be amorphous hydroxylated $Zn(OH)_2$

3.3.3 Solution Analysis by ICP-OES

Inductively coupled plasma-optical emission spectrometry (ICP-OES) was utilized to determine copper ions released from alloys. ICP-OES samples were collected at exposure times corresponding to the removal of copper alloy samples for surface analysis of corrosion products at 12, 48, 96 and 130 hours, and were not acidified.

^{xv} $V_{SCE} = V_{SHE} - 0.241$

^{xvi} $V_{MMSE} = V_{SHE} - 0.650$

Copper alloy samples had a surface to volume ratio of $2.67 \text{ cm}^2/\text{L}$ during the exposure time. A 300 mL aliquot of 0.1 M HCL was used to wash the cell following exposure, where the sample hole was covered with inert parafilm wax to prevent leakage. This wash solution was analyzed in addition to the exposure solution to determine possible corrosion product precipitation along the walls of the cell during exposure. Note that while ICP-OES can detect elements in solution regardless of complexation with other matter in the solution, it cannot differentiate between oxidation states (Cu^+ or Cu^{2+}).

Measurements were conducted using a Thermo Scientific iCAP 6200 with a HF-compatible sample introduction system. A yttrium (Y) internal standard was utilized to account for instrumental fluctuations, and observed a wavelengths 230.6 and 325.6 nm, which were determined to have no interference with elements possible in sample solutions (Cu, Al, Zn, or Sn). Calibration was conducted in Millipore water and concentrated synthetic perspiration after 130 hours (with no exposure to copper alloys) with additions of 0.01-100 ppm Cu using single element ICP-OES standards (Agilent Technologies). Figure 3.6 compares the calibration of the two solutions at 224.7 nm. A calibration of signal intensity versus copper content was used to determine copper content (ppm) in test solutions. A minimum of 3 replicates per corresponding sample and exposure time were analyzed, each analyzed at 224.7 nm in triplicate. Raw concentrations were manipulated as seen in Figure 3.7 to achieve concentration in $\text{Cu ions}/\text{cm}^2$, the surface area of the exposed solution. Table 3.6 lists possible copper precipitates, associated solubility constants (K_{sp}) and maximum concentration of Cu^{2+} or Cu^+ as ions possible in solution 300 mL solution before a product may precipitate. Concentrations for solubility concentrations were assumed as $[\text{Cl}^-] = 2 \text{ M}$, $[\text{H}^+] = .005 \text{ M}$,

$[\text{OH}^-] = 1.9 \times 10^{-12} \text{ M}$. Copper ion release rates (m) are calculated linearly ($mx+b$) from 12 to 130 hours, and initial 12 hour release rate determined by y-intercept (b). ICP-OES was also used to detect Al, Sn, and Zn in solutions exposed to Nordic Gold, with calibration of 0.01-100 ppm of each element. Al and Sn couldn't be detected within the limits of the calibration, and Zn was detected at wavelength 206.2 nm by similar method as described above for Cu.

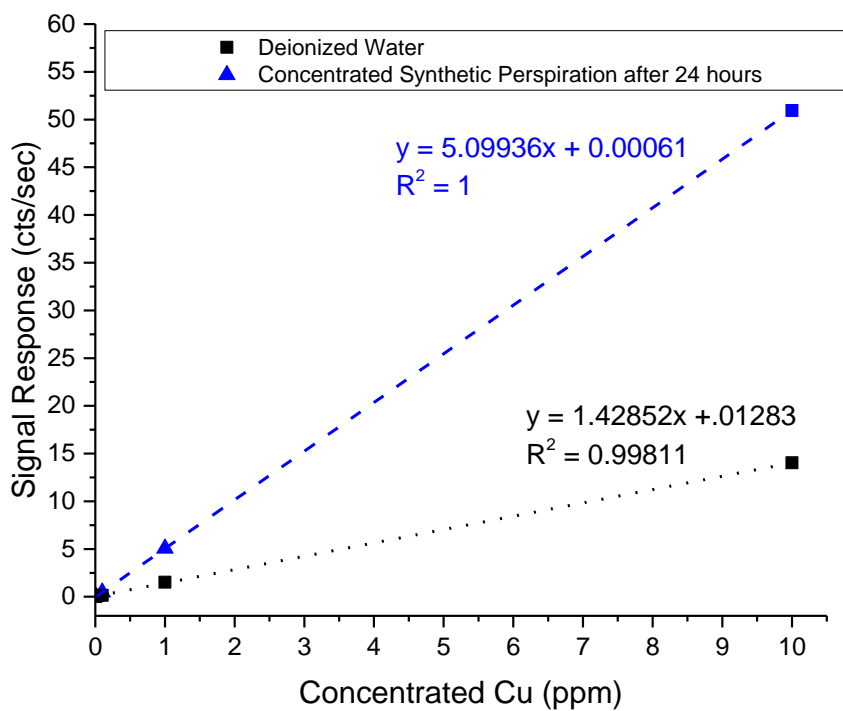


Figure 3.6. Comparative calibration curves of Cu in deionized water and concentrated synthetic perspiration after 130 hours (no exposure to copper alloys) at 224.7 nm.

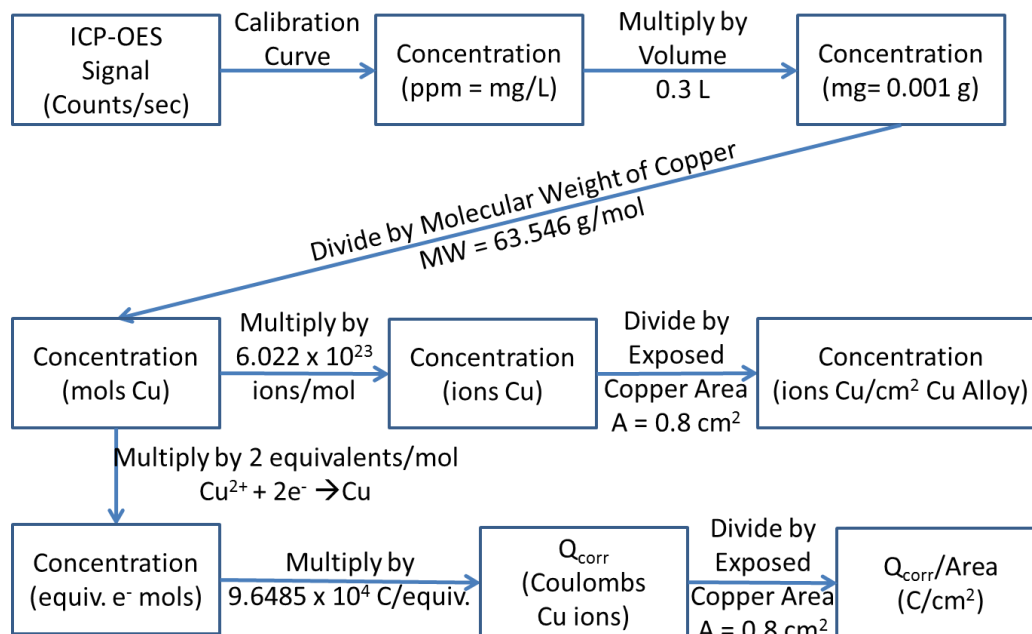


Figure 3.7. Procedural flow chart of converting signal obtained by ICP-OES to copper ion release (ions/cm²).

Chemical Formula	Reaction	K _{sp}	Solubility of Cu ⁺ or Cu ²⁺ (ions/300 mL)
Cu ₂ (OH) ₃ Cl (atacamite)	2Cu ²⁺ + 3 OH ⁻ + Cl ⁻ = Cu ₂ (OH) ₃ Cl	1.72 × 10 ⁻³⁵	2.01 × 10 ²³
Cu ₂ O (cuprite)	2Cu ⁺ + OH ⁻ = Cu ₂ O + H ⁺	2.6 × 10 ⁻²	1.53 × 10 ²⁷
CuCl (nantokite)	Cu ⁺ + Cl ⁻ = CuCl	1.86 × 10 ⁻⁷	1.68 × 10 ¹⁶

3.3.4 Charge Analysis

Charge analysis calculations were obtained from Q_{corr} values by instantaneous corrosion rate, oxide analysis by galvanostatic reduction, solution analysis by ICP-OES and mass loss. Equations 3.12-3.14 describe the process by which Q_{corr} was determined by EIS, where B is 0.057 V.¹²³ The variable n denotes times at 0.5, 12, 48, 96, or 130 hours when EIS was analyzed. Equation 3.15 describes the process by which Q_{corr} was

determined by mass loss. Equations 3.16-3.17 describe the process by which Q_{corr} was determined by oxide analysis. The denotation m represents the different average inflection times (t_m) found for reduction waves of the preceding corrosion product, such t_1 , and t_2 denoted in Figure 3.5. The current (i) is assumed to be the applied current during galvanostatic reduction (0.02 mA/cm^2). Figure 3.7 describes the process by which ICP-OES signal is converted to $Q_{solution}$ determined by solution analysis for Cu, and a similar method followed for additional elements found by ICP-OES in the case of Nordic Gold. Total charge transfer to solution in Nordic Gold is the sum of Q_{corr} for all elements detected. Ideally, Q_{corr} by EIS and mass loss should be equivalent, and equivalent to the sum of Q_{oxide} and $Q_{solution}$ as seen in Equation 3.18.

Q_{corr} by EIS:

$$i_{corr} = \frac{B}{R_p} = \left(\frac{1}{R_p}\right) \left(\frac{1}{2.303}\right) \left(\frac{\beta_a \beta_c}{\beta_a + \beta_c}\right) \quad \text{Equation 3.12}$$

$$Q_{corr_n} = i_{corr} * A * dt = \frac{(t_{n+1} - t_n)(i_{n+1} + i_n)}{2} \quad \text{Equation 3.13}$$

$$Q_{corr} = \Sigma Q_{corr_n} \quad \text{Equation 3.14}$$

Q_{corr} by Mass Loss:

$$Q = \frac{\Delta m F}{E.W.} \quad \text{Equation 3.15}$$

Q_{oxide} by Oxide Analysis:

$$Q_{oxide_m} = i t_m \quad \text{Equation 3.16}$$

$$Q_{oxide} = \Sigma Q_{oxide_m} \quad \text{Equation 3.17}$$

$$Q_{corr} \text{ by EIS} = Q_{corr} \text{ by Mass Loss} = Q_{oxide} + Q_{solution} \quad \text{Equation 3.18}$$

3.4 Results

3.4.1 E-I Behavior and Open Circuit Potential of C11000 and Nordic Gold

The open circuit potential of Nordic Gold is observed to be slightly lower than C11000, likely due to the presence of Zn and Al (Figure 3.8). The open circuit potential behavior of C11000 and Nordic Gold in concentrated synthetic perspiration rapidly increases at first, followed by an equally rapid decrease, as seen in Figure 3.8. Following the initial stage likely involving the dissolution of the passive layer, C11000 returned to a potential -0.005 V above the initial potential (-0.331 V_{SCE}), and increased gradually over time. Nordic Gold returned to the same potential (-0.334 V_{SCE}) and experienced a potential plateau with gradual potential increase.

The anodic behavior of Nordic Gold and C11000 in concentrated synthetic perspiration appears active (Figures 3.9-3.10). This shows a cathodic peak indicative of the reduction of Cu ions. Both C11000 and Nordic Gold appear to reduce one species, C11000 at a greater potential (-0.2 V_{SCE}) compared to Nordic Gold (-0.25 V_{SCE}). This reduction is well below the potential of the oxygen reduction reaction (0.854 V_{SCE}), suggesting the reduction of a corrosion product formed during anodic polarization or ions in the solution. No pitting was observed during either C11000 or Nordic Gold corrosion, suggesting uniform corrosion behavior.

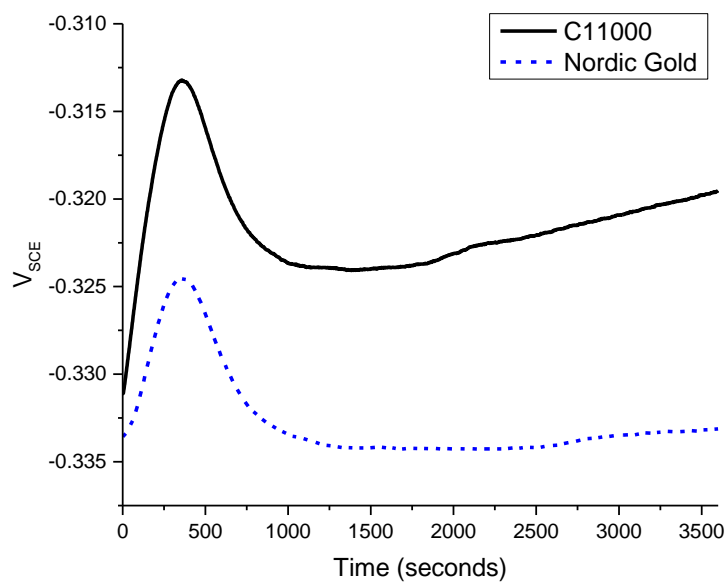


Figure 3.8. Open circuit potential (OCP) of C11000 and Nordic Gold freshly ground to 1200 grit and exposure to concentrated synthetic perspiration (23 °C, ambient aeration) for 1 hour.

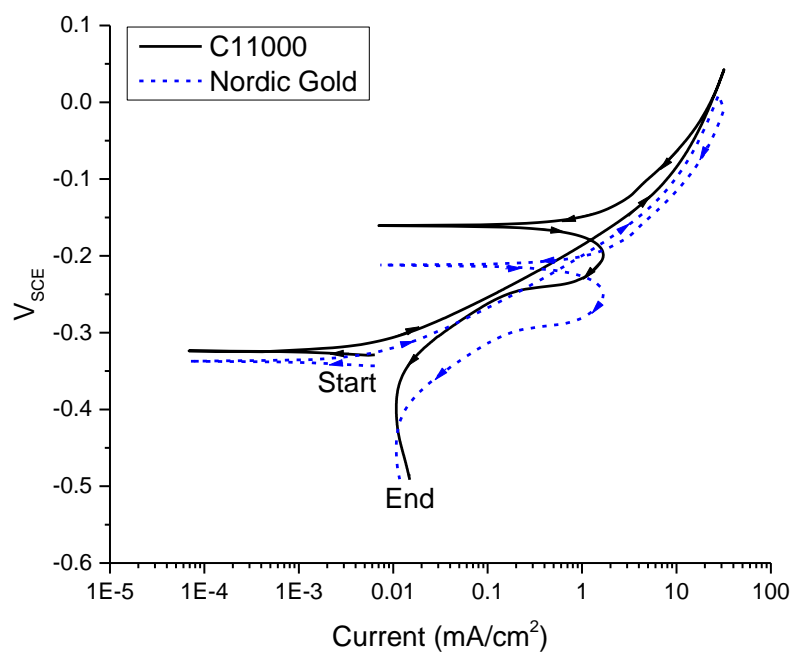
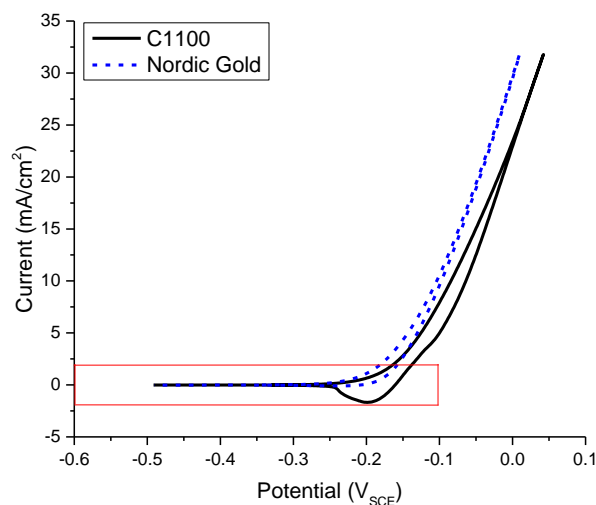
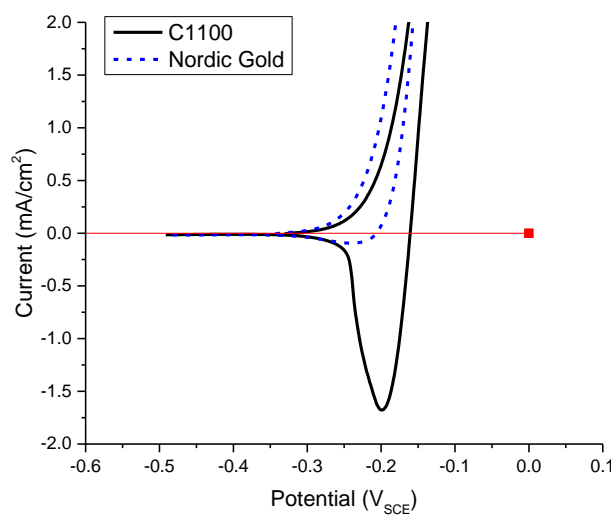


Figure 3.9. Cyclic polarization (CP) of C11000 and Nordic Gold freshly ground to 1200 grit and exposure to concentrated synthetic perspiration (23 °C, ambient aeration) for 1 hour prior to CP.



a



b

Figure 3.10. Cyclic polarization (CP) of C11000 and Nordic Gold freshly ground to 1200 grit and exposure to concentrated synthetic perspiration (23 °C, ambient aeration) for 1 hour prior to CP. Figure b is a close-up of the red-outlined portion of figure a. In figure b, the solid horizontal line indicates 0 mA/cm^2 .

3.4.2 Corrosion Rate by OCP-EIS and Mass Loss

3.4.2.1 Instantaneous Corrosion Rate by EIS

Open circuit potential was held for 30 minutes prior to electrochemical impedance spectroscopy. After exposure to concentrated synthetic perspiration for 30 minutes, all alloys demonstrated complex EIS behavior consistent with diffusional impedance likely due to the occurrence of oxygen reduction reactions perhaps through a porous film¹²². EIS behavior was dependent on time exposed to concentrated synthetic perspiration, alloy composition, but little on pre-treatment conditions (freshly ground or air oxidized). Figures 3.11-3.12 show example Nyquist fits using the fitting method described in experimental procedure, which shows good agreement between data and model fit for a model containing finite diffusional impedance. The data used in the model is reported in each figure caption.

Over time the instantaneous corrosion rate of both C110000 and Nordic Gold increased. Figures 3.13-3.14 demonstrate example progression of EIS behavior over time for freshly ground C11000 and Nordic Gold. Over time, low frequency impedance values decrease and the peak phase shifts to higher frequencies, suggestive of a lower polarization resistance. Nordic Gold is observed to have less of a decrease in $Z_{\text{magnitude}}$ compared to C11000. A comparison of the exposure time dependence of instantaneous corrosion rate can be seen in Figures 3.15-3.16, where the comparison between 0 hours and 130 hours in concentrated synthetic perspiration solution support the notion that regardless of alloy composition or whether samples were freshly ground or air oxidized under ambient lab conditions for 30 days, exposure time increases instantaneous corrosion rate. Nordic Gold consistently exhibits a slightly lower instantaneous corrosion

rate compared to C11000, both when freshly ground and air oxidized. Figures 3.17-3.18 show the averaged polarization resistance values taken as $R_2+R_3+R_D$ of C11000 and Nordic Gold when freshly ground or air oxidized over time.

Table 3.7. Charge analysis by EIS for C11000 and Nordic Gold when freshly ground to 1200 grit or air oxidized at ambient lab conditions for 30 days, then exposed to concentrated synthetic perspiration solution (23 °C, ambient aeration) for 130 hours. $Q_{corr}/area$ by EIS were calculated as seen in Equations 3.12-3.14, where $B= 0.057 V$. ¹²³ Data is the average of a minimum of 3 replicates with one standard deviation.			
Alloy: Treatment	0 Hours Exposure Concentrated Synthetic Perspiration $1/R_p$ (ohms ⁻¹ /cm ²)	130 Hours Exposure Concentrated Synthetic Perspiration $1/R_p$ (ohms ⁻¹ /cm ²)	$Q_{corr}/area$ (C/cm ²) by EIS after 130 hours in Concentrated Synthetic Perspiration
C11000: Freshly Ground	$1.02 \times 10^{-4} (\pm 2.19 \times 10^{-5})$	$1.62 \times 10^{-4} (\pm 2.78 \times 10^{-5})$	4.42 C/cm ²
C11000: Air Oxidized	$1.46 \times 10^{-4} (\pm 7.30 \times 10^{-5})$	$2.45 \times 10^{-4} (\pm 1.17 \times 10^{-4})$	4.64 C/cm ²
Nordic Gold: Freshly Ground	$1.06 \times 10^{-4} (\pm 8.44 \times 10^{-5})$	$1.81 \times 10^{-4} (\pm 3.04 \times 10^{-5})$	4.57 C/cm ²
Nordic Gold: Air oxidized	$1.62 \times 10^{-4} (\pm 3.26 \times 10^{-5})$	$3.05 \times 10^{-4} (\pm 6.08 \times 10^{-5})$	6.94 C/cm ²

The presence of a thin air oxide formed for 30 days in lab air does not reduce the instantaneous corrosion rate when exposed to concentrated synthetic perspiration (Figure 3.19). At 0 hours exposure to concentrated synthetic perspiration (23 °C, ambient aeration), the $1/R_p$ values of C11000 and Nordic Gold when air oxidized were greater than their freshly ground counterparts. Following exposure to concentrated synthetic perspiration (23 °C, ambient aeration) for 130 hours, the trend of greater $1/R_p$ values on air oxidized samples continues (Figure 3.19).

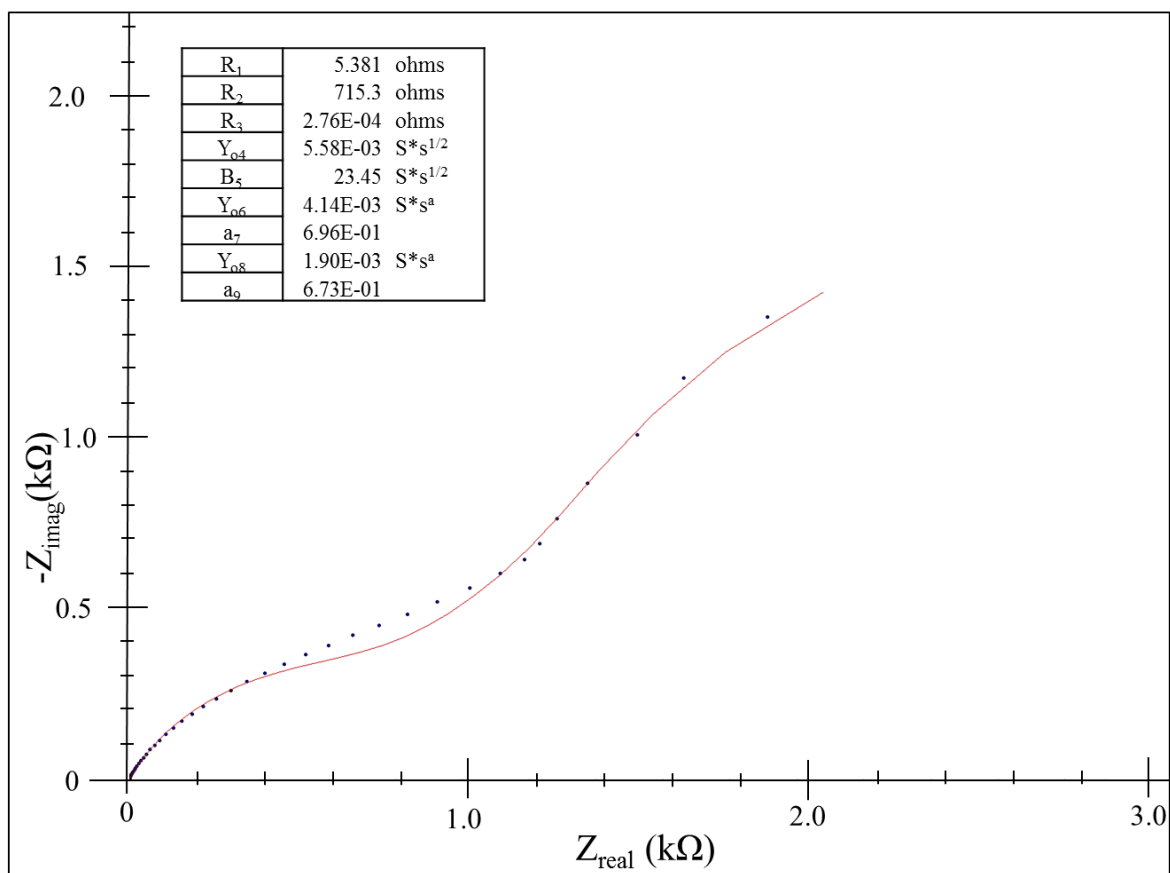


Figure 3.11. Nyquist plot of C11000 freshly ground to 1200 grit, then exposed to concentrated synthetic perspiration solution (23 °C, ambient aeration) for 130 hours, overlaid with model fit by the Simplex method. Exposure area was 0.8 cm². B_5 was bound to between 10 and 70 s^{1/2}/Ω, while the remaining parameters were left unbound to fit the data. Fit resulted in $R_1 = 5.381 \Omega$, $R_2 = 715.3 \Omega$, $R_3 = 2.76 \times 10^{-4} \Omega$, $Y_{o4} = 5.58 \times 10^{-3} s^{1/2}/\Omega$, $B_5 = 23.45 s^{1/2}/\Omega$, $Y_{o6} = 4.14 \times 10^{-3} s^{1/2}/\Omega$, $a_7 = 6.96 \times 10^{-1}$, $Y_{o8} = 1.90 \times 10^{-3} s^{1/2}/\Omega$, $a_9 = 6.73 \times 10^{-1}$.

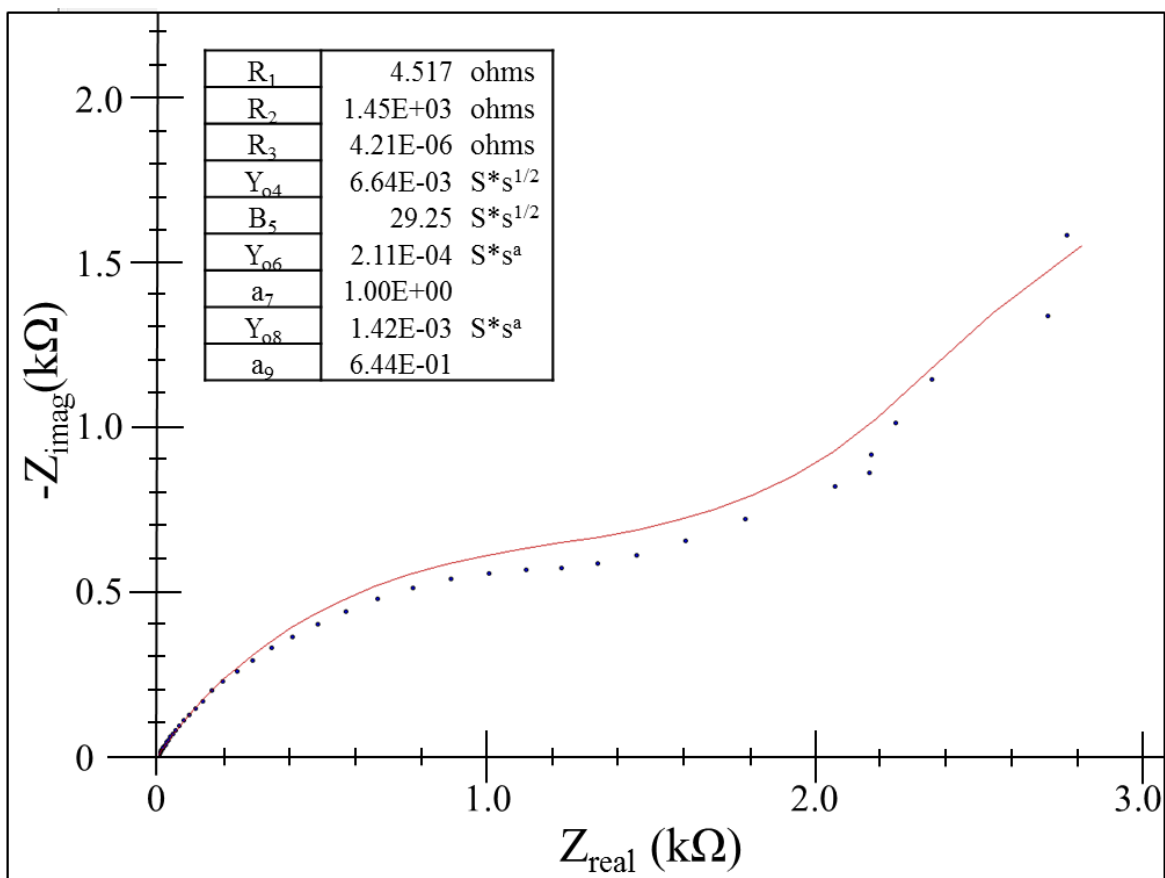


Figure 3.12. Nyquist plot of Nordic Gold freshly ground to 1200 grit, then exposed to concentrated synthetic perspiration solution (23 °C, ambient aeration) for 130 hours, overlaid with model fit by the Simplex method. Exposure area was 0.8 cm². B_5 was bound to between 10 and 70 s^{1/2}/Ω, while the remaining parameters were left unbound to fit the data. Fit resulted in $R_1 = 4.517 \Omega$, $R_2 = 1.45 \times 10^3 \Omega$, $R_3 = 4.21 \times 10^{-6} \Omega$, $Y_{o4} = 6.64 \times 10^{-3} s^{1/2}/\Omega$, $B_5 = 29.25 s^{1/2}/\Omega$, $Y_{o6} = 2.11 \times 10^{-4} s^{1/2}/\Omega$, $a_7 = 1.00$, $Y_{o8} = 1.42 \times 10^{-3} s^{1/2}/\Omega$, $a_9 = 6.44 \times 10^{-1}$.

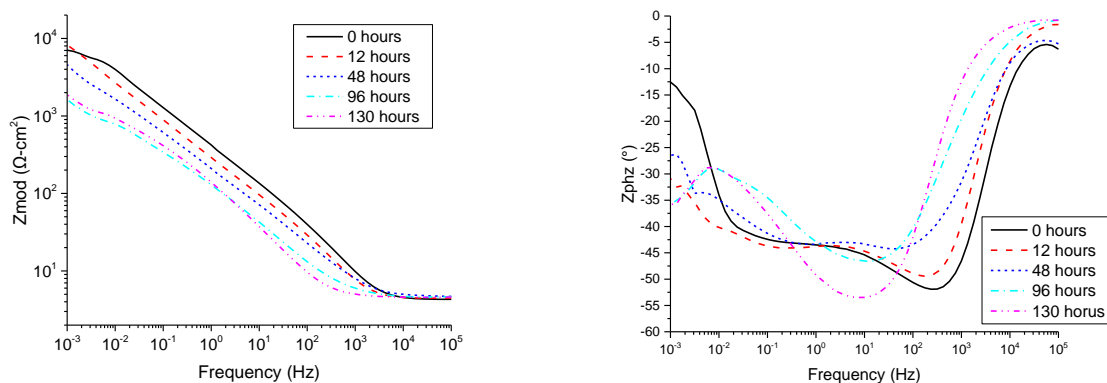


Figure 3.13. Bode plots of C11000 freshly ground to 1200 grit, then exposed to concentrated synthetic perspiration solution (23 °C, ambient aeration) for various times indicated.

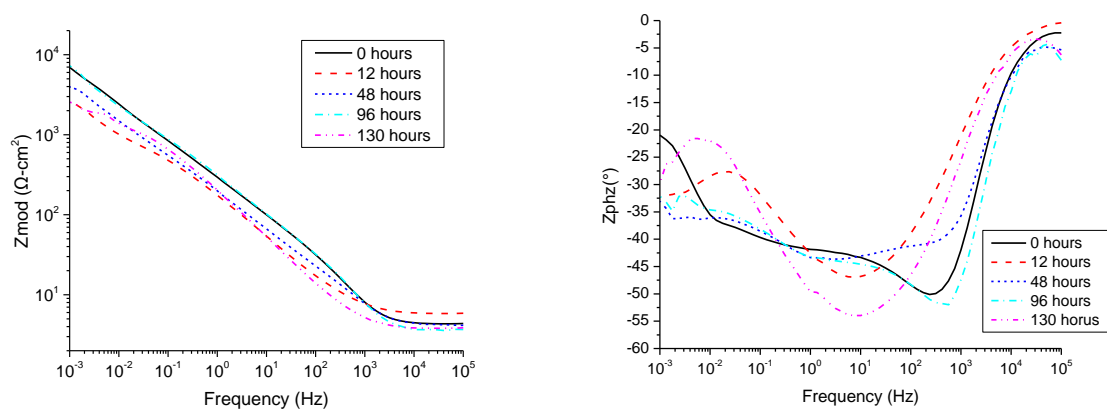


Figure 3.14. Bode plots of Nordic Gold freshly ground to 1200 grit, then exposed to concentrated synthetic perspiration solution (23° C, ambient aeration) for various times indicated.

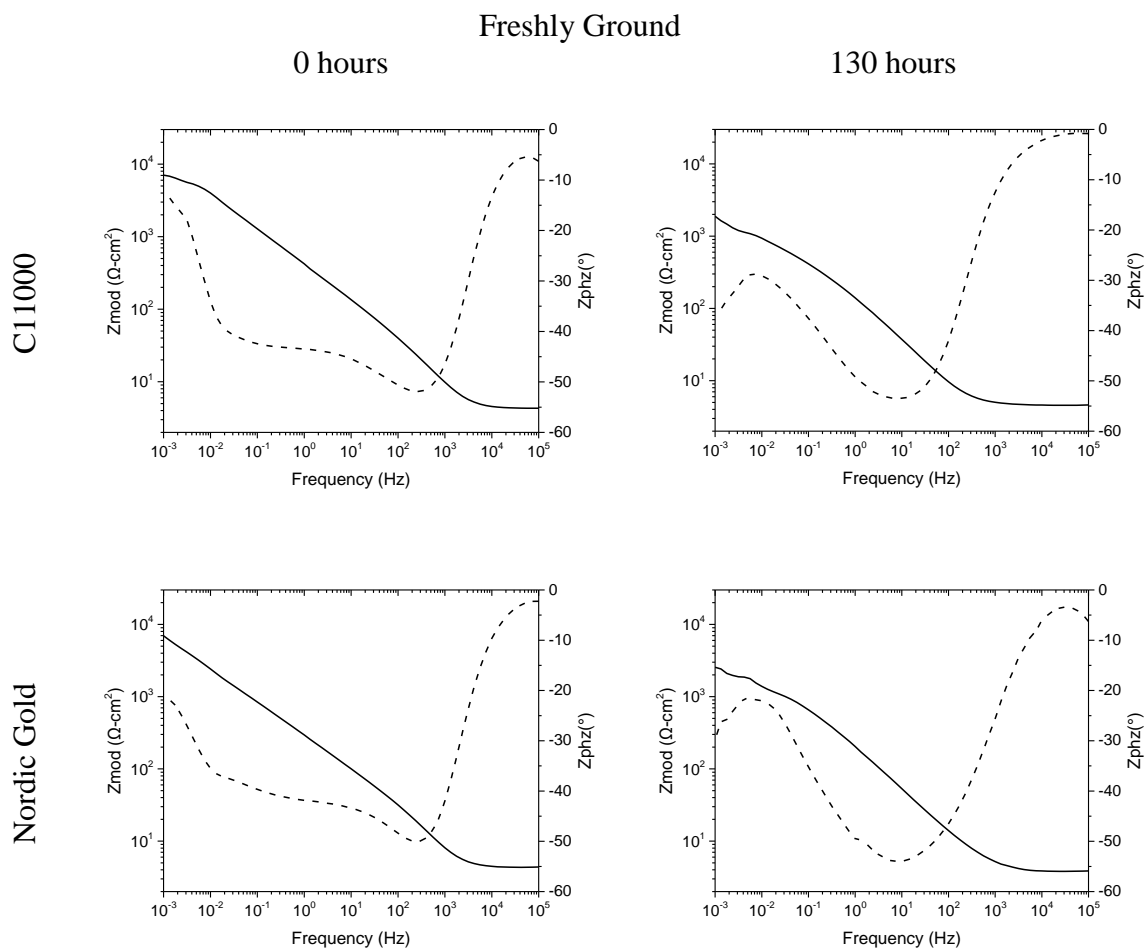


Figure 3.15. Bode plots of C11000 and Nordic Gold freshly ground to 1200 grit, then exposed to concentrated synthetic perspiration solution (23° C, ambient aeration) for 0 and 130 hours.

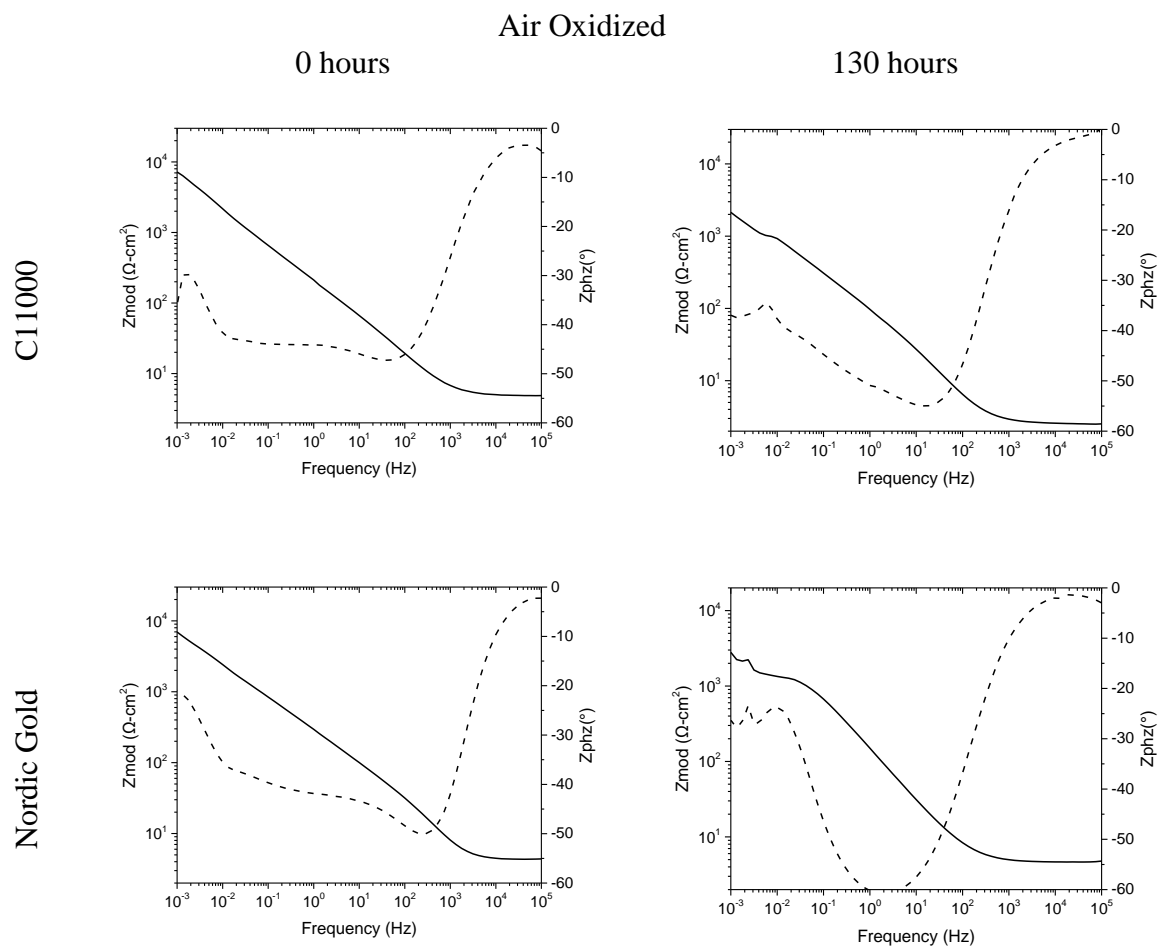


Figure 3.16. Bode plots of C11000 and Nordic Gold freshly ground to 1200 grit, air oxidized at ambient lab conditions for 30 days, then exposed to concentrated synthetic perspiration solution (23 °C, ambient aeration) for 0 and 130 hours.

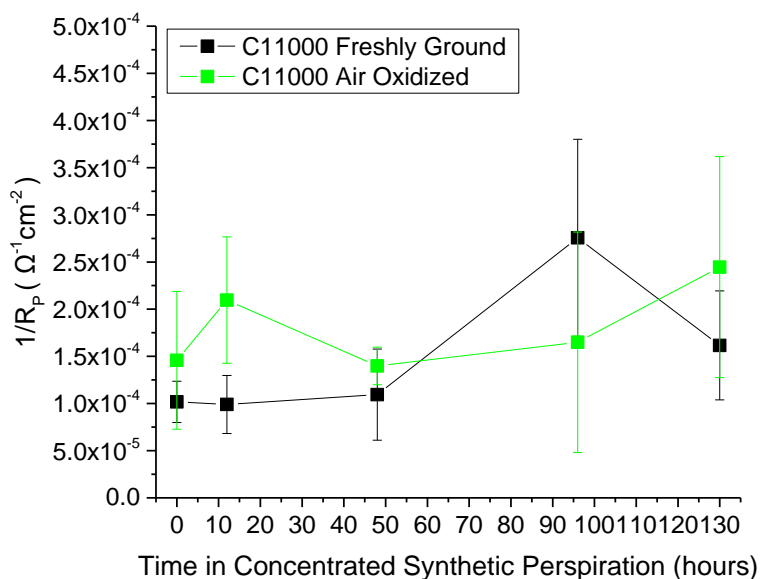


Figure 3.17. Instantaneous corrosion rate ($1/R_p$) over time for C11000 freshly ground to 1200 grit, or air oxidized at ambient lab conditions for 30 days, then exposed to concentrated synthetic perspiration solution (23 °C, ambient aeration). Data is the average of a minimum of 3 replicates and error bars are one standard deviation.

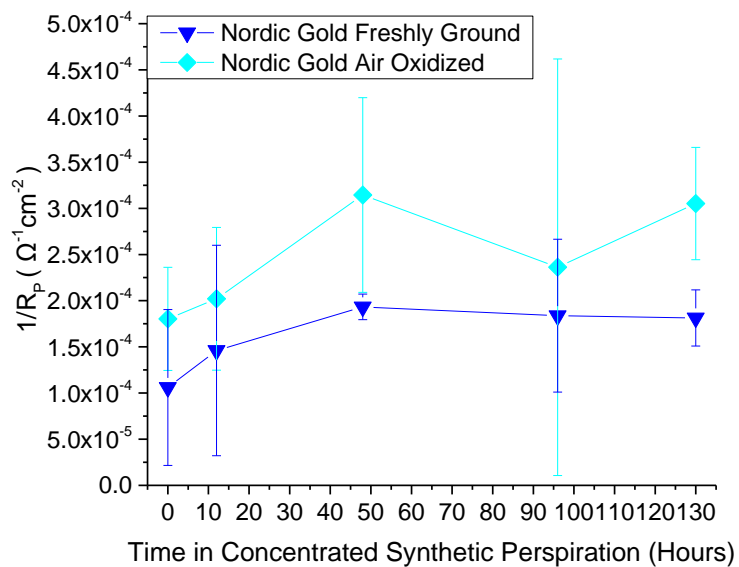


Figure 3.18. Instantaneous corrosion rate ($1/R_p$) over time for Nordic Gold when freshly ground to 1200 grit or air oxidized at ambient lab conditions for 30 days, then exposed to concentrated synthetic perspiration solution (23 °C, ambient aeration). Data is the average of a minimum of 3 replicates and error bars reflect one standard deviation.

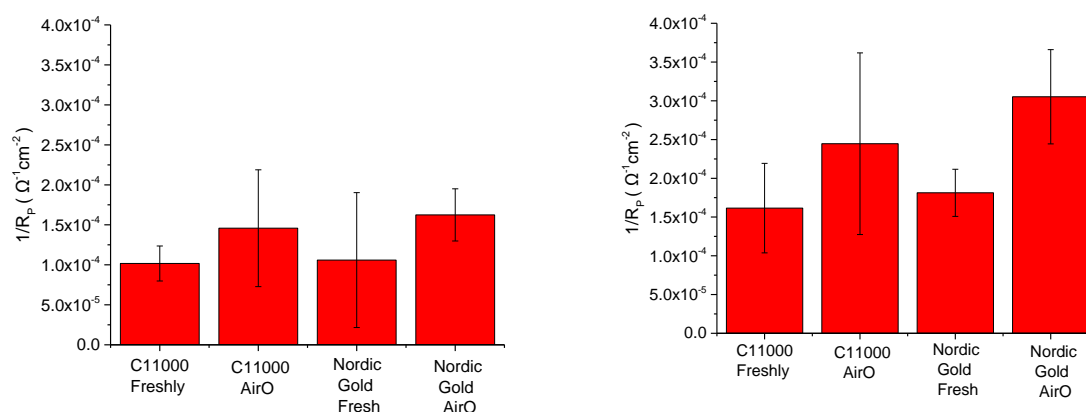


Figure 3.19. Instantaneous corrosion rate ($1/R_p$) at 0 hours (left) and 130 hours (right) for C11000 and Nordic Gold when freshly ground to 1200 grit or air oxidized at ambient lab conditions for 30 days, then exposed to concentrated synthetic perspiration solution (23 °C, ambient aeration). Data is the average of a minimum of 3 replicates and error bars reflect one standard deviation.

3.4.2.2 Mass Loss by Gravimetric Analysis

Mass loss by gravimetric analysis was conducted on freshly ground C10000 and Nordic Gold just after polishing and after being exposed to concentrated synthetic perspiration for 130 hours. This study serves as a qualitative confirmation of corrosion rate dependency on the alloys composition and Q_{corr} by EIS calculations. Mass loss following 130 hours in concentrated synthetic perspiration was determined to be 3.1 (± 2.2) mg for Nordic Gold, and 1.1 (± 0.4) mg for C11000 in an exposure area of 0.8 cm^2 . Table 3.8 lists mass loss (Δm) and associated anodic charge (Q_{corr}) for Nordic Gold and C11000 adjusted for area and depending on Cu^+ or Cu^{2+} . These results are consistent with instantaneous corrosion rates observed by EIS, where Nordic Gold has a slightly higher corrosion rate than C11000. The greater mass loss observed in Nordic Gold is likely the result of dissolution of Zn or Al into solution, as well as Cu. A B value was calculated for C11000 and Nordic Gold based on Q_{corr} calculated by mass loss, as seen in Equation

3.19, utilizing average $1/R_P$ values obtained at 0 and 130 hours. Note t_0 is 0.5 hours, accounting for OCP prior to EIS measurements.

$$B = \frac{\left(\frac{Q_{corr \text{ by Mass Loss}^*2}}{(t_{130 \text{ hours}} - t_0 \text{ hours})}\right)}{\left(\left(\frac{1}{R_{P_{130 \text{ hours}}}}\right) + \left(\frac{1}{R_{P_0 \text{ hours}}}\right)\right)} \quad \text{Equation 3.19}$$

Table 3.8. Charge (Q_{corr}) analysis based on mass loss of 3 specimens with standard deviation after 130 hours exposure of 0.8 cm ² copper alloy freshly ground to 1200 grit to concentrated synthetic perspiration (23 °C, ambient aeration).					
Alloy	Mass Loss (Δm) (mg)	Mass Loss (mg/cm ²)	Q_{corr}/area (C/cm ²) $Cu^+ + e^-$ $= Cu$	Q_{corr}/area (C/cm ²) $Cu^{2+} + 2e^-$ $= Cu$	B (V) Calculated Assuming Q_{corr} (Cu^{2+})
C11000	1.1 (± 0.4)	1.4 (± 0.5)	2.09 ^{xvii}	4.18 ^{xviii}	0.0678
Nordic Gold	3.1 (± 2.2)	3.9 (± 2.9)	7.95 ^{xix}	15.90 ^{xx}	0.1962
			6.36 ^{xxi}	11.83 ^{xxii}	0.1460

3.4.3 Surface Analysis of Corrosion Products

3.4.3.1 Tarnishing in Concentrated Synthetic Perspiration

Optical images of C11000 and Nordic Gold under freshly ground and air oxidized conditions were collected at each exposure time in triplicate. The results are shown in Figures 3.20-3.21. In freshly ground samples of C11000 and Nordic Gold, exposure to concentrated synthetic perspiration for 12 hours resulted in little discoloration, only in slight darkening of the alloys surface. Air oxidized samples exposed for 12 hours experienced more dramatic discoloration, with C11000 having multi-colored regions and Nordic Gold becoming vibrantly yellow and etched revealing grain structure. Following

^{xvii} Equivalent weight, $Cu^+ = 63.55$ equiv./g

^{xviii} Equivalent weight, $Cu^{2+} = 31.77$ equiv./g

^{xix} Equivalent weight, congruent alloy dissolution, $Cu^+ = 47.03$ equiv./g

^{xx} Equivalent weight, congruent alloy dissolution, $Cu^{2+} = 23.52$ equiv./g

^{xxi} Equivalent weight, incongruent alloy dissolution, $Cu^+ = 59.14$ equiv./g

^{xxii} Equivalent weight, incongruent alloy dissolution, $Cu^{2+} = 31.84$ equiv./g

12 hours of exposure to concentrated synthetic perspiration, all C11000 alloy samples became bright salmon-pink in color, and the appearance of grain boundaries can be seen. C11000 air oxidized samples exposed for 130 hours to concentrated synthetic perspiration developed a white-grey appearance along the surface. Following 12 hours of exposure to concentrated synthetic perspiration, all Nordic Gold samples showed etched faceting, where air oxidized samples had a tendency towards a more yellowing appearance. Scanning electron microscope imaging by backscattering electrons confirms crystalline etching in both C11000 and Nordic Gold (Figures 3.22-3.23).^{xxiii}

^{xxiii} Scanning electron microscope images were obtained courtesy of Michael Melia.






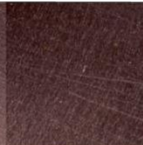
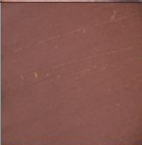














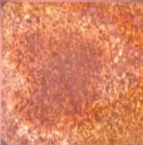





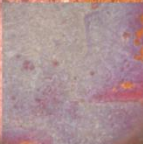


<div style="border: 1px solid black; padding: 5px; display: inline-block;"> Scale <hr style="width: 50%; margin: 0 auto;"/> 0.5 cm </div>	Freshly Ground			Air Oxidized		
	1	2	3	1	2	3
Replicate						
0 Hours						
12 Hours						
48 Hours						
96 Hours						
130 Hours						

Figure 3.20. Visual analysis of C11000 under freshly ground and air oxidized conditions after the indicated time exposure to concentrated synthetic perspiration at 23 °C and ambient aeration.


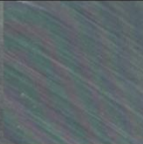


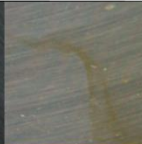
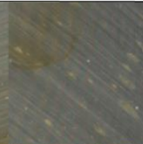




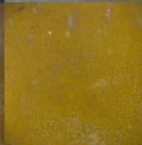

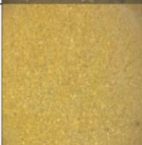

















Scale 0.5 cm	Freshly Ground			Air Oxidized		
	1	2	3	1	2	3
Replicate						
0 Hours						
12 Hours						
48 Hours						
96 Hours						
130 Hours						

Figure 3.21. Visual analysis of Nordic Gold under freshly ground and air oxidized conditions after the indicated time exposure to concentrated synthetic perspiration at 23 °C and ambient aeration.

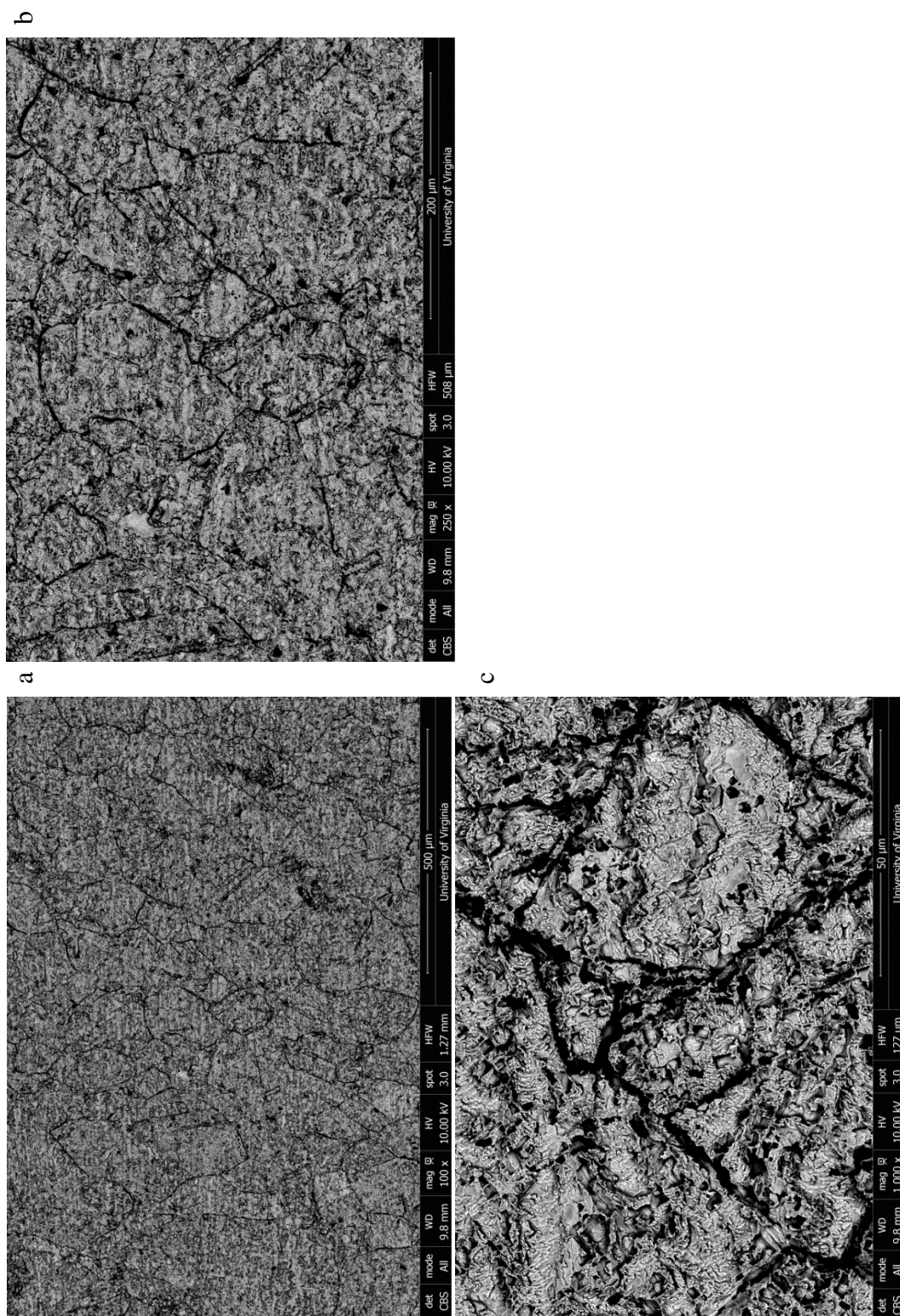


Figure 3.22. SEM micrographs of C11000 exposed to concentrated synthetic perspiration (23 C, ambient aeration) for 130 hours using backscattered electrons at 100x (a), 250x (b) and 1000x (c)

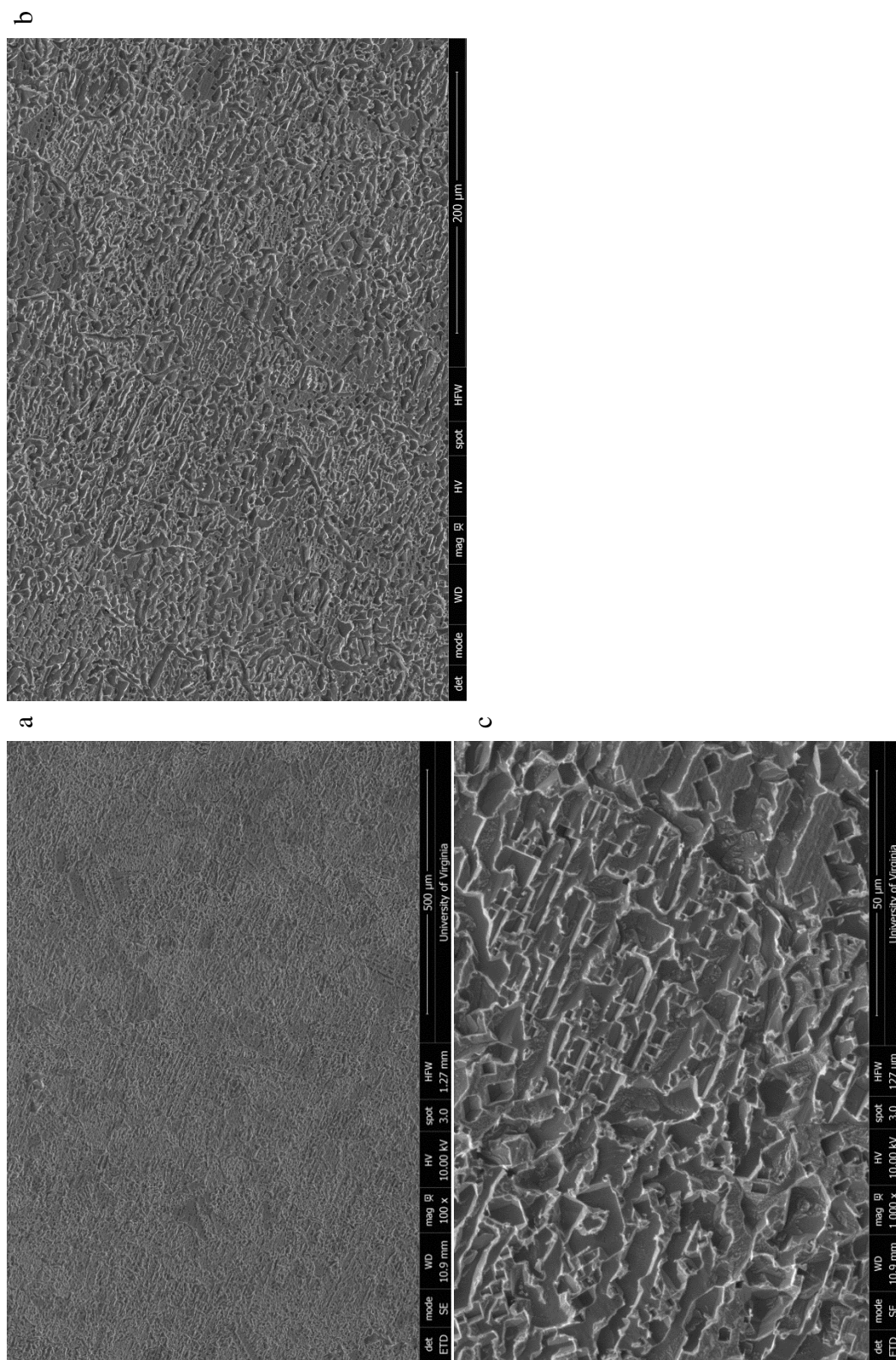


Figure 3.23. SEM micrographs of Nordic Gold exposed to concentrated synthetic perspiration (23 C, ambient aeration) for 130 hours using backscattered electrons at 100x (a), 250x (b) and 1000x (c)

3.4.3.2 Tarnish Analysis by Optical Spectrophotometry

Reflectivity was utilized as a qualitative comparison for the degree of tarnish acquired on samples over time exposed to concentrated synthetic perspiration. In all samples, exposure to concentrated synthetic perspiration caused a decrease in reflectivity in air after only 12 hours of exposure (Figure 3.24). Nordic Gold lost more reflectivity in the first 12 hours compared to C11000, but maintained greater reflectivity after 130 hours of exposure to concentrated synthetic perspiration. The greatest degree of relative reflectivity was observed at 630-730 nm on both materials, corresponding orange to dark red light as was visually observed (Figure 3.25). After 130 hours of exposure to concentrated synthetic perspiration, all alloys have a <16% reflectivity over all wavelengths (Figure 3.26). When air oxidized, Nordic Gold had a lower level of reflectivity before being exposed to concentrated synthetic perspiration, but tarnished to approximately the same degree as Nordic Gold when freshly ground, with a maximum of 14.4% reflectivity on freshly ground Nordic Gold and 15.8% reflectivity on air oxidized Nordic Gold. Therefore, there may be an overall slightly lesser degree of tarnishing occurring when Nordic Gold is air oxidized before being exposed to concentrated synthetic perspiration.

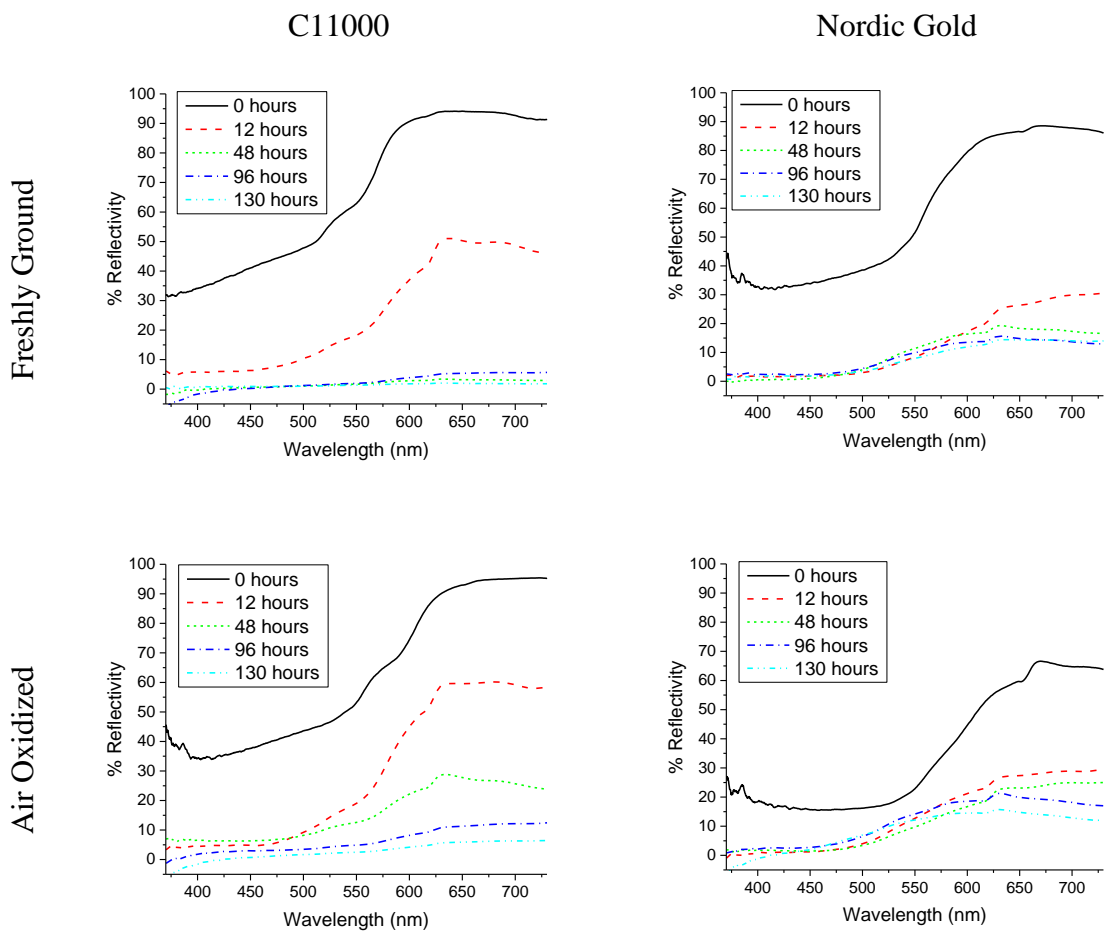


Figure 3.24. Reflectivity of C11000 and Nordic Gold samples when freshly ground to 1200 grit, furnace oxidized at 170 °C for 60 minutes, or air oxidized at ambient lab conditions for 30 days, then exposed to concentrated synthetic perspiration solution at 23 °C and ambient aeration for various times.

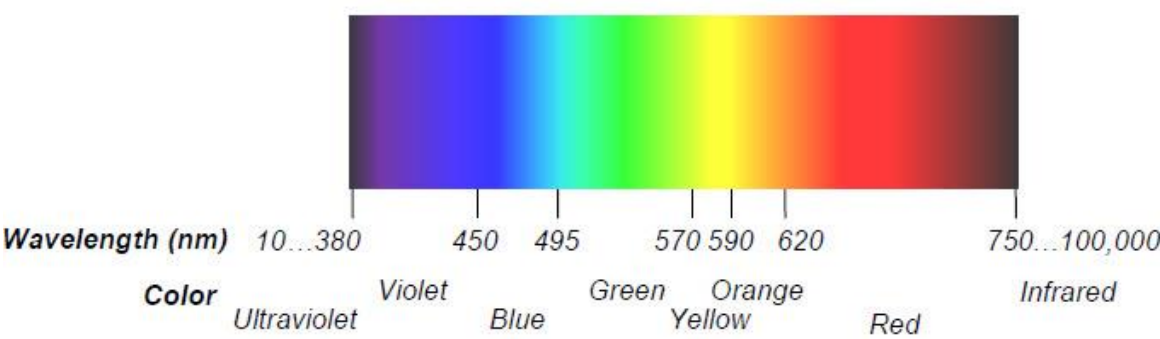


Figure 3.25. Visible light spectrum wavelengths with corresponding observed color.¹²⁹

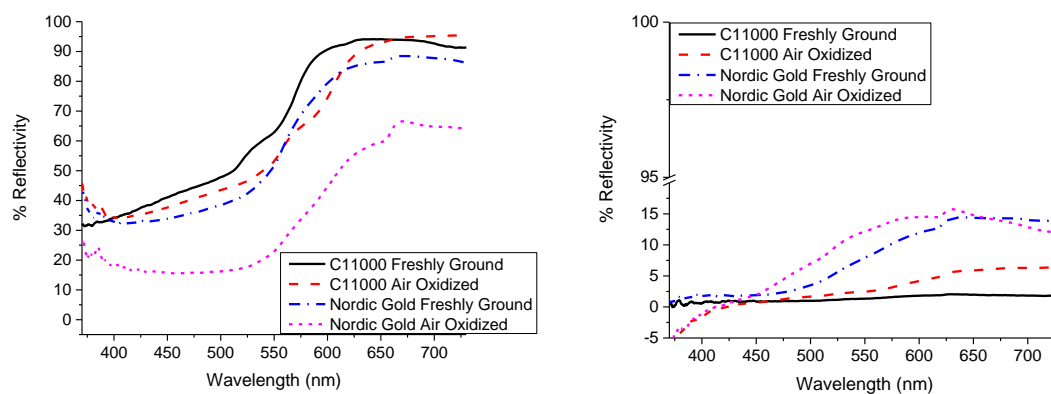


Figure 3.26. Reflectivity of C11000 and Nordic Gold samples when freshly ground to 1200 grit or air oxidized at ambient lab conditions for 30 days, then exposed to concentrated synthetic perspiration solution at 23 °C and ambient aeration for 0 hours (left) and 130 hours (right).

3.4.3.3 Corrosion Product Analysis by GIXRD

Prior to exposure to concentrated synthetic perspiration, all samples exhibited only peaks consistent with fcc copper and no corrosion products, despite the pretreatment of air oxidation suggesting that air formation causes thin oxides (Figure 3.27). GIXRD peaks in Nordic Gold before exposure to concentrated synthetic perspiration were shifted to lower angles, consistent with substitution alloying effects on the Cu fcc lattice parameter.¹⁴⁶

Following exposure to concentrated synthetic perspiration, all samples developed crystalline corrosion products, regardless of pretreatment, as seen in Figure 3.28. Peaks were identified based on International Centre for Diffraction Data (ICDD) PDF cards. In all samples, exposure to concentrated synthetic perspiration results in peaks consistent with Cu_2O ($2\theta = 36.4$) in as little as 12 hours. After 130 hours, all samples had evidence of Cu_2O (Figure 3.30), and air oxidized samples peaks consistent with of $\text{Cu}_2(\text{OH})_3\text{Cl}$ ($2\theta = 31.5468, 32.2113, 32.4512$) (Figure 3.31). Additionally, GIXRD spectra signal-to-noise

increased following exposure to concentrated synthetic perspiration, indicating a roughening of the copper alloys surface during the corrosion process.¹⁴⁷ Figures 3.32-3.33 show comparative GIXRD of C11000 and Nordic Gold after identical pre-treatments to highlight the effect of alloy composition on corrosion behavior.

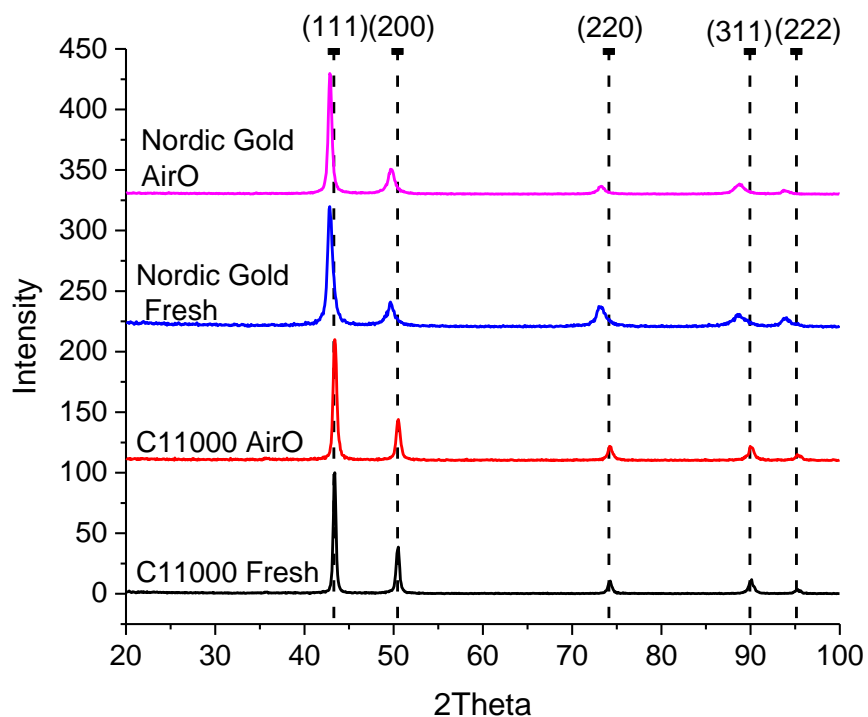


Figure 3.27. GIXRD of C11000 and Nordic Gold samples when freshly ground to 1200 grit, or air oxidized at ambient lab conditions for 30 days, prior to exposure to concentrated synthetic perspiration solution, where only FCC metallic Cu (PDF Card No. 00-004-0836) peaks are evident. Spectra are shown offset ($y=120$ on intensity scale) for ease of comparison.

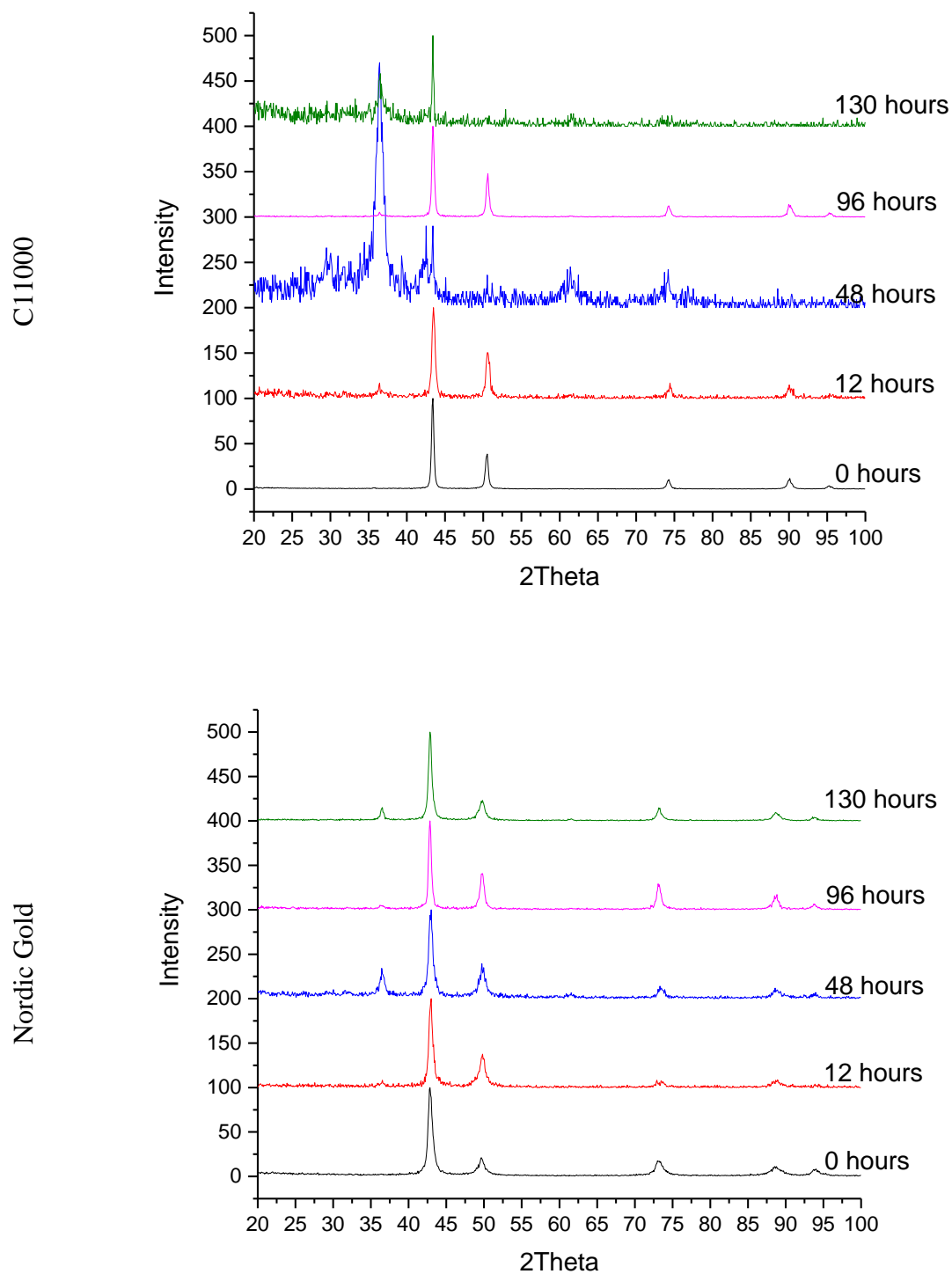


Figure 3.28. GIXRD of C11000 (top) and Nordic Gold (bottom) samples when freshly ground to 1200 grit then exposed to concentrated synthetic perspiration solution at 23 °C and ambient aeration for various times indicated.

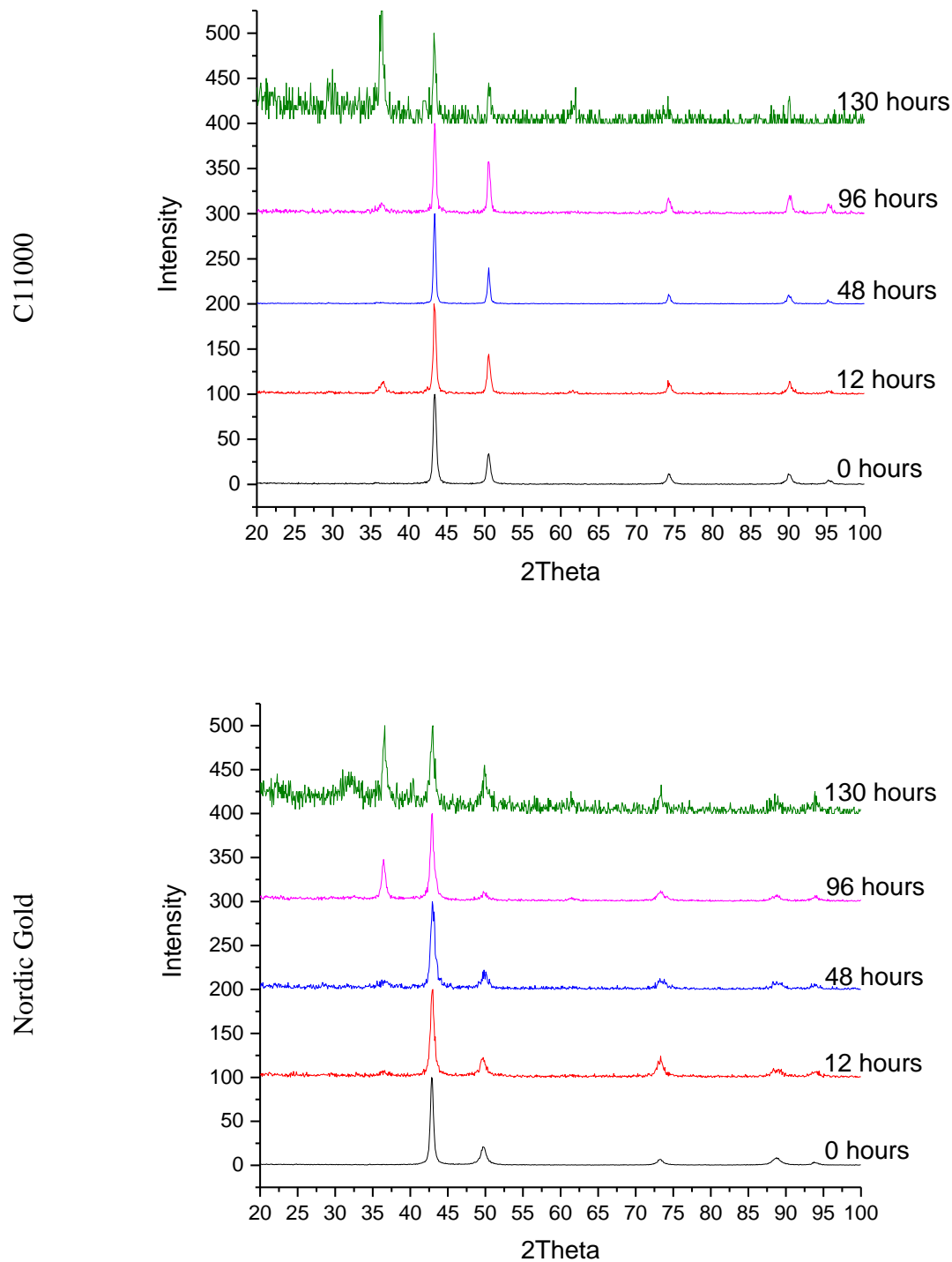


Figure 3.29. GIXRD of C11000 (top) and Nordic Gold (bottom) samples when freshly ground to 1200 grit and air oxidized at ambient lab conditions for 30 days, then exposed to concentrated synthetic perspiration solution at 23 °C and ambient aeration for various times indicated.

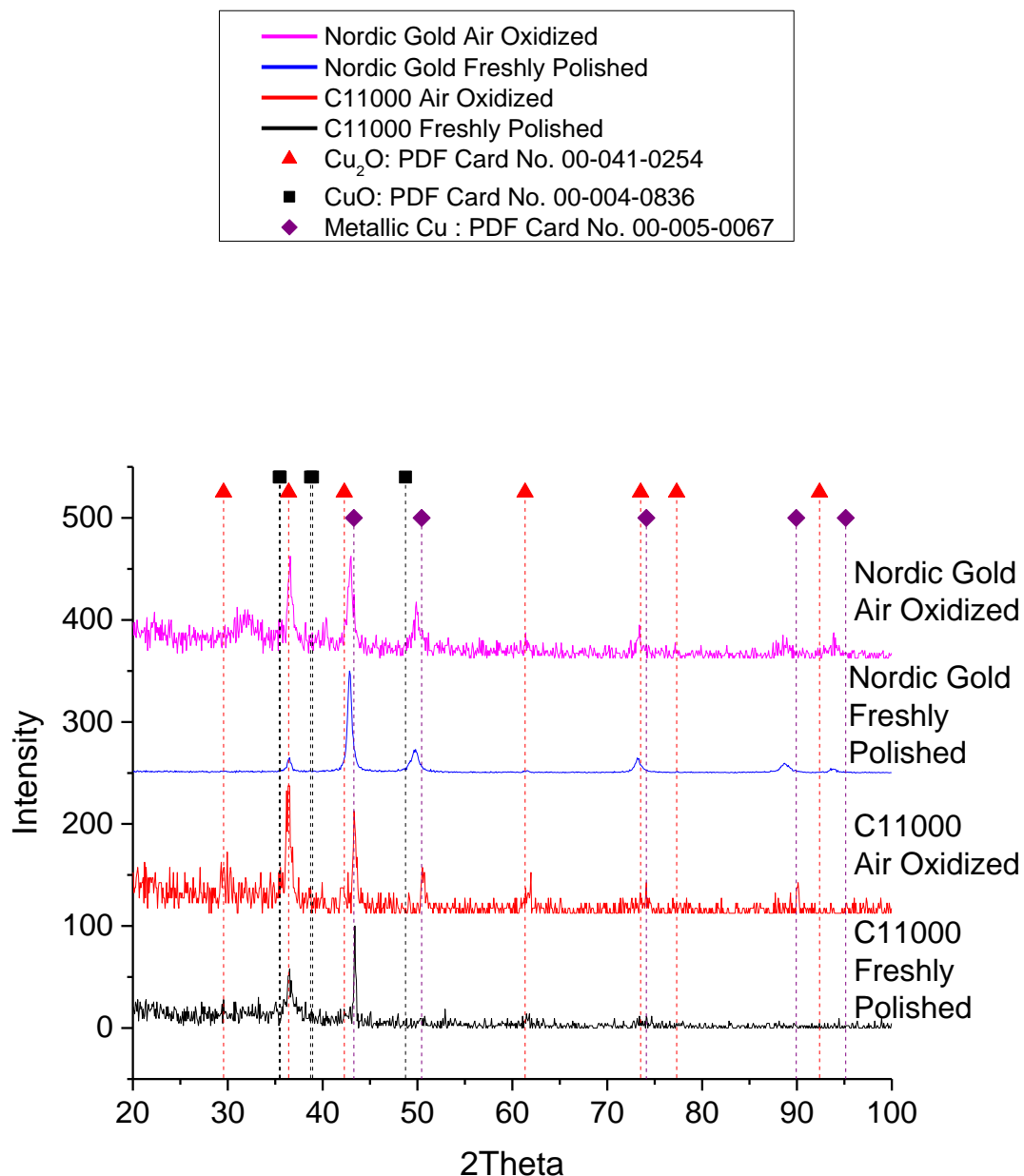


Figure 3.30. GIXRD of C11000 and Nordic Gold samples when freshly ground to 1200 grit or air oxidized at ambient lab conditions for 30 days, after exposure to concentrated synthetic perspiration solution (23 °C, ambient aeration) for 130 hours, with FCC metallic Cu, Cu_2O and CuO peaks highlighted. Spectra are shown offset ($y=150$) for ease of comparison.

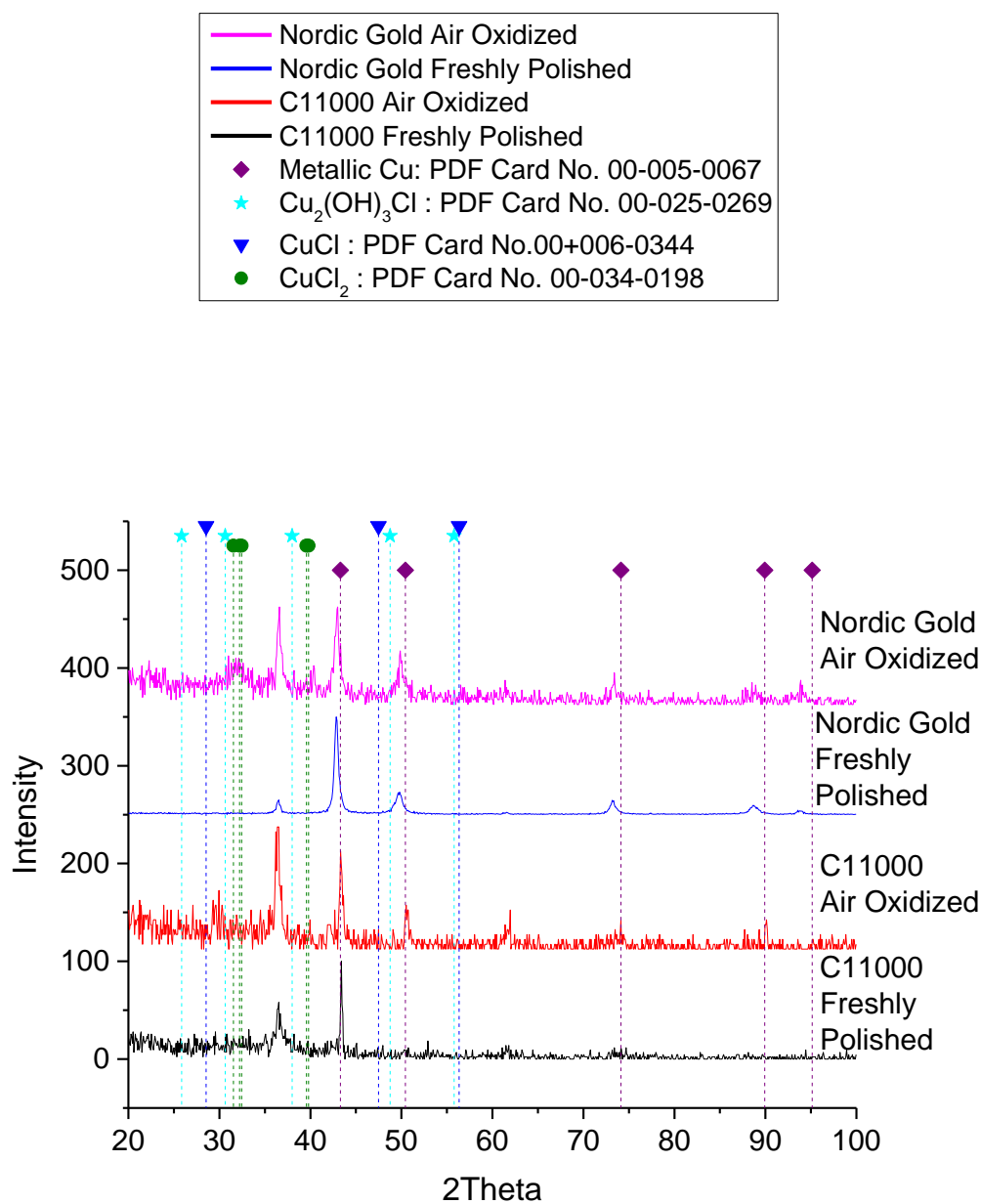


Figure 3.31. GIXRD of C11000 and Nordic Gold samples when freshly ground to 1200 grit or air oxidized at ambient lab conditions for 30 days, after exposure to concentrated synthetic perspiration solution (23 °C, ambient aeration) for 130 hours, with FCC metallic Cu, CuCl, Cu₂Cl, and Cu₂(OH)₃Cl peaks highlighted. Spectra are shown offset (y=150) for ease of comparison.

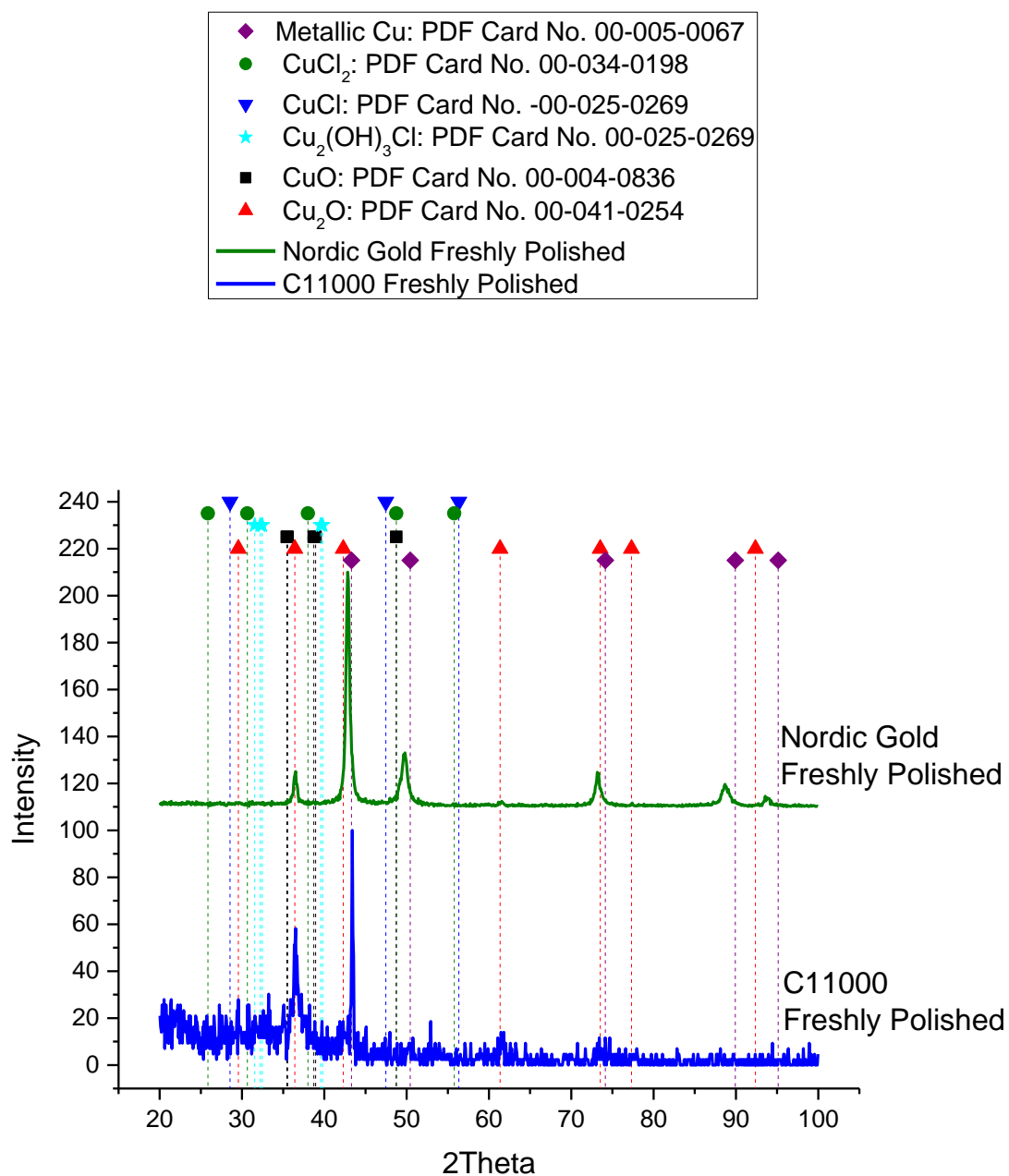


Figure 3.32. Comparative GIXRD of C11000 and Nordic Gold when freshly ground to 1200 grit followed by exposure to concentrated synthetic perspiration solution (23 °C, ambient aeration) for 130 hours. Spectra are shown offset ($y=170$) for ease of comparison.

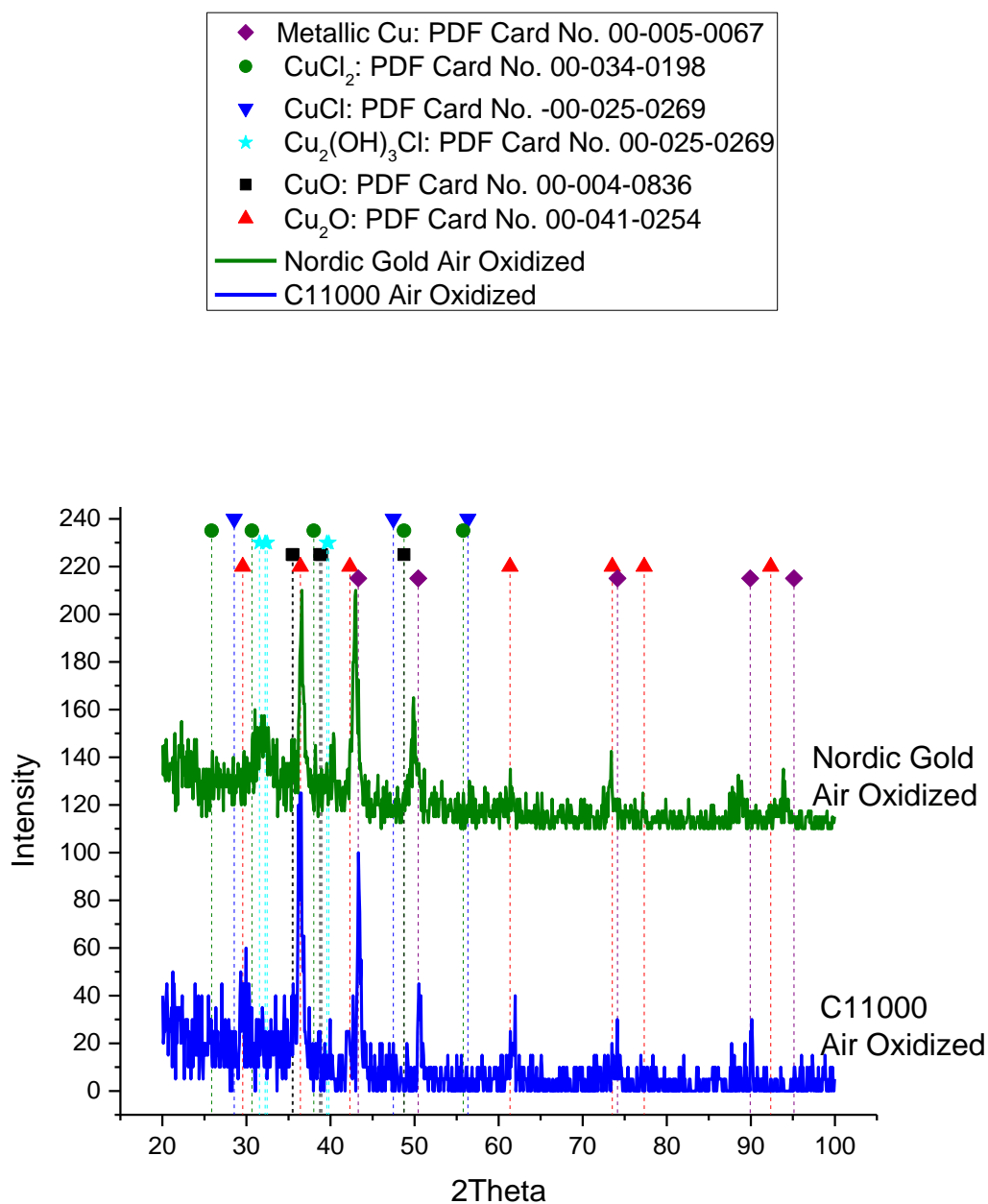


Figure 3.33. Comparative GIXRD of C11000 and Nordic Gold when freshly ground to 1200 grit, then air oxidized at ambient lab conditions, followed by exposure to concentrated synthetic perspiration solution (23 °C, ambient aeration) for 130 hours. Spectra are shown offset ($y=170$) for ease of comparison.

3.4.3.4 Corrosion Product Layer Analysis by Galvanostatic Reduction

Samples were analyzed prior to exposure to concentrated synthetic perspiration to determine composition of oxides formed by air oxidation (Figure 3.34). Before exposure

to concentrated synthetic perspiration (23 °C, ambient aeration), air oxidized C11000 experienced longer reduction times near $-0.8 V_{MMSE}$ compared to freshly ground C11000 and similar reduction times near $-1.2 V_{MMSE}$, but no additional reduction waves were present. Prior to exposure to concentrated synthetic perspiration (23 °C, ambient aeration), air oxidized Nordic Gold experienced a longer reduction times near $-0.75 V_{MMSE}$, similar reductions waves near $-1.05 V_{MMSE}$, and an additional reduction at $-1.3 V_{MMSE}$. The change in reduction behavior between freshly ground samples and air oxidized samples confirms the presences of thin oxides following pre-treatment. The identity of C11000 thin oxides following air oxidation have similar identity judging from reduction potential as the corrosion product ($-0.8 V_{MMSE}$) that forms on C11000 after only minutes of exposure to air during the transfer from methanol to the reaction cell.^{xxiv} The identity of Nordic Gold air formed thin oxides have similar identity as the corrosion product on freshly ground Nordic Gold judging from reduction potentials ($-0.75 V_{MMSE}$ and $-1.05 V_{MMSE}$), but the corrosion product formed by air oxidation contains an additional species ($-1.3 V_{MMSE}$).

Figures 3.34-3.37 illustrate the dependence of exposure time in concentrated synthetic perspiration on the reduction behavior. In cases where the reduction of a species begins at a more negative potentials and increases over time, the corrosion product is likely becoming easier to reduce. C11000 exposed to concentrated synthetic perspiration develops a corrosion layer that is reduced at $-0.6 V_{MMSE}$ which was not seen prior to exposure to concentrated synthetic perspiration solution. A corrosion product at $-0.8 V_{MMSE}$, which was seen prior to exposure to concentrated synthetic perspiration, thickens as indicated by longer reduction times. Following 12 hours of exposure, a new corrosion

^{xxiv} Outer layer of corrosion layer taken as the highest oxidation state

product forms that reduces at $-0.9 V_{MMSE}$, and thickens with time as indicated by longer reduction times. An innermost corrosion product is evident at reduction potential $-1.3 V_{MMSE}$ after exposure to concentrated synthetic perspiration, but due to its thin nature is difficult to discern in some cases from the previous reduction wave. Nordic Gold experiences similar behavior, where the outer layer ($-0.6 V_{MMSE}$) thickens over time, but its identity does not change compared to before exposure to concentrated synthetic perspiration. The inner corrosion layer ($-0.9 V_{MMSE}$) thickens over time, and a corrosion layer reduced at $-1.3 V_{MMSE}$ develops and thickens over time following exposure to concentrated perspiration. Figures 3.38-3.39 and demonstrate example inflection points based on the 1st derivative maximum. Figure 3.39 demonstrates example inflection points determined by differentiation (t_i) and potentials (E_i) associated of C11000 and Nordic Gold that are used to define the points in Figure 3.40.

Figures 3.41-3.42 illustrate the effect of additional alloying elements on corrosion products by comparing C11000 and Nordic Gold after identical pretreatment conditions, as well as attempts to identify corrosion products based on electrochemical reduction potentials. Based on Figure 3.41, oxides on C11000 and Nordic Gold are reduced at similar potentials, though Nordic Gold reduces at significantly shorter times compared to C11000. The composition of freshly ground C11000 and Nordic Gold corrosion layers following 130 hours of exposure to concentrated synthetic perspiration (23 °C, ambient aeration) is suspected (Chapter 2.4.3.4) to consist of an outer layer of CuO and an inner, thicker layer of Cu₂O. Both layers were considerably thicker on C11000 compared to Nordic Gold when freshly ground. An unidentified corrosion product at $-1.3 V_{MMSE}$ is present in both Nordic Gold and C11000, and therefore cannot be related to alloying

elements. Air oxidized samples appear to result in the formation of more complex corrosion layers. When air oxidized, C11000 appears to have a thin outer oxide of either CuO or $\text{Cu}_2(\text{OH})_3\text{Cl}$, and a thicker Cu_2O inner layer. Nordic Gold corrosion layers consist of thin layers of CuO, $\text{Cu}_2(\text{OH})_3\text{Cl}$, and $\text{CuCl}_2 \cdot 3\text{Cu}(\text{OH})_2$ over a thicker Cu_2O layer. As seen in Figure 3.43, the presence of thin air formed oxides on C11000 reduced the thickness of the corrosion layer, but was ineffective at reducing oxide thickness based on reduction times on Nordic Gold when exposed to concentrated perspiration solution for 130 hours. Figure 3.44 demonstrates that while air oxidation of C11000 reduces the thickness of corrosion products developed during exposure to concentrated synthetic perspiration compared to freshly ground C11000, Nordic Gold consistently results in less corrosion products compared to C11000, although with no effect of air oxidation. There may be electrically disconnected corrosion products that are not seen in galvanostatic reduction, but seen in GIXRD due to corrosion product precipitation due to homogeneous chemical reaction.

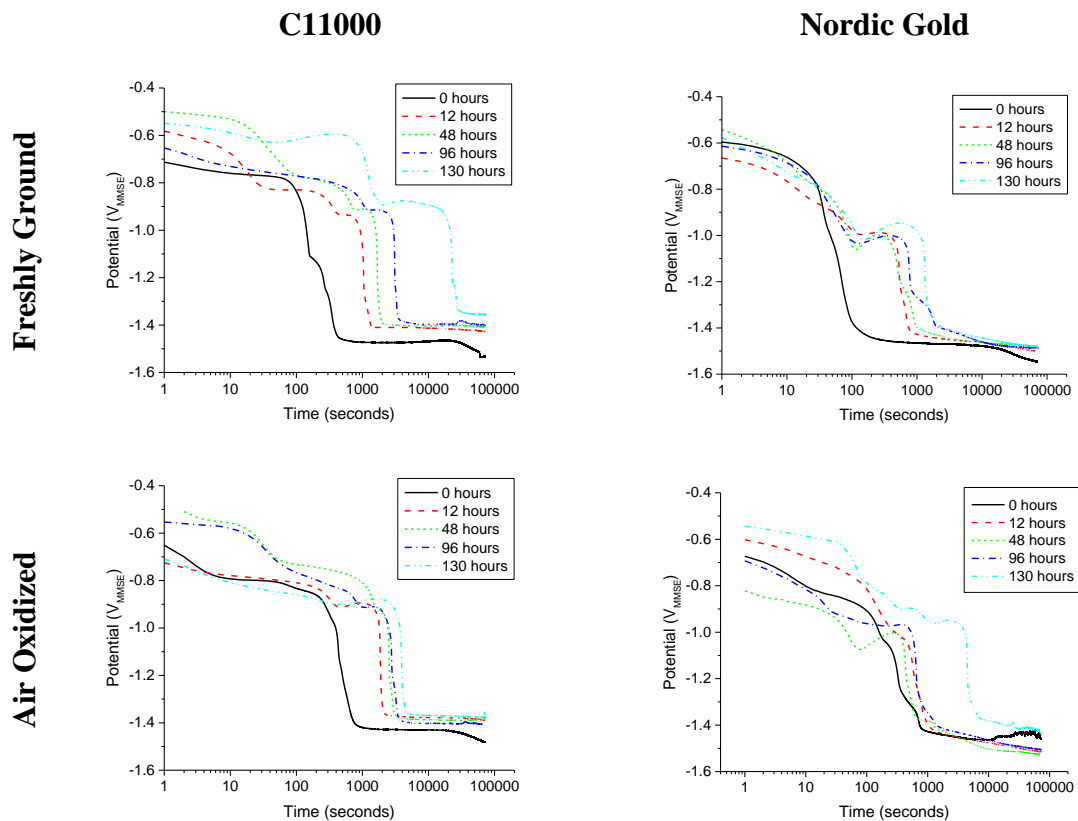


Figure 3.34. Galvaostatic reduction of C11000 and Nordic Gold when freshly ground to 1200 grit or air oxidized at ambient lab conditions for 30 days, followed by exposure to concentrated synthetic perspiration solution (23 °C, ambient aeration) for the various times indicated. Galvanostatic reductions were conducted at 0.02 mA/cm² on an area of 0.8 cm².

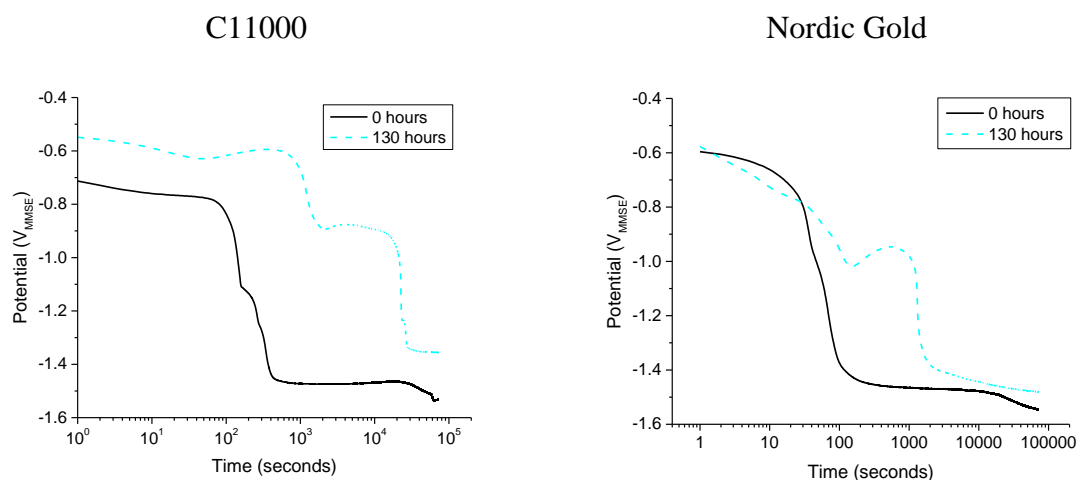


Figure 3.35. Galvanostatic reduction of C11000 (left) and Nordic Gold (right) when freshly ground to 1200 grit followed by exposure to concentrated synthetic perspiration solution (23 °C, ambient aeration) for 0 and 130 hours. Galvanostatic reductions were conducted at 0.02 mA/cm² on an area of 0.8 cm².

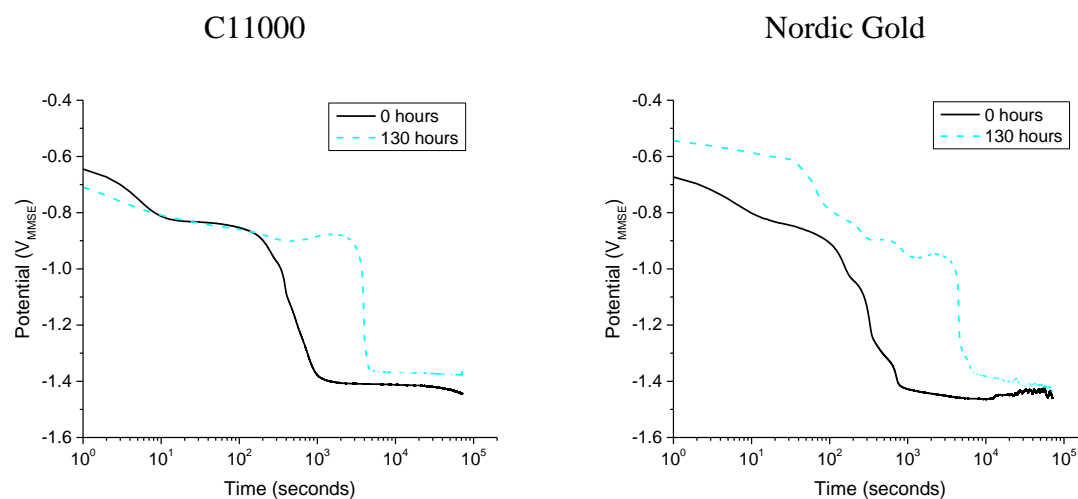


Figure 3.36. Galvanostatic reduction of C11000 (left) and Nordic Gold (right) when freshly ground to 1200 grit, then air oxidized at ambient lab conditions for 30 days followed by exposure to concentrated synthetic perspiration solution (23 °C, ambient aeration) for 0 and 130 hours. Galvanostatic reductions were conducted at 0.02 mA/cm² on an area of 0.8 cm².

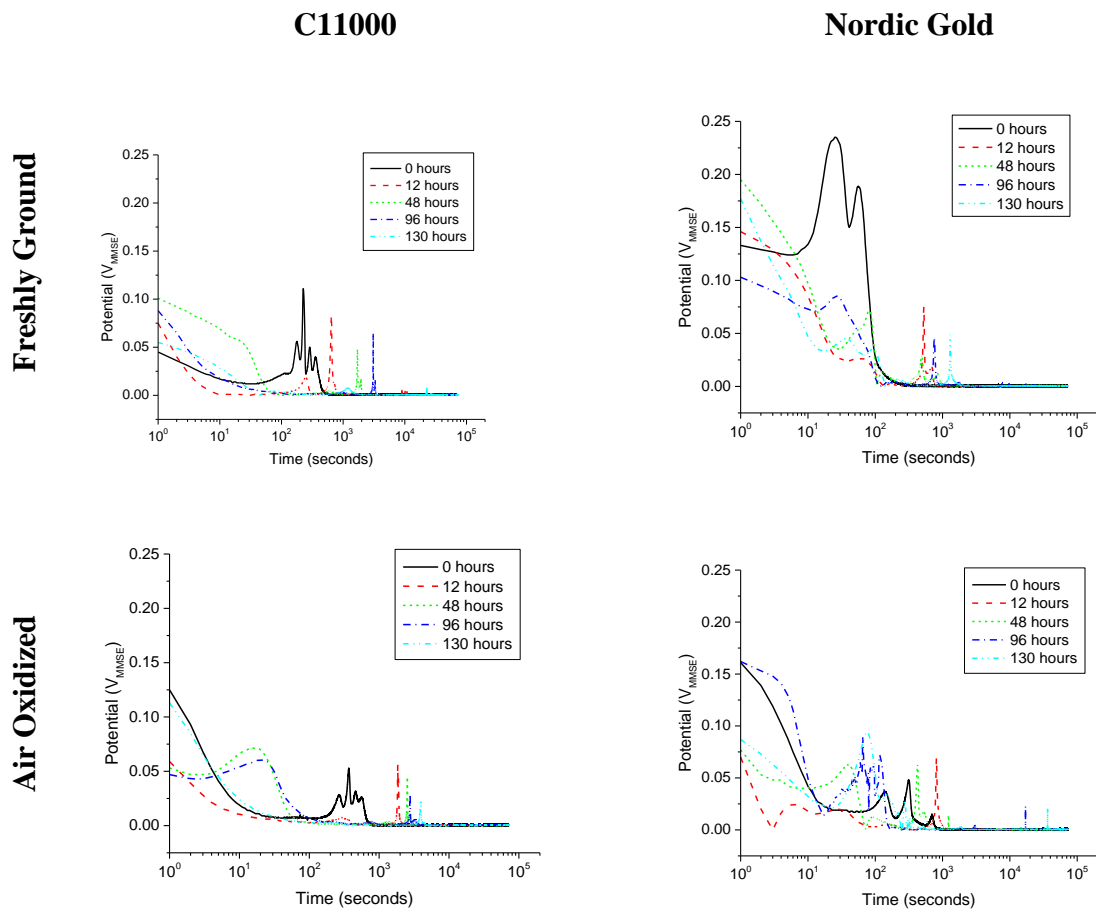


Figure 3.37. Galvanostatic reduction analysis to produce inflection points by taking the first derivative of C11000 and Nordic Gold when freshly ground to 1200 grit or air oxidized at ambient lab conditions for 30 days, followed by exposure to concentrated synthetic perspiration solution (23 °C, ambient aeration) for the various times indicated. Galvanostatic reductions were conducted at 0.02 mA/cm^2 on an area of 0.8 cm^2 .

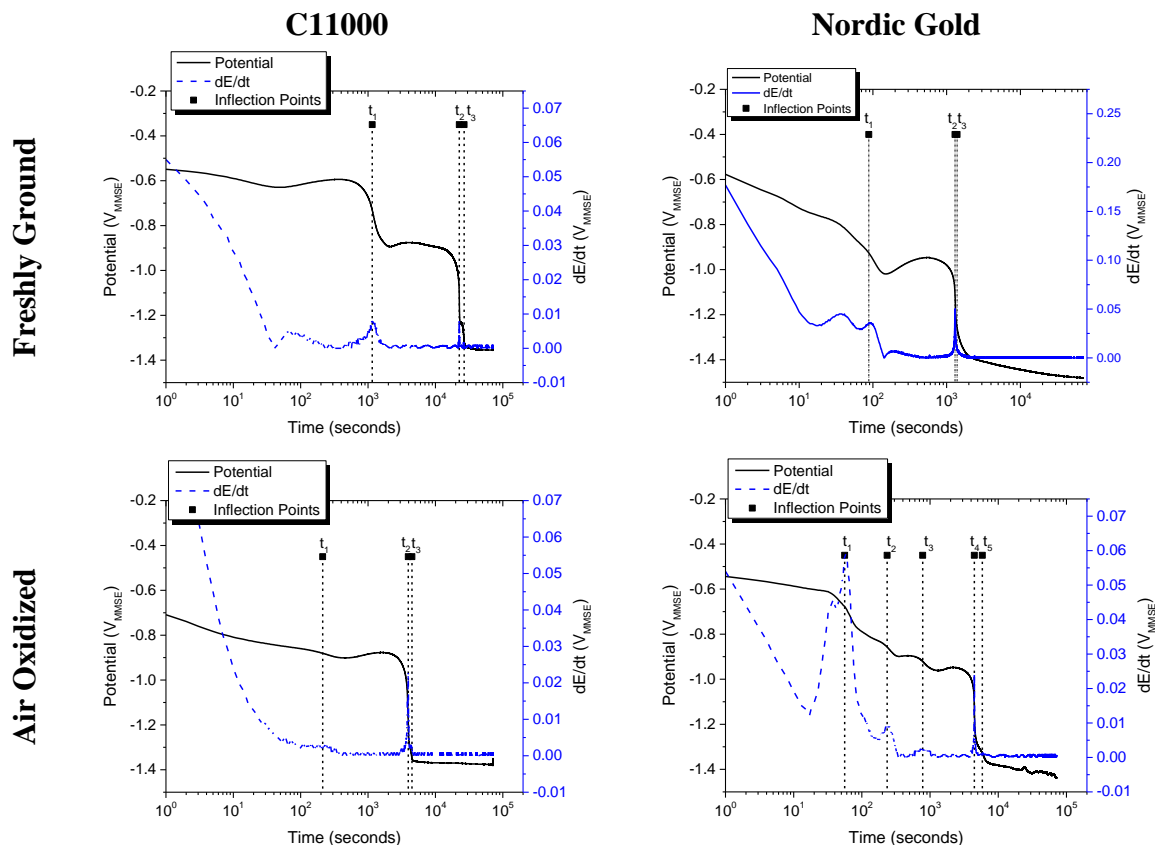


Figure 3.38. Galvanostatic reduction over laid with inflection analysis of C11000 and Nordic Gold when freshly ground to 1200 grit air oxidized at ambient lab conditions for 30 days, followed by exposure to concentrated synthetic perspiration solution (23 °C, ambient aeration) for various times. Galvanostatic reductions were conducted at 0.02 mA/cm² on an area of 0.8 cm².

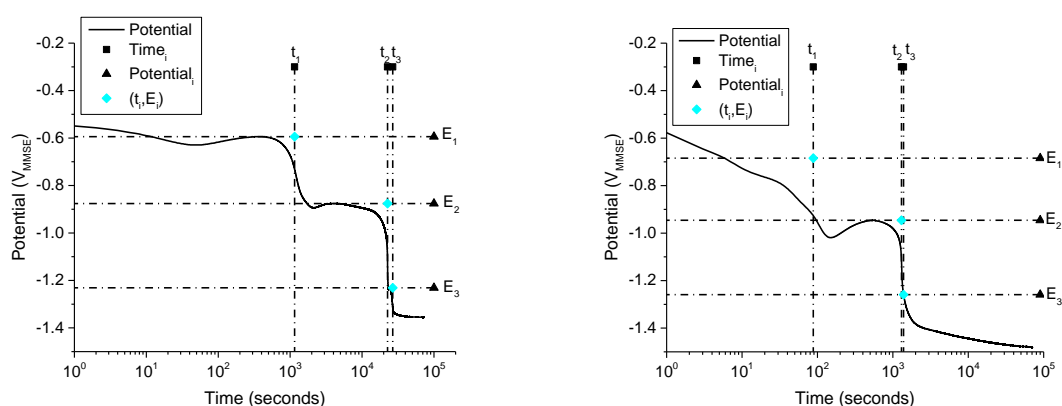


Figure 3.39. Galvanostatic reduction with inflection points (t_i) and associated potentials (E_i) of C11000 (left) and Nordic Gold (right) when freshly ground to 1200 grit then air oxidized at ambient lab conditions for 30 days, followed by exposure to concentrated synthetic perspiration solution (23 °C, ambient aeration) for 130 hours. Galvanostatic reductions were conducted at 0.02 mA/cm² on an area of 0.8 cm².

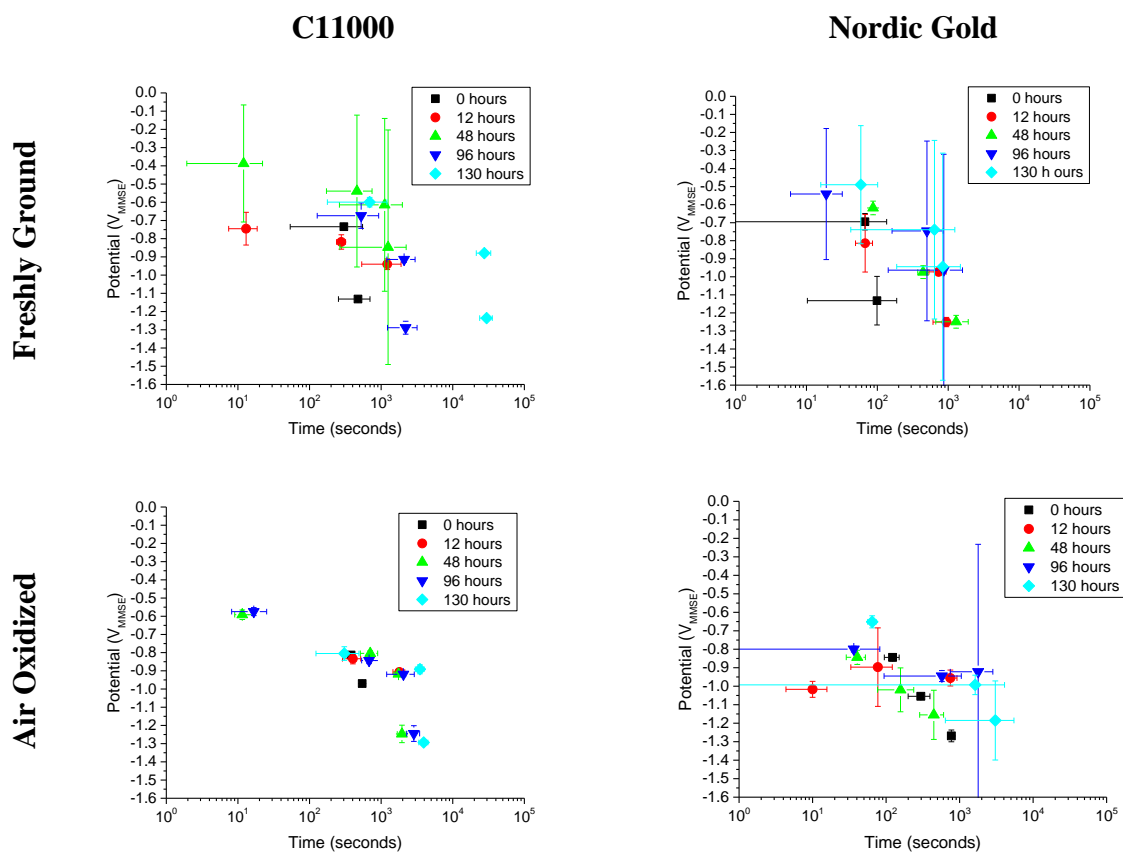


Figure 3.40. Summary of galvanostatic reduction data on C11000 and Nordic Gold when freshly ground to 1200 grit or air oxidized at ambient lab conditions for 30 days, followed by exposure to concentrated synthetic perspiration solution (23 °C, ambient aeration) for various times. Galvanostatic reductions were conducted at 0.02 mA/cm² on an area of 0.8 cm². Data is the average of 3 replicates and error bars are one standard deviation.

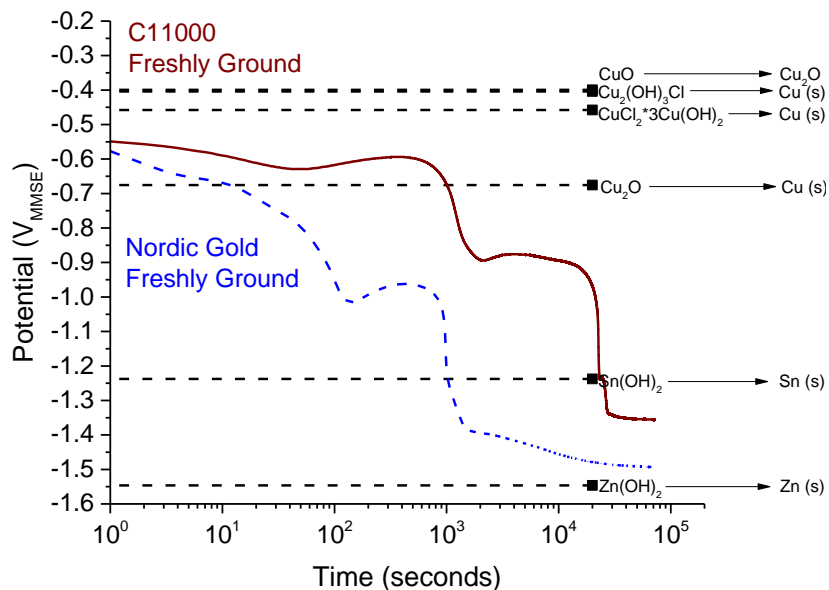


Figure 3.41. Comparative galvanostatic reduction of C11000 (solid red line) and Nordic Gold (dotted blue line) when freshly ground to 1200 grit followed by exposure to concentrated synthetic perspiration solution (23 °C, ambient aeration) for 130 hours. Galvanostatic reductions were conducted at 0.02 mA/cm² on an area of 0.8 cm².

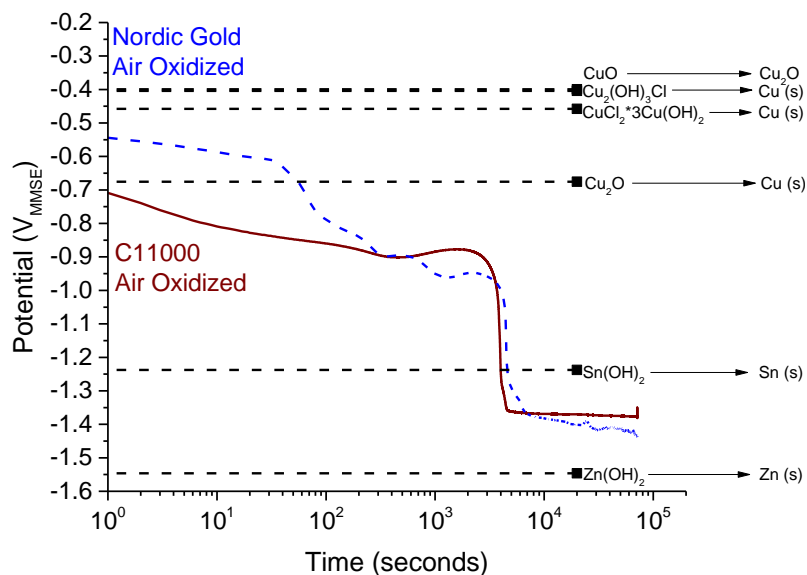


Figure 3.42. Comparative galvanostatic reduction of C11000 (solid red line) and Nordic Gold (dotted blue line) when freshly ground to 1200 grit then air oxidized at ambient lab conditions for 30 days, followed by exposure to concentrated synthetic perspiration solution (23 °C, ambient aeration) for 130 hours. Galvanostatic reductions were conducted at 0.02 mA/cm² on an area of 0.8 cm².

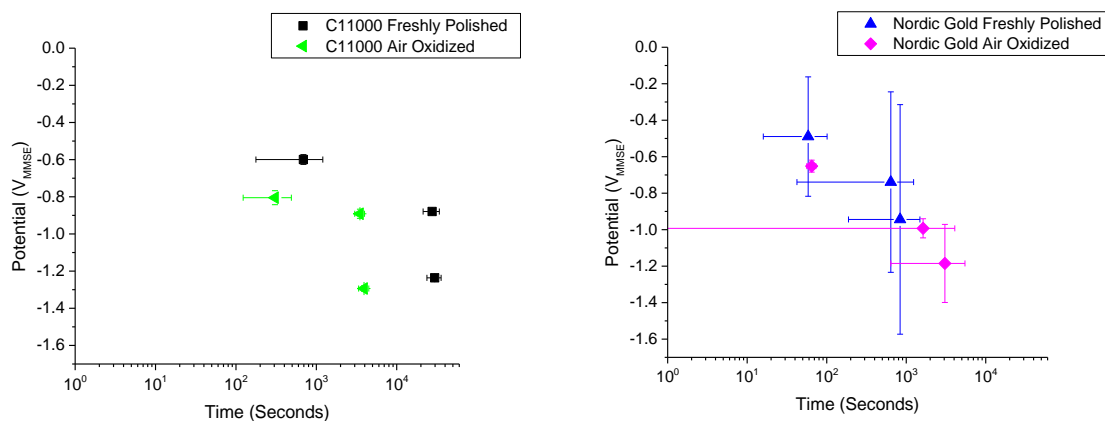


Figure 3.43. Galvanostatic reduction points (t_i, E_i) of C11000 (left) and Nordic Gold (right) when freshly ground to 1200 grit or air oxidized at ambient lab conditions for 30 days, followed by exposure to concentrated synthetic perspiration solution (23 °C, ambient aeration) for 130 hours. Galvanostatic reductions were conducted at 0.02 mA/cm² on an area of 0.8 cm². Data is the average of 3 replicates and error bars are one standard deviation.

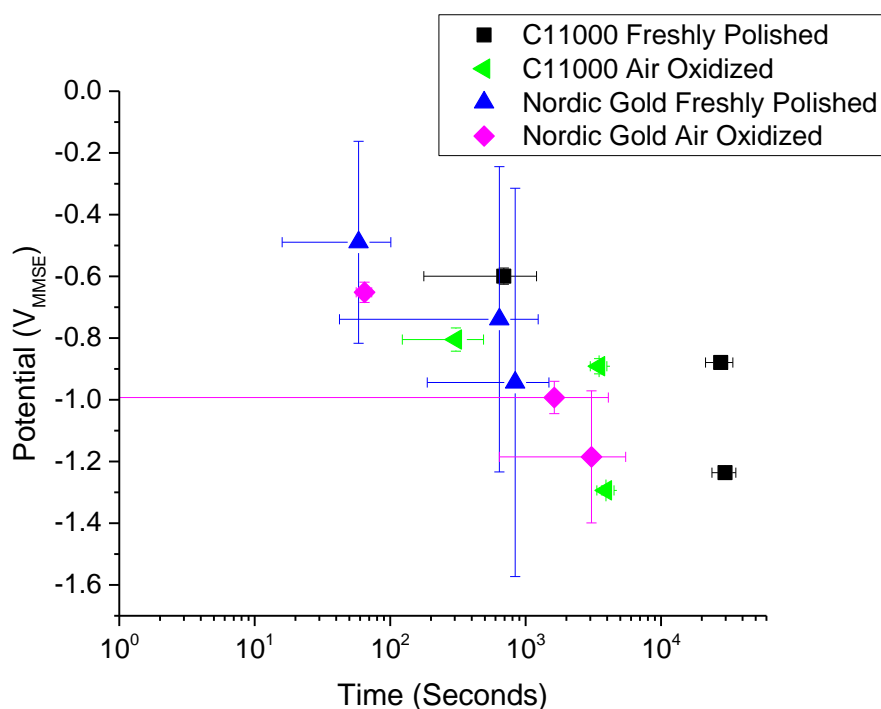


Figure 3.44. Galvanostatic reduction points (t_i, E_i) of C11000 and Nordic Gold when freshly ground to 1200 grit or air oxidized at ambient lab conditions for 30 days, followed by exposure to concentrated synthetic perspiration solution (23 °C, ambient aeration) for 130 hours. Galvanostatic reductions were conducted at 0.02 mA/cm² on an area of 0.8 cm². Data is the average of 3 replicates and error bars are one standard deviation.

3.4.4 Copper Ion Release by ICP-OES

Copper ion release was analyzed in concentrated synthetic perspiration solution by inductively coupled plasma-optical emission spectrometry (ICP-OES). Copper release was assumed to be a factor of time exposure to concentrated synthetic perspiration, pre-treatment condition, and alloy composition. As seen in Figure 3.45, copper release increased over time in a roughly linear trend.

Figures 3.46-3.47 compares copper release from C11000 and Nordic Gold under pre-treatment conditions. Thin oxides formed by air oxidation on C11000 increase the rate of copper release (0.035 ppm/hour for 0.8 cm² area) compared to the freshly ground alloy (0.027 ppm/hour for 0.8 cm² area). Air formed oxides on Nordic Gold result in an increase rate of copper release (0.020 ppm/hour for 0.8 cm² area) compared to freshly ground Nordic Gold (0.012 ppm/hour for 0.8 cm² area).

Figures 3.48-3.49 demonstrate the dependence of alloy composition on copper release over time. When freshly ground, Nordic Gold release less copper across all times compared to C11000. In the presence of thin oxides, initial copper ion release from Nordic Gold and C11000 are similar, but copper release from Nordic Gold is consistently less than C11000 between 48 and 130 hours of exposure to concentrated synthetic perspiration. As seen in Figure 3.50, copper release from C11000 is higher than Nordic Gold following 130 hours of exposure to concentrated synthetic perspiration when both freshly ground and air oxidized. However, while air formed oxides decrease copper release in C11000, it enhances copper release in Nordic Gold when exposed to concentrated synthetic perspiration (23 °C, ambient aeration) solution for 130 hours. Additionally, Nordic Gold released zinc in increasing amounts over time (Figure 3.51),

where after 130 hours in concentrated synthetic perspiration freshly ground samples released 0.11 (± 0.02) and air oxidized samples released 0.17 (± 0.07) ppm Zn, with a surface to volume ratio of 2.67 cm²/L (Figure 3.52). This suggests incongruent dissolution of elements, with a calculated fractional release of 92.1% Cu and 7.9% Zn over 130 hours.

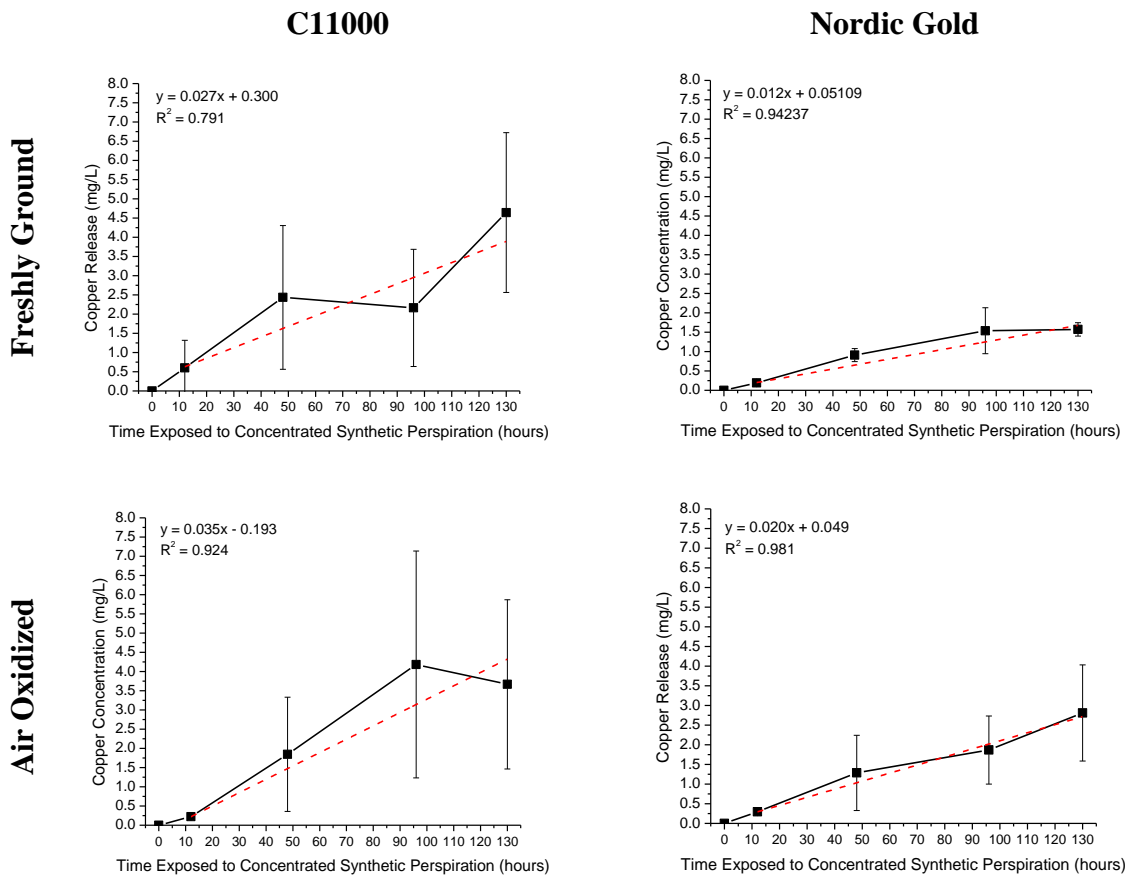


Figure 3.45 Copper concentration as a factor of time for C11000 and Nordic Gold when freshly ground to 1200 grit or air oxidized at ambient lab conditions for 30 days, followed by exposure to concentrated synthetic perspiration solution (23 °C, ambient aeration) over time. Concentrated synthetic perspiration solution was exposed to 0.8 cm² of copper of the copper alloy coupon to 300 mL of solution, with a surface to volume ratio of 2.67 cm²/L. Data is the average of 3 replicates and error bars are one standard deviation.

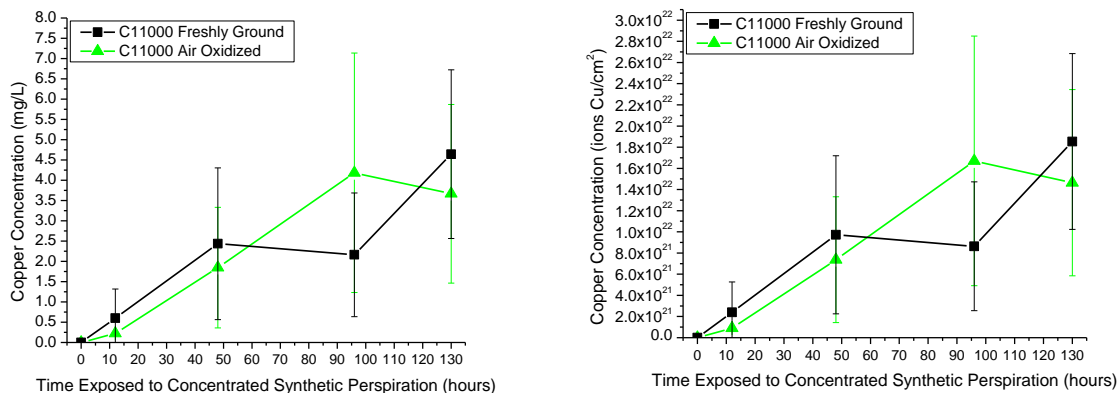


Figure 3.46. Copper concentration as a factor of time for C11000 when freshly ground to 1200 grit or air oxidized at ambient lab conditions for 30 days, followed by exposure to concentrated synthetic perspiration solution (23 °C, ambient aeration) over time, expressed as ppm in solution (left) and amount Cu²⁺ in 300 mL divided by electrode area (0.8 cm²) (right) over time. Concentrated synthetic perspiration solution was exposed to 0.8 cm² of copper of the copper alloy coupon to 300 mL of solution, with a surface to volume ratio of 2.67 cm²/L. Data is the average of 3 replicates and error bars are one standard deviation.

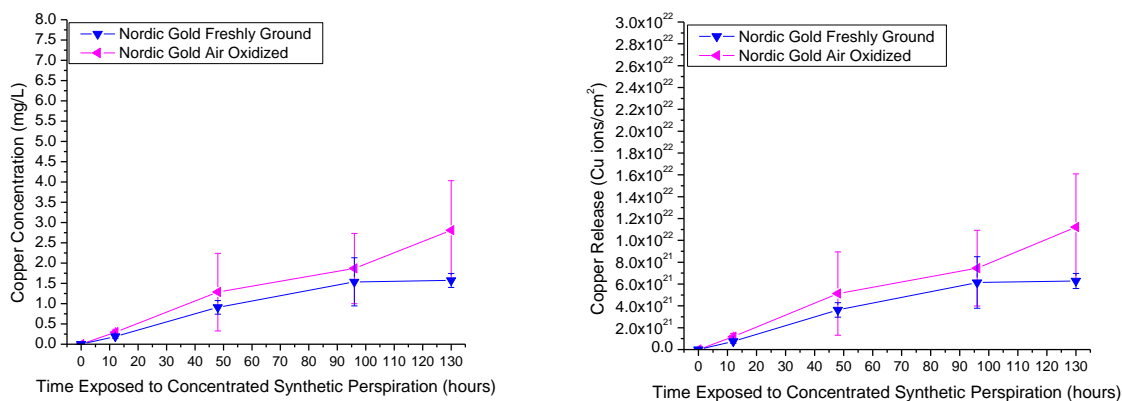


Figure 3.47. Copper concentration as a factor of time for Nordic Gold when freshly ground to 1200 grit or air oxidized at ambient lab conditions for 30 days, followed by exposure to concentrated synthetic perspiration solution (23 °C, ambient aeration) over time, expressed as ppm in solution (left) and amount Cu²⁺ in 300 mL divided by electrode area (0.8 cm²) (right) over time. Concentrated synthetic perspiration solution was exposed to 0.8 cm² of copper of the copper alloy coupon to 300 mL of solution, with a surface to volume ratio of 2.67 cm²/L. Data is the average of 3 replicates and error bars are one standard deviation.

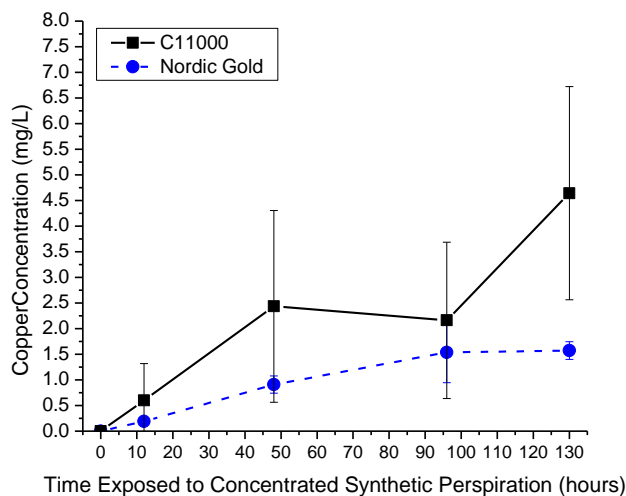


Figure 3.48. Copper concentration as a factor of time for C11000 and Nordic Gold when freshly ground to 1200 grit, followed by exposure to concentrated synthetic perspiration solution (23 °C, ambient aeration) over time expressed as ppm in solution. Concentrated synthetic perspiration solution was exposed to 0.8 cm² of the copper alloy coupon, with a surface to volume ratio of 2.67 cm²/L to 300 mL of solution, with a surface to volume ratio of 2.67 cm²/L. Data is the average of 3 replicates and error bars are one standard deviation.

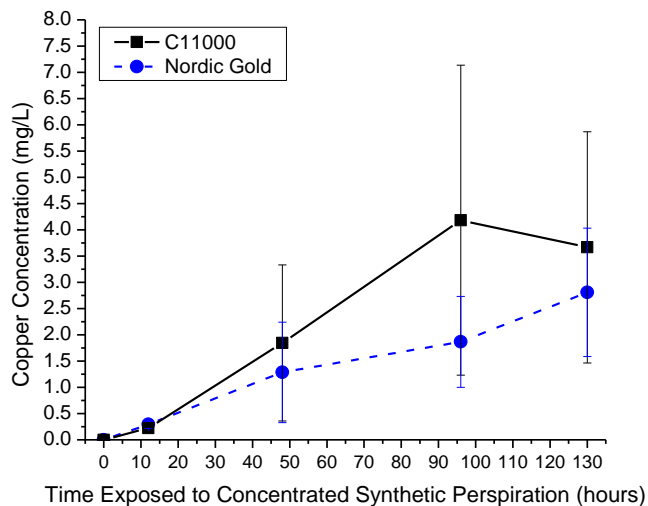


Figure 3.49. Copper concentration as a factor of time for C11000 and Nordic Gold when freshly ground to 1200 grit and air oxidized at ambient lab conditions for 30 days, followed by exposure to concentrated synthetic perspiration solution (23 °C, ambient aeration) over time expressed as ppm in solution. Concentrated synthetic perspiration solution was exposed to 0.8 cm² of the copper alloy coupon to 300 mL of solution, with a surface to volume ratio of 2.67 cm²/L. Data is the average of 3 replicates and error bars are one standard deviation.

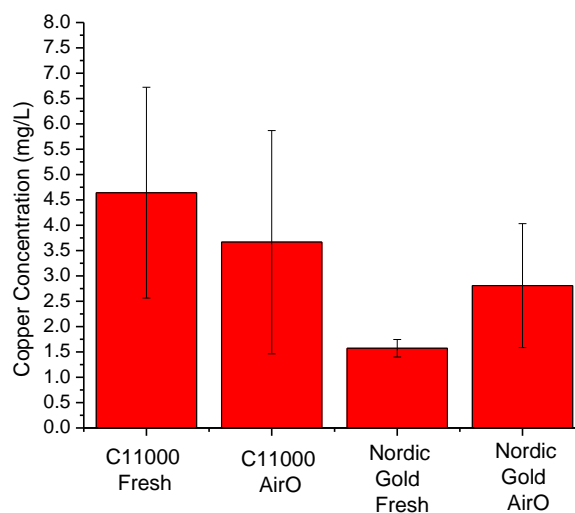


Figure 3.50. Copper concentration as a factor of time for C11000 and Nordic Gold when freshly ground to 1200 grit or air oxidized at ambient lab conditions for 30 days, followed by exposure to concentrated synthetic perspiration solution (23 °C, ambient aeration) over time, expressed as ppm in solution. Concentrated synthetic perspiration solution was exposed to 0.8 cm² of copper of the copper alloy coupon to 300 mL of solution, with a surface to volume ratio of 2.67 cm²/L. Data is the average of 3 replicates and error bars are one standard deviation.

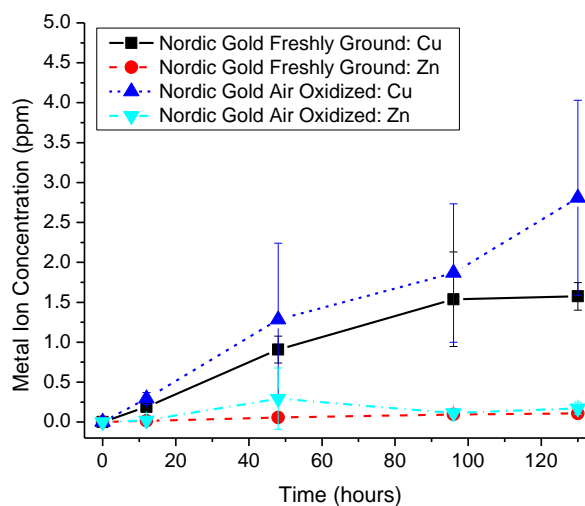


Figure 3.51. Metal ion concentration as a factor of time for Nordic Gold when freshly ground to 1200 grit or air oxidized at ambient lab conditions for 30 days, followed by exposure to concentrated synthetic perspiration solution (23 °C, ambient aeration) for various times, expressed as ppm in solution. No Al or Sn release was detected by ICP-OES from Nordic Gold. Data is the average of 3 replicates and error bars are one standard deviation.

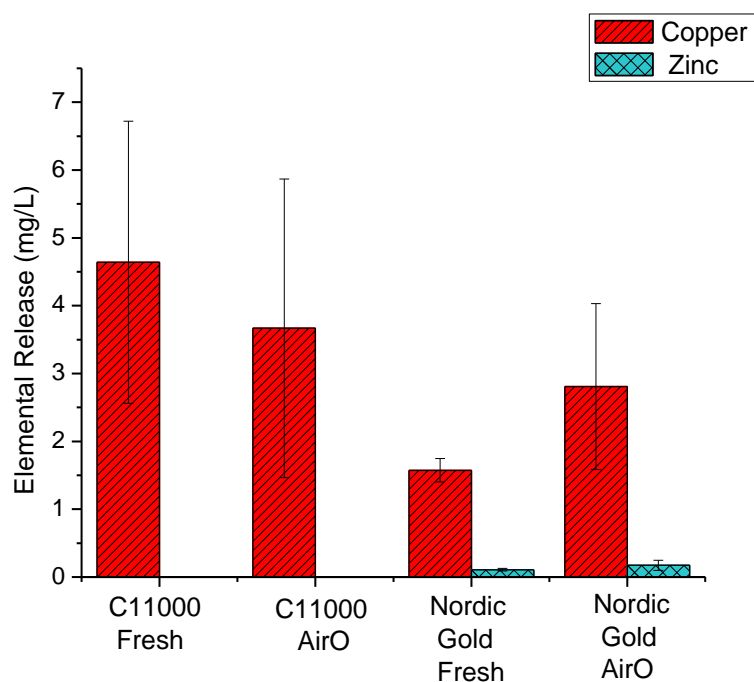


Figure 3.52. Metal concentration as a factor of time for C11000 and Nordic Gold when freshly ground to 1200 grit or air oxidized at ambient lab conditions for 30 days, followed by exposure to concentrated synthetic perspiration solution (23 °C, ambient aeration) for 130 hours, expressed as ppm in solution. No Al or Sn release was detected by ICP-OES from Nordic Gold.

3.5 Discussion

3.5.1 Summary of Findings

Ideally, the fate of copper can be tracked through the corrosion process of a copper alloy through charge transfer to the oxide, evaluated by galvanostatic reduction, and charge transfer to the solution, evaluated by ICP-OES, compared to total oxidation rate monitored by EIS and total oxidation charge based on mass loss with Cu^+ and Cu^{2+} . Figure 3.53a-b shows the charge analysis as a function of exposure time by EIS compared with charge by mass loss assuming equivalent weights for Cu^+ and Cu^{2+} seen in Table 3.3. It is likely that corrosion products are a mix of Cu^+ and Cu^{2+} , as seen by

GIXRD, rather than purely Cu^+ or Cu^{2+} as assumed in Table 3.8. Figure 3.53b includes both mass loss assuming congruent dissolution of all elements in Nordic Gold, and incongruent dissolution based on fractional analysis by ICP-OES, which shows better agreement. In all cases, the majority of the charge is transferred to solution, with C11000 having greater charge transfer to oxide than Nordic Gold. Figure 3.54 demonstrates the charge difference after 130 hours of exposure to concentrated synthetic perspiration solution (23 °C, ambient aeration) between Q_{corr} calculated by EIS and Q_{corr} calculation by the summation of oxide and solution analysis. The greatest difference is present in Nordic Gold samples, likely due to uncompensated effects of alloying additions on corrosion behavior. However, not all corrosion products are thought to be electrochemically connected and therefore not analyzed by galvanostatic reduction, such as copper chloride corrosion products that form by homogeneous precipitation (Table 3.6).

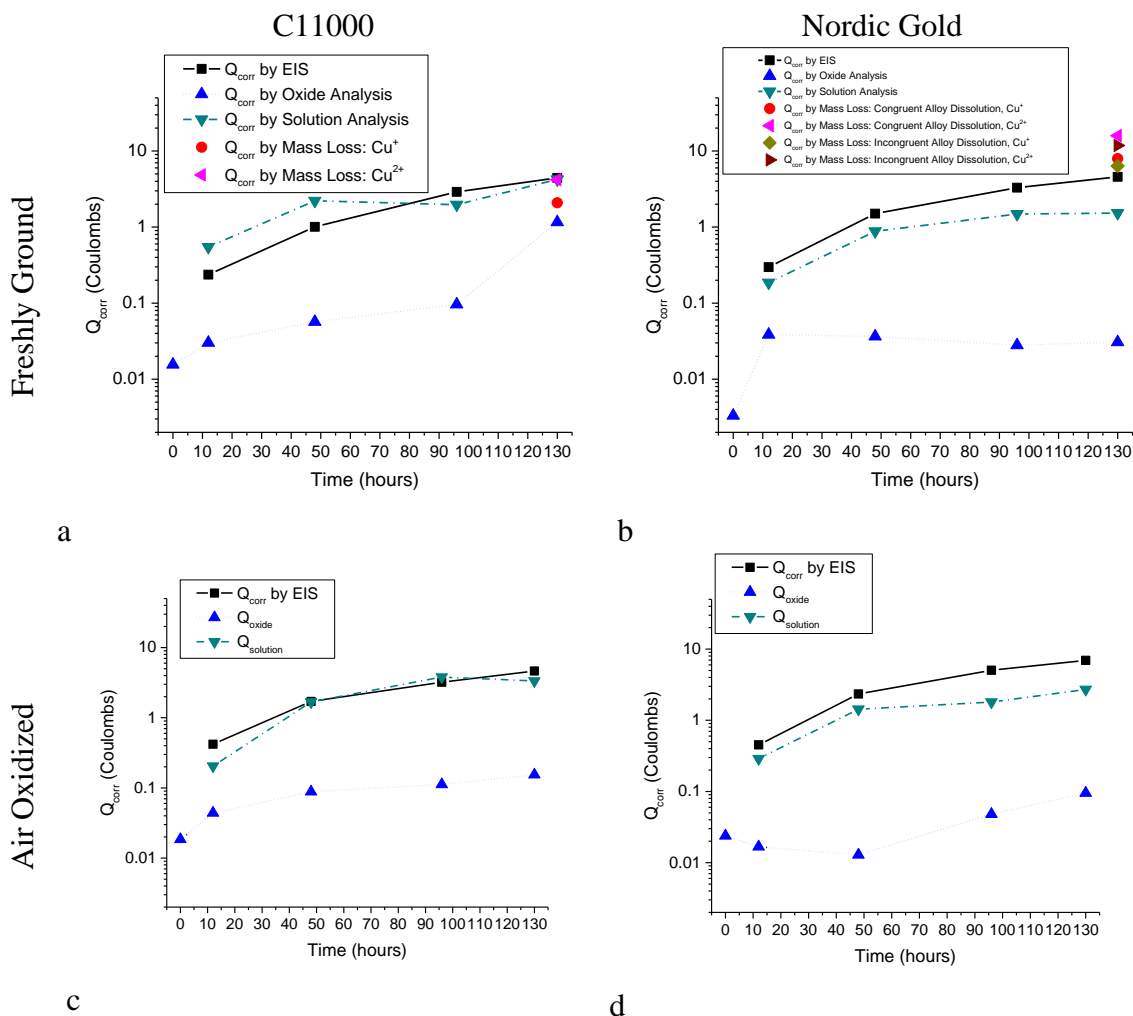


Figure 3.53. Charge analysis of C11000 and Nordic Gold when freshly ground to 1200 grit air oxidized at ambient lab conditions for 30 days, followed by exposure to concentrated synthetic perspiration solution (23 °C, ambient aeration) over time. Exposure area of working electrode (copper alloy) for EIS was 0.8 cm². Galvanostatic reductions were conducted at 0.02 mA/cm² on an area of 0.8 cm². Concentrated synthetic perspiration solution was exposed to 0.8 cm² of copper of the copper alloy coupon, with a surface to volume ratio of 2.67 cm²/L.

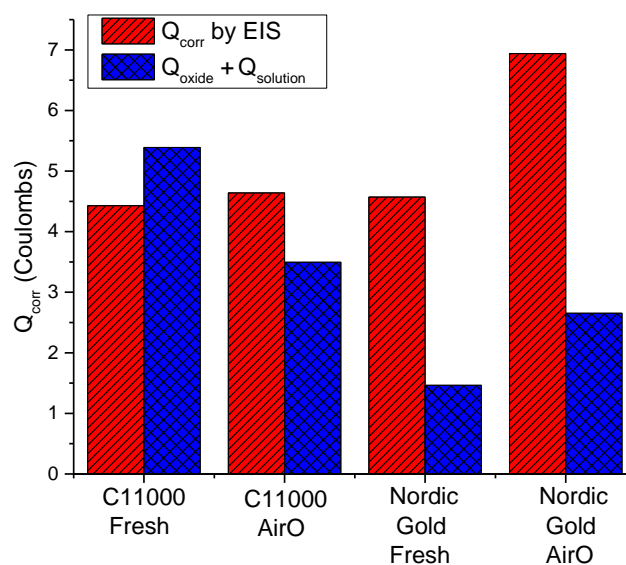


Figure 3.54. Charge comparison of Q_{corr} calculated from EIS versus ($Q_{\text{oxide}} + Q_{\text{solution}}$) of C11000 and Nordic Gold when freshly ground to 1200 grit air oxidized at ambient lab conditions for 30 days, followed by exposure to concentrated synthetic perspiration solution (23 °C, ambient aeration) over time. Exposure area of working electrode (copper alloy) for EIS was 0.8 cm². Galvanostatic reductions were conducted at 0.02 mA/cm² on an area of 0.8 cm². Concentrated synthetic perspiration solution was exposed to 0.8 cm² of copper of the copper alloy coupon, with a surface to volume ratio of 2.67 cm²/L.

3.5.1 Effect of Concentrated Synthetic Perspiration Solution on Corrosion Behavior compared to Normal Concentration Synthetic Perspiration Solution

It is well known that the environment (i.e. solution) effects corrosion behavior. An examination of copper alloys in concentrated synthetic perspiration solution to normal concentration synthetic perspiration solution indicates both a change in corrosion behavior and the fate of copper. As seen in Figure 3.55a, concentrated perspiration solution reduces the OCP of both copper alloys, indicating a stronger driving force towards oxidation in concentrated perspiration versus normal concentration perspiration. As seen in Figure 3.55b, there is also larger potential region of active behavior in

concentrated perspirations versus un-concentrated perspiration solution. Corrosion rate is dramatically altered in concentrated perspiration solution versus un-concentrated perspiration solution (Figure 3.56). Normal concentration perspiration solution results in a decrease in $1/R_p$ values over time. Concentrated perspiration solution results in a gradual increase in $1/R_p$, indicating more rapid corrosion behavior over time. The fate of copper in these two environments varies both in the amount incorporated into the oxide and the amount dissolved directly into solution. Concentrated perspiration solution results in thicker oxides compared to un-concentrated-perspiration solution, with the exception of C11000 when air oxidized (Figure 3.57). Additionally, a greater amount of copper was observed dissolved from both copper alloys in concentrated perspiration solution compared to un-concentrated perspiration solution. The overall effect of concentrated perspiration solution is a greater activity of copper when in concentrated perspiration solution compared to un-concentrated perspiration solution, as seen by an increasing corrosion rate over time, a thicker oxide and a greater dissolution of copper into the solution.

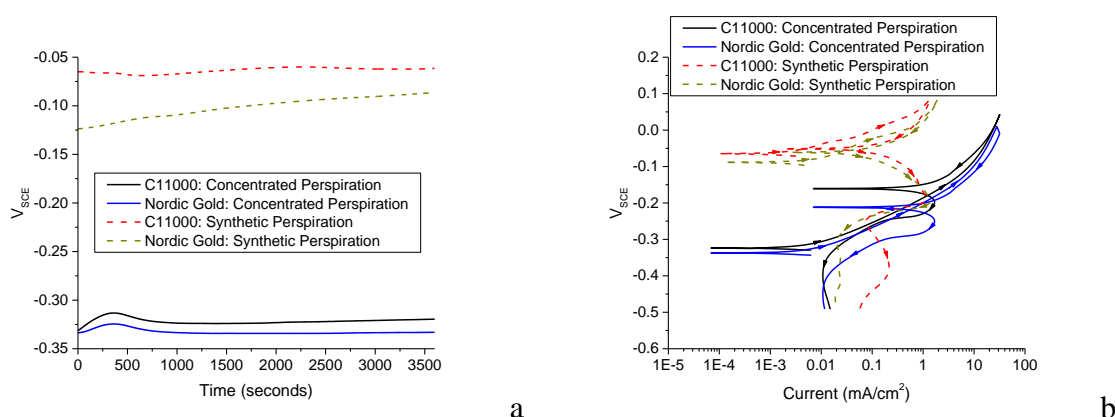
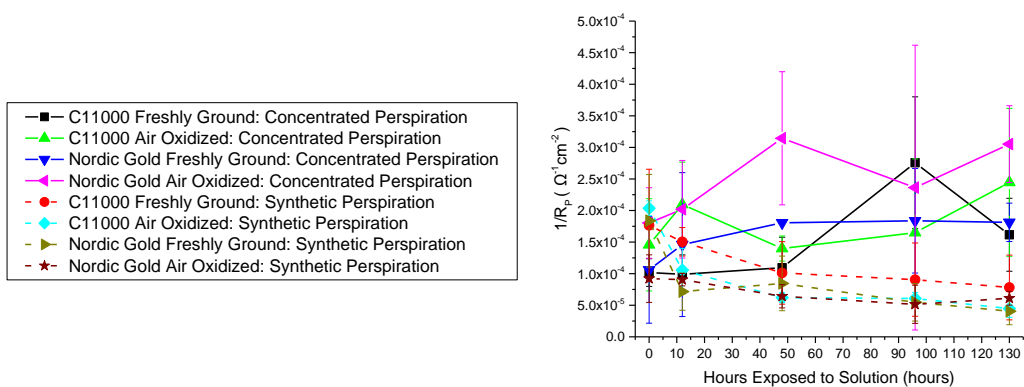


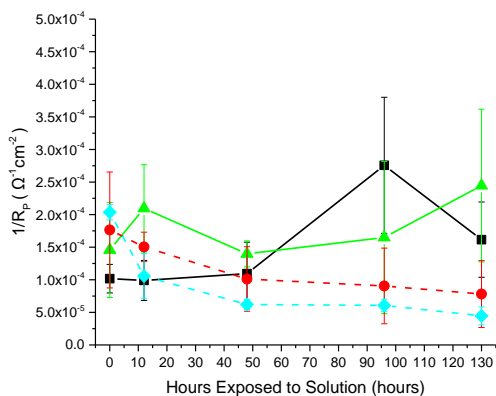
Figure 3.55. Comparison of OCP (a) and cyclic polarization (b) from C11000 and Nordic Gold when freshly ground to 1200 grit followed by exposure solution (23 °C, ambient aeration).



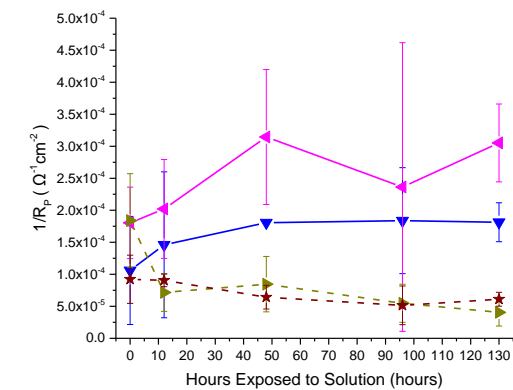
a

C11000

Nordic Gold

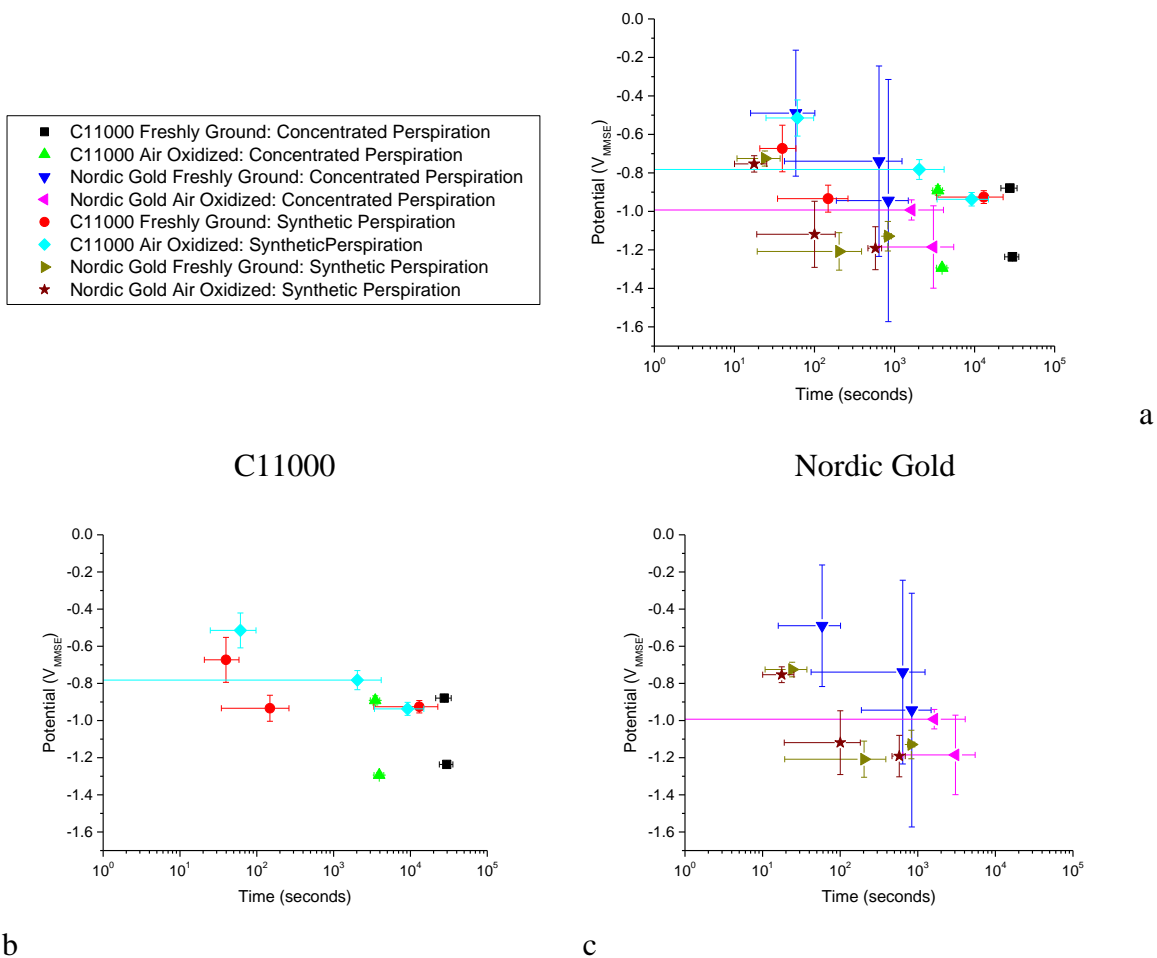


b



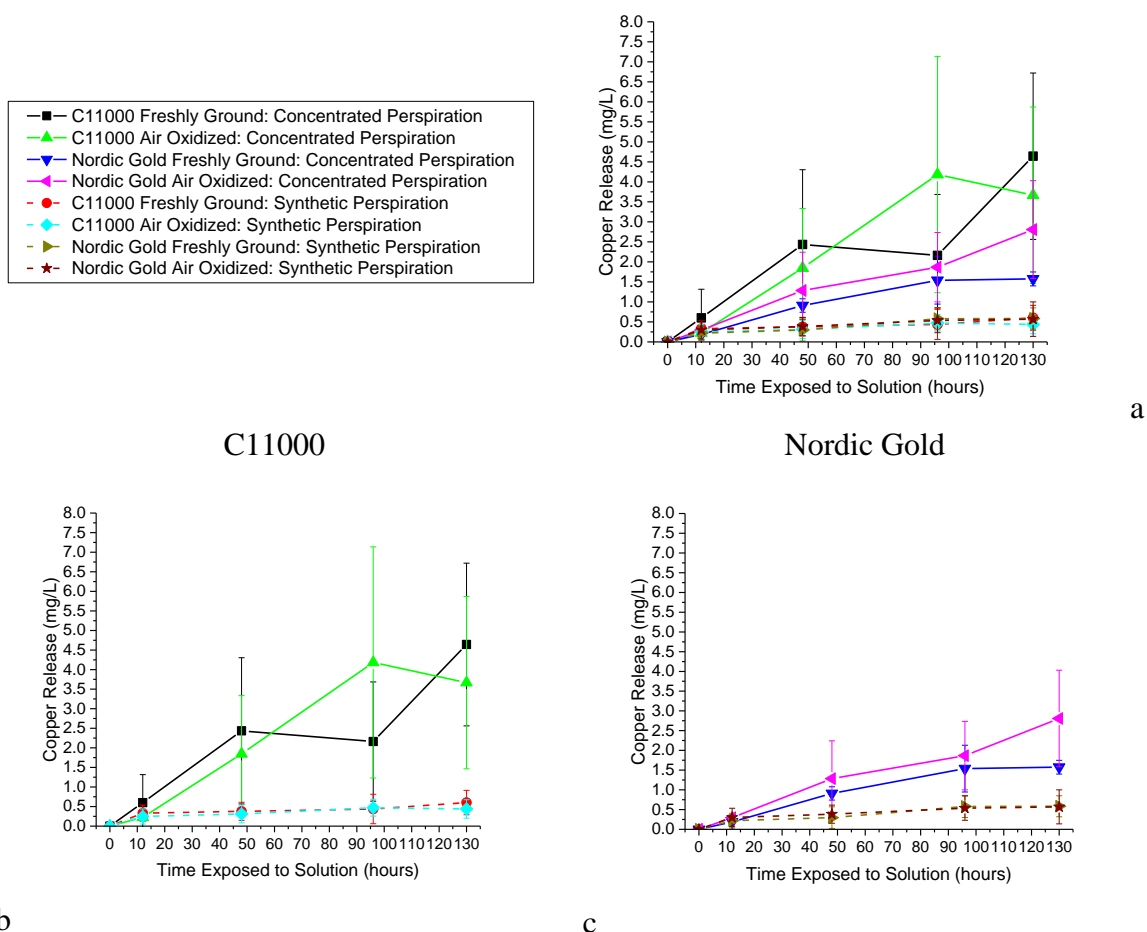
c

Figure 3.56 Comparison of corrosion rate from C11000 and Nordic Gold when freshly ground to 1200 grit or air oxidized at ambient lab conditions for 30 days, followed by exposure solution (23 °C, ambient aeration) over time. Figure a is a complete comparison, whereas figure b compares C11000 and figure c compares Nordic Gold. Data is the average of 3 replicates and error bars are one standard deviation.



b **c**

Figure 3.57 Comparison of galvanostatic reduction points (t_i, E_i) of C11000 and Nordic Gold when freshly ground to 1200 grit or air oxidized at ambient lab conditions for 30 days, followed by exposure to concentrated synthetic perspiration solution (23 °C, ambient aeration) for 130 hours. Galvanostatic reductions were conducted at 0.02 mA/cm² on an area of 0.8 cm². Figure a is a complete comparison, whereas figure b compares C11000 and figure c compares Nordic Gold. Data is the average of 3 replicates and error bars are one standard deviation.



b

c

Figure 3.58. Comparison of copper release from C11000 and Nordic Gold when freshly ground to 1200 grit or air oxidized at ambient lab conditions for 30 days, followed by exposure solution (23 °C, ambient aeration) over time, expressed as ppm in solution. Solution was exposed to 0.8 cm² of copper of the copper alloy coupon, with a surface to volume ratio of 2.67 cm²/L. Figure a is a complete comparison, whereas figure b compares C11000 and figure c compares Nordic Gold. Data is the average of 3 replicates and error bars are one standard deviation.

3.5.2 Effect of Zn, Al, and Sn Alloying Additions and Thin Oxides on Copper

Corrosion Electrochemistry in Concentrated Synthetic Perspiration

It is well known that alloy composition effects corrosion behavior.^{97,98} When exposed to concentrated perspiration solution, C11000 and Nordic Gold exhibit different corrosion behavior due to their different alloying composition. As seen in Figure 3.8, Nordic Gold exhibits a lower OCP than C11000 likely due to the additions of Zn and Al

in the alloys composition. Following 130 hours, Nordic Gold exhibited greater $1/R_p$ values than C11000, and greater mass loss, indicating a faster corrosion rate (Figure 3.19, Table 3.7). However, Nordic Gold maintained better reflectivity over time compared to C11000 (Figure 3.24). Oxide analysis techniques indicate Nordic Gold forms thinner oxides, as suggested by GIXRD in Figures 3.28-3.29 and galvanostatic reduction in Figures 3.40-3.43. As seen in Figure 3.53, charge transfer to the oxide is minimal compared to charge transfer to the solution. The sum of the charge transfer to solution and oxide in C11000 is close to that determined by EIS, while the sum of solution and oxide for Nordic Gold is significantly less than determined by EIS. There is likely precipitation by homogeneous chemical reaction that is not accounted for fully by galvanostatic reduction.

While the effects of environment (i.e. solution) and alloy composition have frequently been explored, little is known regarding the effects of thin oxides on corrosion behavior, such as those developed from extended lab air exposure. The presence of thin, air formed oxides on Nordic Gold and C11000 prior to exposure to concentrated synthetic perspiration does not alter the consistent increase in $1/R_p$ values in both alloys over time periods when they were exposed to concentrated synthetic perspiration solution (Figure 3.19, Table 3.7). The appearance of the copper alloys was altered by air oxidation, as seen in a slower decrease in reflectivity and a change in coloration compared to their freshly ground counterparts (Figures 3.20-3.24). After 130 hours in concentrated synthetic perspiration, C11000 developed a white surface film (Figure 3.20), while Nordic Gold became more yellow compared to the freshly ground Nordic Gold's gold appearance (Figure 3.21). These aesthetic differences are likely the result of

different corrosion product formations on air oxidized alloys versus freshly ground alloys with overall color determined by alloying additions in the alloy, as well as corrosion product roughness and identity. As seen in Figures 3.30-3.33, GIXRD suggests that air oxidized alloys exhibit a copper-chloride corrosion product, suspected to be $\text{Cu}_2(\text{OH})_3\text{Cl}$, which does not appear on freshly ground alloys. Figure 3.34 indicates that a greater variety of corrosion products, assumed to be copper-chlorides, are observed on alloys that have thin air formed oxides present before exposure to concentrated perspiration solution (Figure 3.33), compared to freshly ground alloys which only exhibit CuO and Cu_2O (Figure 3.32). The combination of a greater corrosion rate, differing aesthetic properties and a greater variety of observed corrosion products suggest the presence of thin oxides on copper alloys exposed to concentrated synthetic perspiration solution results in more aggressive corrosion behavior.

3.5.3 Effect of Zn, Al, and Sn Alloying Additions and Thin Oxides on Metal Release Rate in Concentrated Synthetic Perspiration

An evaluation of copper release enables the correlation between corrosion behavior and antimicrobial function of copper alloy surfaces. While individual and/or selected alloying elements (Zn, Sn) have been examined for their effect on copper release³, the complex effect of multiple alloying additions that have opposing suppressing and enhancing effects has not. As seen in Figures 3.45-3.50, C11000 releases more copper into solution than Nordic Gold. However, despite the presence of Zn, Al and Sn in Nordic Gold, only Zn is released into solution in any measurable amount besides Cu. The fraction of Cu compared to Zn released into solution is greater than 90/10, averaging at 92% Cu: 8% Zn metal release compared to the 89% Cu, 5% Zn, 5% Al and 1% Sn alloy

composition. As seen in Figure 3.53, the majority of charge is transferred directly to solution, with a strong correlation between Q_{corr} based on EIS and Q_{corr} based on oxide and solution analysis for C11000 (Figure 3.54). However, corrosion products precipitated on the alloy surface by homogeneous chemical reaction may not be electrically connected, and therefore not indexed by galvanostatic reduction.

In order to relate copper release to antimicrobial efficacy, an evaluation of total copper release from alloys compared to copper content necessary to kill microorganisms is necessary. While previous testing of Nordic gold's antimicrobial efficacy indicated that the presence of thin oxides formed by air inhibited antimicrobial activity, assumed to be a function of copper ion release², the presence of air formed oxides on C11000 and Nordic Gold during corrosion in concentrated perspiration solution enhance copper release (Figures 3.45-3.50). Assuming linear release rates, as seen in Figure 3.59 and Table 3.9, both C11000 and Nordic Gold in the presence of thin air formed oxides surpass 1 ppm Cu release within 2 days, and 10 ppm within 13 and 21 respectively. Figure 3.60 shows the results disinfection "kill curves" performed at the University of Virginia to observe the relative effectiveness of copper ions (Cu^{2+}) at varying concentrations on killing *E. coli* (HCB1) in synthetic perspiration, and enumerated by the most probable number (MPN) method utilizing Colilert® and Quanti-Trays® (Idexx). *E. coli* (HCB1) was obtained from Howard C. Berg at Harvard University. At concentrations above 0.1 ppm Cu^{2+} , such as 1, 10, or 100 ppm, *E. coli* (HCB1) populations dropped faster than natural die off, indicating antimicrobial activity. While not conducted in concentrated perspiration solution, this study can be used as a point of reference that relates rate of die off to copper ion concentration. Therefore, by relating the necessary quantity of Cu^{2+} to kill *E. coli*

(HCB1) to copper release from Nordic Gold and C11000, it is evident that both alloys release sufficient copper within just the first 12 hours to kill *E. coli* (HCB1) before natural die off in normal concentration synthetic perspiration (Figure 3.45). Additionally, C11000 both when freshly ground and air oxidized, and Nordic Gold when air oxidized, could significantly reduce bacteria within less than 2 days, as they reach concentrations greater than 1 ppm Cu.

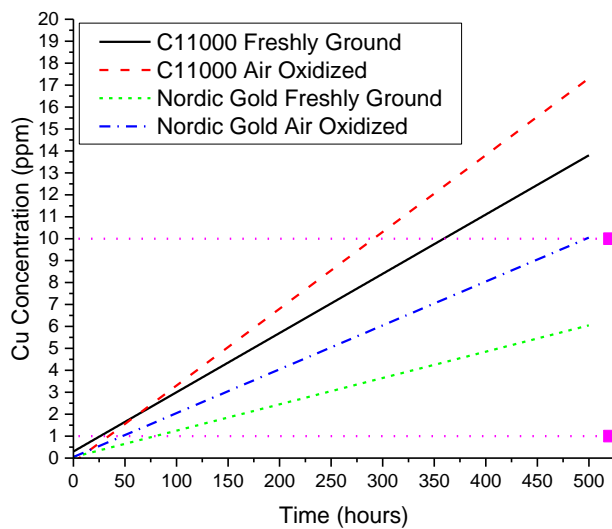


Figure 3.59. Correlation of constant copper release rates from copper alloys to time needed to achieve 1 and 10 ppm Cu^{2+} at a surface to volume ratio of $2.67 \text{ cm}^2/\text{L}$.

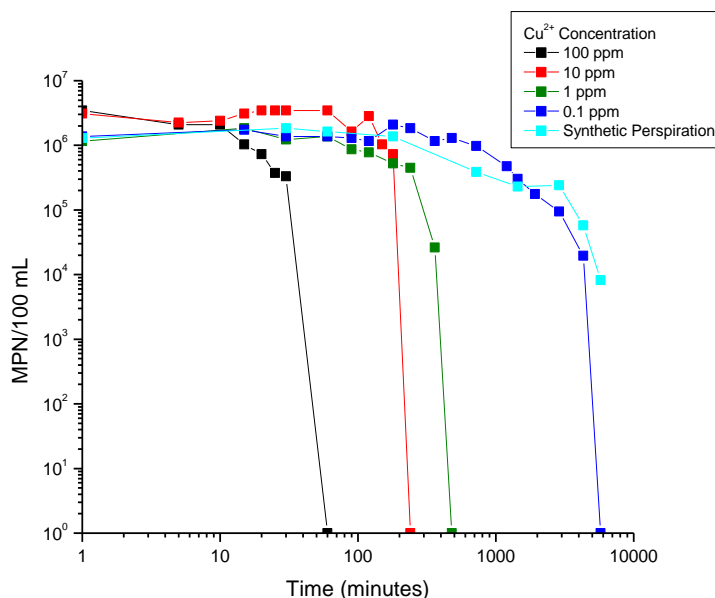


Figure 3.60. University of Virginia disinfection studies of *E. coli* (HCB1) in solution of synthetic perspiration (0.5% NaCl, 0.1% CH₄N₂O, 0.1% C₃H₆O₃, pH 6.5) and Cu²⁺ ions from a CuCl₂ solution at 23 °C, enumerated by most probable number (MPN) method.

Table 3.9. Analysis of constant copper release rates to determine lengths of time needed to achieve antimicrobial copper concentration.

Alloy: Treatment	Concentration (ppm)		
	1	10	100
	Days Needed to Achieve Concentration Based on Constant Release Rates		
C11000: Freshly Ground	2	15	154
C11000: Air Oxidized	2	13	120
Nordic Gold: Freshly Ground	4	35	348
Nordic Gold: Air Oxidized	2	21	209

3.6 Conclusion

For use as hospital high touch surfaces, copper alloys must exhibit an antimicrobial robustness against passivation due to long term air exposure, with well understood corrosion behavior under concentration build-up that may occur due to drying or repeated contamination. While previous studies by the CDA have only analyzed the

empirical survivability of bacteria on the alloy surface in a nutrient broth solution, and previous studies have explored the effects of synthetic perspiration solution on copper alloy corrosion behavior, this series of studies successfully identified the effects of Nordic Gold alloying and thin air formed oxides versus freshly abraded surfaces on corrosion behavior in a concentrated synthetic perspiration solution. Corrosion behavior is a factor of both alloy solid solution composition and the presence or lack of thin oxides. In concentrated synthetic perspiration, both C11000 and Nordic Gold demonstrated increasing $1/R_p$ values suggestive of increasing corrosion rate over time, where Nordic Gold and the presence of thin air formed oxides resulted in a greater increase in i_{corr} . The presence of thin, air formed oxides also resulted in a larger variety of corrosion products, including $Cu_2(OH)_3Cl$ compared to freshly ground alloys where only CuO and Cu_2O were detected. As compared to normal concentration synthetic perspiration where Cu release was similar between copper alloys both when ground and air oxidized, exposure to concentrated synthetic perspiration resulted in less Cu release from Nordic Gold compared to C11000, but an enhanced Cu release in air oxidized samples. Based on the Cu concentrations measured, it is suspected that both alloys would provide sufficient Cu^{2+} necessary to kill *E. coli* (HCB1) before its natural die off, especially in the case of air oxidation.

4 The Fate of Copper during Corrosion of Nordic Gold (89% Cu, 5% Zn, 5% Al, 1% Sn) vs. C11000 (>99.9% Cu) in Synthetic Perspiration Droplets during Wetting and Drying Cycles

4.1 Abstract

The goals of this study is to understand tarnishing, copper release and color stability of a Cu-Al-Zn-Sn alloy (Nordic Gold) when deposited with a droplet of synthetic perspiration (approximately 0.8 cm^2) designed to mimic the effects of hand perspiration transfer and subsequent drying on a copper surface, compared to commercially pure copper, C11000. Previously, no studies have examined the effect of repeated drying-wetting on the alloy's corrosion behavior and copper ion release, as it relates to antimicrobial efficacy. 100 μL droplets of synthetic perspiration were dried by drierite treated lab air (4 hours) and re-wet with water-saturated lab air (4 hours) for total of 12 dry-wet cycles. This was done by tracking the "fate of copper" through the corrosion process by analysis of total copper oxidation, electrochemical analysis of the oxide layer formed, and solution analysis of dissolved copper.

Corrosion behavior as a result of synthetic perspiration deposition and subsequent drying and wetting was determined to be strongly dependent on alloy composition. Despite Al and Sn alloying additions, Nordic Gold was observed to have similar i_{corr} compared to C11000. Evidence of directly formed oxides CuO and Cu₂O, as well as reprecipitated Cu₂(OH)₃Cl and Cu₂(OH)₂CO₃, were observed on both alloys. Nordic Gold resulted in thinner, compact directly formed oxide layers (CuO and Cu₂O), and less precipitated corrosion products formed by homogeneous chemical reaction (Cu₂(OH)₃Cl and Cu₂(OH)₂CO₃) compared to C11000. However, the concentration of Cu ions in the

droplets on Nordic Gold was greater than C11000 at early times due to compact oxides and similar i_{corr} . After 12 cycles, Cu ion concentration of both alloys was comparable, and suggesting similar antimicrobial efficacy when exposed to droplets of synthetic perspiration solution and allowed to dry and rewet. Based on the Cu concentrations measured, it is suspected that both alloys would provide sufficient Cu release necessary to kill *E. coli* (HCB1) observed in lab testing spiked with Cu^{2+} before its natural die off. This determination is based on the comparison of critical Cu concentrations to measured Cu ion release rates.

4.2 Introduction

Due to the rising number of hospital acquired infections in recent years, significant research has explored exploiting copper alloys for their inherent antimicrobial nature to replace high touch surfaces. Current standards to evaluate antimicrobial copper reply only on empirically bacteria viability, and offers no insight into the exact role of corrosion on copper ion release responsible for antimicrobial behavior nor the critical Cu^+ or Cu^{2+} concentration required to serve in this function. Additionally, Environmental Protection Agency qualifications for antimicrobial copper alloys are based on the corrosion of the copper alloy in a nutrient broth ideal for growing bacteria⁴⁹⁻⁵¹, rather than on the medium that would naturally facilitate the alloys corrosion in a hospital environment. The likely relevant environment on high touch surfaces is hand perspiration.^{112,113} Additionally, the effect of wetting and drying cycles that would naturally occur in the environment on the chemistry of surfaces containing perspiration has not been investigated. Therefore, a link has not been established between a cyclic wet/dry corrosive environment and antimicrobial behavior.

As antimicrobial behavior in copper alloys has been established to a result of microorganism's interaction with copper ions, there is a direct correlation between antimicrobial efficacy and corrosion to supply Cu ions. During the corrosion process, copper ions can become part of one of several "fates" as a result of metal oxidation. These include retention of the metal oxide at the interface during incongruent dissolution¹¹⁴, dissolution into the solution¹¹⁵, selective leaching or dealloying of other elements¹¹⁶, dissolution into the solution followed by precipitation on the surface of the oxide as an insoluble corrosion product¹¹⁷ or complexation with species in the environment. Only those copper ions that are dissolved into the solution are responsible for antimicrobial behavior. Moreover, those ions that become part of an oxide may be sequestered.

Nordic Gold (89% Cu, 5% Zn, 5% Al, 1% Sn) is an fcc solid solution alloy that has been examined by several research groups as a possible antimicrobial material due to its high copper content.¹⁰⁶⁻¹⁰⁸ Additionally, due to its development as an alloy for European coinage, Nordic Gold is also tarnish resistant in perspiration¹⁰⁵, which in combination with its high copper content makes it an attractive prospect for hospital applications where both antimicrobial efficacy and non-tarnishing visual appeal are desired.¹¹¹ Previous work (Chapter 2) indicates that Nordic Gold releases comparable amounts of Cu ions to C11000 in synthetic perspiration full immersion studies, but releases less than C11000 in concentrated synthetic perspiration full immersion studies, designed to mimic concentration just before complete drying on a surface. This finding was observed whether surfaces were ground or covered by thin air formed oxides due to prolonged exposure in lab air. This is in disagreement with empirical evidence found by

the Copper Development Association that suggest Nordic Gold passivates completely in the presence of thin air formed oxides, and has no antimicrobial efficacy when air oxidized in lab air for 7 days.² However, these studies were conducted in a bacteria nutrient broth such as tryptone soy broth, rather than synthetic perspiration.

Previous electrochemical studies at the University of Virginia that included Nordic Gold (89% Cu, 5% Zn, 5% Al, 1% Sn) as an alloy of interest determined that the unique combination of alloying elements resulted in unexpected corrosion behavior.¹¹⁹ Alloys containing zinc were observed to have a lower corrosion rate compared to other zinc-free alloys examined¹¹⁹, and studies by Goidanich indicate that the presence of zinc in an alloy decreases the copper ion release.³ Goidanich also reported that copper alloys containing Sn released similar amounts of Cu to commercially pure copper sheets, despite having stoichiometrically less copper content, indicating additions of Sn enhance copper release from an alloy.³ The unique combination of both alloying additions that suppress corrosion rate (Zn) and enhance copper release (Sn) in Nordic Gold result in a unique alloy composition that may have the ability to both be antimicrobial while maintaining relatively low corrosion over time.

However, these results likely depend on environmental severity and environment composition. In applications as antimicrobial high touch surfaces, copper alloys will rely on the perspiration transferred by handling to facilitate the copper ion release necessary for antimicrobial activity.^{112,113} Studies have reported that primary constituents of human perspiration to be salt (NaCl), potassium (K), lactic acid (C₃H₆O₃), and nitrogen containing compounds such as urea (CH₄N₂O), ammonia (NH₃), amino acids, uric acid (C₅H₄N₄O₃), and creatinine (C₄H₇N₃O).¹³⁰ Additionally, calcium (Ca) and magnesium

(Mg) are present, and phosphorous (P), copper (Cu) and manganese (Mn), iron (Fe), iodine (I), fluorine (F) and bromine (Br) in trace amounts have been reported.¹³⁰ Typical pH values range 4-6.8.¹³⁰ The exact composition is highly dependent on the individual, including gender, environmental heat stress, and diet. A variety of synthetic perspiration solutions have been utilized in research, varying in composition and pH (Table 4.1). Based on the chemistry of perspiration, a handled object will be deposited with the full chemical composition of the perspiration, but over time will retain only those chemicals whose vapor pressure less than water, such as NaCl, urea and lactic acid, while those with a greater vapor pressure will be evaporated, such as ammonia. Therefore, the composition of the dried perspiration droplet can differ from the composition of the initially deposited perspiration droplet.

Table 4.1. Composition of synthetic perspiration solutions used in previous exposure studies	
Composition (by mass percentage)	pH
0.87% NaCl, 0.16% CH ₄ N ₂ O, 10.92% C ₃ H ₅ NaO ₃ (60%), 0.016% Na ₂ HPO ₄	7.5 ⁸²
1.96% NaCl, 0.49% CH ₄ N ₂ O, 1.39% C ₃ H ₆ O ₃ , 0.25% C ₂ H ₄ O ₂ , 1.71% NH ₄ Cl	4.7 ⁸³
0.5% NaCl, 0.1% CH ₄ N ₂ O, 0.1% C ₃ H ₆ O ₃	6.5 ^{63,84,85}
0.3% NaCl, 0.1% Na ₂ SO ₄ , 0.2% CH ₄ N ₂ O, 0.2% C ₃ H ₆ O ₃	6.6 or 4.5 ⁸⁶
0.5% NaCl, 0.1% CH ₄ N ₂ O, 0.5% C ₃ H ₆ O ₃	5 ⁸⁷
0.5% NaCl, 0.1% CH ₄ N ₂ O, 0.1% C ₃ H ₆ O ₃	4.5 ⁸⁸

The composition of each salt of the electrolyte is governed by the attainment of a concentration in equilibrium with a particular relative humidity (RH). The thickness of the electrolyte will be partially determined by the RH, as well as by the presence of particulate on the surface. At 20% RH, one monolayer of water is stable along clean surfaces, increasing at 75% RH to ~5 monolayers.¹³¹ The behavior of atmospheric corrosion above 3 monolayers of water are similar to those of bulk water.¹³² In high RH

circumstances, invisible water clusters and water film develop along the surface, resulting in local anode and cathodes that enhance the corrosion process.¹³³ However, if salt particles exist along the metallic surface, a thicker water film can form compared to a clean surface.¹³³ The thickening of the water film results in the ionic connection of spatially separated anodes and cathodes.¹³³ Thicker water films will exist at the points of wetting and connected by thinner layers across the surface.¹³² Electrolyte thickness adjustment phenomenon has several effects on metal corrosion, including concentration build-up, increase in metal ion concentration and passivation.¹³⁶ Concentration build-up causes reduced solubility of oxygen.¹³⁶ It also causes supersaturation of ions and can result in corrosion product formation due to solubility limits.^{136,137} The concentration build-up by drying on carbon steel has resulted in a reduced corrosion rate when the corrosion reaction is controlled by cathodic oxygen reduction, but increases corrosion rate when the corrosion reaction is controlled by anodic dissolution processes.¹³⁶ In Figure 4.1, it is evident that the greatest oxygen reduction current density is accomplished at the transition from “wet” conditions to “dry” conditions in an iron sample, a trend that is expected to be true also in the case of copper.¹³⁴ Concentration build-up during drying results in the thin electrolyte becoming supersaturated with the salts, causing precipitation and possibly drying.^{134,135} Thus, a salt deposit may be present on the surface, in the presence of a thin electrolyte layer dictated by RH. When perspiration is deposited on a surface, the RH of the environment determines whether the area continues to wet the surface in the case of high RH, or begins to evaporate in the case of low RH.¹³² The critical RH, called the deliquescence point, determines the behavior of the solution due to its constituents. At the deliquescence point, the salt fully saturates the water droplets

formed. At RH above the deliquescence point, the compound is considered in solution, due to the accumulation of water from the atmosphere.¹³² Additionally micro-droplets have been observed to form around the deliquescence formed droplet, which occurred at RH greater than the deliquescence point in the presence of oxygen.^{133,148} These micro-droplets are composed to hydroxyl ions formed by oxygen reduction, water accumulated from the atmosphere, and cations that migrate from the main droplet, but no anions from the main droplet.^{133,148} The cathodic reaction results in highly alkaline conditions within these droplets.¹⁴⁹ Water migration from the main droplet and water absorption from the surrounding environment occurs in attempt to decrease the pH in the micro-droplets, thus resulting in a spreading effect away from the main droplet.¹⁴⁹ These factors may affect the corrosion of Cu and Cu alloys in droplets.

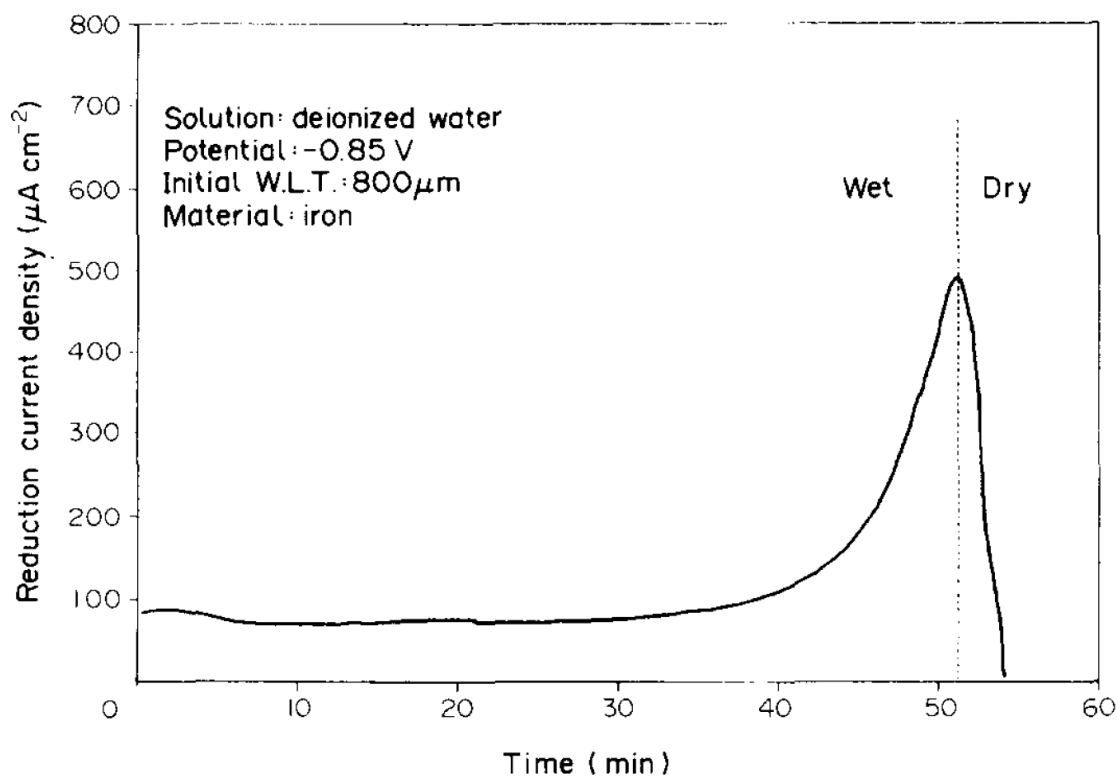


Figure 4.1. Change of oxygen reduction current with the change of the thickness of water layer indicated by the time spent to heat the iron sample.¹³⁴

Atmospheric corrosion of copper is also known to be influenced by gaseous species, specifically CO_2 and SO_2 . Thin layers of water that form along the copper surface at ambient air conditions enable gaseous species to dissolve into the water film. The identity and concentration of the gaseous species can affect corrosion behavior. A study by Leygraf states that in the presence of CO_2 , NaCl-induced atmospheric corrosion depends on NaCl concentration at ambient levels of CO_2 , where lower density of NaCl ($<15 \mu\text{g}/\text{cm}^2$) experience inhibited corrosion and higher density of NaCl ($>15 \mu\text{g}/\text{cm}^2$) experience increased corrosion behavior in the presence of CO_2 .¹⁵⁰ CO_2 levels also dictate the degree of secondary spreading, where low CO_2 levels ($<1-5 \text{ ppm}$) resulted in larger spreading areas compared to ambient CO_2 levels (350 ppm) (Figure 4.2).^{150,151} This is attributed to carbonate formations in ambient CO_2 conditions, resulting in a lowering of the pH in the spreading area, thus increasing surface tension of the oxide and inhibiting spreading.¹⁵¹ However, at low CO_2 levels ($<5 \text{ ppm}$) and in the presence of SO_2 (15 ppb), the larger secondary spreading area was not observed, attributed to the pH lowering effect of SO_2 .¹⁵² The effect of CO_2 on the pH of the droplet strongly determines the formation of corrosion products. At low CO_2 levels, pH values are higher and enable the formation of Cu_2O , CuO , $\text{Cu}_2(\text{OH})_3\text{Cl}$, $\text{Cu}(\text{OH})_2$ and CO_3^{2-} (Figure 4.2).¹⁵⁰ Ambient levels of CO_2 result in lower pH values and the formation of Cu_2O , $\text{Cu}_2(\text{OH})_2\text{CO}_3$, $\text{Cu}_2(\text{OH})_3\text{Cl}$, and CO_3^{2-} .¹⁵⁰ The presence of CuO in low CO_2 environments provides a protective layer, and a lower corrosion rate.¹⁵⁰ These factors should be considered during cyclic wetting/drying corrosion of commercially pure C11000 and Nordic Gold.

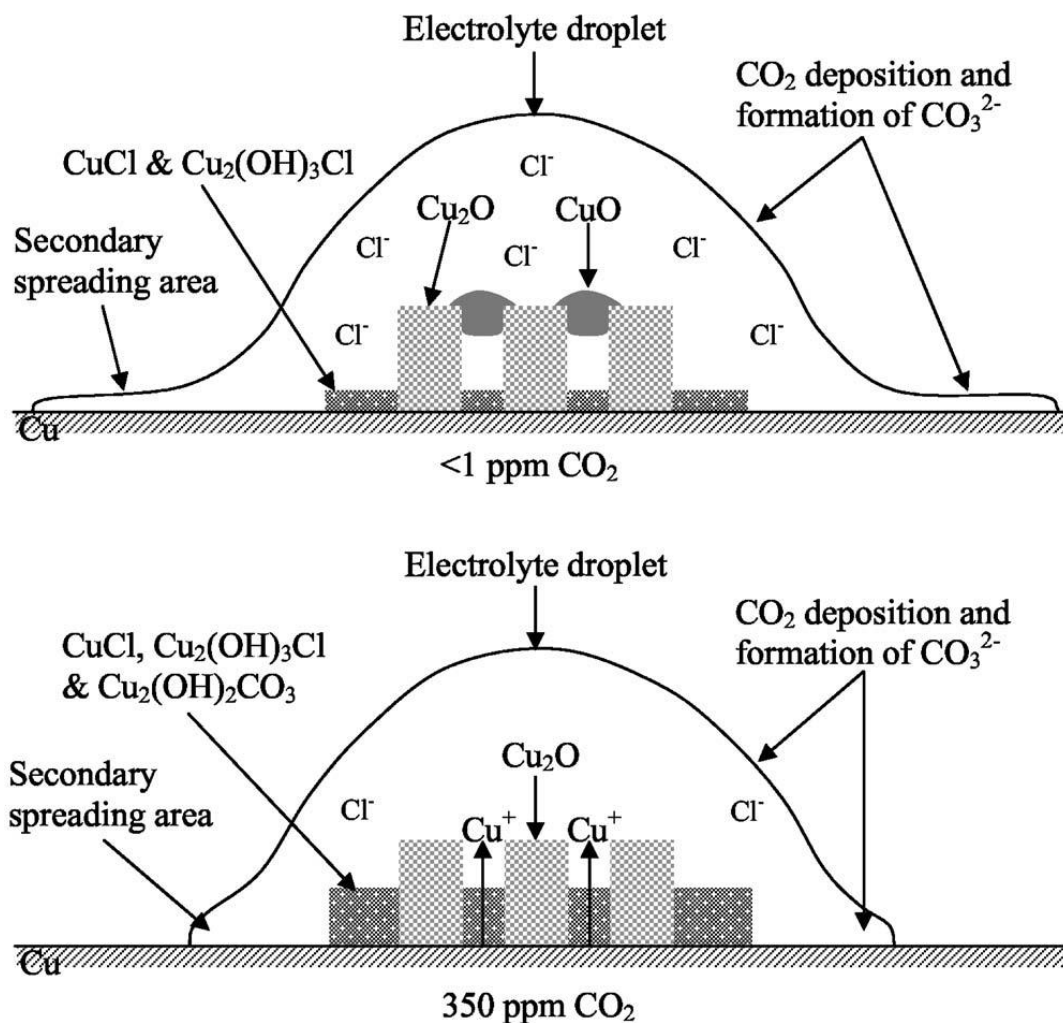


Figure 4.2. Schematic illustration of corrosion product layer formation during copper exposure to CO₂ at low (<1 ppm) and ambient (350 ppm) levels.¹⁵⁰

The objective of this study is to determine the corrosion behavior of Nordic Gold (89% Cu, 5% Zn, 5% Al, 1% Sn) compared to C11000 (>99.9% Cu) during wetting and drying cycling of synthetic perspiration deposited on the surface of the alloy in ambient atmosphere. Tarnishing and the fate of copper through the corrosion process in perspiration will be tracked through analysis of oxides formed during exposure to synthetic perspiration solution, assessed by optical spectrophotometry, grazing incidence x-ray diffraction, galvanostatic reduction, and copper ion release assessed by inductively

coupled plasma-optical emission spectrometry. This study will ultimately provide a link between corrosion behavior and antimicrobial efficacy in an applications based situation, where perspiration may be deposited on copper high touch surface and undergo multiple wetting and drying cycles.

4.3 Experimental Procedure

4.3.1 Sample Preparations

C11000 (>99.9% Cu) and Nordic Gold (89% Cu, 5% Zn, 5% Al, 1% Sn) were obtained as sheets from the Copper Development association and cut in house into 2.5 x 2.5 cm coupons. All C11000 (>99.9% Cu) and Nordic Gold (89% Cu, 5% Zn, 5% Al, 1% Sn) coupons were ground using silicon carbide (SiC) metallography paper to successively finer grits up to 1200 grit. Immediately following grinding, coupons were placed in methanol to minimize oxidation until just before testing. Samples were dried of methanol by compress air.

4.3.2 Exposure Solution and Setup

A synthetic perspiration solution was made based on standard BS EN 1811:2011⁸⁴. Synthetic perspiration was prepared using purified water (resistivity 18.2 M Ω -cm) produced by an Academic MilliQ filtration system (MilliPore) and reagent grade chemicals was used to dissolve 5 g/L NaCl (Sigma-Aldrich), 1 g/L Urea (CH₄N₂O) (Fisher Scientific), and 1 g/L Lactic Acid (C₃H₆O₃) (90%, Acros Organics), and the pH adjusted by addition of ammonium hydroxide (NH₄OH) (Fisher Scientific) to 6.5 (\pm 0.05) (Table 4.2). Synthetic perspiration solution was used at ambient aeration at 23 °C within 24 hours of preparation. The bulk solution was stable at pH 6.5.

Chemical	Molecular Weight	Concentration (g/L)	Molarity (M)
NaCl	58.44	5	0.08556
CH ₄ N ₂ O	60.06	1	0.01665
C ₃ H ₆ O ₃	90.08	1	0.00999

Samples were placed in a custom-built chamber with a programmable wetting-drying sequence. The setup was constructed with sealed chamber, a wet system, a dry system, two solenoid valves, and a programmable switch. In dry cycles, lab air was dried using a drierite column while for wet cycles, lab air was saturated with deionized water before being injected into the chamber. The relative humidity during these cycles was recorded, and a sample segment can be seen in Figure 4.3. The switch was programmed to execute 8 hour cycles, where each cycle was comprised by one 4 hour dry cycle and one 4 hour wet cycle. More information regarding the automated wet/dry cycle system can be found elsewhere.¹⁵³ Samples were deposited with 100 μ L of synthetic perspiration solution by volumetric pipette (0.6-1.8% accuracy)^{xxv}. Droplet was formed with minimal surface area in order to maximize salt density, with an area approximating 0.8 cm². Exact droplet size was not measured, and spreading was governed by the surface energy of the Cu alloy sample. Samples were removed from the chamber <5 minutes before the end of the final wetting cycle in order to collect a sample of the thin electrolyte for Cu content by solution analysis. Copper alloys were washed with 10 mL of synthetic perspiration, and dried with compressed air. Samples were stored in a desiccator fixed at 30% RH until corrosion product analysis.

^{xxv} The re-wetting volume of the droplet is not known.

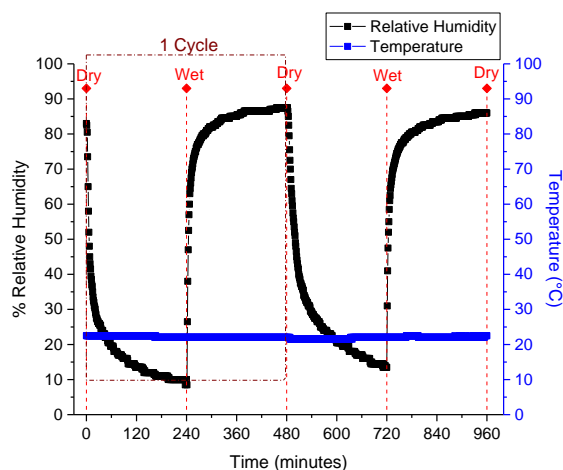


Figure 4.3. Relative humidity and temperature was collected throughout drying and wetting cycles, and a sample portion is displayed here. As seen, temperature remains steady at 22 C, while RH varies depending on the cycle position.

4.3.3 Corrosion Rate: Mass Loss by Gravimetric Analysis

Mass loss was conducted in accordance with ASTM G1-03. Baseline mass loss was conducted on freshly ground (1200 grit) copper alloy samples, preserved in methanol. Copper alloys masses were obtained by an analytical balance (M-220D, Denver Instrument) after freshly ground (1200 grit, preserved in methanol) and after 12 dry-wet cycles exposed to a synthetic perspiration droplet and dried with compressed air. Corrosion products were removed by exposing the corroded surface to 6 M HCl for 3 minutes at ambient lab temperature, washing with Millipore water and drying with compressed air. Mass changes were obtained before and after cleaning on the same instrument. Freshly ground copper alloy mass loss was utilized as a baseline measurement to determine the effect of corrosion product removal on the bare metal. The effect of cleaning was established to cause negligible dissolution of the metallic alloy, with no mass loss occurring in Nordic Gold before and after cleaning, and 0.1 mg/cm² mass loss occurring in C11000. Mass loss (Δm) was equated to charge (Q_{corr}) utilizing

Equation 4.1, where F is Faraday's constant (96500 C/equivalent), and $E.W.$ is equivalent weight (g/equiv.). Equivalent weights were calculated for both Cu^+ and Cu^{2+} for comparison, as shown in Equation 4.2, where f is the weight fraction of alloying elements, n is the number of equivalent electrons exchanged (equiv./mol), and a is atomic weight of each element in the alloy. The $E.W.$ for C11000 was defined as 63.546 g/equiv. (Cu^+) or 31.773 g/equiv. (Cu^{2+}). Table 4.3 defines calculations for $E.W.$ for an alloy such as Nordic Gold. Congruent dissolution was first assumed in all cases involving all elements. The $E.W.$ for an alloy such as Nordic Gold is also shown assuming incongruent dissolution of 94.7% Cu and 5.3% Zn.

$$Q_{corr} \text{ by Mass Loss} = \Delta m F / (E.W.) \quad \text{Equation 4.1}$$

$$E.W. = \sum \frac{f_i n_i}{a_i} \quad \text{Equation 4.2}$$

Table 4.3. Calculation of equivalent weight of Nordic Gold using either Cu^+ or Cu^{2+} . In each $E.W.$ reported, all elements were considered to dissolve congruently or proportional to their mass fraction reported. Additionally, a case of incongruent dissolution is assumed, with 94.7 wt% Cu and 5.3 wt% Zn. The difference arises from Cu^+ vs. Cu^{2+} assumption.

Reaction	Nernst Potential (E°/V) (SHE)	Equivalent Electrons (equiv./mol)	Atomic Weight (g/mol)	Weight Fraction (wt%)	Equivalent Weight (E.W): Congruent (g/equiv.)	Equivalent Weight (E.W): Incongruent (g/equiv.)
$Cu^+ + e^- = Cu$	0.521	1	63.546	.89	47.03	60.52
$Cu^{2+} + 2e^- = Cu$	0.342	2	63.546	.89	28.35	31.82
$Al^{3+} + 3e^- = Al$	-1.662	3	26.982	.05		
$Zn^{2+} + 2e^- = Zn$	-0.762	2	65.38	.05		
$Sn^{2+} + 2e^- = Sn$	-0.138	2	118.71	.01		

4.3.4 Corrosion Product Analysis

4.3.4.1 Optical Spectrophotometry

Reflectivity was used as a means to determine the degree of tarnish, and thus aesthetic appeal, of the tarnished surfaces. Optical reflectance as a function of wavelength was determined by using a tungsten halogen lamp (LS-1, Ocean Optics), reflection probe (R400-7-VIS/NIR, Ocean Optics) and coupled optical spectrometer (Jaz, Ocean Optics) using SpectraSuite software. The light source was held at a fixed distance perpendicular (90°) to the sample surface using a RPH-1 reflection probe holder. A STAN-SSH High-reflectivity specular reflectance standard was used for calibration of the light reference (100%) which guarantees 85-90% reflectance across 250-800 nm and 85-98% reflectance across 800-2500 nm. Integration time was set automatically using SpectraSuite software, and measurements were conducted using 10 scans to average, with a boxcar width of 5 to increase signal to noise ratio. Particular interest was paid to the visible light region, with wavelengths from 370-730 nm. One sample per alloy, pre-exposure treatment, and time was conducted as a representative of the 3 samples exposed. The test area was a 11.16 mm² circle at the center, and color distinct regions of the corroded area.

4.3.4.2 Grazing Incidence X-Ray Diffraction

Grazing incidence X-ray diffraction measurements were carried out on a PanalyticalX'Pert Pro MPD diffractometer applying the associated software (DataCollector). Cu-K α radiation ($\lambda = 1.5406 \text{ \AA}$) was used in all experiments. The incident beam was conditioned using a parallel beam X-ray mirror for Cu radiation with a $1/32^\circ$ divergent slit and 20 mm mask. The use of a 20 mm mask ensured that signal was measured from a line across the entire sample, resulting in the averaging of potentially

heterogeneous sections of the oxide. A beam attenuator with 0.125 mm Ni foil was employed for the alignment of the sample following standard alignment procedures. Samples were placed in the center of an Eulerian cradle mounting stage, and an incident angle of 0.5° was used for measurements, limiting depth of interaction to $0.2 \mu\text{m}$ ¹²⁴. The diffracted beam was conditioned with a parallel plate collimator, parallel plate collimator slit (with alignment only), and 0.04 radians Soller slits, then recorder using a proportional Xe detector. The 2θ scan range was 20-100°.

4.3.4.3 Galvanostatic Reduction to Analyze Oxides

Galvanostatic reduction operates on the principle of electrochemically reducing corrosion products sequentially through the application of constant current. The corrosion products with the highest reduction potentials are reduced first. Based on worked by Nakayama, Kaji, Shibata, Notoya, and Osakai, galvanostatic reduction can be used to identify the order of reduction in copper oxides (CuO, Cu₂O) that was previously debated.¹²⁵ As seen in Figure 4.4, CuO is known to reduce first, followed by the reduction of Cu₂O, a result of the oxides sandwich like oxide layer arrangement where Cu₂O is contained by CuO and metallic Cu.

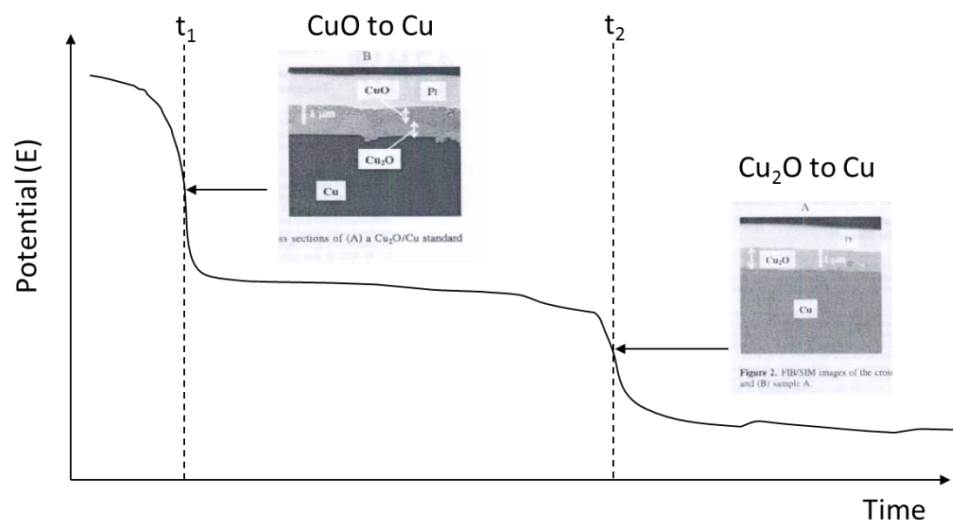


Figure 4.4. Reduction order of copper oxides CuO and Cu₂O.¹²⁵ However, other papers suggest CuO reduces to Cu₂O, rather than to CuO to Cu as reported here.^{126,127}

Galvanostatic reduction experiments were conducted on Princeton Applied Research Model 273A potentiostats with CorrWare software. Experiments were conducted in chloride free electrochemical flat cells utilizing a conventional 3-electrode setup. This utilized a mercury-mercury sulfate electrode (MSSE), a platinum-mesh counter electrode, and the sample as a working electrode. Tests were conducted at 0.02 mA/cm² in deaerated borate buffer solution (Na₂B₄O₇+H₃BO₃), pH 8.4, with a collection rate of 1 point/sec. A minimum of 3 replicates per corresponding sample and exposure time were obtained. Table 4.4 compares the galvanostatic reduction method utilized compared to methods used in ASTM B825¹²⁸ and Nakayama, et al.¹²⁵

Table 4.4. Comparison of galvanostatic reduction methods utilized in ASTM standard, Nakayama's previous study and previously used in house method.			
Method	Solution	pH	<i>i</i> _{corr}
ASTM B825 ¹²⁸	1 M KCl	7	1.0 mA/cm ²
Nakayama ¹²⁵	0.1 M KCl	7	0.5 mA/cm ²
	1 M KOH	14	
	6 M KOH + 1 M LiOH	14	
Experimental Procedure	0.019 M Na ₂ B ₄ O ₇ + 0.131 M H ₃ BO ₃	8.4	0.02 mA/cm ²

ASTM B825 was utilized to determine the precise time associated with reduction peak characteristics by determination of differential inflection points (Figure 4.5).¹²⁸ Derivatives were manually calculated as the difference of potential between 15 consecutive seconds, and inflection points determined by visual evaluation of the maximum potential plateau. Inflection peaks were taken to represent times when a full reduction of a species occurred. For example, Figure 4.5 shows the reduction of CuO and Cu₂O, where t_1 corresponds to the time at which the full reduction of CuO is achieved, and t_2 corresponds to the time at which the full reduction of Cu₂O is achieved. Potentials that correspond to the inflection point time were determined by the peak preceding the inflection point, by the average of the first 15 seconds in the case of the first reduction peak and visual evaluation for those following. In Figure 4.5, E_1 corresponds to the potential at which CuO is reduced, and E_2 corresponds to the potential at which Cu₂O is reduced. Data is often represented as inflection point-reduction potential pairs (t_i, E_i), indicated by circles in Figure 4.5. Table 4.5 lists the half-cell reactions for possible corrosion products that could be reduced by galvanostatic reduction. Chloride concentration ($[Cl^-]$) was assumed to be 10^{-8} M as reductions were conducted in Cl^- free cells. Hydrogen ($[H^+]$) and hydroxide ($[OH^-]$) concentrations were derived from pH (8.4). The exposure spot size (0.8 cm^2) was matched precisely to the reduction spot size (0.8 cm^2).

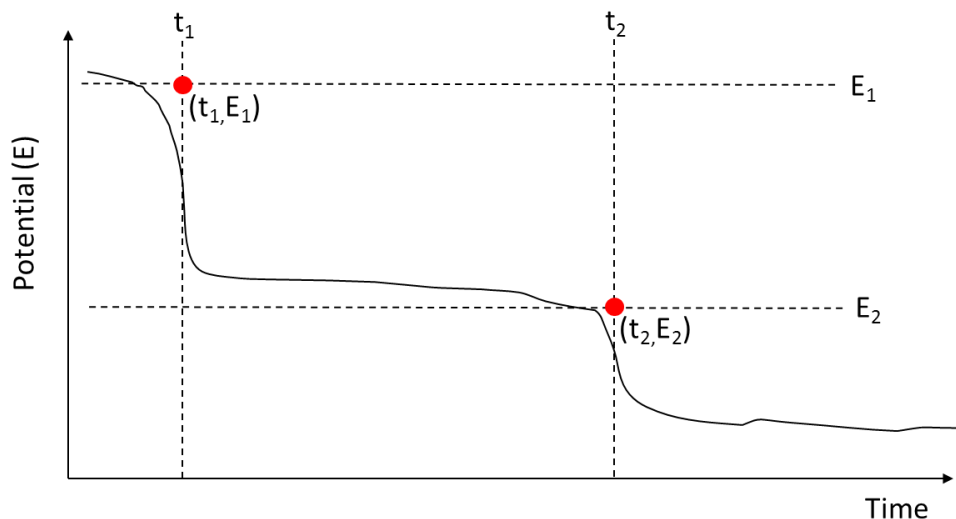


Figure 4.5. Galvanostatic reduction analysis corresponds time to completely reduce a corrosion species (t_i) to inflection points on the galvanostatic reduction spectra, and reduction potential (E_i) to the plateau preceding the inflection point.

Table 4.5. Possible corrosion products reduced by galvanostatic reduction at potentials below associated half-cell potentials. Assumptions were that $[Cl^-]$ is 10^{-8} M, $[H^+]$ is 3.98×10^{-9} M, and $[OH^-]$ is 2.51×10^{-6} M for pH 8.4.			
Half-Cell Reaction	V_{SHE}	V_{SCE}^{xxvi}	V_{MMSE}^{xxvii}
$2CuO \bullet H_2O + 2e^- \rightarrow Cu_2O + 2OH^- + H_2O$	0.25056	0.00956	-0.39944
$Cu_2(OH)_3Cl + 4e^- \rightarrow 2Cu + Cl^- + 3OH^-$	0.24588	0.00488	-0.40412
$CuCl_2 \bullet 3Cu(OH)_2 + 8e^- \rightarrow 4Cu + 2Cl^- + 6OH^-$	0.19228	-0.04872	-0.45772
$Cu_2O + H_2O + 2e^- \rightarrow 2Cu + 2OH^-$	-0.02544	-0.26644	-0.67544
$Sn(O)^* + 2H^+ + 2e^- \rightarrow Sn + H_2O$	-0.58744	-0.82844	-1.23744
$Zn(O)^{**} + 2H^+ + 2e^- \rightarrow Zn + H_2O$	-0.89644	-1.13744	-1.54644
* Assumed to be hydroxylated $Sn(OH)_2$			
** Assumed to be amorphous hydroxylated $Zn(OH)_2$			

4.3.5 Solution Analysis by ICP-OES

Inductively coupled plasma-optical emission spectrometry (ICP-OES) was utilized to determine copper ions released from alloys. ICP-OES samples were collected at times corresponding to the removal of copper alloy samples for surface analysis of corrosion products at 1, 3, 6, 9, and 12 dry-wet cycles, and were not acidified. A 10 mL aliquot of synthetic perspiration solution was used to wash the copper alloy coupon <5

^{xxvi} $V_{SCE} = V_{SHE} - 0.241$

^{xxvii} $V_{MMSE} = V_{SHE} - 0.650$

minutes before the end of the final wet cycle, when thin electrolyte was still visibly apparent on the alloy surface. Samples were further diluted 1:10 in synthetic perspiration solution. Note that while ICP-OES can detect elements in solution regardless of complexation with other matter in the solution, it cannot differentiate between oxidation states (Cu^+ or Cu^{2+}).

Measurements were conducted using a Thermo Scientific iCAP 6200 with a HF-compatible sample introduction system. A yttrium (Y) internal standard was utilized to account for instrumental fluctuations, and observed at wavelengths 230.6 and 325.6 nm, which were determined to have no interference with elements possible in sample solutions (Cu, Al, Zn, or Sn). Calibration was conducted in Millipore water and synthetic perspiration after 130 hours (with no exposure to copper alloys) with additions of 0.01-100 ppm Cu using single element ICP-OES standards (Agilent Technologies). Figure 4.6 compares the calibration of the two solutions at 224.7 nm. A calibration of signal intensity versus copper content was used to determine copper content (ppm) in test solutions. A minimum of 3 replicates per corresponding sample and exposure time were analyzed, each analyzed at 224.7 nm in triplicate. Raw concentrations were manipulated as seen in Figure 4.7 to achieve concentration in Cu ions/cm^2 , the surface area of the exposed solution.

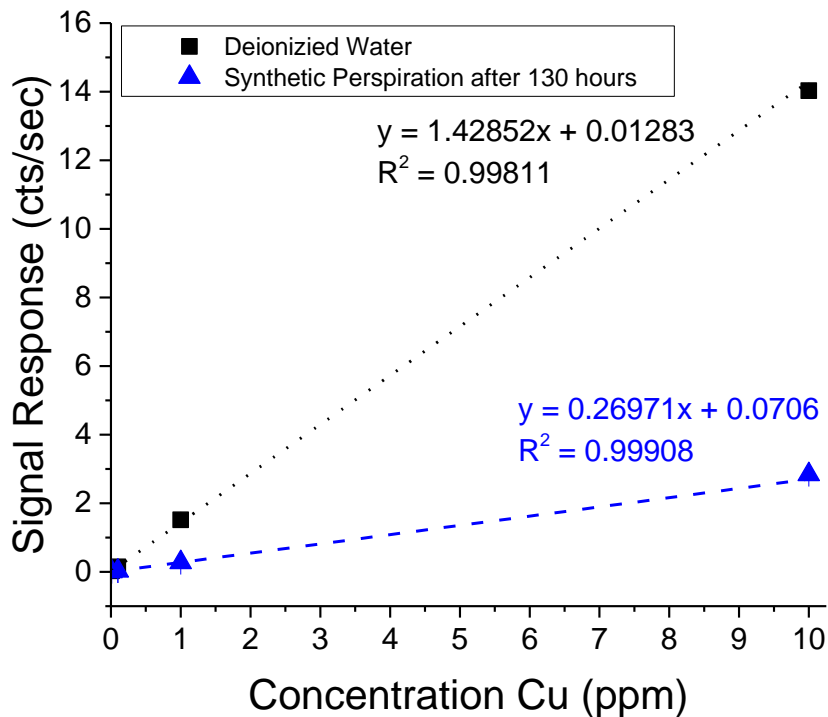


Figure 4.6. Comparative calibration curves of Cu in deionized water and synthetic perspiration after 130 hours (no exposure to copper alloys) at 224.7 nm.

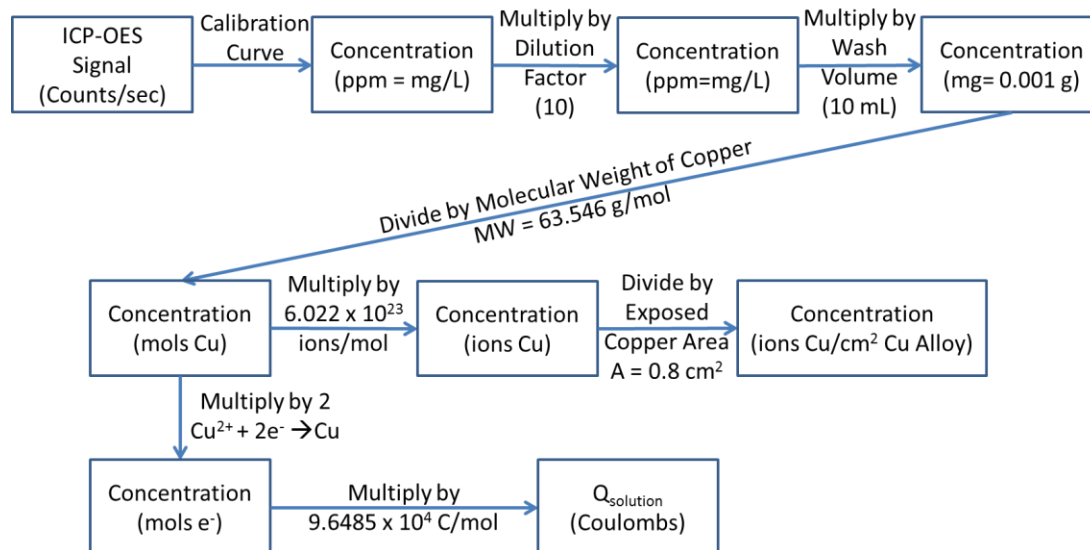


Figure 4.7. Procedural flow chart of converting signal obtained by ICP-OES to copper ion release (ions/cm²).

4.4 Results

4.4.1 Corrosion Rate: Mass Loss by Gravimetric Analysis

Mass loss by gravimetric analysis was conducted on freshly ground C10000 and Nordic Gold just after grinding to 1200 grit and after being deposited with 100 μL synthetic perspiration then exposed to 12 dry-wet cycles. Mass gain following deposition of synthetic perspiration and 12 dry-wet cycles was determined to be 1.4 (± 0.1) mg for Nordic Gold, and 1.6 (± 0.2) mg for C11000 in an approximated droplet area of 0.8 cm^2 , on a total area of approximately 6.25 cm^2 . Mass loss following deposition of synthetic perspiration and 12 dry-wet cycles was determined to be 1.3 (± 0.2) mg for Nordic Gold, and 1.5 (± 0.5) mg for C11000 in an approximated exposure area of 0.8 cm^2 , indicating no statistical difference. Table 4.6 lists mass loss (Δm) and associated charge (Q_{corr}) for Nordic Gold and C11000 normalized by droplet size and depending on Cu^+ or Cu^{2+} . Results indicate a mass gain before cleaning due to O^{2-} , Cl^- , or OH^- addition to the sample surface during the formation of corrosion products (Table 4.6). Following removal of corrosion products in 6 M HCl, there is a mass loss associated with metal lost either to corrosion products or direct dissolution into solution (Table 4.6). There is no statistical difference of Q_{corr} between C11000 and Nordic Gold, despite alloying additions (Table 4.6).

Table 4.6. Charge (Q_{corr}) analysis based on mass loss of 3 specimens with standard deviation after exposure to 100 μL synthetic perspiration (droplet area=0.8 cm^2) and 12 dry-wet cycles on copper alloy freshly ground to 1200 grit (23 $^{\circ}\text{C}$, ambient aeration).						
Alloy	Mass Gain (Δm) (mg)	Mass Gain Prior to Cleaning (mg/cm^2)	Mass Loss After Cleaning (Δm) (mg)	Mass Loss (mg/cm^2)	$Q_{\text{corr}}/\text{area}$ (C/cm^2) $\text{Cu}^+ + e^- = \text{Cu}$	$Q_{\text{corr}}/\text{area}$ (C/cm^2) $\text{Cu}^{2+} + 2e^- = \text{Cu}$
C11000	1.6 (± 0.2)	2.0 (± 0.3)	1.5 (± 0.5)	1.9 (± 0.6)	2.8 (± 0.9) ^{xxviii}	5.7 (± 2.0) ^{xxix}
Nordic Gold	1.4 (± 0.1)	1.8 (± 0.1)	1.3 (± 0.2)	1.6 (± 0.2)	3.2 (± 0.4) ^{xxx}	5.44 (± 0.7) ^{xxx1}
					2.6(± 0.3) ^{xxxii}	4.9(± 0.6) ^{xxxiii}

4.4.1 Surface Analysis of Corrosion Products

4.4.2 Tarnishing in Synthetic Perspiration

Optical images of C11000 and Nordic Gold when freshly ground to 1200 grit prior to deposition with synthetic perspiration and exposure to dry-wet cycling were collected after 1, 3, 6, 9 and 12 cycles. The results are shown in Figures 4.8-4.9. Both alloys experienced significant discoloration in the region of salt deposition by synthetic perspiration droplet after as little as 1 dry-wet cycle (8 hours). Additionally, both alloys discolor in a narrow region outside the initial droplet area in as little as 1 dry-wet cycle, which expands over time, suggesting secondary wetting effects. Primary discoloration of C11000 appeared red-brown that darkened to black with time (Figure 4.8). A blue-green region at the edge of the droplet appears after only 1 dry-wet cycle, grows at 3 dry-wet cycles, and remains relatively constant from 3-12 dry-wet cycles. Nordic Gold discolored primarily to a dull yellow color after 1 dry-wet cycle with darker yellow regions which expand at 3 dry-wet cycles (Figure 4.9). After 3 dry-wet cycles, a blue-green edge

^{xxviii}Equivalent weight, $\text{Cu}^+ = 63.55$ equiv./g

^{xxix}Equivalent weight, $\text{Cu}^{2+} = 31.77$ equiv./g

^{xxx}Equivalent weight, congruent alloy dissolution, $\text{Cu}^+ = 47.03$ equiv./g

^{xxx1}Equivalent weight, congruent alloy dissolution, $\text{Cu}^{2+} = 28.35$ equiv./g

^{xxxii}Equivalent weight, incongruent alloy dissolution, $\text{Cu}^+ = 60.52$ equiv./g

^{xxxiii}Equivalent weight, incongruent alloy dissolution, $\text{Cu}^{2+} = 31.82$ equiv./g

appears which continues to expand inward through 12 dry-wet cycles. Scanning electron microscope (SEM)^{xxxiv} imaging by secondary electron imaging suggests the formation of precipitates along the surface of both C11000 and Nordic Gold following 12 dry-wet cycles and before cleaning (Figures 4.10-4.11). Following the removal of corrosion products with 6 M HCl, both C11000 and Nordic Gold show evidence of uniform corrosion (Figures 4.12-4.13).

^{xxxiv} Scanning electron microscope images were obtained courtesy of Michael Melia.

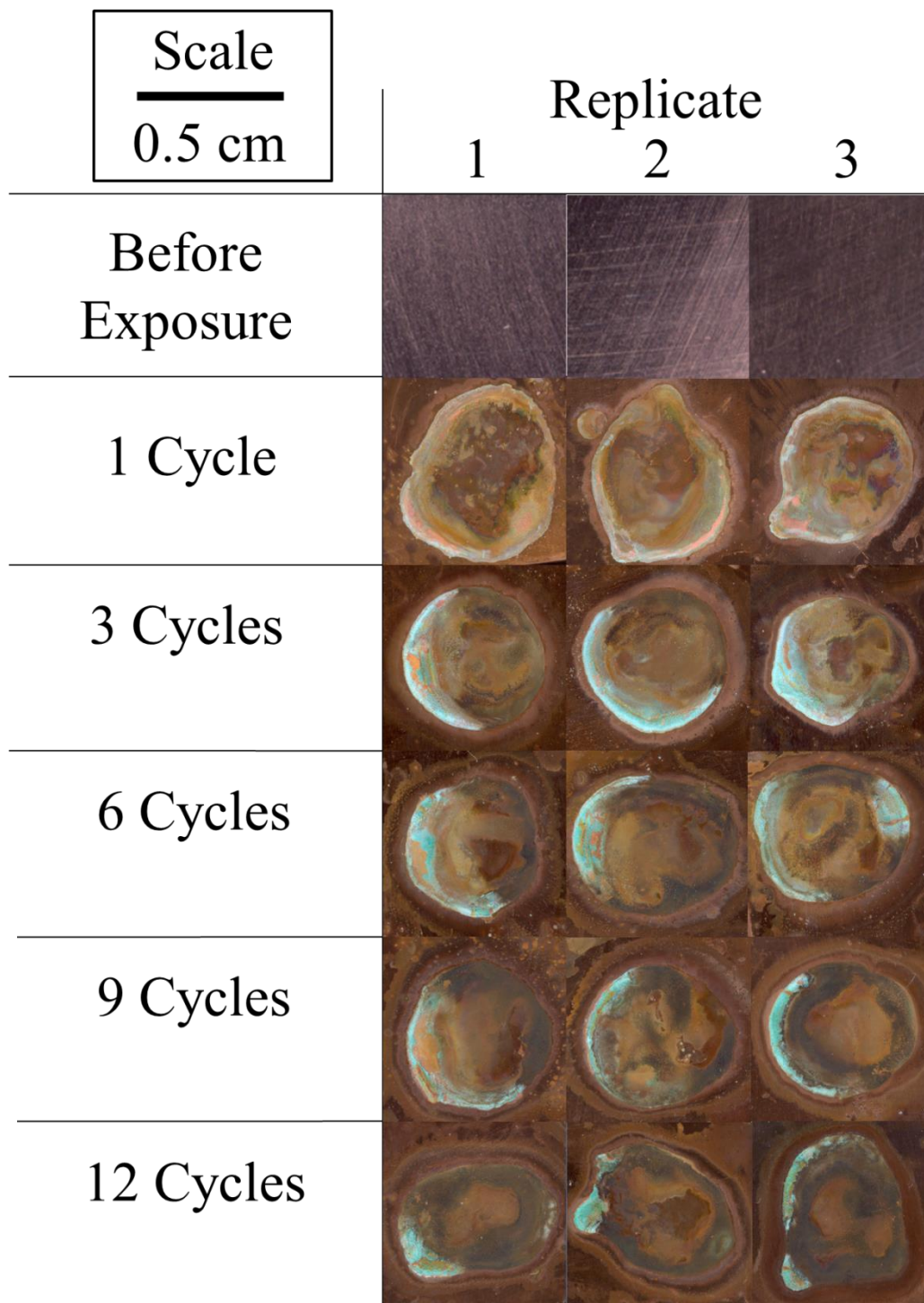


Figure 4.8. Visual analysis of C11000 when freshly ground to 1200 grit, deposited with 100 μ L of synthetic perspiration solution (23 °C, ambient aeration) and exposed to 4 hour wetting-4 hour drying cycles.

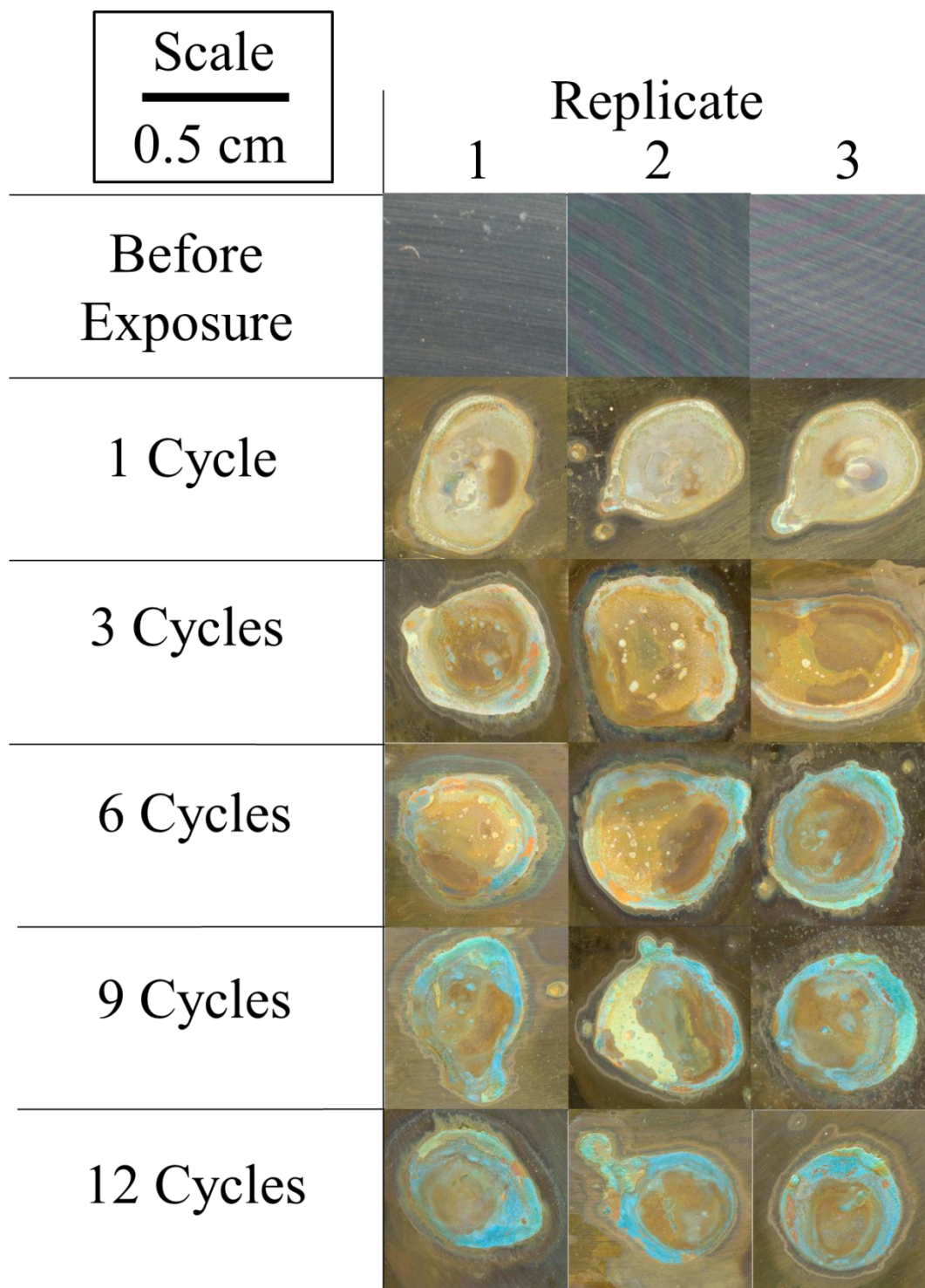


Figure 4.9. Visual analysis of Nordic Gold when freshly ground to 1200 grit, exposed to 100 μL of synthetic perspiration solution (23 $^{\circ}\text{C}$, ambient aeration) and exposed to 4 hour wetting-4 hour drying cycles.

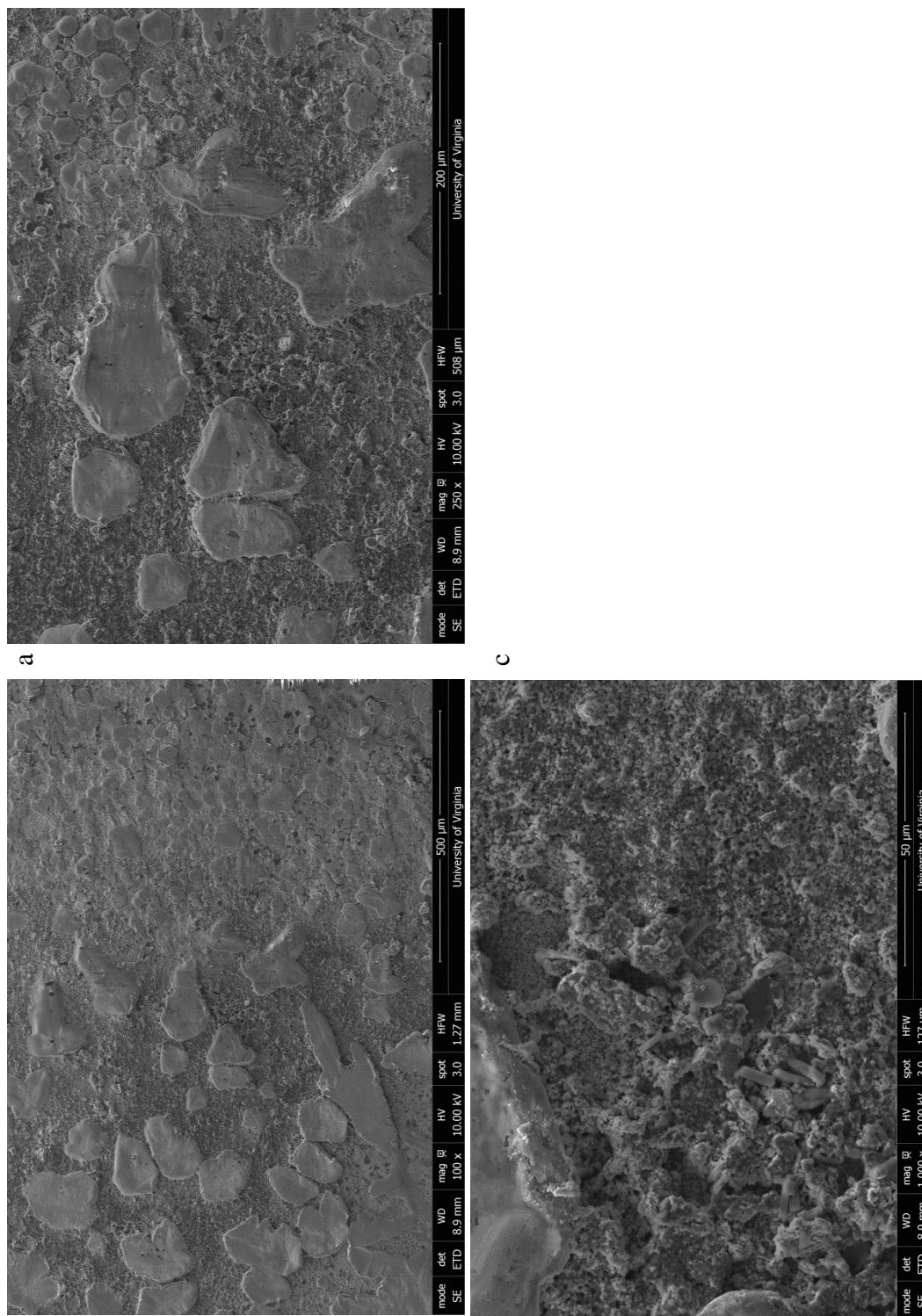


Figure 4.10. SEM micrographs of C11000 exposed to 100 μL synthetic perspiration (23 $^{\circ}\text{C}$, ambient aeration) for 12 dry-wet cycles and left uncleaned using SEI at 100x (a), 250x (b) and 1000x (c).

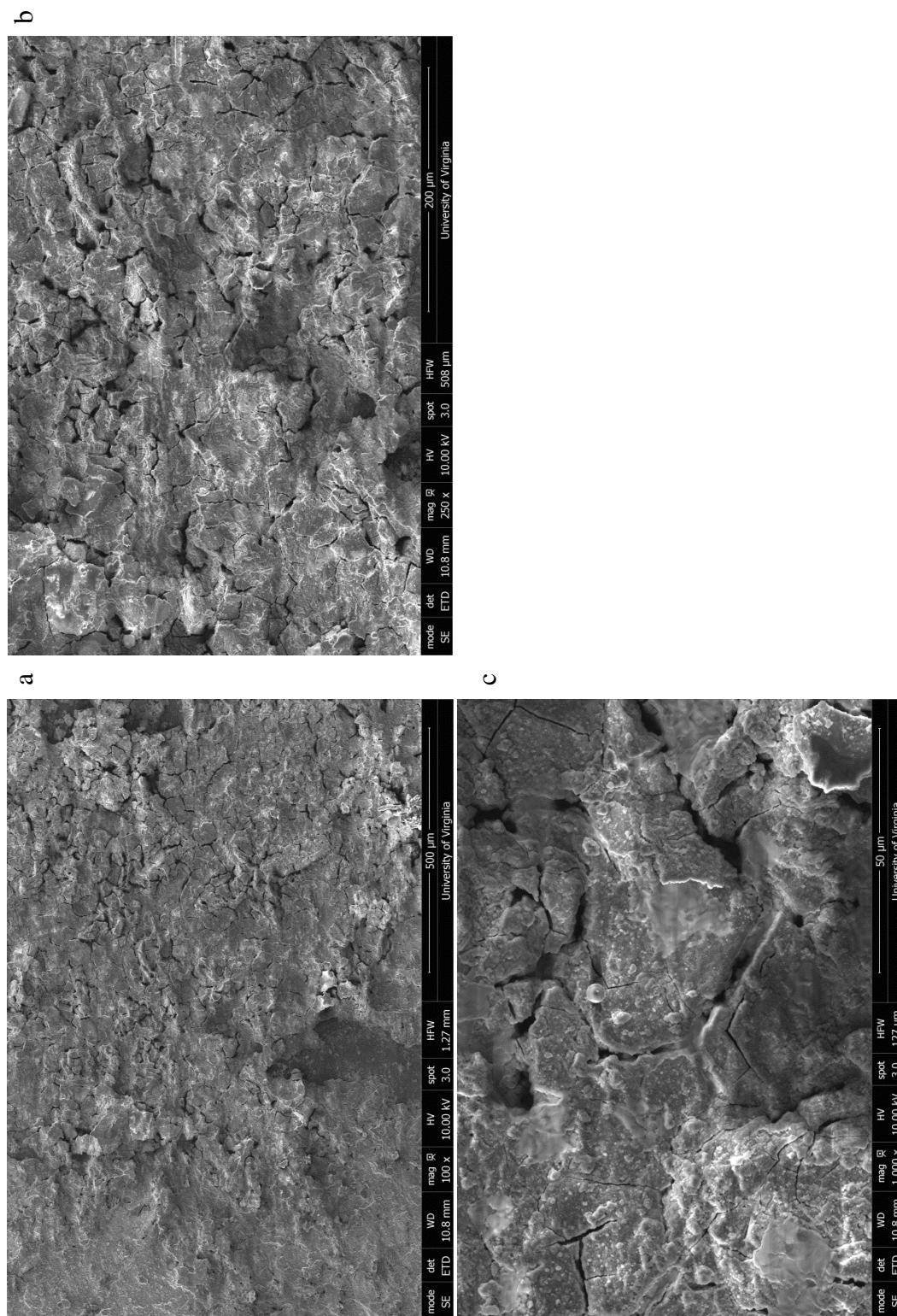


Figure 4.1.1. SEM micrographs of Nordric Gold exposed to 100 μL synthetic perspiration (23 $^{\circ}\text{C}$, ambient aeration) for 12 dry-wet cycles and left uncleaned using SEI at 100x (a), 250x (b) and 1000x (c)

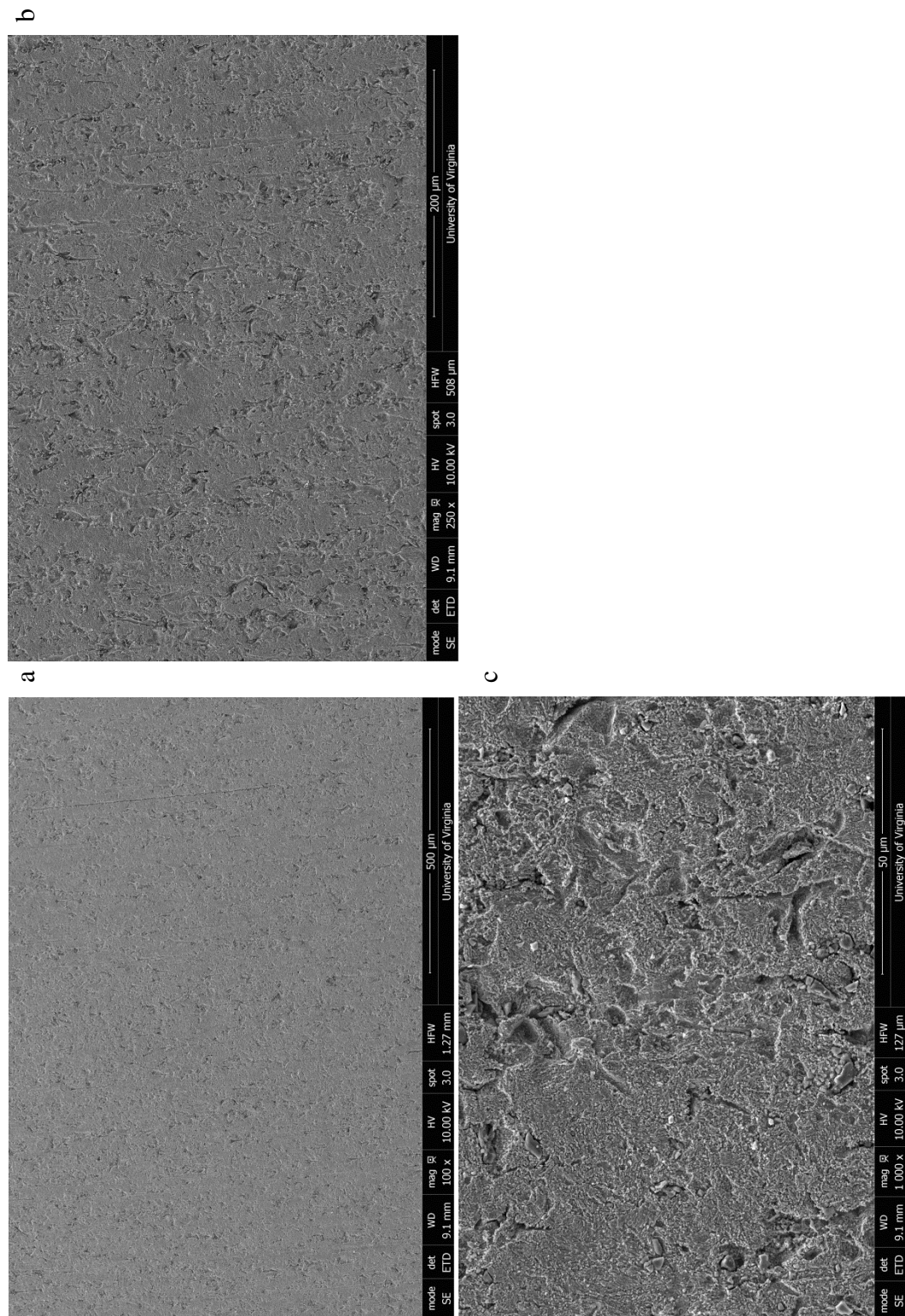


Figure 4.12. SEM micrographs of C11000 exposed to 100 μL synthetic perspiration (23 $^{\circ}\text{C}$, ambient aeration) for 12 dry-wet cycles and cleaned with 6 M HCl for 3 minutes using SEI at 100x (a), 250x (b) and 1000x (c)

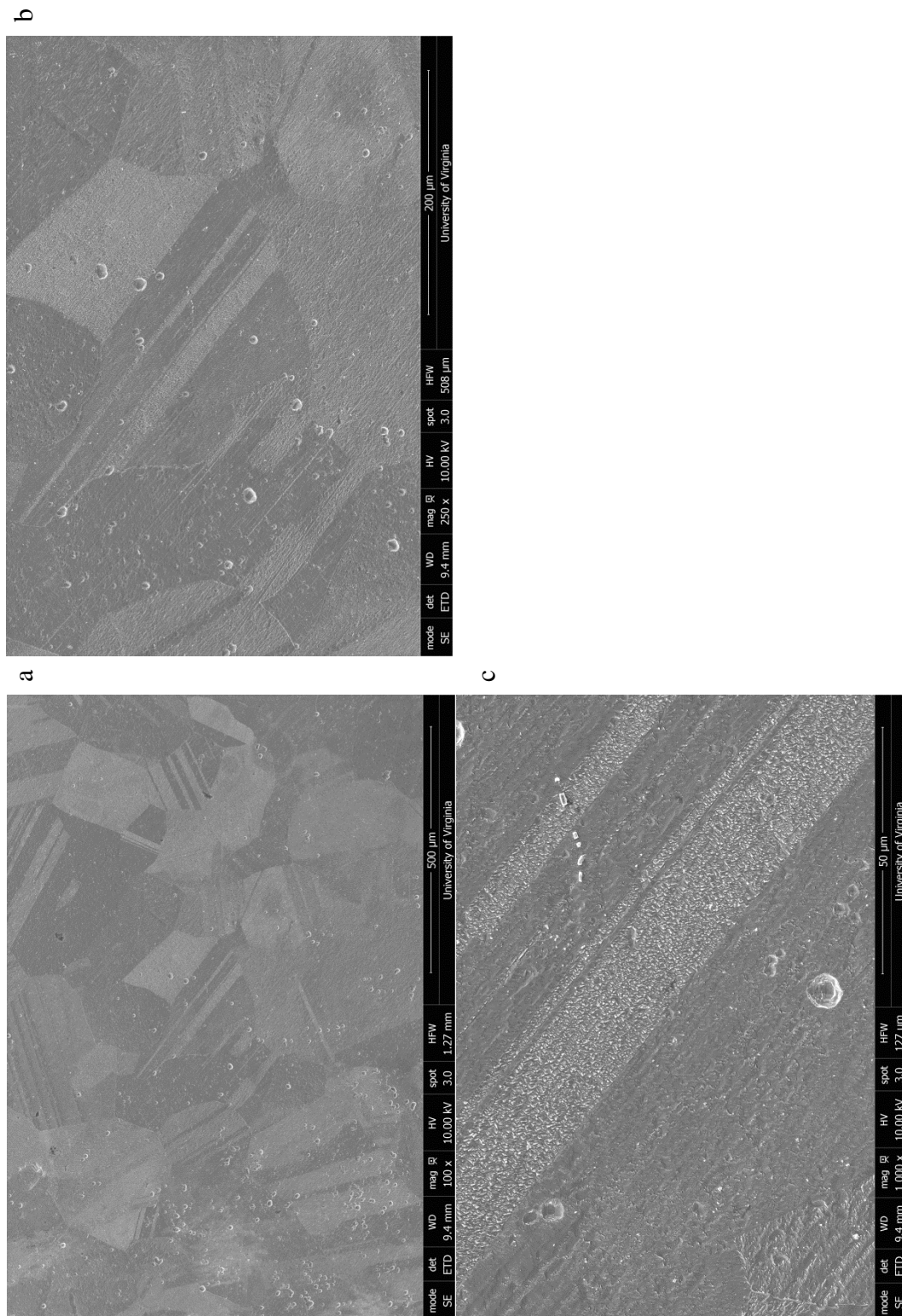


Figure 4.13. SEM micrographs of Nordic Gold exposed to 100 μL synthetic perspiration (23 $^{\circ}\text{C}$, ambient aeration) for 12 dry-wet cycles and cleaned with 6 M HCl for 3 minutes using SEI at 100x (a), 250x (b) and 1000x (c)

4.4.3 Tarnish Analysis by Optical Spectrophotometry

Reflectivity was utilized as a qualitative comparison for the degree of tarnish acquired on samples over time exposed to concentrated synthetic perspiration. In all samples, exposure to synthetic perspiration caused a significant decrease in reflectivity in air after only 1 dry-wet cycle (Figures 4.14-4.15). Reflectivity decreased in both alloys with increasing number of dry-wet cycles, both at the edge and center. The greatest degree of reflectivity was observed from the center region on C11000 at 730 nm (5.1% reflectivity, Figure 4.14c) and 630 nm (3.8% reflectivity, Figure 4.15b) on Nordic Gold, corresponding to dark red light and orange light, respectively (Figure 4.16). The visibly blue-green edge had a lower degree of reflectivity compared to the center region, while maximum reflectivity on C11000 was at 756 nm (4.8% reflectivity, Figure 4.14a) and 530 nm (1.8% reflectivity, Figure 4.15a) on Nordic Gold, corresponding to yellow-green and green light respectively (Figure 4.16).

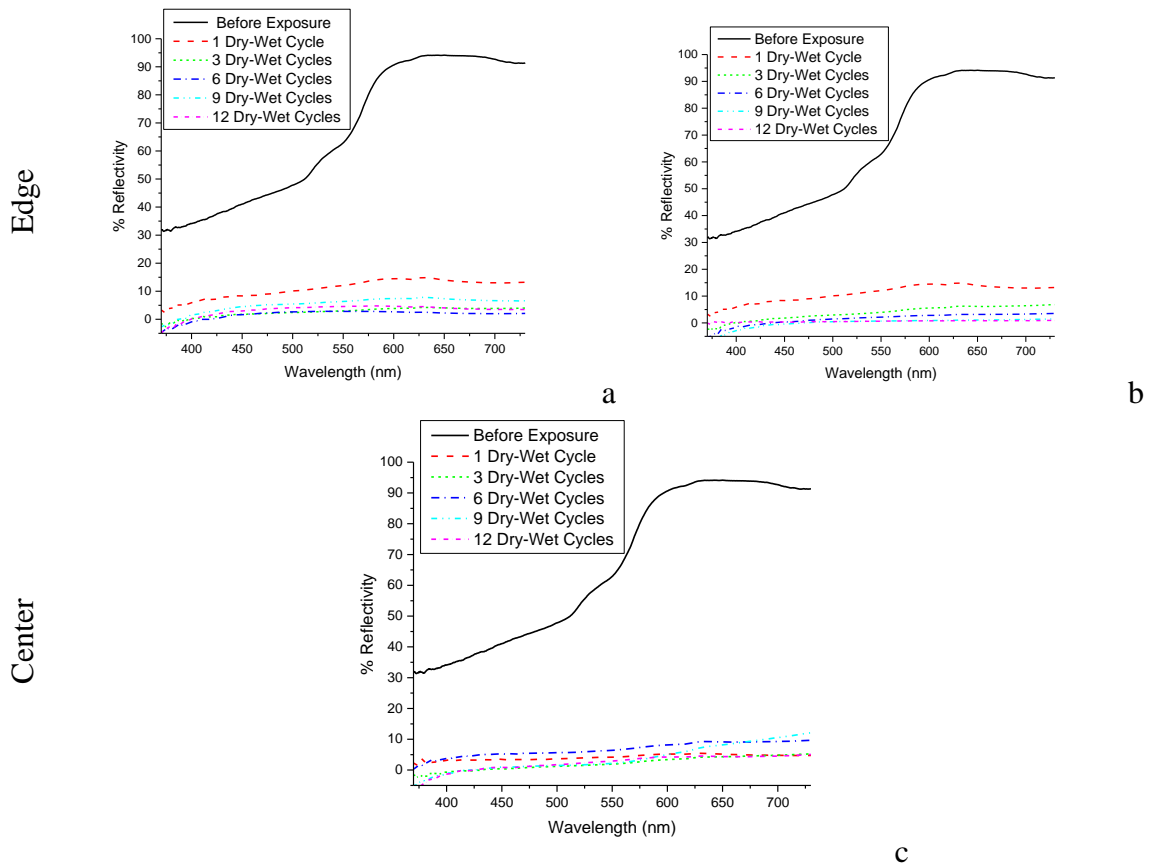


Figure 4.14. Reflectivity of C11000 when freshly ground to 1200 grit, deposited with 100 μL of synthetic perspiration solution (23 $^{\circ}\text{C}$, ambient aeration) and exposed to 4 hour wetting-4 hour drying cycles. Image a is the reflectivity of a visually blue edge, b is the reflectivity of a visually dark-black edge, and c is reflectivity of the center of the dried droplet area.

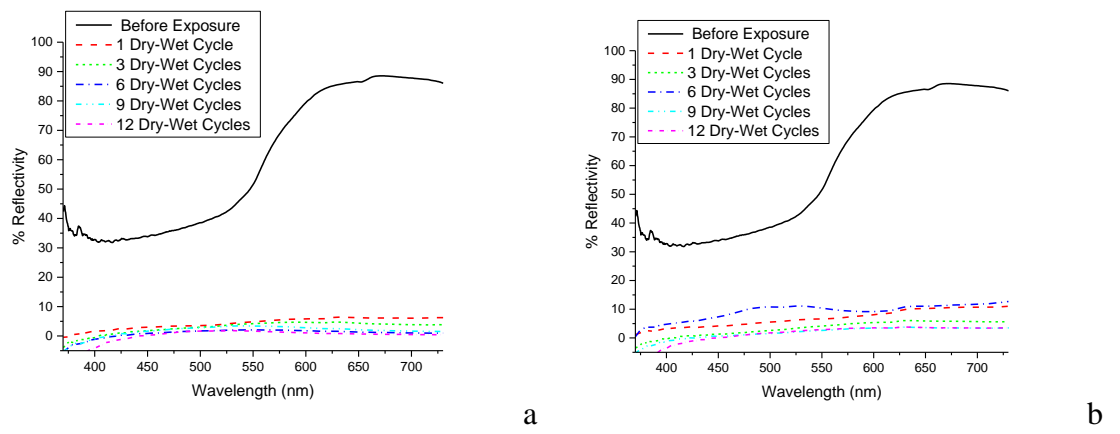


Figure 4.15. Reflectivity of Nordic Gold when freshly ground to 1200 grit, deposited with 100 μL of synthetic perspiration solution (23 $^{\circ}\text{C}$, ambient aeration) and exposed to 4 hour wetting-4 hour drying cycles. Image a is reflectivity of a visually blue edge, b is reflectivity of the center of the dried droplet area.

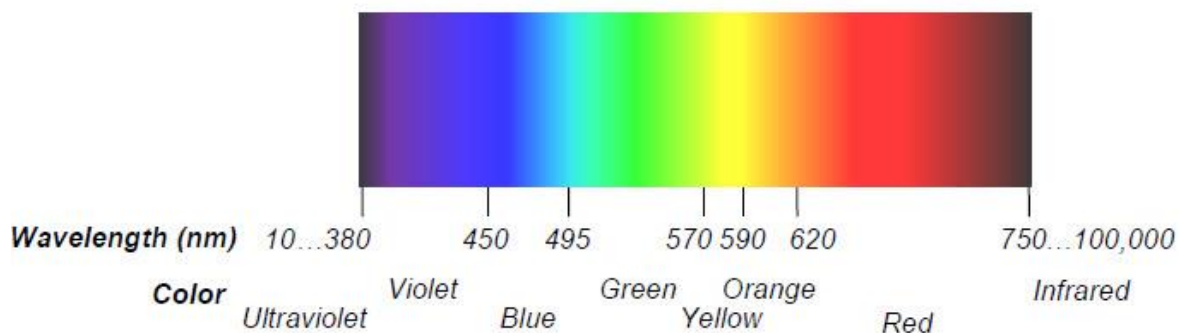


Figure 4.16. Visible light spectrum wavelengths with corresponding observed color.¹²⁹

4.4.4 Corrosion Product Analysis by GIXRD

Prior to exposure to synthetic perspiration, all samples exhibited only peaks consistent with fcc copper and no corrosion products, despite the pre-treatment of air oxidation suggesting that air formation causes thin oxides (Figure 4.17). GIXRD peaks in Nordic Gold before exposure to synthetic perspiration droplets were shifted to lower angles, consistent with substitutional solid solution alloying effects on the Cu fcc lattice parameter.¹⁴⁶

Following exposure to synthetic perspiration droplets and dry-wet cycles, all samples developed crystalline corrosion products, as seen in Figure 4.17. Additionally, GIXRD spectra signal-to-noise increased with increased numbers of dry-wet cycles, indicating a roughening of the copper alloys surface during the corrosion process.¹⁴⁷

Figures 4.18-4.19 show GIXRD of C11000 and Nordic Gold following exposure to synthetic perspiration droplet and 12 dry-wet cycles, with peak identification.

Identified corrosion species include oxides, chlorides and carbonates on both C11000 and Nordic Gold based on International Centre for Diffraction Data (ICDD) PDF cards.

Copper oxides identified were Cu_2O ($2\theta = 36.4183, 61.3435, 73.5263$) and CuO ($2\theta =$

34.4367, 35.5383, 38.7304, 38.9396, 48.7419, 61.5468). The only copper chloride identified was $\text{Cu}_2(\text{OH})_3\text{Cl}$ ($2\theta = 32.2113, 35.2113, 35.7003, 39.5612, 53.3581, 57.3741, 67.3689$). Copper carbonate identified were of $\text{Cu}_2(\text{OH})_2\text{CO}_3$ ($2\theta = 24.1848, 31.2753$) and CuCO_3 ($2\theta = 29.8728, 33.8779, 38.3001, 43.8866, 48.3629$).

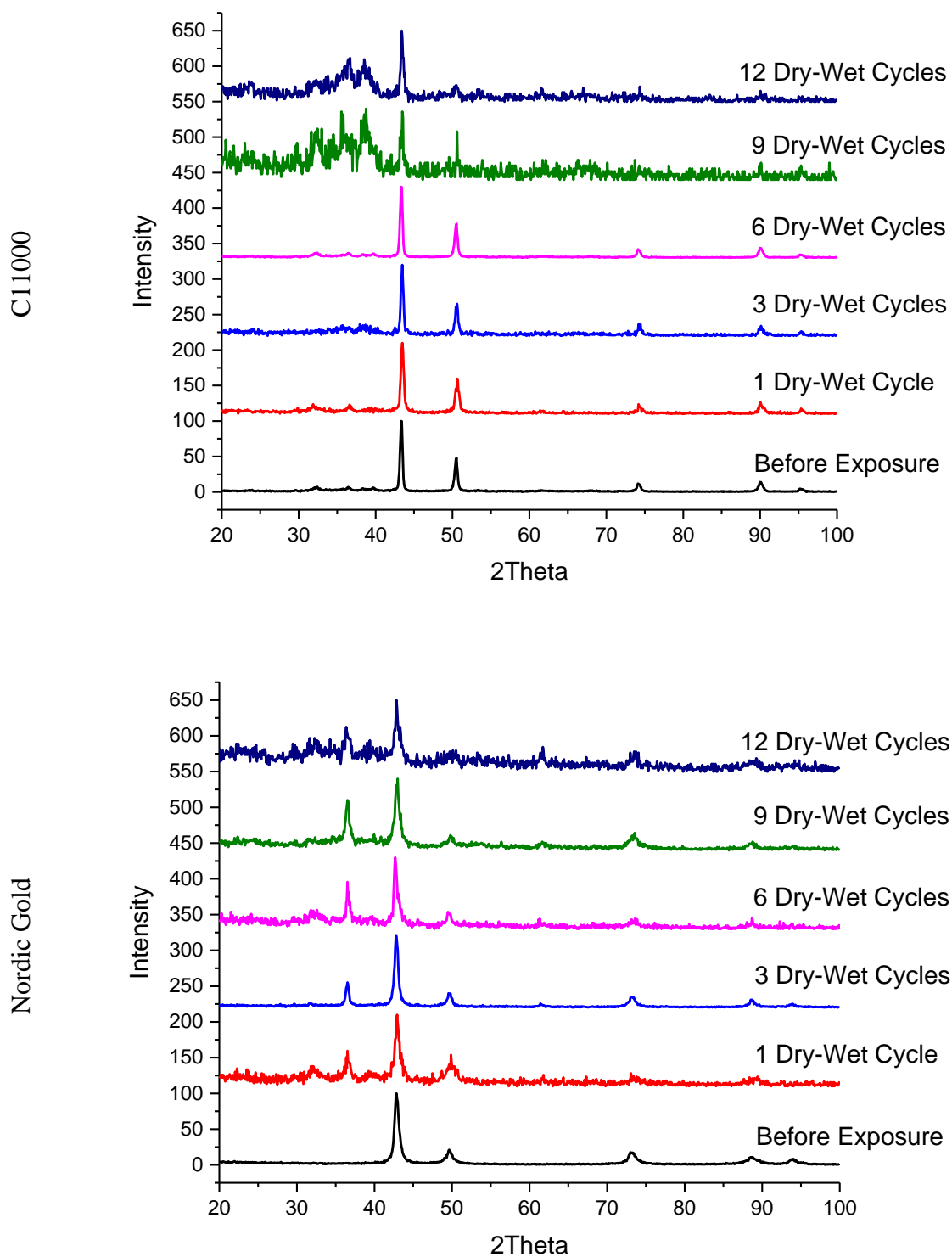


Figure 4.17. GIXRD of C11000 and Nordic Gold samples when to 1200 grit, deposited with 100 μL of synthetic perspiration solution (23 $^{\circ}\text{C}$, ambient aeration) and exposed a number of 4 hour drying-4 hour wetting cycles.

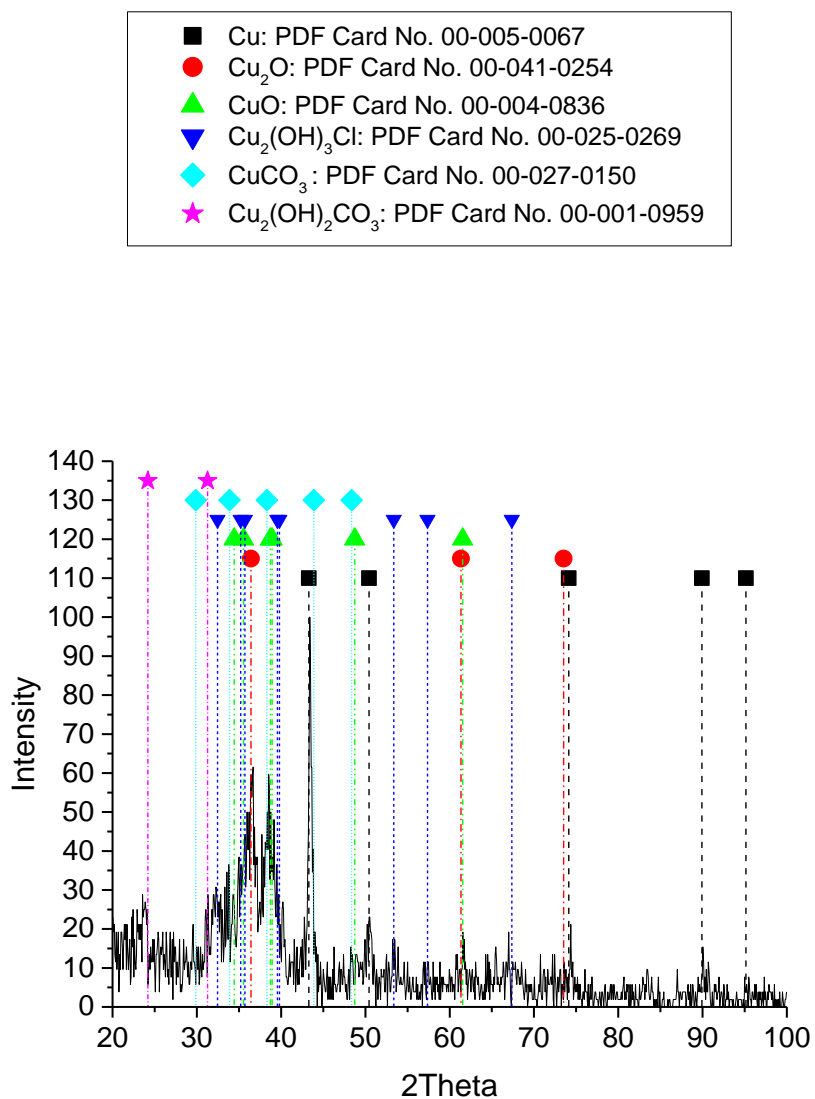


Figure 4.18. GIXRD of C11000 sample when to 1200 grit, deposited with 100 μL of synthetic perspiration solution (23 $^{\circ}\text{C}$, ambient aeration) and exposed to 4 hour wetting-4 hour drying cycles. Spectra highlights FCC metallic Cu, copper oxide, chloride and carbonate corrosion product peaks.

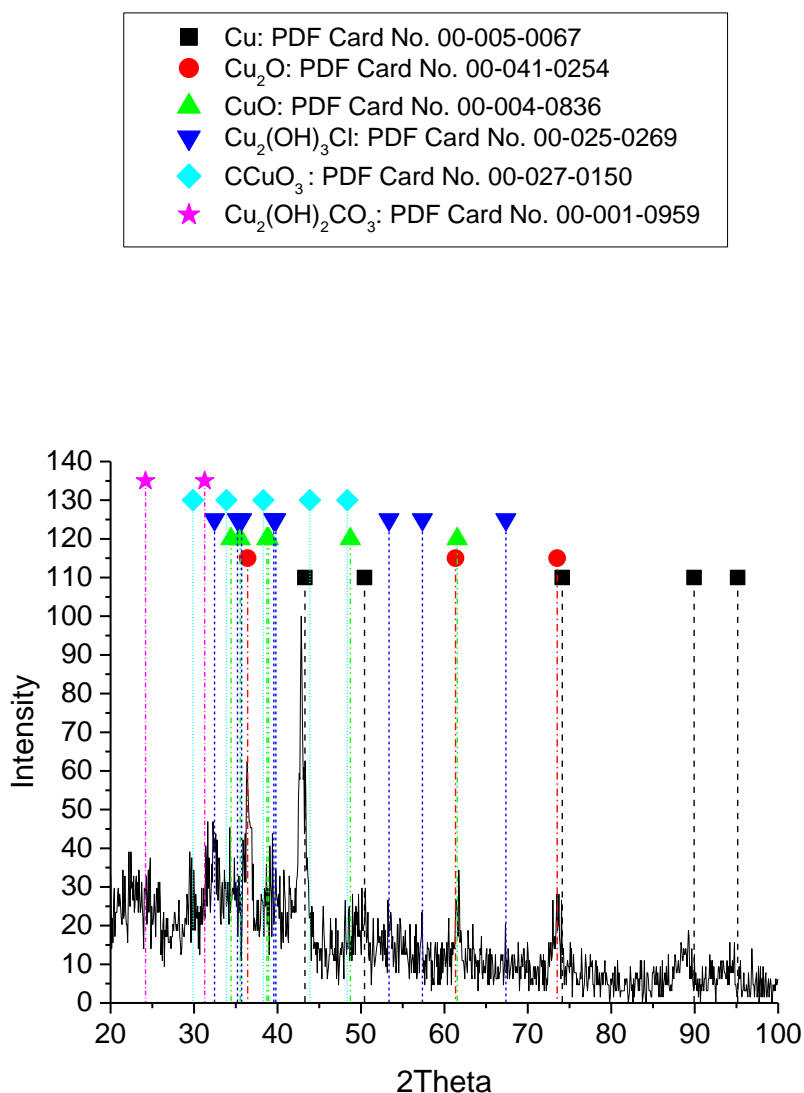


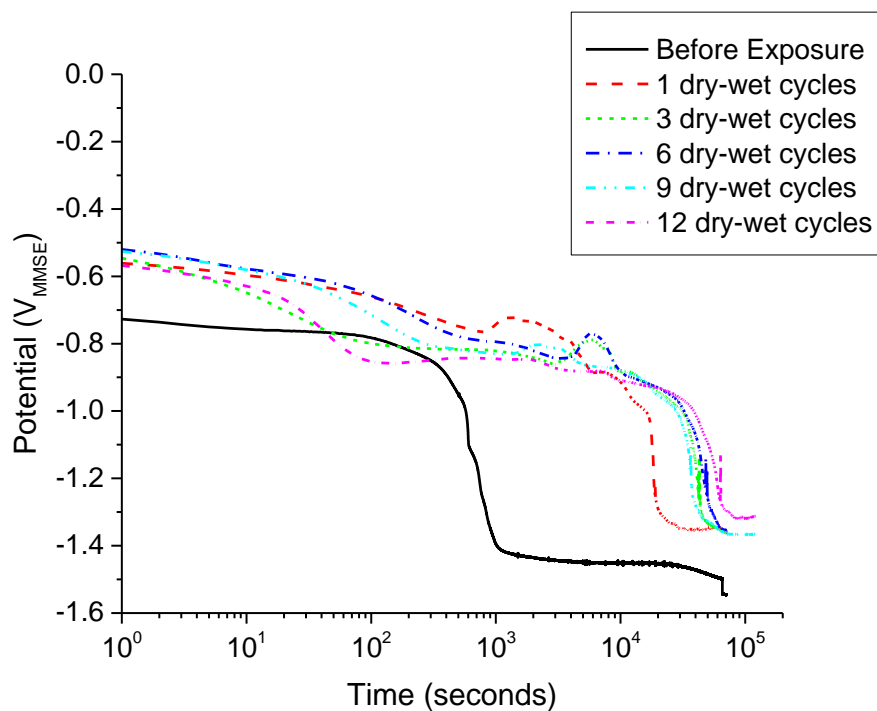
Figure 4.19. GIXRD of Nordic Gold sample when to 1200 grit, deposited with 100 μL of synthetic perspiration solution (23 $^{\circ}\text{C}$, ambient aeration) and exposed to 4 hour wetting-4 hour drying cycles. Spectra highlights FCC metallic Cu, copper oxide, chloride and carbonate corrosion product peaks.

4.4.5 Corrosion Product Layer Analysis by Galvanostatic Reduction

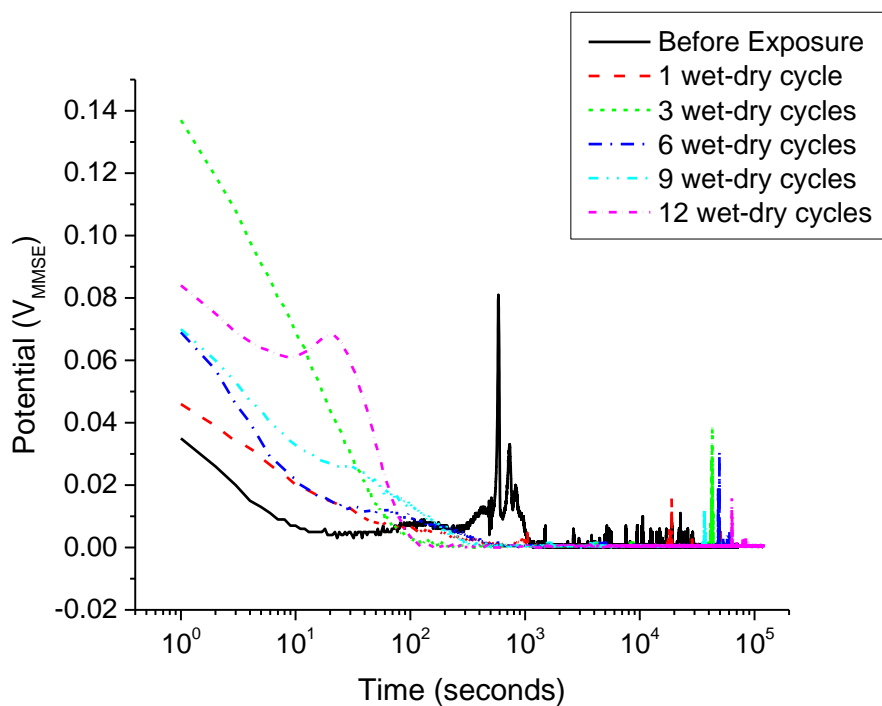
Galvanostatic reduction was utilized as a method to compare corrosion product charge density and identify corrosion species from reduction waves. Figures 4.20-4.21 illustrate the dependence of the number of dry-wet cycles (time) following exposure to

synthetic perspiration solution droplet on the reduction behavior. Following only 1 dry-wet cycle, C11000 develops a significantly thicker corrosion layer that includes a corrosion product that reduces at $-0.5 V_{MMSE}$ which was not seen prior to deposition of synthetic perspiration solution (Figure 4.20). A corrosion product reduced at $-0.8 V_{MMSE}$, which was seen prior to exposure to deposition with synthetic perspiration solution, and which thickens as indicated by longer reduction times. Following synthetic perspiration deposition and 1 dry-wet cycle, a new corrosion product forms that reduces at $-0.75 V_{MMSE}$, but becomes more difficult to identify at 9 and 12 dry-wet cycles. At ≥ 3 dry-wet cycles, a distinct peak occurs during the end of the reduction of corrosion product at $-0.8 V_{MMSE}$. These are not believed to be a result of corrosion species reduction, and is instead a result of the surface of the alloy becoming more catalytic and galvanostatic current being supported with less polarization. Nordic Gold experiences similar behavior, where the outer layer ($-0.6 V_{MMSE}$) thickens over time, but its apparent identity does not change compared to prior to deposition with synthetic perspiration solution (Figure 4.21). The inner corrosion layer ($-0.9 V_{MMSE}$) thickens over time, and a corrosion layer reduced at $-1.2 V_{MMSE}$ develops following deposition with synthetic perspiration solution. Figure 4.23 illustrates the effect of additional alloying elements on corrosion products by comparing C11000 and Nordic Gold after identical conditions, as well as attempts to identify corrosion products based on electrochemical half-cell reduction potentials. Based on Figure 4.23, corrosion products on Nordic Gold are reduced at more negative potentials compared to C11000. The outer corrosion product on Nordic Gold is relatively thicker than C11000, but thinner inner oxides result in an overall thinner corrosion product layer following deposition of synthetic perspiration and 12 dry-wet cycles. Figure

4.22 compares freshly ground samples to those exposed to synthetic perspiration for 1 and 9 dry-wet cycles, confirming the growth of an oxide layer over time as indicated by longer reduction times, and a relatively thinner oxide layer on Nordic Gold compared to C11000. The composition of freshly ground C11000 and Nordic Gold corrosion layers following deposition of synthetic perspiration and 12 dry-wet cycles is suspected (Chapter 2.4.3.4) to consist of a compact, conformed outer layer of CuO and an inner, thicker layer of Cu₂O.¹²⁵ An unidentified corrosion product at -1.3 V_{MMSE} is present in both Nordic Gold and C11000, and therefore cannot be related to exclusively Nordic Gold alloying elements. Another unidentified corrosion product observed prior to 12 dry-wet cycles at -0.85 V_{MMSE}, but not apparent in these galvanostatic reduction waves, also appears on both Nordic Gold and C11000, as seen in Figures 4.20-4.21. There may be electrically disconcerted corrosion products that are not seen in galvanostatic reduction, but seen in GIXRD (Figure 4.24). Figures 4.10-4.11 support the notion of outer deposits.

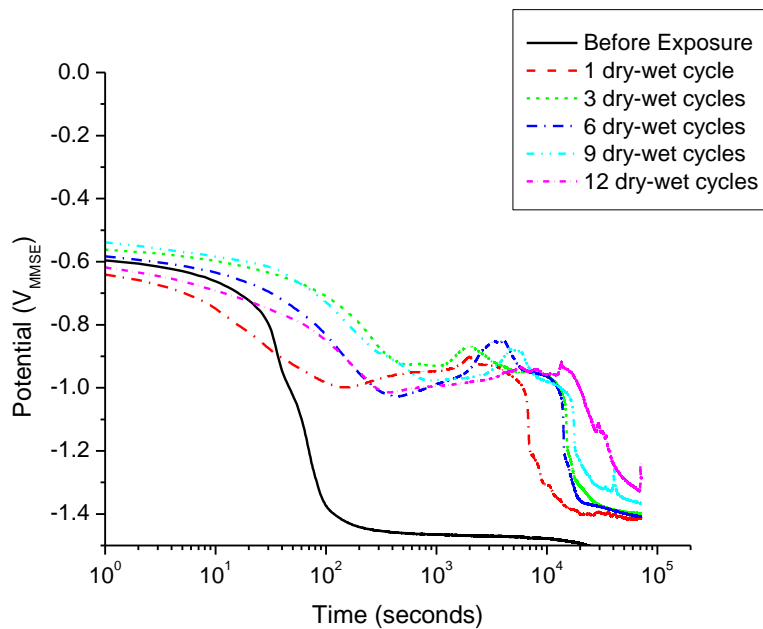


a

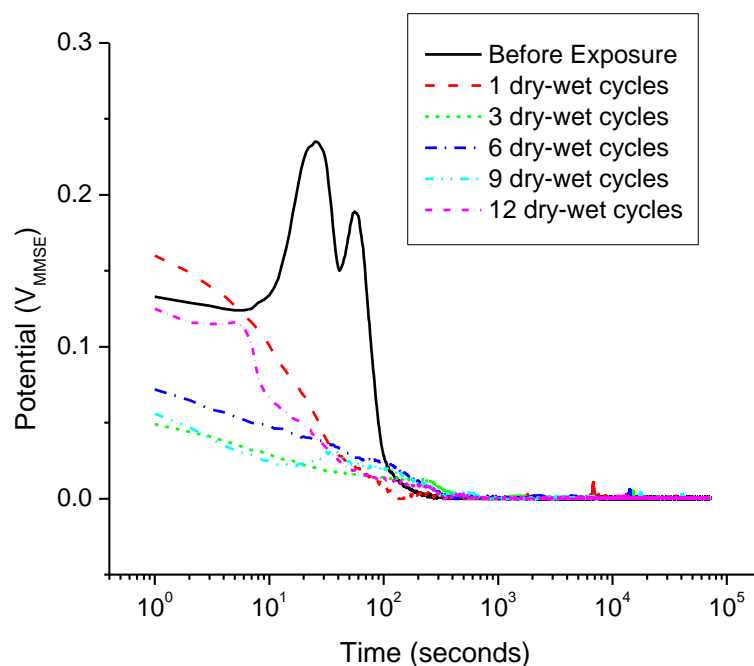


b

Figure 4.20. Galvanostatic reduction of C11000 when freshly ground to 1200 grit, deposited with 100 μL of synthetic perspiration solution (23 $^{\circ}\text{C}$, ambient aeration) and exposed to 4 hour wetting-4 hour drying cycles. Galvanostatic reductions were conducted at 0.02 mA/cm^2 on an area of 0.8 cm^2 . Figure a shows the reduction waves, while figure b shows the inflection points used to determine time of complete reduction.



a



b

Figure 4.21. Galvanostatic reduction of Nordic Gold when freshly ground to 1200 grit, deposited with 100 μL of synthetic perspiration solution (23 $^{\circ}\text{C}$, ambient aeration) and exposed to 4 hour wetting-4 hour drying cycles. Galvanostatic reductions were conducted at 0.02 mA/cm^2 on an area of 0.8 cm^2 . Figure a shows the reduction waves, while figure b shows the inflection points used to determine time of complete reduction.

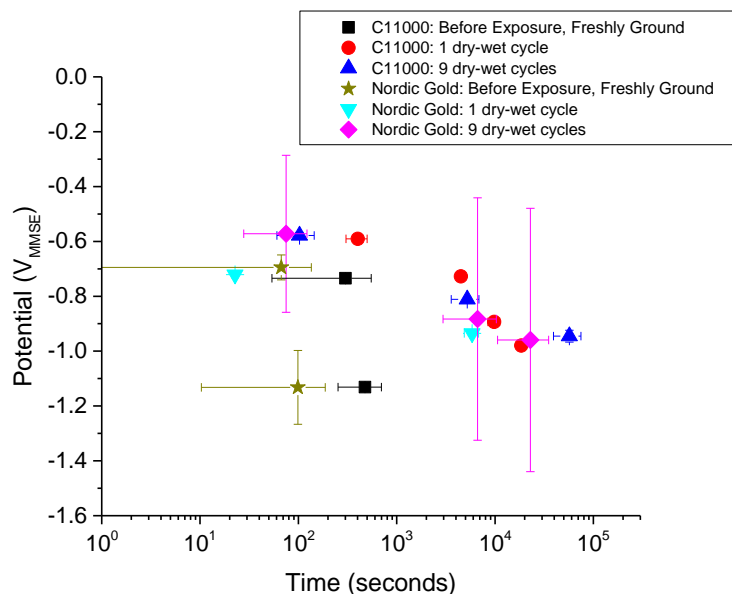


Figure 4.22. Galvanostatic reduction of C11000 and Nordic Gold when freshly ground to 1200 grit, followed by deposition of synthetic perspiration and expose for 1 and 9 dry-wet cycles. Galvanostatic reductions were conducted at 0.02 mA/cm^2 on an area of 0.8 cm^2 . Data is the average of 3 replicates and error bars are one standard deviation.

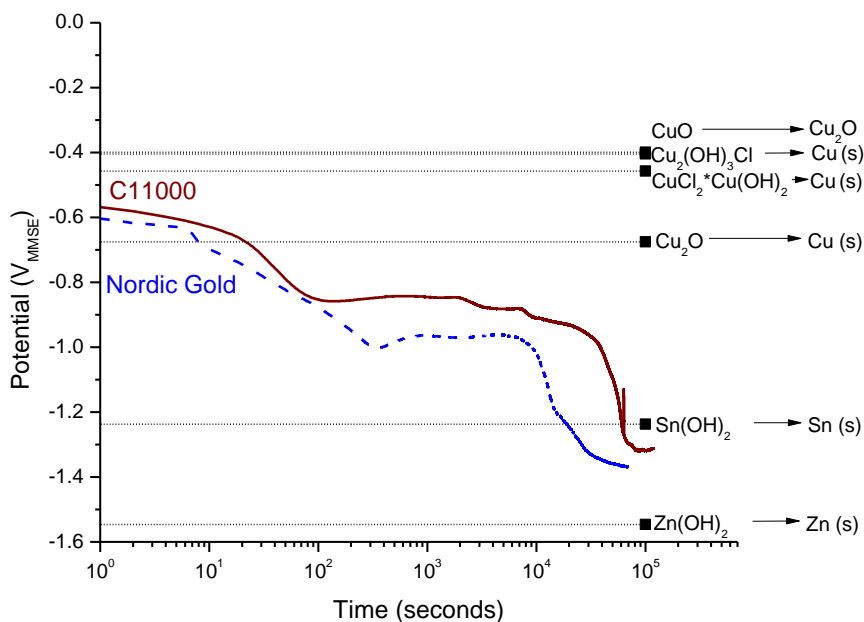


Figure 4.23. Comparative galvanostatic reduction of C11000 (solid red line) and Nordic Gold (dotted blue line) when freshly ground to 1200 grit followed by deposition of synthetic perspiration and 12 dry-wet cycles. Galvanostatic reductions were conducted at 0.02 mA/cm^2 on an area of 0.8 cm^2 .

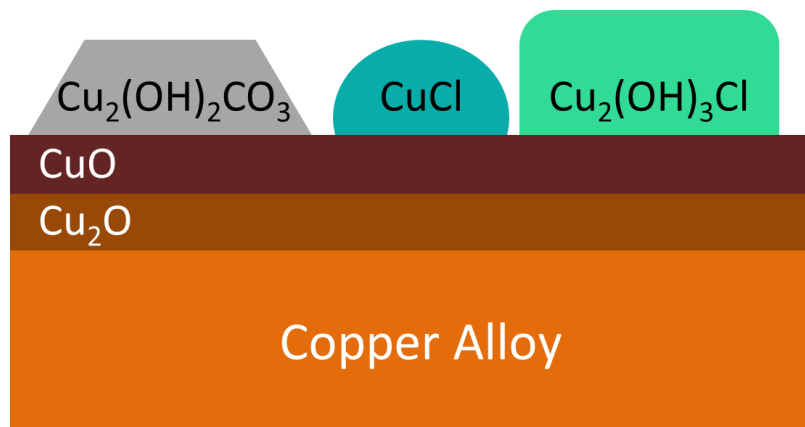


Figure 4.24. Schematic representation of inner directly formed oxides and outer corrosion precipitates formed by homogeneous chemical reaction.

4.4.6 Copper Ion Release Assessed by ICP-OES

Copper ion release was analyzed in the thin electrolyte layer formed during re-wetting conditions by inductively coupled plasma-optical emission spectrometry (ICP-OES). Copper release was assumed to be a factor of both exposure time with synthetic perspiration and alloy composition. As seen in Figure 4.25, copper release tends to decrease as the number of wet-dry cycles (time) increase. This indicates that the solubility level of Cu in the droplet has been reached, and after 1 dry-wet cycle, Cu ions are more likely to end up in corrosion products than as free Cu ions in the restricted volume of the droplet. This issue is discussed further below.

As seen in Figure 4.25, the amount of Cu found in the thin electrolyte layer of Nordic Gold maintained higher values through 3 cycles, unlike C11000 which begins to decrease after only 1 cycle. Following 3 dry-wet cycles, copper release into the thin electrolyte layer between alloys is comparable. Cu ion concentrations are greater than the solubility for CuCl (3.07×10^{18} ions/cm²) and Cu₂(OH)₃Cl (6.79×10^{19} ions/cm²), but below that of Cu₂O (2.53×10^{25} ions/cm²) in water at 25 °C, assuming 0.8 cm². The lower

solubility limit of chloride corrosion products, coupled with the decrease in Cu ions detected at later exposure times, suggest that copper chloride corrosion precipitate from solution by homogeneous chemical reaction. In addition to Cu, Zn was detected in the thin electrolyte on the surface of Nordic Gold by ICP-OES, and was observed to also decrease with the number of cycles (Figure 4.26). Zn to Cu elemental release ratio ranged from 5.9% Zn: 94.1% Cu at maximum (6 cycles) and 4.7% Zn: 95.3% Cu at minimum (9 cycles) compared to an alloy composition of 89% Cu, 5% Zn, 5% Al, 1% Sn in Nordic Gold. No Al or Sn was observed within the calibration range (0.01-100 ppm). This suggests slightly greater Zn release than congruent dissolution.

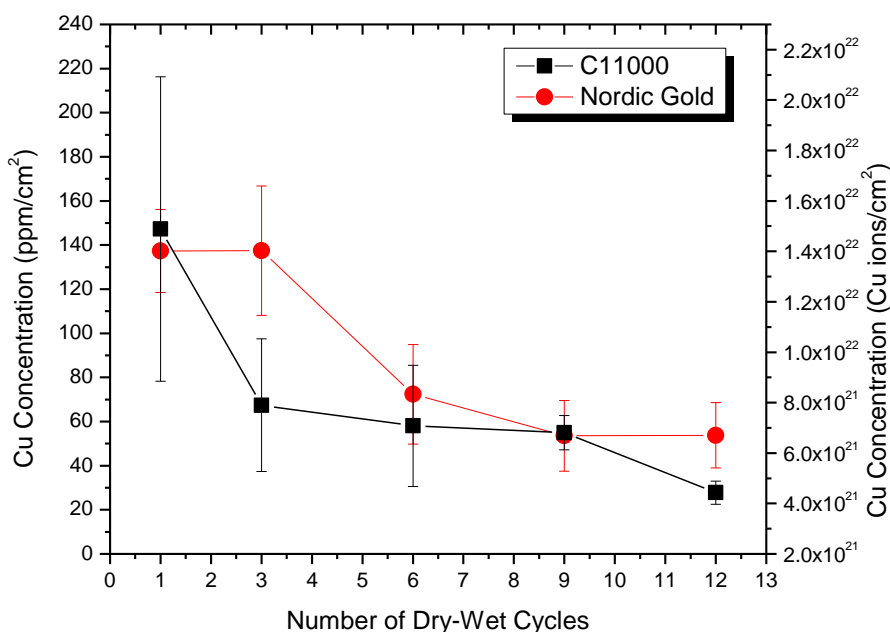


Figure 4.25. Copper concentration as a factor of time for C11000 and Nordic Gold when freshly ground to 1200 grit, deposited with 100 μL of synthetic perspiration solution (23 $^{\circ}\text{C}$, ambient aeration) and exposed to a number of 4 hour drying-4 hour wetting cycles, then washed with 10 mL of synthetic perspiration solution. Average area of droplet size is assumed to be 0.8 cm^2 . Data is the average of 3 replicates and error bars are one standard deviation.

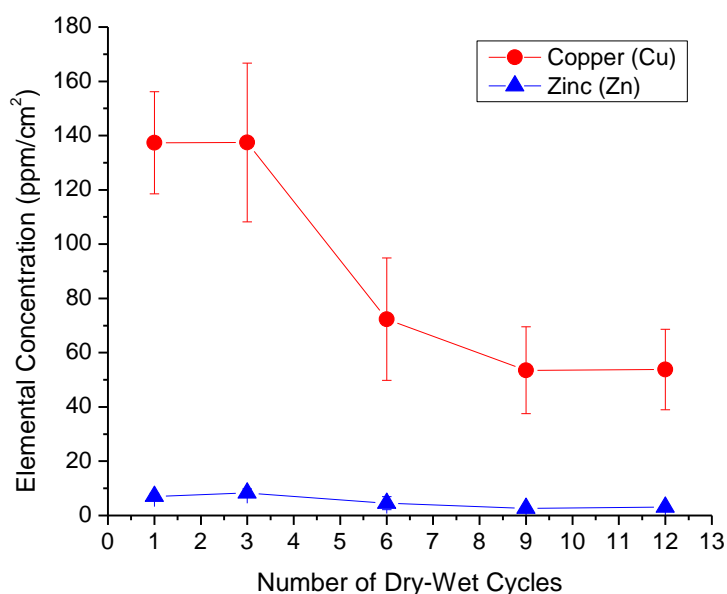


Figure 4.26. Metal concentration as a factor of time for Nordic Gold when freshly ground to 1200 grit, deposited with 100 μL of synthetic perspiration solution (23 $^{\circ}\text{C}$, ambient aeration) and exposed to a number of 4 hour drying-4 hour wetting cycles, then washed with 10 mL of synthetic perspiration solution. Average area of droplet size is assumed to be 0.8 cm^2 . Data is the average of 3 replicates and error bars are one standard deviation.

4.5 Discussion

4.5.1 Summary of Findings

Ideally, the fate of copper can be tracked through the corrosion process of a copper alloy through charge transfer leading to oxide, evaluated by galvanostatic reduction, and charge transfer to the solution, evaluated by ICP-OES, compared to total oxidation charge based on mass loss. Figure 4.27 shows the oxidation charge determined by mass loss assuming Cu^+ , Cu^{2+} and a mix of $\text{Cu}^+/\text{Cu}^{2+}$ justified from GIXRD and galvanostatic reduction compared to the sum of the oxidation charge accounted for by ICP-OES of the electrolyte solution and corrosion products evaluated by galvanostatic

reduction^{xxxv}. As seen by Nordic Gold's lower overall corrosion rate compared to C11000, both have similar charge transfer to solution. Additionally, Nordic Gold has less charge transfer to corrosion products. The sum of the charge transfer to the electrolyte solution and corrosion products is ideally equal to total charge transfer assessed by mass loss (Table 4.6). Figure 4.28 indicates moderate agreement of charge transfer in C11000 and Nordic Gold. It is likely that corrosion products are a mix of Cu^+ and Cu^{2+} , as seen by GIXRD, rather than purely Cu^+ or Cu^{2+} are represented in these calculations. Additionally, not all corrosion products are thought to be electrochemically connected, such as copper chloride corrosion products that form by homogeneous precipitation (Table 4.7), which contributes to discrepancy between the higher Q_{corr} measured by mass loss and Q_{oxide} characterized by galvanostatic reduction. This is supported by substantial mass gain observed on both C11000 and Nordic Gold following exposure to a synthetic perspiration droplet, but before cleaning (Table 4.6).

Table 4.7. Solubility limits of copper corrosion products in 100 μL droplet of synthetic perspiration. $[\text{Cl}^-]$ is 8.6×10^{-2} M, $[\text{H}^+]$ is 3.2×10^{-7} M, and $[\text{OH}^-]$ is 3.2×10^{-8} M.			
Chemical Formula	Reaction	K_{sp}	Solubility of Cu^+ or Cu^{2+} (ions/ cm^2)
$\text{Cu}_2(\text{OH})_3\text{Cl}$ (atacamite)	$2\text{Cu}^{2+} + 3 \text{OH}^- + \text{Cl}^- = \text{Cu}_2(\text{OH})_3\text{Cl}$	1.72×10^{-35}	3.07×10^{18}
Cu_2O (cuprite)	$2\text{Cu}^+ + \text{OH}^- = \text{Cu}_2\text{O} + \text{H}^+$	2.6×10^{-2}	2.53×10^{25}
CuCl (nantokite)	$\text{Cu}^+ + \text{Cl}^- = \text{CuCl}$	1.86×10^{-7}	6.79×10^{19}

^{xxxv} Some corrosion products formed by homogeneous chemical reaction will not be detected by galvanostatic reduction as they are electrically and therefore electrochemically disconnected.

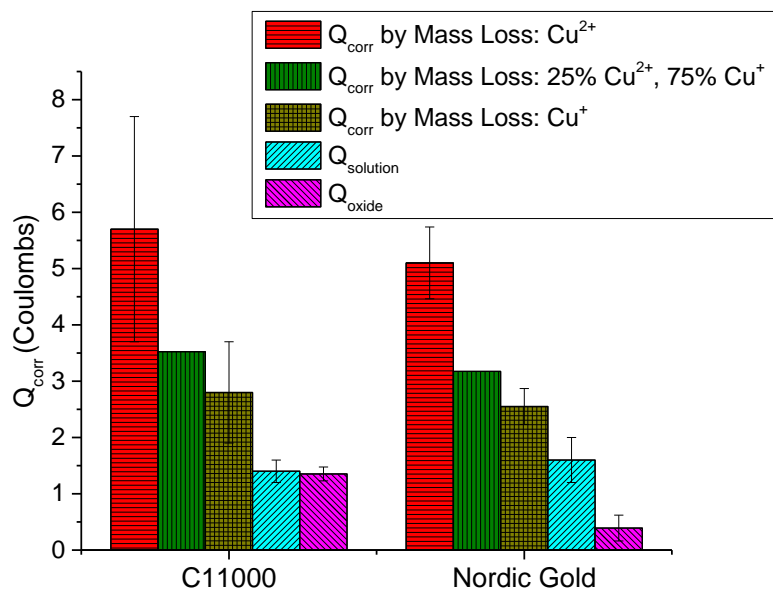


Figure 4.27. Charge analysis of C11000 and Nordic Gold when freshly ground to 1200 grit followed by deposition of 100 μL of synthetic perspiration solution (23 $^{\circ}\text{C}$, ambient aeration) and exposed to 12 dry-wet cycles. Galvanostatic reductions were conducted at 0.02 mA/cm^2 on an area of 0.8 cm^2 . Solution analysis was conducted on 10 mL of synthetic perspiration wash solution utilized to gather thin electrolyte layer <5 minutes before the end of the final dry cycle, with an average droplet area to be 0.8 cm^2 . Incongruent dissolution was determined by ICP-OES and factored into Q_{corr} calculations for Nordic Gold. Corrosion products are likely a mixture of Cu^+ and Cu^{2+} , and precipitate copper chloride products are likely not analyzed by galvanostatic reduction. Data is the average of 3 replicates and error bars are one standard deviation.

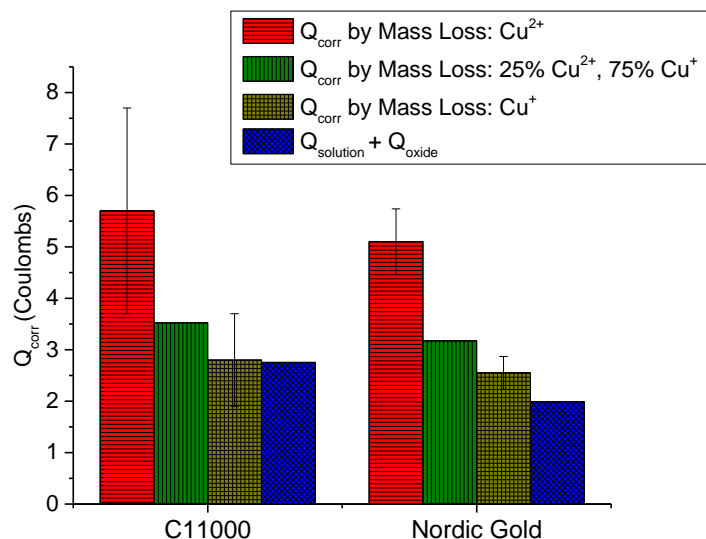


Figure 4.28. Charge analysis of C11000 and Nordic Gold when freshly ground to 1200 grit followed by deposition of 100 μL of synthetic perspiration solution (23 $^{\circ}\text{C}$, ambient aeration) and exposed to 12 dry-wet cycles. Galvanostatic reductions were conducted at 0.02 mA/cm^2 on an area of 0.8 cm^2 . Solution analysis was conducted on 10 mL of synthetic perspiration wash solution utilized to gather thin electrolyte layer <5 minutes before the end of the final dry cycle, with an average droplet area to be 0.8 cm^2 . Summation of Q_{solution} and Q_{oxide} were calculated from the average Q_{solution} and Q_{oxide} values. Incongruent dissolution was determined by ICP-OES and factored into Q_{corr} calculations for Nordic Gold. Corrosion products are likely a mixture of Cu^+ and Cu^{2+} , and precipitate copper chloride products are likely not analyzed by galvanostatic reduction. Data is the average of 3 replicates and error bars are one standard deviation.

4.5.2 Effect of Zn, Al, and Sn Alloying Additions on Copper Corrosion

Electrochemistry and Metal Ion Release during Drying and Wetting of Synthetic Perspiration Solution

It is well known that alloy composition, microstructure and environmental severity effect corrosion behavior. When deposited with synthetic perspiration and subjected to drying-wetting cycles, C11000 and Nordic Gold exhibit different corrosion behavior due to their different alloying composition. Despite the presence of Al and Sn to improve the alloys corrosion resistance^{97,98}, Q_{corr} analysis by mass loss suggests Nordic Gold and C11000 have similar corrosion rate, even when incongruent dissolution has

been accounted for. (Table 4.6). However, Nordic Gold results in thinner oxides compared to C11000 based on galvanostatic reduction (Figures 4.20-4.21), but yields comparable Cu release over time (Figure 4.25). Based on the comparable Cu release between Nordic Gold and C11000, this suggests that the Cu ion release enhancing effect of Sn seen by Goidanich³ is also operative in Nordic Gold. GIXRD and galvanostatic reduction suggest both alloys have similar identity corrosion products, including CuO, Cu₂O, Cu₂(OH)₃Cl and Cu₂(OH)₂CO₃. However, Nordic Gold compact oxide layer thickness is considerably less than C11000, and has a lower mass gain indicative of less corrosion product build-up, likely a result of the alloys corrosion resistant alloying additions Al and Sn (Figures 4.20-4.21, Table 4.6). An evaluation of copper release enables the correlation between corrosion behavior and antimicrobial function of copper alloy surfaces. While individual and/or selected alloying elements (Zn, Sn) have been examined for their effect on copper release³, the effect of multiple alloying additions that have opposing suppressing and enhancing effects has not. As seen in Figure 4.25, copper release from Nordic Gold is greater than C11000 at early times due to compact oxides and similar i_{corr} . After 12 cycles, Cu ion concentration of both alloys was comparable. This suggests that the enhancing effect of Sn is able to overcome both any inhibiting effect from other alloying elements that support passivation, and the lower stoichiometric availability of Cu from Nordic Gold.

Therefore, oxide formation occurs by direct oxidation as compact oxide film that is alloy dependent and homogeneous chemical precipitation due to supersaturation of the droplet volume that is not alloy dependent. Based on total mass gained following exposure to 100 μL droplet of perspiration and 12 dry-wet cycles, Nordic Gold and

C11000 accumulate similar amounts of corrosion products as these products are governed by solution chemistry, not alloy type (Table 4.6). However, galvanostatic reduction indicates a thinner compact oxide film formed by direct oxidation on Nordic Gold compared to C11000, which enables greater copper release at short time periods and comparable copper release at long times (Figures 4.20-4.21).

4.5.3 Ability to Achieve Critical Concentration for Antimicrobial Efficacy

Figure 4.29 shows the results disinfection “kill curves” performed at the University of Virginia to observe the relative effectiveness of copper ions (Cu^{2+}) at varying concentrations on killing *E. coli* (HCB1) in synthetic perspiration, and enumerated by the most probable number (MPN) method utilizing Colilert® and Quanti-Trays® (Idexx). At concentrations above 0.1 ppm Cu^{2+} , such as 1, 10, or 100 ppm, *E. coli* (HCB1) populations dropped faster than natural die off, indicating antimicrobial activity. The volume of the thin electrolyte layer formed during re-wetting was not determined, and therefore no calculations can determine the exact concentration (ppm) of Cu in only the thin electrolyte layer to correlate with antimicrobial behavior observed in congruent testing. However, in the 10 mL wash sample collected including the thin electrolyte layer, initial values exceeded 100 ppm, and remain above 40 ppm for the extent of the study. The fact that concentrations would be significantly greater in the small volume of thin electrolytes, Figure 4.29 suggests both alloys would release enough Cu after one drying-wetting cycle to result in antimicrobial efficacy in less than 8 hours.

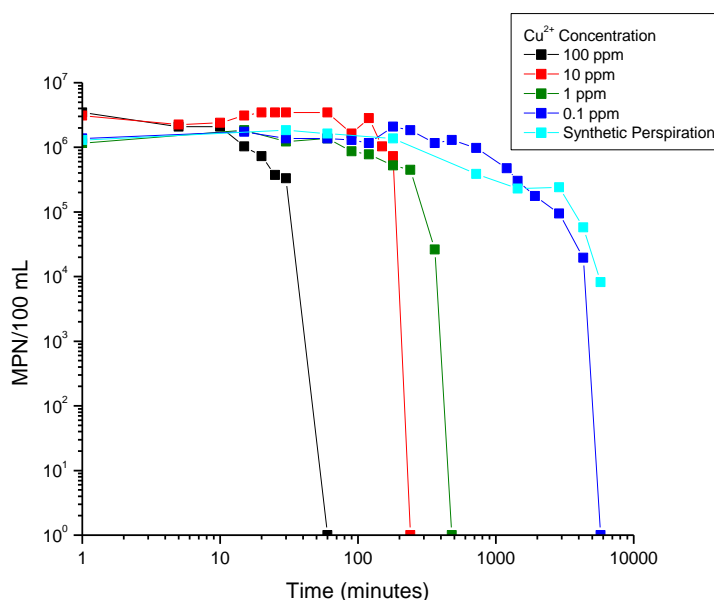


Figure 4.29. University of Virginia disinfection studies of *E. coli* (HCB1) in solution of synthetic perspiration (0.5% NaCl, 0.1% CH₄N₂O, 0.1% C₃H₆O₃, pH 6.5) and Cu²⁺ ions from a CuCl₂ solution at 23 °C, enumerated by most probable number (MPN) method.

4.5.4 Effect of Drying and Wetting Synthetic Perspiration Testing on Corrosion Behavior compared to Full Immersion Synthetic Perspiration Solution and Full Immersion Concentrated Synthetic Perspiration Solution

It is well known that the environment effects corrosion behavior, particularly the relative humidity of the surroundings and the composition of the electrolyte solution. An examination of copper alloys deposited with synthetic perspiration prior to drying-wetting experiments compared to full immersion experiments utilizing synthetic perspiration and concentrated synthetic perspiration (2 M NaCl, 1 M CH₄N₂O, 0.11 M C₃H₆O₃) indicates both a change in corrosion behavior and the fate of copper. As seen in Figure 4.30a, drying-wetting experiments resulted in greater mass loss in C11000 over 96 hours compared to either full immersion testing solution over 130 hours, normalized by the number of hours exposed to perspiration. Mass loss in Nordic Gold was greater in

drying-wetting experiments than full immersion in synthetic perspiration, but lower than full immersion in concentrated perspiration (Figure 4.30a). This result suggests that wetting-drying conditions are more severe than full immersion synthetic perspiration at regular strength. These trends are also reflected in the total oxidation charge for corrosion (Q_{corr}) (Figure 4.30b). The corrosion rate of Nordic Gold is slightly lower than C11000 in the case of full immersion and drying-wetting testing with synthetic perspiration. However, full immersion testing with concentrated perspiration solution result in greater Q_{corr} in Nordic Gold compared to C11000 (Figure 4.30b). This indicates that cyclic wetting-drying with a droplet of synthetic perspirations solution is not well represented by either full immersion testing or synthetic perspirations solution or concentrated synthetic perspiration solution. While concentrated synthetic perspiration may mimic concentration build-up just before drying, other complexities are not simulated.

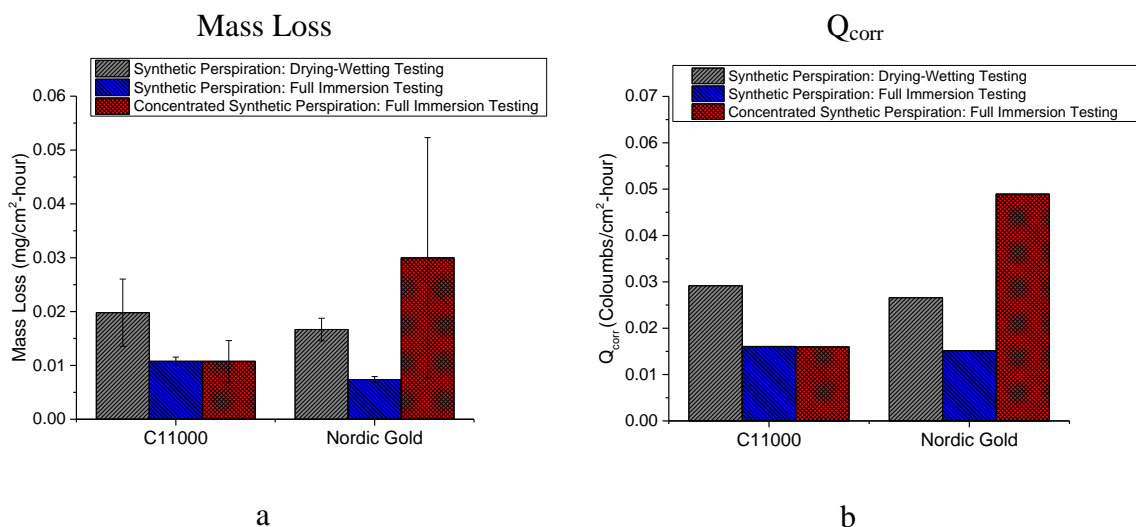


Figure 4.30. A comparison of C11000 and Nordic Gold corrosion behavior exposed to different testing environments, when freshly ground to 1200 grit. Drying-wetting testing was conducted by the deposition of 100 L of synthetic perspiration, approximate area of 0.8 cm². Full immersion testing was conducted by the exposure of 300 mL solution to a 0.8 cm² area of alloy. Mass loss and Q_{corr} are normalized by the number of hours testing occurred over (130 hours for full immersion testing, 96 hours for drying-wetting testing). In the case of concentrated perspiration full immersion and synthetic perspiration drying-wetting testing, incongruent dissolution was determined by ICP-OES and factored into Q_{corr} calculations. Data is the average of 3 replicates and error bars are one standard deviation.

As seen in Figure 4.31, corrosion product analysis by galvanostatic reduction differed in both alloys depending on testing environment. On both alloys, drying-wetting testing resulted in significantly thicker corrosion product layers compared to either full immersion testing solutions. Additionally, galvanostatic reductions following drying-wetting testing were observed to include more small waves that could not be assigned to a specific corrosion species. Concerning C11000, full immersion concentrated perspiration solution resulted in the thinnest corrosion layer as assessed by reduction charge, followed by full immersion synthetic perspiration then drying-wetting testing with synthetic perspiration. On Nordic Gold, both full immersion testing solutions are similar in oxide thickness as assessed by reduction charge, and significantly thinner than

that formed by drying-wetting testing. The identities of the corrosion species in all cases were primarily CuO and Cu₂O, with an unknown species reduction at -1.3 V_{MSE} that occurred in both full immersion with concentrated perspiration solution and drying-wetting testing with synthetic perspiration solution.

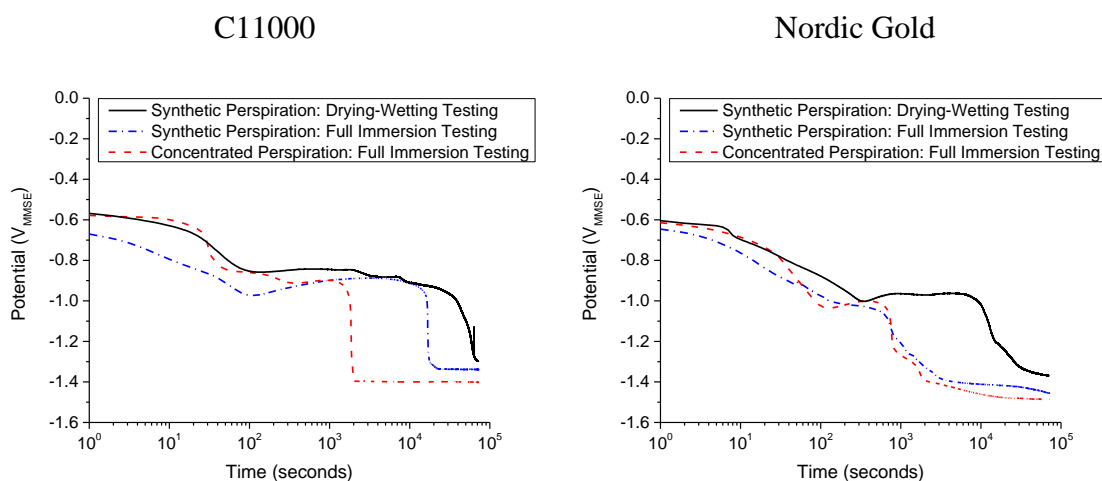


Figure 4.31. A comparison of C11000 and Nordic Gold corrosion behavior exposed to different testing environments, when freshly ground to 1200 grit. Drying-wetting testing was conducted by the deposition of 100 L of synthetic perspiration, approximate area of 0.8 cm². Full immersion testing was conducted by the exposure of 300 mL solution to a 0.8 cm² area of alloy. Galvanostatic reduction waves were compared at 96 hours of exposure for full immersion testing, and 12 dry-wet cycles (96 total hours) for drying-wetting testing.

An evaluation of copper release enables the correlation between corrosion behavior and antimicrobial function of copper alloy surfaces, and is highly dependent on environment. Figure 4.32 indicates that while both full immersion testing solutions indicate an increase in copper ions released over time, drying-wetting testing with synthetic perspiration is initially highest in early cycles and decreases over time likely due to precipitation by homogeneous chemical reactions subject to solubilities of specific corrosion products in the finite volume of the droplet. Drying-wetting testing with

synthetic perspiration solution results in significantly higher copper ion release compared to full immersion testing with synthetic perspiration solution. Compared to full immersion testing with concentrated perspiration solution (pH=2.8), drying-wetting testing with synthetic perspiration has regions of time when copper ion release is comparable between the two, but deviates at the two extremes tested (short times and long times). At long times, release is more severe in concentrated synthetic perspiration solution. This is the result of the high driving force for oxidation combined with high oxide solubility in the large volume acidic solution.

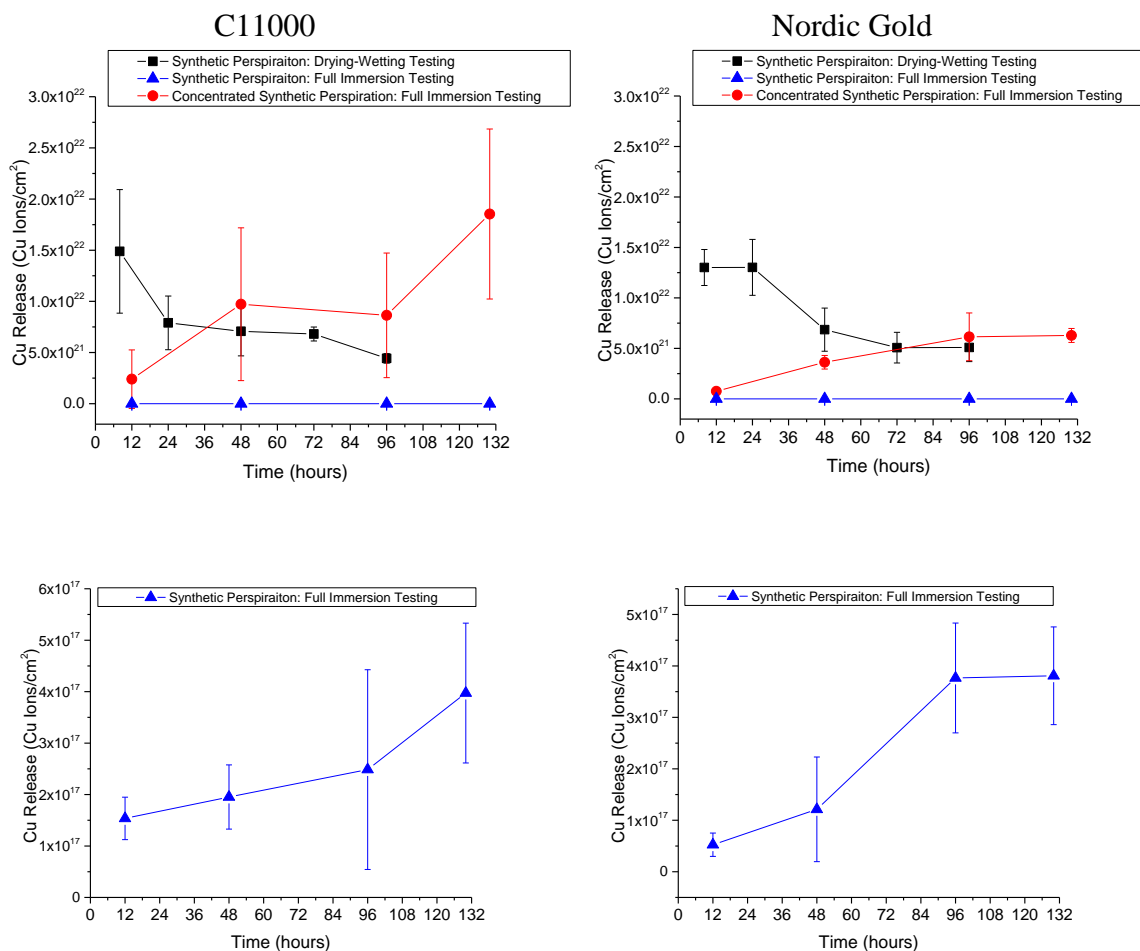


Figure 4.32. Copper release from C11000 (left) and Nordic Gold (right) when freshly ground to 1200 grit. Drying-wetting testing was conducted by the deposition of 100 μL of synthetic perspiration, approximate area of 0.8 cm^2 , and washing of the thin electrolyte layer with 10 mL of synthetic perspiration for ICP-OES analysis. Full immersion testing was conducted by the exposure of 300 mL solution to a 0.8 cm^2 area of alloy, and an aliquot of exposure solution was collected for ICP-OES analysis. Data is the average of 3 replicates and error bars are one standard deviation.

4.6 Conclusion

This study showed that Al, Zn, and Sn in the Cu-Al-Zn-Sn alloy (Nordic Gold) suppress film formation during cyclic drying-wetting corrosion conditions compared to commercially pure C11000. Despite Al and Sn alloying additions, Nordic Gold and C11000 was observed to have no statistical difference in total oxidation charge

determined by mass loss. Evidence of CuO, Cu₂O, Cu₂(OH)₃Cl and Cu₂(OH)₂CO₃ were observed on both alloys. CuO and Cu₂O were theorized to form by direct oxidation while Cu₂(OH)₃Cl and Cu₂(OH)₂CO₃ were formed by supersaturation of the droplet, resulting in precipitation by homogeneous chemical reaction. C11000 and Nordic Gold had slightly lower mass gain over 12 dry-wet cycles, suggesting less precipitated corrosion product. However, Nordic Gold resulted in thinner electrochemically connected compact oxide layer. This thinner corrosion film enables more copper release from the bulk alloy despite comparable corrosion rate and a lower percentage of Cu in the bulk alloy. Based on the dissolved Cu concentrations measured, it is argued that both alloys would provide sufficient Cu²⁺ necessary to kill *E. coli* (HCB1) in time periods less than 8 hours.

5 Future Work

The following future work is suggested to further the study of Nordic Gold for antimicrobial hospital applications:

1. Explore additional characterization techniques for oxide analysis following full immersion studies and wet-dry studies using synthetic perspiration solution. Examining corrosion products formed using X-ray photoelectron spectroscopy and Raman spectroscopy could detect possible Al and Sn oxides formed during the corrosion of Nordic Gold, while glow discharge optical emission spectrometry and auger depth profiling can obtain interfacial composition between oxides.
2. Further exploration of corrosion behavior during cyclic wetting and drying with droplets of synthetic perspiration would include scanning Kelvin probe studies to observe the potential during the corrosion process.
3. Explore the fate of copper of Nordic Gold and C11000 during full immersion exposure to a nutrient broth, such as tryptone soy broth. This investigation would be designed to quantitatively determine the copper ion release of Nordic Gold in a medium reported to be used for the evaluation of antimicrobial efficacy by EPA testing procedures. By utilizing full immersion testing procedures similar to those already explored for synthetic perspiration solutions, insight into the results of EPA testing evaluations will be gained, as this study will be a factor of both alloy composition and a comparative study to previous solutions tested. This study is necessary to address the discrepancy between CDA reported findings and findings presented in this thesis.

4. Explore the fate of copper of model binary and ternary alloys during full immersion testing exposure to synthetic perspiration. This study is designed to identify individual alloying elemental effects of Al, Sn, and Zn on the fate of copper through the use of model binary alloys. The use of model ternary alloys will enable insight into multi-elemental effects, such as in the case of Zn and Sn, where one element is suspected to suppress copper ion release and the other to promote copper ion release or something else such as passivation.
5. Explore the empirical antimicrobial effect of Nordic Gold and C11000 compared while tracked copper ion release in synthetic perspiration solution. By utilizing shavings of Nordic Gold and C11000 as a source of copper ions in bacteria kill rate studies, the rate of bacteria die-off can be related to the rate of copper-ion release measured at identical sampling periods. This study would serve to link the reported behavior found in EPA testing procedures to the full immersion testing procedures.

References

1. H.T. Michels, J.O. Noyce, and C.W. Keevil, "Effects of temperature and humidity on the efficacy of methicillin-resistant *Staphylococcus aureus* challenged antimicrobial materials containing silver and copper," *Letters in Applied Microbiology* 49, 2 (2009): p. 191-195.
2. J. Michel, L.L. Foster and J.R. Scully, Editors. 2014.
3. S. Goidanich, I.O. Wallinder, G. Herting, and C. Leygraf, "Corrosion induced metal release from copper based alloys compared to their pure elements," *Corros Eng Sci Techn* 43, 2 (2008): p. 134-141.
4. S. Harbarth and D. Pittet, "Control of nosocomial methicillin-resistant *Staphylococcus aureus*: Where shall we send our hospital director next time?," *Infect Cont Hosp Ep* 24, 5 (2003): p. 314-316.
5. G.L. French, J.A. Otter, K.P. Shannon, N.M.T. Adams, D. Watling, and M.J. Parks, "Tackling contamination of the hospital environment by methicillin-resistant *Staphylococcus aureus* (MRSA): a comparison between conventional terminal cleaning and hydrogen peroxide vapour decontamination," *Journal of Hospital Infection* 57, 1 (2004): p. 31-37.
6. A.P. Johnson, A. Pearson, and G. Duckworth, "Surveillance and epidemiology of MRSA bacteraemia in the UK," *J Antimicrob Chemoth* 56, 3 (2005): p. 455-462.
7. N.A. Office, *The management and control of hospital acquired infection in acute NHS trusts in England*. 2000: London: The Stationary Office.
8. K. Huslage, W.A. Rutala, E. Sickbert-Bennett, and D.J. Weber, "A Quantitative Approach to Defining "High-Touch" Surfaces in Hospitals " *Infection Control and Hospital Epidemiology* 31, 8 (2010): p. 850-853.
9. C.f.D.C.a. Prevention, *National and State Healthcare-Associated Infections Standardized Infection Ratio Report, in January-December 2010*. 2010.
10. H.F.L. Wertheim, M.C. Vos, H.A.M. Boelens, A. Voss, C.M.J.E. Vandembroucke-Grauls, M.H.M. Meester, J.A.J.W. Kluytmans, P.H.J. van Keulen, and H.A. Verbrugh, "Low prevalence of methicillin-resistant *Staphylococcus aureus* (MRSA) at hospital admission in the Netherlands: the value of search and destroy and restrictive antibiotic use," *Journal of Hospital Infection* 56, 4 (2004): p. 321-325.
11. B.M. Farr, "Political versus epidemiological correctness," *Infect Cont Hosp Ep* 28, 5 (2007): p. 589-593.
12. S.P. Barrett, R.V. Mummery, and B. Chattopadhyay, "Trying to control MRSA causes more problems than it solves," *Journal of Hospital Infection* 39, 2 (1998): p. 85-93.
13. E. Girou, G. Pujade, P. Legrand, F. Cizeau, and C. Brun-Buisson, "Selective screening of carriers for control of methicillin-resistant *Staphylococcus aureus* (MRSA) in high-risk hospital areas with a high level of endemic MRSA," *Clin Infect Dis* 27, 3 (1998): p. 543-550.
14. K.J. Hardy, B.A. Oppenheim, S. Gossain, F. Gao, and P.M. Hawkey, "Study of the relationship between environmental contamination with methicillin-resistant *Staphylococcus aureus* (MRSA) and patients' acquisition of MRSA," *Infect Cont Hosp Ep* 27, 2 (2006): p. 127-132.

15. T.A.S.o.H.E.S.o.t.A.H. Association, *Practice Guidance for Healthcare Environmental Cleaning*. 2010.
16. S. Harbarth, C. Fankhauser, J. Schrenzel, J. Christenson, P. Gervaz, C. Bandiera-Clerc, G. Renzi, N. Vernaz, H. Sax, and D. Pittet, "Universal screening for methicillin-resistant *Staphylococcus aureus* at hospital admission and nosocomial infection in surgical patients," *Jama-J Am Med Assoc* 299, 10 (2008): p. 1149-1157.
17. A. Copper, *Practical Aspects of Reducing Bioburden with Copper: Clinical Case Study: Selly Oak Hospital, Birmingham*. 2009.
18. L. Weaver, H.T. Michels, and C.W. Keevil, "Survival of *Clostridium difficile* on copper and steel: futuristic options for hospital hygiene," *Journal of Hospital Infection* 68, 2 (2008): p. 145-151.
19. S.J. Dancer, "Mopping up hospital infection," *Journal of Hospital Infection* 43, 2 (1999): p. 85-100.
20. J.J. Shim and J.G. Kim, "Copper corrosion in potable water distribution systems: influence of copper products on the corrosion behavior," *Materials Letters* 58, 14 (2004): p. 2002-2006.
21. A. Copper, *Antimicrobial Copper: The Only Touch Surfaces Approved by the U.S. Environmental Protection Agency (EPA) to Make Human Health Claims*.
22. M.T. Madigan, J.M. Martinko, D.A. Stahl, and D.P. Clark, *Brock Biology of Microorganisms*. 13 ed: Benjamin Cummings, 2010). p. 1152.
23. H.H.A. Dollwet and J.R.J. Sorenson, "Historic Uses of Copper-Compounds in Medicine," *Trace Elem Med* 2, 2 (1985): p. 80-87.
24. G. Grass, C. Rensing, and M. Solioz, "Metallic Copper as an Antimicrobial Surface," *Appl Environ Microb* 77, 5 (2011): p. 1541-1547.
25. S.A. Wilks, H. Michels, and C.W. Keevil, "The survival of *Escherichia coli* O157 on a range of metal surfaces," *Int J Food Microbiol* 105, 3 (2005): p. 445-454.
26. J. Elguindi, J. Wagner, and C. Rensing, "Genes involved in copper resistance influence survival of *Pseudomonas aeruginosa* on copper surfaces," *J Appl Microbiol* 106, 5 (2009): p. 1448-1455.
27. C.E. Santo, E.W. Lam, C.G. Elowsky, D. Quaranta, D.W. Domaille, C.J. Chang, and G. Grass, "Bacterial Killing by Dry Metallic Copper Surfaces," *Appl. Environ. Microbiol.* 77, 3 (2011): p. 794-802.
28. Y. Ohsumi, K. Kitamoto, and Y. Anraku, "Changes Induced in the Permeability Barrier of the Yeast Plasma-Membrane by Cupric Ion," *J Bacteriol* 170, 6 (1988): p. 2676-2682.
29. S.L. Warnes, S.M. Green, H.T. Michels, and C.W. Keevil, "Biocidal Efficacy of Copper Alloys against Pathogenic Enterococci Involves Degradation of Genomic and Plasmid DNAs," *Appl Environ Microb* 76, 16 (2010): p. 5390-5401.
30. D.R. Lloyd and D.H. Phillips, "Oxidative DNA damage mediated by copper(II), iron(II) and nickel(II) Fenton reactions: evidence for site-specific mechanisms in the formation of double-strand breaks, 8-hydroxydeoxyguanosine and putative intrastrand cross-links," *Mutat Res-Fund Mol M* 424, 1-2 (1999): p. 23-36.
31. K.W.v. Nägeli, "Über oligodynamische Erscheinungen in lebenden Zellen," *Neue Denkschr. Allgemein. Schweiz. Gesellsch. Ges. Naturwiss.* Bd XXXIII Abt 1. (1893).

32. A. Top and S. Ulku, "Silver, zinc, and copper exchange in a Na-clinoptilolite and resulting effect on antibacterial activity," *Appl Clay Sci* 27, 1-2 (2004): p. 13-19.
33. W.L. Du, S.S. Niu, Y.L. Xu, Z.R. Xu, and C.L. Fan, "Antibacterial activity of chitosan tripolyphosphate nanoparticles loaded with various metal ions," *Carbohydr Polym* 75, 3 (2009): p. 385-389.
34. T.N. Kim, Q.L. Feng, J.O. Kim, J. Wu, H. Wang, G.Q. Chen, and F.Z. Cui, "Antimicrobial effects of metal ions (Ag⁺, Cu²⁺, Zn²⁺) in hydroxyapatite," *J Mater Sci-Mater M* 9, 3 (1998): p. 129-134.
35. M. Yamada, K. Kato, K. Shindo, M. Nomizu, M. Haruki, N. Sakairi, K. Ohkawa, H. Yamamoto, and N. Nishi, "UV-irradiation-induced DNA immobilization and functional utilization of DNA on nonwoven cellulose fabric," *Biomaterials* 22, 23 (2001): p. 3121-3126.
36. V.K. Sharma, R.A. Yngard, and Y. Lin, "Silver nanoparticles: Green synthesis and their antimicrobial activities," *Adv Colloid Interfac* 145, 1-2 (2009): p. 83-96.
37. J.V. Rogers, C.V. Parkinson, Y.W. Choi, J.L. Speshock, and S.M. Hussain, "A preliminary assessment of silver nanoparticle inhibition of monkeypox virus plaque formation," *Nanoscale Res Lett* 3, 4 (2008): p. 129-133.
38. P.V. AshaRani, M.P. Hande, and S. Valiyaveetil, "Anti-proliferative activity of silver nanoparticles," *Bmc Cell Biol* 10, (2009).
39. O. Choi, K.K. Deng, N.J. Kim, L. Ross, R.Y. Surampalli, and Z.Q. Hu, "The inhibitory effects of silver nanoparticles, silver ions, and silver chloride colloids on microbial growth," *Water Res* 42, 12 (2008): p. 3066-3074.
40. Q. Bao, D. Zhang, and P. Qi, "Synthesis and characterization of silver nanoparticle and graphene oxide nanosheet composites as a bactericidal agent for water disinfection," *J Colloid Interf Sci* 360, 2 (2011): p. 463-470.
41. Q.L. Li, S. Mahendra, D.Y. Lyon, L. Brunet, M.V. Liga, D. Li, and P.J.J. Alvarez, "Antimicrobial nanomaterials for water disinfection and microbial control: Potential applications and implications," *Water Res* 42, 18 (2008): p. 4591-4602.
42. I. Codita, D. Caplan, E.-C. Dragulescu, E.B. Lixandru, L. Coldea, C. Dragomirescu, C. Surdu-Bob, and M. Badulescu, "ANTIMICROBIAL ACTIVITY OF COPPER AND SILVER NANOFILMS ON NOSOCOMIAL BACTERIAL SPECIES," *Arch. Microbiol. Immunol.* 69, (2010): p. 204-212.
43. K.Y. Yoon, J.H. Byeon, J.H. Park, and J. Hwang, "Susceptibility constants of *Escherichia coli* and *Bacillus subtilis* to silver and copper nanoparticles," *Sci Total Environ* 373, 2-3 (2007): p. 572-575.
44. J.P. Ruparelia, A.K. Chatterjee, S.P. Duttagupta, and S. Mukherji, "Strain specificity in antimicrobial activity of silver and copper nanoparticles," *Acta Biomater* 4, 3 (2008): p. 707-716.
45. J.F. Hernandez-Sierra, F. Ruiz, D.C.C. Pena, F. Martinez-Gutierrez, A.E. Martinez, A.D.P. Guillen, H. Tapia-Perez, and G.A. Martinez-Castanon, "The antimicrobial sensitivity of *Streptococcus mutans* to nanoparticles of silver, zinc oxide, and gold," *Nanomed-Nanotechnol* 4, 3 (2008): p. 237-240.
46. M.M. Abd-Elzaher, "Synthesis, characterization, and antimicrobial activity of cobalt(II), nickel(II), copper(II) and zinc(II) complexes with ferrocenyl Schiff bases containing a phenol moiety," *Appl Organomet Chem* 18, 4 (2004): p. 149-155.

47. L.P.T.M. Zevenhuizen, J. Dolfing, E.J. Eshuis, and I.J. Scholtenkoerselman, "Inhibitory Effects of Copper on Bacteria Related to the Free Ion Concentration," *Microbial Ecol* 5, 2 (1979): p. 139-146.
48. R.A. MacLeod, S.C. Kuo, and R. Gelinas, "Metabolic injury to bacteria. II. Metabolic injury induced by distilled water or Cu⁺⁺ in the plating diluent.," *J. Bacteriol* 93, 3 (1967): p. 961-969.
49. *Test Method for Efficacy of Copper Alloy Surfaces as a Sanitizer*, E.P. Agency, Editor.
50. *Test Method for Residual Self-Sanitizing Activity of Copper Alloy Surfaces*, E.P. Agency, Editor.
51. *Test Method for the Continuous Reduction of Bacterial Contamination on Copper Alloy Surfaces*, E.P. Agency, Editor.
52. R.W. Bennett and G.A. Lancette. *Staphylococcus aureus*. Bacteriological Analytical Manual 2001 2/10/14].
53. H.J. Hoben and P. Somasegaran, "Comparison of the Pour, Spread, and Drop Plate Methods for Enumeration of Rhizobium Spp in Inoculants Made from Pre-Sterilized Peat," *Appl Environ Microb* 44, 5 (1982): p. 1246-1247.
54. C.D. Association. *Laboratory testing of Antimicrobial Copper reveals 3 key benefits*. April 4, 2014]; Available from: <http://antimicrobialcopper.com/us/scientific-proof/epa-registration.aspx>.
55. J.O. Noyce, H. Michels, and C.W. Keevil, "Potential use of copper surfaces to reduce survival of epidemic meticillin-resistant Staphylococcus aureus in the healthcare environment," *J Hosp Infect* 63, 3 (2006): p. 289-297.
56. J.O. Noyce, H. Michels, and C.W. Keevil, "Use of Copper Cast Alloys To Control Escherichia coli O157 Cross-Contamination during Food Processing," *Appl Environ Microb* 72, 6 (2006): p. 4239-4244.
57. H.T. Michels, *Copper Alloys for Human Infectious Disease Control*, in *Materials Science and Technology Conference*. 2005: Pittsburg, PA.
58. C. Leygraf and T.E. Graedel, Atmospheric corrosion. The Electrochemical Society series (New York: Wiley-Interscience, 2000). p. xii, 354 p.
59. D.W. Rice, P. Peterson, E.B. Rigby, P.B.P. Phipps, R.J. Cappell, and R. Tremoureux, "Atmospheric Corrosion of Copper and Silver," *J Electrochem Soc* 128, 2 (1981): p. 275-284.
60. H.M. Ha and J.R. Scully, "Artificial Pit Study on Effects of Bulk Solution Composition Changes on Copper Pitting Propagation in Synthetic Potable Waters," *Journal of the Electrochemical Society* 159, 12 (2012): p. C571-C582.
61. W. He, I.O. Wallinder, and C. Leygraf, "A Comparison Between Corrosion Rates and Runoff Rates from New and Aged Copper and Zinc as Roofing Material," *Water, Air, & Soil Pollution: Focus* 1, 3-4 (2001): p. 67-82.
62. I.O. Wallinder and C. Leygraf, "Seasonal variations in corrosion rate and runoff rate of copper roofs in an urban and a rural atmospheric environment," *Corros Sci* 43, 12 (2001): p. 2379-2396.
63. S. Colin, E. Beche, R. Berjoan, H. Jolibois, and A. Chambaudet, "An XPS and AES study of the free corrosion of Cu-, Ni- and Zn-based alloys in synthetic sweat," *Corros Sci* 41, 6 (1999): p. 1051-1065.

64. T. Aastrup and C. Leygraf, "Simultaneous infrared reflection absorption spectroscopy and quartz crystal microbalance measurements for in situ studies of the metal/atmosphere interface," *J Electrochem Soc* 144, 9 (1997): p. 2986-2990.
65. W.H.J. Vernon, "The Formation of Protective oxide Films on Copper and Brass by Exposure to Air at Various Temperatures," *J. Chem. Soc.* (1926): p. 2278.
66. W.E. Cambell and U.B. Thomas, *Tarnishing and Contamination of Metals*, in *Electrical Contacts*. 1968, Illinois Institute of Tech.: Chicago. p. 233.
67. R. Schubert and S.M. Degidio, "The Surface-Composition of Copper with Indoor Exposures Ranging from 3 to 49 Years," *Corros Sci* 30, 10 (1990): p. 999-1008.
68. E. Cano, J.L. Polo, A. La Iglesia, and J.M. Bastidas, "Rate control for copper tarnishing," *Corros Sci* 47, 4 (2005): p. 977-987.
69. J.H. Payer. *Corrosion Processes in the Development of Thin Tarnish Films*. in *Thirty-Sixth IEEE Holm Conference on Electrical Contacts and the Fifteenth International Conference on Electric Contacts* 1990. Montreal, Que.
70. E. Cano, M.F. Lopez, J. Simancas, and J.M. Bastidas, "X-ray photoelectron spectroscopy study on the chemical composition of copper tarnish products formed at low humidities," *J Electrochem Soc* 148, 1 (2001): p. E26-E30.
71. J.M. Bastidas and T. Simancas, "Characterization of corrosion products on a copper-containing intrauterine device during storage at room temperature," *Biomaterials* 18, 3 (1997): p. 247-250.
72. N. Fredj, J.S. Kolar, D.M. Prichard, and T.D. Burleigh, "Study of relative color stability and corrosion resistance of commercial copper alloys exposed to hand contact and synthetic hand sweat," *Corros Sci* 76, (2013): p. 415-423.
73. F.L. Laque, *Marine Corrosion: Causes and Prevention* (New York: John Wiley & Sons, 1975).
74. A. International, *Standard Practice for the Preparation of Substitute Ocean Water*. 2003.
75. M. Schumacher, *Seawater corrosion handbook* (Park Ridge, N.J.: Noyes Data Corp., 1979). p. vii, 494 p.
76. G.J. Danek and J.L. Basil, *Sea-water Corrosion Behavior of ACI-CD-4M Cu Alloy*. August 1964, Navy Marine Engineering Lab. p. 14.
77. H.P. Hack and H.W. Pickering, "Ac Impedance Study of Cu and Cu-Ni Alloys in Aerated Salt-Water .1. Pd Coating and Corrosion Product Stripping," *J Electrochem Soc* 138, 3 (1991): p. 690-695.
78. N.W. Farro, L. Veleva, and P. Aguilar, "Copper Marine Corrosion: I. Corrosion Rate in Atmospheric and Seawater Environments of Peruvian Port," *The Open Corrosion Journal* 2, (2009): p. 130-138.
79. F.O. Nestle, H. Speidel, and M.O. Speidel, "Metallurgy - High nickel release from 1-and 2-euro coins," *Nature* 419, 6903 (2002): p. 132-132.
80. S. Colin, G. Krier, H. Jolibois, A. Hachimi, J.F. Muller, and A. Chambaudet, "Characterization of the corrosion layer of copper-nickel alloys in a synthetic sweat medium by FTMS and LAMMA laser microprobes," *Applied Surface Science* 125, 1 (1998): p. 29-45.
81. J.J. Hostýnek and H.I. Maibach, *Copper and the skin. Dermatology : clinical & basic science series* (New York: Informa Healthcare, 2006). p. xv, 305 p.

82. ASTM, Standard Test Methods for Chemical Analysis of Copper Alloys. Vol. 03.03 Nondestructive Testing (West Conshohocken, PA: ASTM International, 2005).
83. I.O.f. Standardization, *Watch-cases and accessories -- Gold alloy coverings -- Part 2: Determination of fineness, thickness, corrosion resistance and adhesion*. 2013. p. 12.
84. T.L.A.t.B.A. Office, *Reference test method for release of nickel from all post assemblies which are inserted into pierced parts of the human body and articles intended to come into direct and prolonged contact with the skin*. 2011.
85. O. Nygren and J.E. Wahlberg, "Speciation of chromium in tanned leather gloves and relapse of chromium allergy from tanned leather samples," *Analyst* 123, 5 (1998): p. 935-937.
86. P. Haudrechy, J. Foussereau, B. Mantout, and B. Baroux, "Nickel Release from 304 and 316 Stainless-Steels in Synthetic Sweat - Comparison with Nickel and Nickel-Plated Metals - Consequences on Allergic Contact-Dermatitis," *Corros Sci* 35, 1-4 (1993): p. 329-336.
87. Y.W. Song, D.Y. Shan, and E.H. Han, "Corrosion behaviors of electroless plating Ni-P coatings deposited on magnesium alloys in artificial sweat solution," *Electrochim Acta* 53, (2007): p. 2009-2015.
88. F.F. Larese, F. D'Agostin, M. Crosera, G. Adami, N. Renzi, M. Bovenzi, and G. Maina, "Human skin penetration of silver nanoparticles through intact and damaged skin," *Toxicology* 255, 1-2 (2009): p. 33-37.
89. A.L. Casey, D. Adams, T.J. Karpanen, P.A. Lambert, B.D. Cookson, P. Nightingale, L. Miruszenko, R. Shillam, P. Christian, and T.S.J. Elliott, "Role of copper in reducing hospital environment contamination," *Journal of Hospital Infection* 74, 1 (2010): p. 72-77.
90. S. Mehtar, I. Wiid, and S.D. Todorov, "The antimicrobial activity of copper and copper alloys against nosocomial pathogens and Mycobacterium tuberculosis isolated from healthcare facilities in the Western Cape: an in-vitro study," *Journal of Hospital Infection* 68, 1 (2008): p. 45-51.
91. S.A. Wilks, H.T. Michels, and C.W. Keevil, "Survival of *Listeria monocytogenes* Scott A on metal surfaces: Implications for cross-contamination," *International Journal of Food Microbiology* 111, 2 (2006): p. 93-98.
92. P. Airey and J. Verran, "Potential use of copper as a hygienic surface; problems associated with cumulative soiling and cleaning," *Journal of Hospital Infection* 67, 3 (2007): p. 271-277.
93. ASM Handbook Committee. and A.I.H. Committee., *ASM Handbook. Properties and Selection: Nonferrous Alloys and Special-Purpose Materials Vol. 2*, 1992.
94. *Unified Numbering System for Copper + Copper Alloys*. April 4, 2014]; Available from: <http://unscopperalloys.org/>.
95. J. William D. Nielsen. *Metallurgy of Copper-Base Alloys*. Available from: http://www.copper.org/resources/properties/703_5/.
96. D.G. Kolman, *ASM Handbook. Corrosion: Materials*, ed. S.D. Cramer, Bernard, S.C., Jr. Vol. 13A (Materials Park, OH: ASM International, 2005).

97. R.A. Wilkins and E.S. Bunn, *Copper and Copper Base Alloys: The Physical and Mechanical Properties of Copper and Its Commercial Alloys in Wrought Form* (New York; London: McGraw-Hill Book Company, Inc., 1943.
98. C.L. Trybus, R.P. Vierod, and P.W. Robinson, *Antitarnish, Antimicrobial Copper Alloys and Surface Made from Such Alloys*. 2011: United States.
99. H. Ha, H. Bindig, K. Williams, and J.R. Scully. *Tarnishing and Cu Ion release In Selected Copper-Base Alloys: Implications Towards Anti-Microbial Functionality*. in *220th ECS Meeting and Electrochemical Energy Summit*. 2011. Boston, MA.
100. J.D. Johansen, T. Menne, J. Christophersen, K. Kaaber, and N. Veien, "Changes in the pattern of sensitization to common contact allergens in Denmark between 1985-86 and 1997-98, with a special view to the effect of preventive strategies," *Brit J Dermatol* 142, 3 (2000): p. 490-495.
101. E. Nucera, D. Schiavino, A. Calandrelli, C. Roncallo, A. Buonomo, C. Pedone, C. Lombardo, V. Pecora, T. De Pasquale, E. Pollastrini, and G. Patriarca, "Positive patch tests to Euro coins in nickel-sensitized patients," *Brit J Dermatol* 150, 3 (2004): p. 500-503.
102. C.R. Hamann, D. Hamann, C. Hamann, J.P. Thyssen, and C. Liden, "The cost of nickel allergy: a global investigation of coin composition and nickel and cobalt release," *Contact Dermatitis* 68, 1 (2013): p. 15-22.
103. P.G. Fournier and T.R. Govers, "Contamination by nickel, copper and zinc during the handling of euro coins," *Contact Dermatitis* 48, 4 (2003): p. 181-188.
104. *Applications: Coins*. [cited 2014; Available from: <http://www.copperinfo.co.uk/coins/>.
105. *Nordic Gold in our pockets*. [cited 2014; Available from: <http://www.sdda.com/copper/development-history.html#>.
106. H.-G. Neumann, C. Prinz, and U. Lembke, *Fitting with Antibacterial Coating and Method for Manufacturing the Same*. 2013: United States.
107. D. Quaranta, T. Krans, C.E. Santo, C.G. Elowsky, D.W. Domaille, C.J. Chang, and G. Grass, "Mechanisms of Contact-Mediated Killing of Yeast Cells on Dry Metallic Copper Surfaces," *Appl Environ Microb* 77, 2 (2011): p. 416-426.
108. C. de Carvalho and M.J. Caramujo, "Bacterial diversity assessed by cultivation-based techniques shows predominance of Staphylococcus species on coins collected in Lisbon and Casablanca," *FEMS Microbiology Ecology* (2013).
109. D.M. Prichard, *DEVELOPMENT OF A NOVEL COLOR-STABLE, ANTI-MICROBIAL COPPER ALLOY*, in *Materials and Metallurgical Engineering*. 2010, New Mexico Institute of Mining and Technology: Socorro, New Mexico. p. 100.
110. J.F. Dante and R.G. Kelly, "The Evolution of the Adsorbed Solution Layer during Atmospheric Corrosion and Its Effects on the Corrosion Rate of Copper," *J Electrochem Soc* 140, 7 (1993): p. 1890-1897.
111. S.J. Dancer, "How do we assess hospital cleaning? A proposal for microbiological standards for surface hygiene in hospitals," *Journal of Hospital Infection* 56, 1 (2004): p. 10-15.

112. O. Jensen and E. Nielsen, "Rusters - Corrosive Action of Palmar Sweat .2. Physical and Chemical Factors in Palmar Hyperhidrosis," *Acta Derm-Venereol* 59, 2 (1979): p. 139-143.
113. O. Jensen, "Rusters - Corrosive Action of Palmar Sweat .1. Sodium-Chloride in Sweat," *Acta Derm-Venereol* 59, 2 (1979): p. 135-138.
114. Y.-Y. Su and R.M. Shemanski, "Qualitative and quantitative identification of copper oxides," *Surface and Interface Analysis* 40, 8 (2008): p. 1183-1189.
115. G. Kear, B.D. Barker, and F.C. Walsh, "Electrochemical corrosion of unalloyed copper in chloride media—a critical review," *Corrosion Science* 46, 1 (2004): p. 109-135.
116. M. Forslund, C. Leygraf, C.J. Lin, and J.S. Pan, "Radial Spreading of Localized Corrosion-Induced Selective Leaching on alpha-Brass in Dilute NaCl Solution," *Corrosion* 69, 5 (2013): p. 468-476.
117. A.E. Broo, B. Berghult, and T. Hedberg, "Copper corrosion in water distribution systems—the influence of natural organic matter (nom) on the solubility of copper corrosion products," *Corros Sci* 40, 9 (1998): p. 1479-1489.
118. H.T. Michels, J.P. Noyce, S.A. Wilks, and C.W. Keevil. *Antimicrobial effects of cast copper alloy surfaces on the bacterium E. coli O157:H7*. in *AFS Transactions*. 2005. Schaumburg, IL, USA: Amecican Foundry Society.
119. D. Horton, H. H., H. Bindig, and J.R. Scully, "Tarnishing and Cu Ion release In Selected Copper-Base Alloys: Implications towards Anti-Microbial Functionality," (2014).
120. C.B. Beggs, K.G. Kerr, C.J. Noakes, E.A. Hathway, and P.A. Sleight, "The ventilation of multiple-bed hospital wards: Review and analysis," *Am J Infect Control* 36, 4 (2008): p. 250-259.
121. H.M. Ha and J.R. Scully, "Effects of Phosphate on Pit Stabilization and Propagation in Copper in Synthetic Potable Waters," *Corrosion* 69, 7 (2013): p. 703-718.
122. M. Metikos-Hukovic, R. Babic, and I. Paic, "Copper corrosion at various pH values with and without the inhibitor," *J Appl Electrochem* 30, 5 (2000): p. 617-624.
123. B.C. Syrett, "The Mechanism of Accelerated Corrosion of Copper-Nickel-Alloys in Sulfide-Polluted Seawater," *Corros Sci* 21, 3 (1981): p. 187-&.
124. S. Sembiring, B. O'Connor, D. Li, A.v. Risessen, C. Buckley, and I. Low, "Grazing Incidence X-Ray Diffraction Characterization of Corrosion Deposits Induced by Carbon Dioxide on Mild Steel," *Advances in X-Ray Analysis* 43, (2000).
125. S. Nakayama, T. Kaji, M. Shibata, T. Notoya, and T. Osakai, "Which Is Easier to Reduce, Cu[₂]O or CuO?," *Journal of The Electrochemical Society* 154, 1 (2007): p. C1-C6.
126. M.R.G. Dechialvo, J.O. Zerbino, S.L. Marchiano, and A.J. Arvia, "Correlation of Electrochemical and Ellipsometric Data in Relation to the Kinetics and Mechanism of Cu₂O Electroformation in Alkaline-Solutions," *J Appl Electrochem* 16, 4 (1986): p. 517-526.
127. J. Morales, P. Esparza, G.T. Fernandez, S. Gonzalez, J.E. Garcia, J. Caceres, R.C. Salvarezza, and A.J. Arvia, "A Comparative-Study on the Passivation and

- Localized Corrosion of Alpha-Brass and Beta-Brass in Borate Buffer Solutions Containing Sodium-Chloride .2. X-Ray Photoelectron and Auger-Electron Spectroscopy Data," *Corros Sci* 37, 2 (1995): p. 231-239.
128. A. International, *ASTM B825-13: Standard Test Method for Coulometric Reduction of Surface Films on Metallic Test Samples*, in *Nonferrous Metals-Nickel, Cobalt, Lead, Tin, Zinc, Cadmium, Precious, Reactive, Refractory Metals and Alloys; Materials for Thermostats, Electrical Heating and Resistance Contact, and Connectors* 2011.
 129. A. Lindsay. *Introducing the Phototransistor*. 2012 04/23/2014]; Available from: <http://learn.parallax.com/lightpectrum>.
 130. S. Robinson and A.H. Robinson, "Chemical Composition of Sweat," *Physiological Reviews* 34, (1954): p. 202.
 131. B. Harris and B.P. Phipps, "Role of Adsorbed Water in Atmospheric Corrosion," *J Electrochem Soc* 126, 8 (1979): p. C332-C332.
 132. Z.Y. Chen, S. Zakipour, D. Persson, and C. Leygraf, "Effect of sodium chloride particles on the atmospheric corrosion of pure copper," *Corrosion* 60, 5 (2004): p. 479-491.
 133. J. Zhang, J. Wang, and Y. Wang, "Micro-droplets formation during the deliquescence of salt particles in atmosphere," *Corrosion* 61, 12 (2005): p. 1167-1172.
 134. S.H. Zhang and S.B. Lyon, "The Electrochemistry of Iron, Zinc and Copper in Thin-Layer Electrolytes," *Corros Sci* 35, 1-4 (1993): p. 713-718.
 135. A. Nishikata, Y. Ichihara, Y. Hayashi, and T. Tsuru, "Influence of electrolyte layer thickness and pH on the initial stage of the atmospheric corrosion of iron," *J Electrochem Soc* 144, 4 (1997): p. 1244-1252.
 136. K.W. Chung and K.B. Kim, "A study of the effect of concentration build-up of electrolyte on the atmospheric corrosion of carbon steel during drying," *Corros Sci* 42, 3 (2000): p. 517-531.
 137. A. Yasunishi, "Solubilities of Sparingly Soluble Gases in Aqueous Sodium-Sulfate and Sulfite Solutions," *J Chem Eng Jpn* 10, 2 (1977): p. 89-94.
 138. T.E. Graedel, J.P. Franey, G.W. Kammlott, J.M. Vandenberg, and P.L. Key, "The Atmospheric Sulfidation of Copper Single Crystals," *J Electrochem Soc* 134, 7 (1987): p. 1632-1635.
 139. A. Kratschmer, I.O. Wallinder, and C. Leygraf, "The evolution of outdoor copper patina," *Corros Sci* 44, 3 (2002): p. 425-450.
 140. I. Odnevall and C. Leygraf, "Formation of $\text{Na}_2\text{Zn}_4\text{Cl}(\text{OH})_6\text{SO}_4 \cdot 6\text{H}_2\text{O}$ in a Marine Atmosphere," *Corros Sci* 34, 8 (1993): p. 1213-1229.
 141. H. Strandberg and L.G. Johansson, "Some aspects of the atmospheric corrosion of copper in the presence of sodium chloride," *J Electrochem Soc* 145, 4 (1998): p. 1093-1100.
 142. S.B. Adeloju and Y.Y. Duan, "Influence of bicarbonate ions on stability of copper oxides and copper pitting corrosion," *British Corrosion Journal* 29, 4 (1994): p. 315-320.
 143. P. Eriksson, L.G. Johansson, and J. Gullman, "A Laboratory Study of Corrosion Reactions on Statue Bronze," *Corros Sci* 34, 7 (1993): p. 1083-1097.

144. J.S. Garner and B.P. Simmons, "Guideline for Isolation Precautions in Hospitals," *Infect Cont Hosp Ep* 4, 4 (1983): p. 245-325.
145. M. Hutchison, "Effect of Drying Synthetic Perspiration Droplets on pH," (2014).
146. G.S. Rohrer, *Structure and bonding in crystalline materials* (Cambridge ; New York: Cambridge University Press, 2001). p. x, 540 p.
147. M. Birkholz, P.F. Fewster, and C. Genzel, *Thin film analysis by X-ray scattering* (Weinheim: Wiley-VCH, 2006). p. xxii, 356 p.
148. J.B. Zhang, J. Wang, and Y.H. Wang, "Electrochemical investigations of microdroplets formed on metals during the deliquescence of salt particles in atmosphere," *Electrochem Commun* 7, 4 (2005): p. 443-448.
149. T. Tsuru, K.I. Tamiya, and A. Nishikata, "Formation and growth of microdroplets during the initial stage of atmospheric corrosion," *Electrochim Acta* 49, 17-18 (2004): p. 2709-2715.
150. Z.Y. Chen, D. Persson, F. Samie, S. Zakipour, and C. Leygraf, "Effect of carbon dioxide on sodium chloride-induced atmospheric corrosion of copper," *J Electrochem Soc* 152, 12 (2005): p. B502-B511.
151. Z.Y. Chen, D. Persson, A. Nazarov, S. Zakipour, D. Thierry, and C. Leygraf, "In Situ Studies of the Effect of CO₂ on the Initial NaCl-Induced Atmospheric Corrosion of Copper," *J Electrochem Soc* 152, 9 (2005): p. B342-B351.
152. Z.Y. Chen, D. Persson, and C. Leygraf, "In situ studies of the effect of SO₂ on the initial NaCl-induced atmospheric corrosion of copper," *J Electrochem Soc* 152, 12 (2005): p. B526-B533.
153. B. Troconis and J.R. Scully, "Paper in Progress."

Appendix A: Broth Medium Compositions



BAIRD PARKER AGAR (7112)

Intended Use

Baird Parker Agar is used for detection and enumeration of *Staphylococcus aureus* in foods.

Product Summary and Explanation

Baird Parker Agar was first described in 1962.¹ It is a selective medium for the isolation and presumptive identification of coagulase-positive staphylococci. This medium is used extensively for detecting *Staphylococcus aureus* in foods, dairy products, and other materials.²⁻⁶ Coagulase-positive staphylococci can grow and reproduce in cosmetic products. These products are tested for the presence of coagulase-positive staphylococci using standard microbiological methods.⁴

Principles of the Procedure

Enzymatic Digest of Casein and Beef Extract are the carbon and nitrogen sources in Baird Parker Agar. Yeast Extract supplies B-complex vitamins that stimulate bacterial growth. Glycine and Sodium Pyruvate stimulate growth of staphylococci. The selectivity of the medium is due to Lithium Chloride and a 1% Potassium Tellurite Solution, suppressing growth of organisms other than staphylococci. The differentiation of coagulase-positive staphylococci is based on Potassium Tellurite and Egg Yolk Emulsion. Staphylococci that contain lecithinase break down the Egg Yolk and cause clear zones around the colonies. An opaque zone of precipitation may form due to lipase activity. Reduction of Potassium Tellurite is a characteristic of coagulase-positive staphylococci, and causes blackening of colonies. Agar is the solidifying agent.

Formula / Liter

Enzymatic Digest of Casein	10 g
Beef Extract	5 g
Yeast Extract.....	1 g
Lithium Chloride	5 g
Glycine	12 g
Sodium Pyruvate.....	10 g
Agar	*17 g

*15 - 20 g according to gel strength

Enrichment (# 7983)

Egg Yolk Tellurite, 100 mL
(Chicken egg yolk and egg, 100%)
(Potassium Tellurite, 0.21 g)

Enrichments (# 7982 & # 7989)

Chicken egg yolk & egg, 50% (# 7982)
Tellurite Supplement (1%) (# 7989)

Final pH: 7.0 ± 0.2 at 25°C

Formula may be adjusted and/or supplemented as required to meet performance specifications.

Precautions

1. For Laboratory Use.
2. HARMFUL. Harmful if swallowed, inhaled, or absorbed through skin. Skin irritation may be severe. Irritating to eyes, respiratory system, and skin. May cause central nervous system effects.

Directions

1. Suspend 60 g of the medium in one liter of purified water.
2. Heat with frequent agitation and boil for one minute to completely dissolve the medium.
3. Autoclave at 121°C for 15 minutes.
4. After cooling to 45 - 50°C, add 50 mL of Egg Yolk Tellurite Supplement (# 7983). Alternatively, add 50 mL of Egg Yolk Emulsion (# 7982) and 10 mL of Tellurite Supplement (1%), (# 7989).
5. Mix thoroughly before dispensing.

Quality Control Specifications

Dehydrated Appearance: Powder is homogeneous, free flowing, and beige.

Prepared Appearance (Plain): Prepared medium is trace to slightly hazy and light amber.



Prepared Appearance (with Egg Yolk Tellurite Supplement): Prepared medium is canary yellow and opaque.

Expected Cultural Response: Cultural response on Baird Parker Agar with Egg Yolk Tellurite Supplement (# 7983) at 35 ± 2°C after 24 - 48 hours incubation in anaerobic atmosphere.

Microorganism	Approx. Inoculum (CFU)	Expected Results	
		Growth	Reaction
<i>Enterococcus faecalis</i> ATCC® 29212	10 - 300	Poor to fair	Black colonies suppressed, no halo
<i>Escherichia coli</i> ATCC® 25922	10 ⁸	Inhibited	-----
<i>Proteus mirabilis</i> ATCC® 12453	10 - 300	Partially inhibited	Black colonies, no halo
<i>Staphylococcus aureus</i> ATCC® 25923	10 - 300	Fair to good	Black colonies with a clear halo
<i>Staphylococcus epidermidis</i> ATCC® 12228	10 - 300	Poor	Grey to Black colonies, suppressed, no halo

The organisms listed are the minimum that should be used for quality control testing.

Test Procedure

1. Prepare dilutions of test samples, if indicated by references.²⁻⁵
2. Transfer 1 mL of the sample to each of 3 Baird Parker Agar plates, distribute over the surface using a sterile, bent glass rod.
3. Allow inoculum to be absorbed by the medium before inverting the plates.
4. Incubate at 35 - 37°C for 45 - 48 hours.
5. Examine plates having 20 - 200 colonies, counting colonies typical of *Staphylococcus aureus*.

Results

Coagulase-positive staphylococci produce black, shiny, convex colonies with entire margins and clear zones, with or without an opaque zone. Coagulase-negative staphylococci produce poor or no growth. If growth occurs, colonies are black; clear or opaque zones are rare. The majority of other organisms are inhibited or grow poorly. If growth appears, colonies are light to brown-black, with no clear or opaque zones.

Storage

Store sealed bottle containing the dehydrated medium at 2 - 30°C. Once opened and recapped, place the container in a low humidity environment at the same storage temperature. Protect from moisture and light by keeping container tightly closed.

Expiration

Refer to expiration date stamped on the container. The dehydrated medium should be discarded if not free flowing, or if the appearance has changed from the original color. Expiry applies to medium in its intact container when stored as directed.

Limitation of the Procedure

Due to nutritional variation, some strains may grow poorly or fail to grow on this medium.

Packaging

Baird Parker Agar	Code No.	7112A	500 g
		7112B	2 kg
		7112C	10 kg
Egg Yolk Tellurite		7983	100 mL
Egg Yolk Emulsion		7982	100 mL
Tellurite Supplement (1%) Chapman		7989	10 mL



References

1. **Baird-Parker, A. C.** 1962. An improved diagnostic and selective medium for isolating coagulase-positive staphylococci. *J. Appl. Bacteriol.* 25:12-19.
2. **Vanderzant, C., and D. F. Splittstoesser (eds.)**. 1992. *Compendium of methods for the microbiological examination of food*. 3rd ed. American Public Health Association, Washington, D.C.
3. **Marshall, R. T. (ed.)**. 1993. *Standard methods for the microbiological examination of dairy products*, 16th ed. American Public Health Association, Washington, D.C.
4. www.fda.gov/Food/ScienceResearch/LaboratoryMethods/BacteriologicalAnalyticalmanualBAM/default.htm.
5. **Cunnif, P. (ed.)**. 1995. *Official Methods of Analysis AOAC International*, 16th ed. AOAC International, Gaithersburg, MD.
6. **United States Pharmacopeial Convention**. 2007. *The United States pharmacopeia*, 31st ed., Amended Chapters 61, 62, 111. The United States Pharmacopeial Convention, Rockville, MD.

Technical Information

Contact Acumedia Manufacturers, Inc. for Technical Service or questions involving dehydrated culture media preparation or performance at (517)372-9200 or fax us at (517)372-2006.



620 Leisher Place, Lansing MI 48912
517/372-9200 • 800/783-3212 • fax: 800/875-8563
neogen-info@neogen.com • www.neogen.com

PI 7112 Rev 6, March 2012



TRYPTIC SOY AGAR (7100)

Intended Use

Tryptic Soy Agar is used for the cultivation of a wide variety of microorganisms. Tryptic Soy Agar conforms to Harmonized USP/EP/JP Requirements.^{1,2,3}

Product Summary and Explanation

In 1955, Leavitt et al.⁴ discovered Tryptic Soy Agar (TSA) facilitated vigorous growth of aerobic and anaerobic microorganisms. TSA, a general purpose medium, is commonly referred to as Soybean-Casein Digest Agar USP 23. TSA is a nutritious base, and a variety of supplements can be added to enhance this medium. The addition of 5% sterile, defibrinated sheep, horse, or rabbit blood provides an excellent non-selective medium, used to determine hemolytic reactions of bacteria. TSA supplemented with lecithin and Tween 80[®] is widely used in environmental monitoring.⁵

TSA is recommended in multiple water & wastewater applications,⁶ and numerous standard methods for food testing.⁷ This medium also conforms to Harmonized United States Pharmacopoeia (USP), European Pharmacopoeia (EU), and Japanese Pharmacopoeia (JP).^{1,2,3} Clinically, TSA is used in the differentiation of Haemophilus species (the X and V factors are omitted from this medium), and widely used for blood cultures. TSA is commonly used as a maintenance medium for culture collections, and testing bacterial contaminants in cosmetics.⁸

Principles of the Procedure

Enzymatic Digest of Casein and Enzymatic Digest of Soybean Meal provide the nitrogen, vitamins and carbon in TSA. Sodium Chloride maintains osmotic balance in the medium. Agar is the solidifying agent.

Formula / Liter

Enzymatic Digest of Casein.....	15 g
Enzymatic Digest of Soybean Meal.....	5 g
Sodium Chloride	5 g
Agar	15 g

Final pH 7.3 ± 0.2 at 25°C

Formula may be adjusted and/or supplemented as required to meet performance specifications.

Precautions

1. For Laboratory Use.
2. IRRITANT. Irritating to eyes, respiratory system, and skin.

Directions

1. Suspend 40 g of the medium in one liter of purified water.
2. Heat with frequent agitation and boil for one minute to completely dissolve the medium.
3. Autoclave at 121°C for 15 minutes.
4. Optional: Prepare 5 to 10% blood agar by adding appropriate volume of sterile defibrinated blood to melted sterile agar medium, cooled to 45 – 50°C.

Quality Control Specifications

Dehydrated Appearance: Powder is homogeneous, free flowing and light beige.

Prepared Appearance: Prepared medium without enrichment is trace to slight hazy and yellow beige in color. Prepared medium with 5% sheep blood is red and opaque.



Expected Cultural Response and USP/EP/JP Growth Promotion Testing: Cultural response on TSA tested at Harmonized USP/EP/JP specified temperatures and incubation times.^{1,2,3}

Microorganism	Approx. Inoculum (CFU)	Expected Results
		Growth
<i>Aspergillus niger</i> ATCC ® 16404	10 - 100	Growth
<i>Bacillus subtilis</i> ® ATCC 6633	10 - 100	Growth
<i>Candida albicans</i> ® 10231	10 - 100	Growth
<i>Pseudomonas aeruginosa</i> ATCC® 9027	10 - 100	Growth
<i>Staphylococcus aureus</i> ATCC ® 6538	10 - 100	Growth

Tryptic Soy Agar was prepared according to label directions with 5% sheep blood and inoculated. Cultures were incubated at 30 - 35°C under the appropriate atmosphere and examined for growth at 18 – 24 hours.

Microorganism	Approx. Inoculum (CFU)	Expected Results	
		Growth	Hemolysis
<i>Escherichia coli</i> ATCC® 25922	10 - 100	Good to excellent	Beta hemolysis
<i>Staphylococcus aureus</i> ATCC® 25923	10 - 100	Good to excellent	Beta hemolysis
<i>Streptococcus pneumoniae</i> ATCC® 6305	10 - 100	Fair to excellent	Alpha hemolysis
<i>Streptococcus pyogenes</i> ATCC® 19615	10 - 100	Fair to excellent	Beta hemolysis

The organisms listed are the minimum that should be used for quality control testing.

Test Procedure

Refer to appropriate references for specific procedures using Tryptic Soy Agar.^{1,2,4-7}

Results

Refer to appropriate references for test results.

Storage

Store sealed bottle containing the dehydrated medium at 2 - 30°C. Once opened and recapped, place the container in a low humidity environment at the same storage temperature. Protect from moisture and light by keeping container tightly closed.

Expiration

Refer to expiration date stamped on the container. The dehydrated medium should be discarded if it is not free flowing, or if medium has changed from the original color. Expiry applies to medium in its intact container when stored as directed.

Limitations of the Procedure

Due to nutritional variation, some strains may be encountered that grow poorly or fail to grow on this medium.

Packaging

Tryptic Soy Agar	Code No.	7100A	500 g
		7100B	2 kg
		7100C	10 kg



References

1. **United States Pharmacopeial Convention.** 2007. The United States pharmacopeia, 31st ed., Amended Chapters 61, 62, 111. The United States Pharmacopeial Convention, Rockville, MD.
2. **Directorate for the Quality of Medicines of the Council of Europe (EDQM).** 2007. The European Pharmacopoeia, Amended Chapters 2.6.12, 2.6.13, 5.1.4, Council of Europe, 87075 Strasbourg Cedex, France.
3. **Japanese Pharmacopoeia.** 2007. Society of Japanese Pharmacopoeia. Amended Chapters 35.1, 35.2, 7. The Minister of Health, Labor, and Welfare.
4. **Leavitt, J. M., I. J. Naidorf and P. Shugaevsky.** 1955. The undetected anaerobe in endodontics: a sensitive medium for detection of both aerobes and anaerobes. *The NY J. Dentist.* 25:377-382.
5. **Orth, D. S.** 1993. Handbook of cosmetic microbiology. Marcel Dekker, Inc., New York, NY.
6. **Greenberg, A. E., L. S. Clesceri, and A. D. Eaton (eds.).** 1995. Standard methods for the examination of water and wastewater, 19th ed. American Public Health Association, Washington, D.C.
7. **U.S. Food and Drug Administration.** Bacteriological analytical manual, 8th ed., AOAC International, Gaithersburg, MD.
8. **Curry, A. S., G. G. Joyce, and G. N. McEwen, Jr.** 1993. CTFA Microbiology guidelines. The Cosmetic, Toiletry, and Fragrance Association, Inc. Washington, D.C.

Technical Information

Contact Acumedia Manufacturers, Inc. for Technical Service or questions involving dehydrated culture media preparation or performance at (517)372-9200 or fax us at (517)372-2008.



620 Lasher Place, Lansing MI 48912
 517/372-9200 • 800/783-3212 • fax: 800/875-8563
 neogen-info@neogen.com • www.neogen.com

PI 7100, Rev 6, November 2010



BRAIN-HEART INFUSION BROTH (7116)

Intended Use

Brain-Heart Infusion Broth is used for the cultivation of a wide variety of fastidious organisms.

Product Summary and Explanation

Rosenow¹ prepared a rich medium for culturing streptococci by combining dextrose broth and brain tissue. Hayden² modified the original formula while working with dental pathogens. The current formula is a modification of Rosenow¹ and Hayden², using dehydrated infusions of porcine brain and heart tissue.

Brain-Heart Infusion Broth can be supplemented with antibiotics, varying amounts of sodium chloride, yeast extract, and serum to provide a rich medium for bacteria, yeasts and pathogenic fungi.³ The addition of 0.1% agar can be used to lower oxygen tension, providing an atmosphere to support the growth of aerobic, microaerophilic, and obligate anaerobic microorganisms.

Brain-Heart Infusion Broth, abbreviated as BHI, is specified in many references for food and water testing.⁴⁻⁷ NCCLS, National Committee for Clinical Laboratory Standards, cites Brain-Heart Infusion Broth for preparing the inoculum used in antimicrobial susceptibility tests.⁸

Principles of the Procedure

The nitrogen, vitamin, and carbon sources are provided by Brain-Heart Infusion and Enzymatic Digest of Gelatin in BHI Broth. Dextrose is the carbohydrate source, and Sodium Chloride maintains the osmotic environment. Disodium Phosphate is the buffering agent in this medium.

Formula / Liter

Brain Heart Infusion	17.5 g
Enzymatic Digest of Gelatin	10 g
Dextrose	2 g
Sodium Chloride	5 g
Disodium Phosphate	2.5 g

Final pH: 7.4 ± 0.2 at 25°C

Formula may be adjusted and/or supplemented as required to meet performance specifications.

Precautions

1. For Laboratory Use.
2. IRRITANT. Irritating to eyes, respiratory system, and skin.

Directions

1. Dissolve 37 g of the medium in one liter of purified water.
2. Heat with frequent agitation to completely dissolve the medium.
3. Autoclave at 121°C for 15 minutes.

Quality Control Specifications

Dehydrated Appearance: Powder is homogeneous, free flowing, and light beige.

Prepared Appearance: Prepared broth is brilliant to clear, with none to light precipitate, and light to medium amber in color.



Expected Cultural Response: Cultural response in Brain-Heart Infusion Broth incubated at $35 \pm 2^\circ\text{C}$ under aerobic atmosphere and temperature and examined for growth at 1 – 3 days.

Microorganism	Approx. Inoculum (CFU)	Expected Results
<i>Escherichia coli</i> ATCC® 25922	10 - 300	Good to excellent
<i>Staphylococcus aureus</i> ATCC® 25923	10 - 300	Good to excellent

The organisms listed are the minimum that should be used for quality control testing.

Test Procedure

Refer to appropriate references for specific procedures using Brain-Heart Infusion Broth.

Results

Refer to appropriate references for test results.

Storage

Store sealed bottle containing the dehydrated medium at 2 - 30°C. Once opened and recapped, place container in a low humidity environment at the same storage temperature. Protect from moisture and light by keeping container tightly closed.

Expiration

Refer to expiration date stamped on the container. The dehydrated medium should be discarded if not free flowing, or if the appearance has changed from the original color. Expiry applies to medium in its intact container when stored as directed.

Limitation of the Procedure

Due to nutritional variation, some strains may be encountered that grow poorly or fail to grow on this medium.

Packaging

Brain-Heart Infusion Broth	Code No.	7116A	500 g
		7116B	2 kg
		7116C	10 kg

References

- Rosenow, E. C. 1919. Studies on elective localization. J. Dent. Research 1:205-249.
- Hayden, R. L. 1923. Elective localization in the eye of bacteria from infected teeth. Arch. Int. Med. 32:828-849.
- Atlas, R. M. 1993. Handbook of microbiological media, p. 147-153, CRC Press, Boca Raton, FL.
- Cunniff, P. (ed.). 1995. Official Methods of Analysis AOAC International, 16th ed. AOAC International, Gaithersburg, MD.
- U.S. Food and Drug Administration. Bacteriological analytical manual, 8th ed., AOAC International, Gaithersburg, MD.
- Vanderzant, C., and D. F. Splittstoesser (eds.). 1992. Compendium of methods for the microbiological examination of food., 3rd ed. American Public Health Association, Washington, D.C.
- Greenberg, A. E., L. S. Clesceri, and A.D. Eaton (eds.). 1995. Standard methods for the examination of water and wastewater, 19th ed. American Public Health Association, Washington, D.C.
- National Committee for Clinical Laboratory Standards. 1994. M11-A3, Vol. 13, No. 26, Methods for antimicrobial susceptibility testing of anaerobic bacteria. National Committee for Clinical Laboratory Standards, Villanova, PA.

Technical Information

Contact Acumedia Manufacturers, Inc. for Technical Service or questions involving dehydrated culture media preparation or performance at (517)372-9200 or fax us at (517)372-2006.



620 Leshar Place, Lansing MI 48912
 517/372-9200 • 800/783-3212 • fax: 800/875-8563
 neogen-info@neogen.com • www.neogen.com

PI 7116, Rev 03, Nov. 2010



MANNITOL SALT AGAR (7143)

Intended Use

Mannitol Salt Agar is used for the isolation of staphylococci. Conforms to Harmonized USP/EP/JP Requirements.^{1,2,3}

Product Summary and Explanation

Chapman formulated Mannitol Salt Agar to isolate staphylococci by inhibiting growth of most other bacteria with a high salt concentration.⁴ Chapman added 7.5% Sodium Chloride to Phenol Red Mannitol Agar, and noted pathogenic strains of staphylococci (coagulase-positive staphylococci) grew luxuriantly and produced yellow colonies with yellow zones. Nonpathogenic staphylococci produced small red colonies with no color change to the surrounding medium.

Mannitol Salt Agar is highly selective, and specimens from heavily contaminated sources may be streaked onto this medium without danger of overgrowth.⁵ Mannitol Salt Agar is recommended for isolating pathogenic staphylococci from clinical specimens, cosmetics, and microbial limit tests.^{1,2,3,5,6}

Principles of the Procedure

Enzymatic Digest of Casein, Enzymatic Digest of Animal Tissue, and Beef Extract provide the nitrogen, vitamins, and carbon in Mannitol Salt Agar. D-Mannitol is the carbohydrate source. In high concentrations, Sodium Chloride inhibits most bacteria other than staphylococci. Phenol Red is the pH indicator. Agar is the solidifying agent.

Bacteria that grow in the presence of a high salt concentration and ferment mannitol produce acid products, turning the Phenol Red pH indicator from red to yellow. Typical pathogenic staphylococci ferment mannitol and form yellow colonies with yellow zones. Typical non-pathogenic staphylococci do not ferment mannitol and form red colonies.

Formula / Liter

Enzymatic Digest of Casein	5 g
Enzymatic Digest of Animal Tissue	5 g
Beef Extract	1 g
D-Mannitol	10 g
Sodium Chloride	75 g
Phenol Red	0.025 g
Agar	15 g

Final pH: 7.4 ± 0.2 at 25°C

Formula may be adjusted and/or supplemented as required to meet performance specifications.

Precautions

1. For Laboratory Use.
2. IRRITANT. Irritating to eyes, respiratory system, and skin.

Directions

1. Suspend 111 g of the medium in one liter of purified water.
2. Heat with frequent agitation and boil for one minute to completely dissolve the medium.
3. Autoclave at 121°C for 15 minutes.

Quality Control Specifications

Dehydrated Appearance: Powder is homogeneous, free flowing, and light red-orange to light beige.

Prepared Appearance: Prepared medium is trace to slightly hazy and peach to pink.



Expected Cultural Response and USP/EP/JP Growth Promotion Testing: Cultural response on Mannitol Salt Agar incubated at Harmonized USP/EP/JP specified temperatures and incubation times.^{1,2,3}

Microorganism	Approx. Inoculum (CFU)	Expected Results	
		Recovery	Reactions
<i>Staphylococcus aureus</i> ATCC® 6538	10 - 100	Fair to good	Yellow colonies; may have yellow halo around colonies.
<i>Staphylococcus aureus</i> ATCC® 25923	10 - 100	Fair to good	Yellow colonies; may have yellow halo around colonies
<i>Staphylococcus epidermidis</i> ATCC® 12228	10 - 100	Fair to good	Colorless to pink colonies
<i>Escherichia coli</i> ATCC® 8739	300 - 1000	Inhibited	---

The organisms listed are the minimum that should be used for quality control testing.

Test Procedure

Inoculate specimen on medium as a primary isolation or inoculate isolated colonies onto medium for differentiation.

Results

Staphylococci will grow on this medium, while the growth of most other bacteria will be inhibited. Coagulase-positive staphylococci will produce luxuriant growth of yellow colonies and may have a yellow halo around the colony. Coagulase-negative staphylococci will produce small colorless to pink colonies with no color change to the medium.

Storage

Store sealed bottle containing the dehydrated medium at 2 - 30°C. Once opened and recapped, place container in a low humidity environment at the same storage temperature. Protect from moisture and light by keeping container tightly closed.

Expiration

Refer to expiration date stamped on the container. The dehydrated medium should be discarded if not free flowing, or if appearance has changed from the original color. Expiry applies to medium in its intact container when stored as directed.

Limitation of the Procedure

Due to nutritional variation, some strains may be encountered that grow poorly or fail to grow on this medium.

Packaging

Mannitol Salt Agar	Code No.	7143A	500 g
		7143B	2 kg
		7143C	10 kg

References

1. **United States Pharmacopeial Convention.** 2007. The United States pharmacopeia, 31st ed., Amended Chapters 61, 62, 111. The United States Pharmacopeial Convention, Rockville, MD.
2. **Directorate for the Quality of Medicines of the Council of Europe (EDQM).** 2007. The European Pharmacopoeia, Amended Chapters 2.6.12, 2.6.13, 5.1.4, Council of Europe, 67075 Strasbourg Cedex, France.
3. **Japanese Pharmacopoeia.** 2007. Society of Japanese Pharmacopoeia. Amended Chapters 35.1, 35.2, 7. The Minister of Health, Labor, and Welfare.
4. **Chapman, G. H.** The significance of sodium chloride in studies of staphylococci. *J. bacteriol.* **50**:201.
5. **Kloos, W. E., and T. L. Bannerman.** 1995. *Staphylococcus and Micrococcus.* In P. R. Murray, E. J. Baron, M. A. Pfaller, F. C. Tenover, and R. H. Tenover (eds.), *Manual of clinical microbiology*, 6th ed. American Society for Microbiology, Washington, D.C.
6. **Hitchins, A. D., T. T. Tran, and J. E. McCarron.** 1995. Microbiology methods for cosmetics, p. 23.01-23.12. *In* *Bacteriological analytical manual*, 8th ed. AOAC International, Gaithersburg, MD.

Technical Information

Contact Acumedia Manufacturers, Inc. for Technical Service or questions involving dehydrated culture media preparation or performance at (517)372-9200 or fax us at (517)372-2006.



NEOGEN
CORPORATION

620 Leshar Place, Lansing MI 48912
517/372-9200 • 800/783-3212 • fax: 800/875-8563
neogen-info@neogen.com • www.neogen.com

PI 7143, Rev 6, March 2011



TRYPTIC SOY BROTH (7164)

Intended Use

Tryptic Soy Broth is used for the cultivation of a wide variety of microorganisms. Tryptic Soy Broth conforms to Harmonized USP/EP/JP Requirements.^{1,2,3}

Product Summary and Explanation

Tryptic Soy Broth, a general purpose medium, is commonly referred to as Soybean-Casein Digest Medium, and abbreviated as TSB. This medium was originally developed for use without blood in determining the effectiveness of sulfonamides against pneumococci and other organisms.⁴ Clostridia and non-sporulating anaerobes grow luxuriantly in this broth when incubated under anaerobic conditions. TSB is recommended for testing bacterial contaminants in cosmetics⁵ and complies with established standards^{6,7} in the food industry. TSB was chosen by the USDA Animal and Plant Health Inspection Service for detecting viable bacteria in live vaccines.⁸

Tryptic Soy Broth is recommended by the National Committee for Clinical Laboratory Standards (NCCLS)⁹ for inoculum preparation in disk diffusion sensitivity tests. TSB conforms to Harmonized United States Pharmacopoeia (USP), European Pharmacopoeia (EU), and Japanese Pharmacopoeia (JP).^{1,2,3} The rich nutritional base of TSB, supplemented with SPS and CO₂ is an excellent broth for blood cultures in clinical applications.¹⁰ With the addition of 6.5% NaCl, TSB can be used for the selective growth of group D streptococci.

Principles of the Procedure

Enzymatic Digest of Casein and Enzymatic Digest of Soybean Meal are nitrogen sources in TSB. Dextrose is the carbon energy source that facilitates organism growth. Sodium Chloride maintains osmotic balance; Dipotassium Phosphate is a buffering agent.

Formula / Liter

Enzymatic Digest of Casein	17.0 g
Enzymatic Digest of Soybean Meal	3.0 g
Sodium Chloride	5.0 g
Dipotassium Phosphate	2.5 g
Dextrose.....	2.5 g

Final pH: 7.3 ± 0.2 at 25°C

Formula may be adjusted and/or supplemented as required to meet performance specifications.

Precautions

1. For Laboratory Use.
2. IRRITANT. Irritating to eyes, respiratory system, and skin.

Directions

1. Dissolve 30 g of the medium in one liter of purified water.
2. Mix thoroughly.
3. Autoclave at 121°C for 15 minutes.

Quality Control Specifications

Dehydrated Appearance: Powder is homogeneous, free flowing, and light beige.

Prepared Appearance: Prepared medium is brilliant to clear, yellow to amber, with none to light precipitate.



Expected Cultural Response and USP/EP/JP Growth Promotion Testing: Cultural response in Tryptic Soy Broth tested at Harmonized USP/EP/JP specified temperatures and incubation times.^{1,2,3}

Microorganism	Approx. Inoculum (CFU)	Incubation Period	Expected Growth
<i>Aspergillus niger</i> ATCC® 16404	10 - 100	Within 5 days	Growth
<i>Bacillus subtilis</i> ATCC® 6633	10 - 100	18 – 72 hours	Growth
<i>Bacteroides vulgatus</i> ATCC® 8482	10 - 100	18 – 72 hours	Fair to excellent growth
<i>Candida albicans</i> ATCC® 10231	10 - 100	18 – 72 hours	Growth
<i>Clostridium sporogenes</i> ATCC® 11437	10 - 100	18 – 72 hours	Fair to excellent growth
<i>Escherichia coli</i> ATCC® 25922	10 - 100	18 – 72 hours	Good to excellent growth
<i>Micrococcus luteus</i> ATCC® 9341	10 - 100	18 – 72 hours	Growth
<i>Neisseria meningitidis</i> ATCC® 13090	10 - 100	18 – 72 hours	Poor to good growth
<i>Pseudomonas aeruginosa</i> ATCC® 9027	10 - 100	18 – 72 hours	Growth
<i>Staphylococcus aureus</i> ATCC® 25923	10 - 100	18 – 72 hours	Good to excellent growth
<i>Staphylococcus aureus</i> ATCC® 6538	10 - 100	18 – 72 hours	Growth
<i>Staphylococcus epidermidis</i> ATCC® 12228	10 - 100	18 – 72 hours	Fair to excellent growth
<i>Streptococcus pneumoniae</i> ATCC® 6305	10 - 100	18 – 72 hours	Fair to excellent growth
<i>Streptococcus pyogenes</i> ATCC® 19615	10 - 100	18 – 72 hours	Good to excellent growth

The organisms listed are the minimum that should be used for Growth Promotion testing.

Test Procedure

Refer to appropriate references for specific procedures using Tryptic Soy Broth.^{1,2,3,4-9}

Results

Refer to appropriate references for test results. Growth is indicated by turbidity.

Storage

Store sealed bottle containing the dehydrated medium at 2 - 30°C. Once opened and recapped, place container in a low humidity environment at the same storage temperature. Protect from moisture and light by keeping container tightly closed.

Expiration

Refer to expiration date stamped on the container. The dehydrated medium should be discarded if not free flowing, or if the appearance has changed from the original pale to light beige. Expiry applies to medium in its intact container when stored as directed.

Limitation of the Procedure

Due to nutritional variation, some strains may grow poorly or fail to grow on this medium.

Packaging

Tryptic Soy Broth	Code No.	7164A	500 g
		7164B	2 kg
		7164C	10 kg

References

1. **United States Pharmacopeial Convention.** 2007. The United States pharmacopeia, 31st ed., Amended Chapters 61, 62, 111. The United States Pharmacopeial Convention, Rockville, MD.
2. **Directorate for the Quality of Medicines of the Council of Europe (EDQM).** 2007. The European Pharmacopoeia, Amended Chapters 2.6.12, 2.6.13, 5.1.4, Council of Europe, 67075 Strasbourg Cedex, France.
3. **Japanese Pharmacopoeia.** 2007. Society of Japanese Pharmacopoeia. Amended Chapters 35.1, 35.2, 7. The Minister of Health, Labor, and Welfare.
4. **McCullough, N. B.** 1949. Laboratory tests in the diagnosis of brucellosis. *Amer. J. of Public Health.* 39:866-869.



5. **Curry, A. S., G. G. Joyce, and G. N. McEwen, Jr.** 1993. CTFA Microbiology guidelines. The Cosmetic, Toiletry, and Fragrance Association, Inc. Washington, D.C.
6. **U.S. Food and Drug Administration.** 1995. Bacteriological analytical manual, 8th ed. AOAC International, Gaithersburg, MD.
7. **Cunniff, P.** 1995. Official methods of analysis AOAC International, 16th ed. AOAC International, Arlington, VA.
8. **Federal Register.** 1992. Detection of viable bacteria and fungi except in live vaccine. Fed. Regist. **21**:113.26.
9. **National Committee for Clinical Laboratory Standards.** 1994. Performance standards for antimicrobial disk susceptibility tests, M2-A5, vol.13, No.24. National Committee for Clinical Laboratory Standards, Villanova, PA.
10. **Murray, P. R., E. J. Baron, M. A. Pfaller, F. C. Tenover, and R. H. Tenover (eds).** 1995. Manual of clinical microbiology, 6th ed. American Society for Microbiology, Washington, D.C.

Technical Information

Contact Acumedia Manufacturers, Inc. for Technical Service or questions involving dehydrated culture media preparation or performance at (517)372-9200 or fax us at (517)372-2008.



VOGEL AND JOHNSON AGAR (7207)

Intended Use

Vogel and Johnson Agar is used for the isolation of staphylococci.

Product Summary and Explanation

Coagulase-positive staphylococci, primarily *Staphylococcus aureus*, are among the microorganisms that cause spoilage or chemical changes in cosmetic products.¹ To isolate coagulase-positive, mannitol fermenting staphylococci, Vogel and Johnson² modified Tellurite-Glycine Agar by Zebovitz, Evans, and Niven.³ The modification included increasing mannitol and adding a pH indicator. Vogel and Johnson Agar selects and differentiates coagulase-positive staphylococci that ferment mannitol and reduce tellurite.⁴

Vogel and Johnson (VJ) Agar is specified in standard methods testing for cosmetics,^{1,5} pharmaceutical articles,⁶ nutritional supplements.⁷

Principles of the Procedure

Enzymatic Digest of Casein provides nitrogen, amino acids, and minerals in Vogel and Johnson Agar. Yeast Extract is a vitamin source to stimulate bacterial growth. Mannitol is the fermentable carbohydrate. Dipotassium Phosphate is the buffering agent. Lithium Chloride, Glycine, and 1% Potassium Tellurite Solution inhibit the growth of most microorganisms except staphylococci. Phenol Red is the pH indicator. Agar is the solidifying agent.

Formula / Liter

Enzymatic Digest of Casein	10
Yeast Extract.....	5 g
Mannitol	10 g
Dipotassium Phosphate	5 g
Lithium Chloride	5 g
Glycine	10 g
Phenol Red	0.025 g
Agar	15 g

Final pH: 7.2 ± 0.2 at 25°C

Formula may be adjusted and/or supplemented as required to meet performance specifications.

Supplement # 7989

Tellurite Solution (1%) Chapman
Potassium Tellurite, 100 mg
10 mL

Precautions

1. For Laboratory Use.
2. HARMFUL. Harmful if swallowed, inhaled, or absorbed through skin. Skin irritation may be severe. May cause central nervous system effects.

Directions

1. Suspend 60 g of the medium in one liter of purified water.
2. Heat with frequent agitation and boil for one minute to completely dissolve the medium.
3. Autoclave at 121°C for 15 minutes.
4. After cooling to 45 - 50°C add 2 vials (20 mL) of Tellurite Solution (1%) Chapman Supplement (7989) or 20 mL of a sterile 1% Potassium Tellurite Solution.
5. Mix thoroughly before dispensing.

Quality Control Specifications

Dehydrated Appearance: Powder is homogeneous, free flowing, and red-beige.

Prepared Appearance: Prepared medium is trace to slightly hazy and red-orange.



Expected Cultural Response: Cultural response on Vogel and Johnson Agar at incubated aerobically 35 ± 2°C and examined for growth after 18 - 48 hours.

Microorganism	Approx. Inoculum (CFU)	Expected Results	
		Response	Reaction
<i>Enterococcus faecalis</i> ATCC® 29212	~ 1000	Partial to complete inhibition	Black colonies
<i>Escherichia coli</i> ATCC® 25922	~ 1000	Inhibition	---
<i>Staphylococcus aureus</i> ATCC® 25923	10 - 300	Growth	Black colonies w/ yellow zones
<i>Staphylococcus epidermidis</i> ATCC® 12228	~ 1000	Partial to complete inhibition	Black colonies

The organisms listed are the minimum that should be used for quality control testing.

Test Procedure

Refer to appropriate references for the isolation and identification of staphylococci.

Results

Coagulase-positive strains of *S. aureus* reduce tellurite and form black colonies on the medium. These strains typically ferment mannitol and exhibit yellow halos around black colonies. Most organisms other than coagulase - positive staphylococci are inhibited during the first 24 hours of incubation. After 24 hours, other organisms, especially fecal streptococci and coagulase - negative *S. epidermidis* may grow.

Storage

Store sealed bottle containing the dehydrated medium at 2 - 30°C. Once opened and recapped, place container in a low humidity environment at the same storage temperature. Protect from moisture and light.

Expiration

Refer to expiration date stamped on container. The dehydrated medium should be discarded if not free flowing, or if appearance has changed from the original color. Expiry applies to medium in its intact container.

Limitation of the Procedure

Due to nutritional variation, some strains may be encountered that grow poorly or fail to grow on this medium.

Packaging

Vogel and Johnson Agar	Code No.	7207A	500 g
		7207B	2 kg
		7207C	10 kg
Tellurite Solution (1%) Chapman		7989	10 mL

References

1. www.fda.gov/Food/ScienceResearch/LaboratoryMethods/BacteriologicalAnalyticalManualBAM/default.htm.
2. Vogel, T. A., and M. Johnson. 1960. A modification of the Tellurite-Glycine Medium for use in the identification of *Staphylococcus aureus*. Public Health Lab. 18:131.
3. Zebovitz, E., J. B. Evans, and C. F. Niven, Jr. 1955. Tellurite-Glycine Agar; a selective plating medium for the quantitative detection of coagulase-positive staphylococci. J. Bacteriol. 70:888.
4. MacFaddin, J. F. 1985. Media for isolation-cultivation-identification-maintenance of medical bacteria, vol.1, p. 848-849. Williams & Wilkins, Baltimore, MD.
5. Curry, A. S., J. G. Graf, and G. N. McEwen, Jr. (eds.). 1993. CTFa microbiology guidelines. The Cosmetic, Toiletry, and Fragrance Association, Washington, D.C.
6. United States Pharmacopeial Convention. 1995. The United States pharmacopeia, 23rd ed. The United States Pharmacopeial Convention, Rockville, MD.

Technical Information

Contact Acumedia Manufacturers, Inc. for Technical Service or questions involving dehydrated culture media preparation or performance at (517)372-9200 or fax us at (517)372-2006.



620 Leshar Place, Lansing MI 48912
 517/372-9200 • 800/783-3212 • fax: 800/875-8563
 neogen-info@neogen.com • www.neogen.com

PI 7207, Rev 3, May 2011